Deltares

Samenvatting hydraulische belastingen op de aanlandingsconstructie nabij Wijk aan Zee

Samenvatting hydraulische belastingen op de aanlandingsconstructie nabij Wijk aan Zee

Samenvatting Hydraulische belastingen op de aanlandingsconstructie nabij Wijk aan Zee

Client	Van Vulpen
Contact	
Referentie	
Trefwoorden	Golfbelasting, ontgronding, strand, aanlanding, Wijk aan Zee, HKN

Document control	
Versie	1.0
Datum	14-1-2021
Project nr.	11206427-000
Document ID	11206427-000-HYE-0001
Status	**definitief**

Doc. Versie	Auteurs	Reviewer	Goedkeuring	
1.0				
				

Inhoudsopgave

1 Introductie

De NRG-Groep is bezig met de voorbereiding van een ontwerp voor de kabel aanlandingsconstructie van het Hollandse Kust Noord Offshore Windpark. Om het ontwerp van de tijdelijke aanlandingsconstructie verder te detailleren, is Deltares gevraagd input te leveren dat betrekking heeft op de golfbelasting die zowel op de Geotube als op de damwand werkt. Bovendien is informatie over de te verwachten ontgronding rondom de structuur vereist.

De doelstellingen van deze studie zijn daarom zowel het beoordelen van de golfbelasting op de Geotubes en de damwand als het beoordelen van de te verwachten ontgronding rond de constructie. Daarom wordt de volgende stapsgewijze aanpak gevolgd:

- Taak 1: Bepaling van de offshore extreme metocean condities
- Taak 2: Bepaling van de nearshore metocean condities
- Taak 3: Beoordeling van de golfbelastingen op de Geotubes en de damwand
- Taak 4: Beoordeling van de te verwachten ontgronding rond de constructie
- Taak 5: Aandachtspunten voor het ontwerp van de tijdelijke aanlandingsconstructie

NB Dit Nederlandstalige rapport betreft een vertaling van een samenvattende uitsnede van de uitgebreidere Engelstalige versie (opgenomen als bijlage) om zodoende de vergunningsverlening te vergemakkelijken.

2 Extreme metocean condities op zee

Om de lokale golfbelastingen en de te verwachten ontgronding te beoordelen is informatie over de lokale hydrodynamische omstandigheden rond de constructie vereist. Om de vereiste informatie te verkrijgen werden eerst de offshore extreme condities afgeleid, op basis van extreme waarde analyses (EVA) van historische data die beschikbaar is uit de door Deltares beheerde Noordzee metocean database. Extreme wind en golf (H_s en bijbehorende T_p) condities en waterstanden (totale waterstand en stormvloed) werden afgeleid op basis van gekalibreerde 39-jarige tijdseries (1980-2018) op een totaal van 6 uitvoer locaties langs de buitenste randen van de voorziene domeinen van de numerieke modellering (zie Figuur 2.1).

Figuur 2.1 Uitvoerlocaties voor de afleiding van extreme condities. De projectlocatie wordt gemarkeerd door de witte stip.

In Tabel 2.1, Tabel 2.2 en Tabel 2.3 worden de significante golfhoogten (H_s, kolom 3) en 1 uur gemiddelde windsnelheden op 10 m (U_{10}, kolom 5) voor verschillende terugkeer perioden (RP) gepresenteerd voor respectievelijk locaties WS, WC en WN. In de vierde kolom van elke tabel zijn ook de piek golf perioden (T_p) gepresenteerd. Deze staan in verband met de significante golfhoogten.

Tabel 2.1 Golf (H_s en bijbehorende T_p) en windextremen voor locatie WS.

Sector	RP	H_s (m)	T_p (s)	U_{10} (m/s)
Omni	1	5.2	10.5	21.5
	2	5.6	11.1	22.4
	5	6.1	11.7	23.5
	10	6.5	12.1	24.4
	20	6.8	12.6	25.2
	50	7.2	13.1	26.4
	100	7.5	13.4	27.2
240	1	4.4	9.4	20.3
	2	4.8	9.7	21.5
	5	5.3	10.2	23.0
	10	5.7	10.5	24.1
	20	6.0	10.8	25.1
	50	6.4	11.1	26.3
	100	6.8	11.4	27.2
270	1	4.5	9.2	19.8
	2	5.0	9.5	21.0
	5	5.5	10.0	22.4
	10	6.0	10.3	23.4
	20	6.4	10.6	24.3
	50	7.0	11.0	25.3
	100	7.4	11.2	26.1
300	1	4.7	9.9	18.7
	2	5.1	10.3	19.6
	5	5.6	10.8	20.8
	10	5.9	11.0	21.7
	20	6.2	11.2	22.6
	50	6.4	11.5	23.8
	100	6.6	11.6	24.6
330	1	4.6	10.8	17.3
	2	5.2	11.5	18.6
	5	5.9	12.2	20.2
	10	6.4	12.7	21.2
	20	6.7	13.1	22.2
	50	7.2	13.5	23.4
	100	7.5	13.8	24.3

Tabel 2.2 Golf (H_s en bijbehorende T_p) en windextremen voor locatie WC.

Sector	RP	H_s (m)	T_p (s)	U_{10} (m/s)
Omni	1	5.4	10.7	21.5
	2	5.8	11.3	22.4
	5	6.4	11.9	23.5
	10	6.8	12.3	24.4
	20	7.1	12.7	25.2
	50	7.6	13.2	26.4
	100	7.9	13.5	27.2
240	1	4.5	9.5	20.3
	2	4.9	9.9	21.5
	5	5.4	10.3	23.0
	10	5.8	10.6	24.1
	20	6.1	10.9	25.1
	50	6.5	11.2	26.3
	100	6.8	11.5	27.2
270	1	4.7	9.3	19.8
	2	5.1	9.7	21.0
	5	5.7	10.2	22.4
	10	6.1	10.5	23.4
	20	6.5	10.8	24.3
	50	7.0	11.1	25.3
	100	7.3	11.4	26.1
300	1	4.9	10.1	18.7
	2	5.4	10.5	19.6
	5	5.8	11.0	20.8
	10	6.1	11.3	21.7
	20	6.4	11.5	22.6
	50	6.7	11.7	23.8
	100	6.8	11.9	24.6
330	1	4.8	10.9	17.3
	2	5.4	11.6	18.6
	5	6.2	12.4	20.2
	10	6.6	12.9	21.2
	20	7.1	13.3	22.2
	50	7.5	13.8	23.4
	100	7.9	14.1	24.3

Tabel 2.3 Golf (H_s en bijbehorende T_p) en windextremen voor locatie WN.

Sector	RP	H_s (m)	T_p (s)	U_{10} (m/s)
Omni	1	5.5	10.8	21.5
	2	6.0	11.3	22.4
	5	6.5	11.9	23.5
	10	6.9	12.3	24.4
	20	7.3	12.7	25.2
	50	7.7	13.1	26.4
	100	8.0	13.4	27.2
240	1	4.7	9.5	20.3
	2	5.1	9.9	21.5
	5	5.6	10.4	23.0
	10	6.0	10.7	24.1
	20	6.4	10.9	25.1
	50	6.8	11.3	26.3
	100	7.1	11.5	27.2
270	1	4.8	9.3	19.8
	2	5.2	9.7	21.0
	5	5.8	10.2	22.4
	10	6.2	10.5	23.4
	20	6.6	10.8	24.3
	50	7.1	11.1	25.3
	100	7.5	11.4	26.1
300	1	5.0	10.0	18.7
	2	5.4	10.4	19.6
	5	5.9	10.8	20.8
	10	6.2	11.0	21.7
	20	6.5	11.3	22.6
	50	6.9	11.5	23.8
	100	7.1	11.7	24.6
330	1	5.0	11.0	17.3
	2	5.6	11.6	18.6
	5	6.3	12.4	20.2
	10	6.8	12.8	21.2
	20	7.2	13.2	22.2
	50	7.7	13.6	23.4
	100	8.0	13.9	24.3

De verticale getijdenniveaus op de locaties FS, FC en FN worden weergegeven in respectievelijk Tabel 2.4, Tabel 2.5 en Tabel 2.6.

Tabel 2.4 Getijdenniveaus voor locatie FS.

Tidal levels	Reference level	
	m MSL	m LAT
Highest Astronomical Tide, HAT	1.32	2.27
Mean High High Water, MHHW	1.00	1.95
Mean Low High Water, MLHW	0.46	1.41
Mean Sea Level, MSL	0.00	0.95
Mean High Low Water, MHLW	-0.45	0.51
Mean Low Low Water, MLLW	-0.73	0.23
Lowest Astronomical Tide	-0.95	0.00

Tabel 2.5 Getijdenniveaus voor locatie FC.

Tidal levels	Reference level	
	m MSL	m LAT
Highest Astronomical Tide, HAT	1.29	2.24
Mean High High Water, MHHW	0.98	1.94
Mean Low High Water, MLHW	0.61	1.57
Mean Sea Level, MSL	0.00	0.96
Mean High Low Water, MHLW	-0.49	0.47
Mean Low Low Water, MLLW	-0.73	0.22
Lowest Astronomical Tide	-0.96	0.00

Tabel 2.6 Getijdenniveaus voor locatie FN.

Tidal levels	Reference level	
	m MSL	m LAT
Highest Astronomical Tide, HAT	1.24	2.20
Mean High High Water, MHHW	0.95	1.91
Mean Low High Water, MLHW	0.68	1.63
Mean Sea Level, MSL	0.00	0.96
Mean High Low Water, MHLW	-0.53	0.43
Mean Low Low Water, MLLW	-0.74	0.22
Lowest Astronomical Tide	-0.96	0.00

In Tabel 2.7, Tabel 2.8 en Tabel 2.9 zijn de schattingen voor de totale waterstanden (getij + stormvloed, kolom 3), het stormvloedpeil (kolom 4) en de 1-uur gemiddelde windsnelheden op 10 m hoogte (U_{10}, kolom 5) gepresenteerd voor respectievelijk locaties FS, FC en FN. Ook deze karakteristieken zijn voor verschillende terugkeer perioden weergegeven.

Tabel 2.7 Totale waterstanden (WL), stormvloedpeil en windextremen voor locatie FS.

Sector	RP	Total WL (mMSL)	Surge (m)	U_{10} (m/s)
Omni	1	2.1	1.6	21.5
	2	2.2	1.8	22.4
	5	2.4	2.0	23.5
	10	2.6	2.1	24.4
	20	2.7	2.2	25.2
	50	2.9	2.4	26.4
	100	3.1	2.5	27.2
240	1	1.6	1.2	20.3
	2	1.7	1.3	21.5
	5	1.8	1.4	23.0
	10	1.8	1.5	24.1
	20	1.9	1.6	25.1
	50	2.0	1.6	26.3
	100	2.0	1.7	27.2
270	1	1.9	1.4	19.8
	2	2.1	1.6	21.0
	5	2.3	1.8	22.4
	10	2.4	1.9	23.4
	20	2.6	2.0	24.3
	50	2.8	2.2	25.3
	100	2.9	2.3	26.1
300	1	1.9	1.3	18.7
	2	2.1	1.5	19.6
	5	2.3	1.8	20.8
	10	2.5	1.9	21.7
	20	2.6	2.1	22.6
	50	2.8	2.3	23.8
	100	3.0	2.4	24.6
330	1	1.8	1.1	17.3
	2	2.0	1.3	18.6
	5	2.2	1.6	20.2
	10	2.4	1.7	21.2
	20	2.5	1.9	22.2
	50	2.8	2.1	23.4
	100	2.9	2.3	24.3

Tabel 2.8 Totale waterstanden (WL), stormvloedpeil en windextremen voor locatie FC.

Sector	RP	Total WL (mMSL)	Surge (m)	U_{10} (m/s)
Omni	1	2.1	1.6	21.5
	2	2.2	1.8	22.4
	5	2.4	2.0	23.5
	10	2.6	2.1	24.4
	20	2.7	2.2	25.2
	50	2.9	2.4	26.4
	100	3.0	2.4	27.2
240	1	1.6	1.2	20.3
	2	1.7	1.3	21.5
	5	1.8	1.5	23.0
	10	1.8	1.6	24.1
	20	1.9	1.7	25.1
	50	1.9	1.8	26.3
	100	2.0	1.9	27.2
270	1	1.9	1.4	19.8
	2	2.1	1.6	21.0
	5	2.3	1.8	22.4
	10	2.4	1.9	23.4
	20	2.6	2.0	24.3
	50	2.8	2.2	25.3
	100	2.9	2.3	26.1
300	1	1.9	1.3	18.7
	2	2.1	1.5	19.6
	5	2.3	1.8	20.8
	10	2.5	1.9	21.7
	20	2.6	2.1	22.6
	50	2.8	2.3	23.8
	100	3.0	2.4	24.6
330	1	1.8	1.1	17.3
	2	2.0	1.3	18.6
	5	2.2	1.5	20.2
	10	2.4	1.7	21.2
	20	2.5	1.9	22.2
	50	2.7	2.2	23.4
	100	2.9	2.4	24.3

Tabel 2.9 Totale waterstanden (WL), stormvloedpeil en windextremen voor locatie FN.

Sector	RP	Total WL (mMSL)	Surge (m)	U_{10} (m/s)
Omni	1	2.1	1.6	21.5
	2	2.2	1.8	22.4
	5	2.4	2.0	23.5
	10	2.6	2.1	24.4
	20	2.7	2.3	25.2
	50	2.9	2.4	26.4
	100	3.1	2.5	27.2
240	1	1.6	1.2	20.3
	2	1.7	1.3	21.5
	5	1.8	1.5	23.0
	10	1.8	1.6	24.1
	20	1.9	1.7	25.1
	50	2.0	1.8	26.3
	100	2.0	1.9	27.2
270	1	1.9	1.4	19.8
	2	2.0	1.6	21.0
	5	2.2	1.8	22.4
	10	2.4	1.9	23.4
	20	2.5	2.0	24.3
	50	2.7	2.2	25.3
	100	2.9	2.3	26.1
300	1	1.9	1.3	18.7
	2	2.1	1.5	19.6
	5	2.3	1.7	20.8
	10	2.5	1.9	21.7
	20	2.6	2.1	22.6
	50	2.8	2.2	23.8
	100	3.0	2.4	24.6
330	1	1.8	1.1	17.3
	2	1.9	1.3	18.6
	5	2.2	1.5	20.2
	10	2.3	1.7	21.2
	20	2.5	1.9	22.2
	50	2.7	2.2	23.4
	100	2.9	2.3	24.3

3 Metocean condities langs de kust

Om nauwkeurige stroom- en golfcondities nabij de constructie te bepalen, wordt een numeriek model met hoge resolutie opgesteld voor het projectgebied. Simulaties in dit model lossen het getij, de wind en golf gedreven stromingen op en maken het dus mogelijk om langs de kust tijdseries voor studierelevante parameters zichtbaar te maken. In dit geval zijn voor verschillende scenario's waterdiepten, stroomsnelheden en golfhoogten bepaald voor twaalf locaties rond de constructie.

3.1 Modelopzet

Het numerieke model is opgezet met DELFT3D-FM (rekenrooster is aangegeven met de blauwe rechthoek in Figuur 2.1) en SWAN (rekenrooster is aangegeven met de rode rechthoek in Figuur 2.1). Beide rekenroosters hebben een resolutie van 10 m kustdwars en 20 m in kustlangs richting t.p.v. de projectlocatie. Voor de bodem van het numerieke model zijn drie verschillende 2D bronnen verwerkt:

1. Vaklodingen (vrij beschikbaar, 2017, t.o.v. MSL)
2. MBES Buitenhaven IJmuiden (interne RWS data, 2011, t.o.v. MSL)
3. MBES TenneT (verstrekt door NRG, 2018, t.o.v. LAT)

De vaklodingen data uit 2017 bestrijken bijna de volledige omvang van zowel het rode als het blauwe rooster (zie Figuur 2.1), terwijl de haven van IJmuiden niet gedekt is in deze dataset. Het bodemniveau in dit gebied wordt geleverd door de data van Rijkswaterstaat (RWS), afkomstig uit 2011.

Op de projectlocatie voerde TenneT in 2018 een extra multi-beam (MBES) meting uit. Deze data is ook verwerkt in de bathymetrie. Het vervangt echter niet de data van Vaklodingen in het gebied. Er zijn aanzienlijke verschillen tussen de data tot 2017 en de TenneT MBES uit 2018. Zoals te zien in Figuur 3.1, bereiken de verticale verschillen in het bodemniveau (door Vaklodingen 2017 en TenneT 2018 data te vergelijken) ongeveer 0,9 m bij de damwand aan zeezijde en 0,25 m bij de damwand aan de duinzijde. Daarnaast is er ook een significant verschil in de helling van de bodemniveaus uit verschillende bronnen.

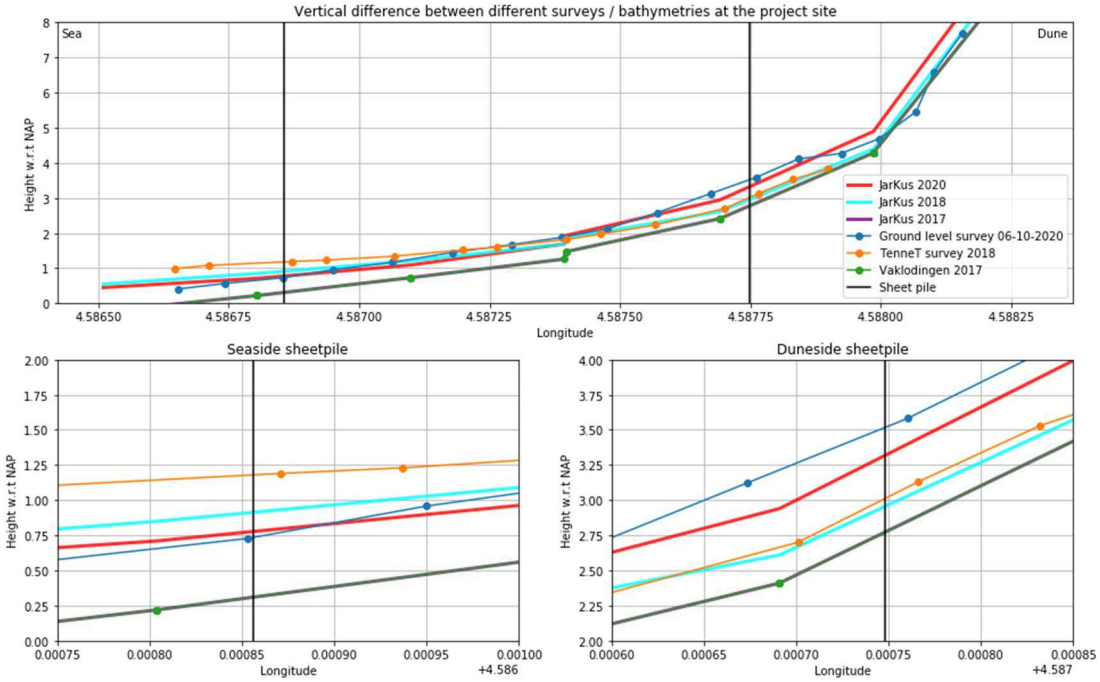

Figuur 3.1: Bodemliggingen (in m t.o.v. NAP) van verschillende databronnen langs een willekeurig lijn loodrecht op de kust in het projectgebied. Het bovenste paneel toont de volledige doorsnede van de willekeurige lijn, waar de locatie van de damwanden aan de zee en duinzijde zijn aangegeven met verticale zwarte lijnen. De linker- en rechterbeneden panelen zoomen in op de bodemligging rond respectievelijk de damwanden aan zee- en duinzijde.

De bovenstaande paragraaf geeft aan dat de verschillen in bathymetrie verkregen uit de vergeleken databronnen aanzienlijk zijn in zowel de verticaal als horizontaal (helling). Dit laatste is een indicatie dat er waarschijnlijk seizoensgebonden verschillen in het bodemniveau, aangeduid als de zomer en winterprofielen, bestaan. Aangezien het ontwerp van de aanlandingsconstructie sterk afhankelijk is van de bodemligging, is besloten om twee verschillende bathymetrieen te beschouwen in de numerieke modellering om zodoende de condities voor beide situaties te verkrijgen.

Één bathymetrie is gebaseerd op de gegevens tot 2017 (bronnen 1 en 2 in de bovenstaande lijst) en wordt in de rest van het rapport de Vaklodingen ‘bathymetrie’ genoemd. Door de Vaklodingen bathymetrie in deze studie op te nemen (zie Figuur 3.2 en groene / paarse lijn in Figuur *3.1*), zijn we conservatief voor de damwand aan de kust en duinzijde. Deze bathymetrie bevat namelijk lagere bodem niveaus die eerder kunnen worden overspoeld of worden onderworpen aan hogere stroomsnelheden als gevolg van grotere waterdiepten.

De andere bathymetrie bestaat uit alle drie de bronnen in de bovenstaande lijst en wordt in de rest van het rapport de TenneT bathymetrie genoemd. Door de TenneT bathymetrie in deze studie op te nemen (zie Figuur 3.3 en oranje lijn in Figuur 3.1) wordt de meest recente bodemdata benaderd, wat waarschijnlijk zal resulteren in de meest realistische resultaten. Er moet echter worden opgemerkt dat deze bathymetrie leidt tot een onderschatting van de waterdiepten en stromingssnelheden die voor de damwand aan de zeezijde worden berekend, aangezien het bodemhoogteonderzoek van 06-10-2020 onder het niveau van de TenneT bathymetrie ligt.

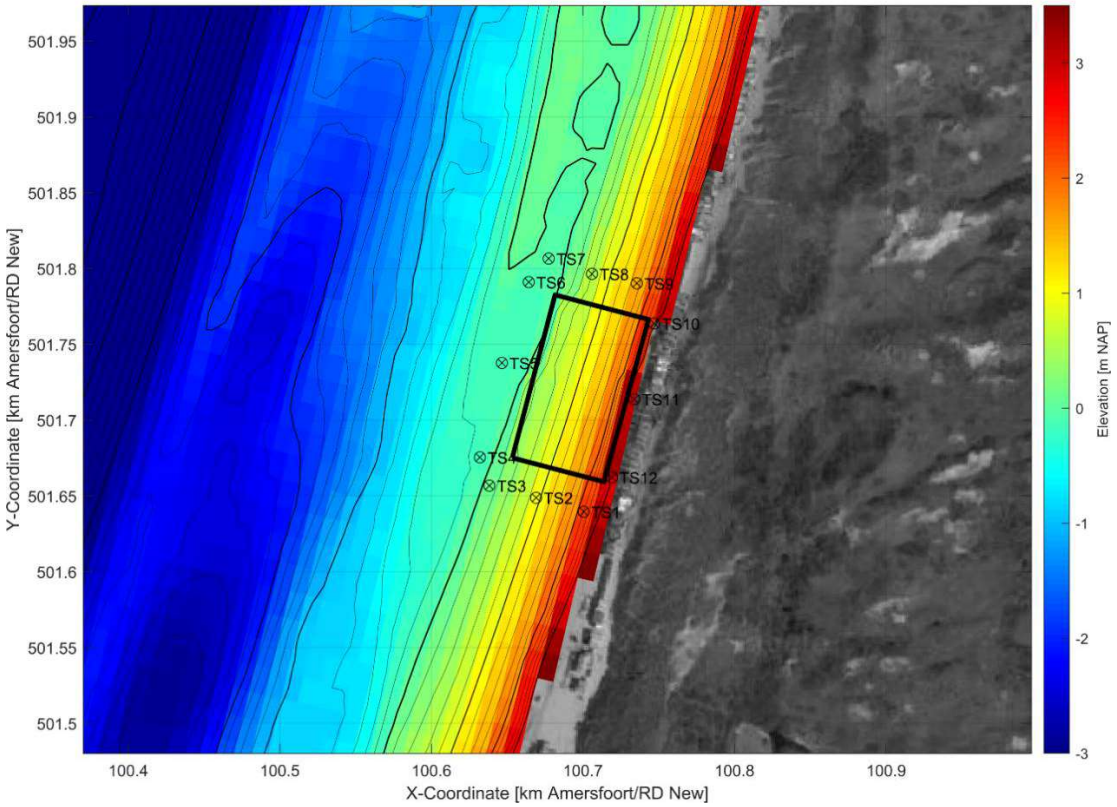

Figuur 3.2: Bodemligging van de Vaklodingen bathymetrie (2017) samen met de geschematiseerde damwanden (zwarte rechthoek) en uitvoerlocaties (TS1 t/m 12) van het numerieke model.

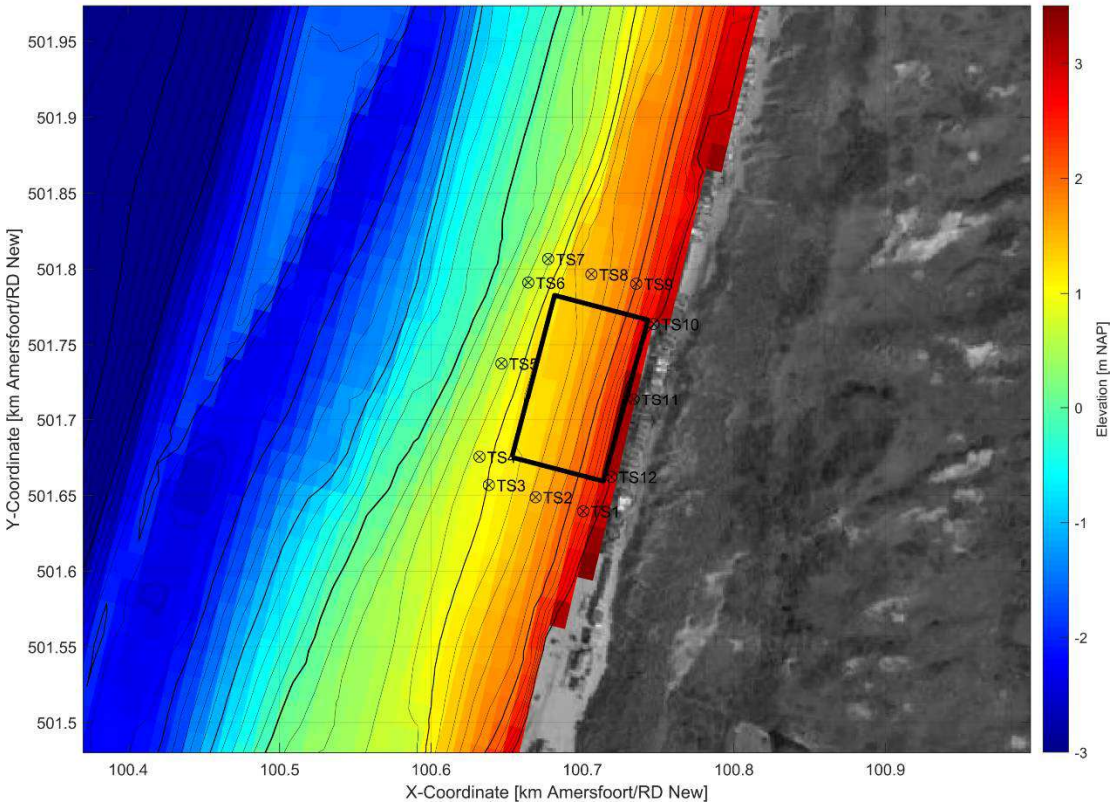

Figuur 3.3: Bodemligging van de TenneT bathymetrie (2018) samen met de geschematiseerde damwanden (zwarte rechthoek) en uitvoerlocaties (TS1 t/m 12) van het numerieke model.

Samen met de klant is besloten om de volgende vijf numerieke simulaties uit te voeren:

1. Een getijde simulatie (flow) met de TenneT bathymetrie (verwijzing F_TenneT)
2. Een simulatie (flow-wave) met een golfklimaat representatief voor de periode (1 jr) waarin de aanlandingsconstructie op het strand wordt geplaatst met de TenneT bathymetrie (verwijzing FW_1yr_TenneT)
3. Een simulatie (flow-wave) met een storm met een hogere terugkeerperiode (5 jr) met de TenneT bathymetrie (verwijzing FW_5yr_TenneT)
4. Een simulatie (flow-wave) met een storm met een hogere terugkeerperiode (20 jr) met de TenneT bathymetrie (verwijzing FW_20yr_TenneT)
5. Een simulatie (flow-wave) met een storm met een hogere terugkeerperiode (20 jr) met de Vaklodingen bathymetrie (referentie FW_20yr_Vakl)

3.2 Resultaten

De resultaten van alle vijf simulaties (zie lijst hierboven) worden gepresenteerd zoals weergegeven in Figuur 3. 4 hieronder, in dit geval voor de vierde simulatie op uitvoerlocatie TS5. Het bovenste paneel toont de locatie van de damwanden samen met de uitvoerlocaties TS1 tot 12, welke aan de voorzijde van de Geotubes en aan de achterzijde van de damwanden zijn geschematiseerd. Het tweede paneel toont de waterhoogte in m t.o.v. NAP samen met het bodemniveau waarop de uitvoerlocatie zich bevindt. De berekende maximale waterdiepte op die locatie wordt aangegeven in de titel van het paneel. Het derde paneel toont de resulterende stroomsnelheid, die te wijten is aan getijden, wind en golven voor deze simulatie. Net als bij het tweede paneel wordt de maximale stroomsnelheid aangegeven in de titel van het paneel. Het laatste paneel bevat de tijdserie van de golfhoogten op de uitvoerlocatie, waar de maximale golfhoogte opnieuw wordt weergegeven in de titel van het paneel.

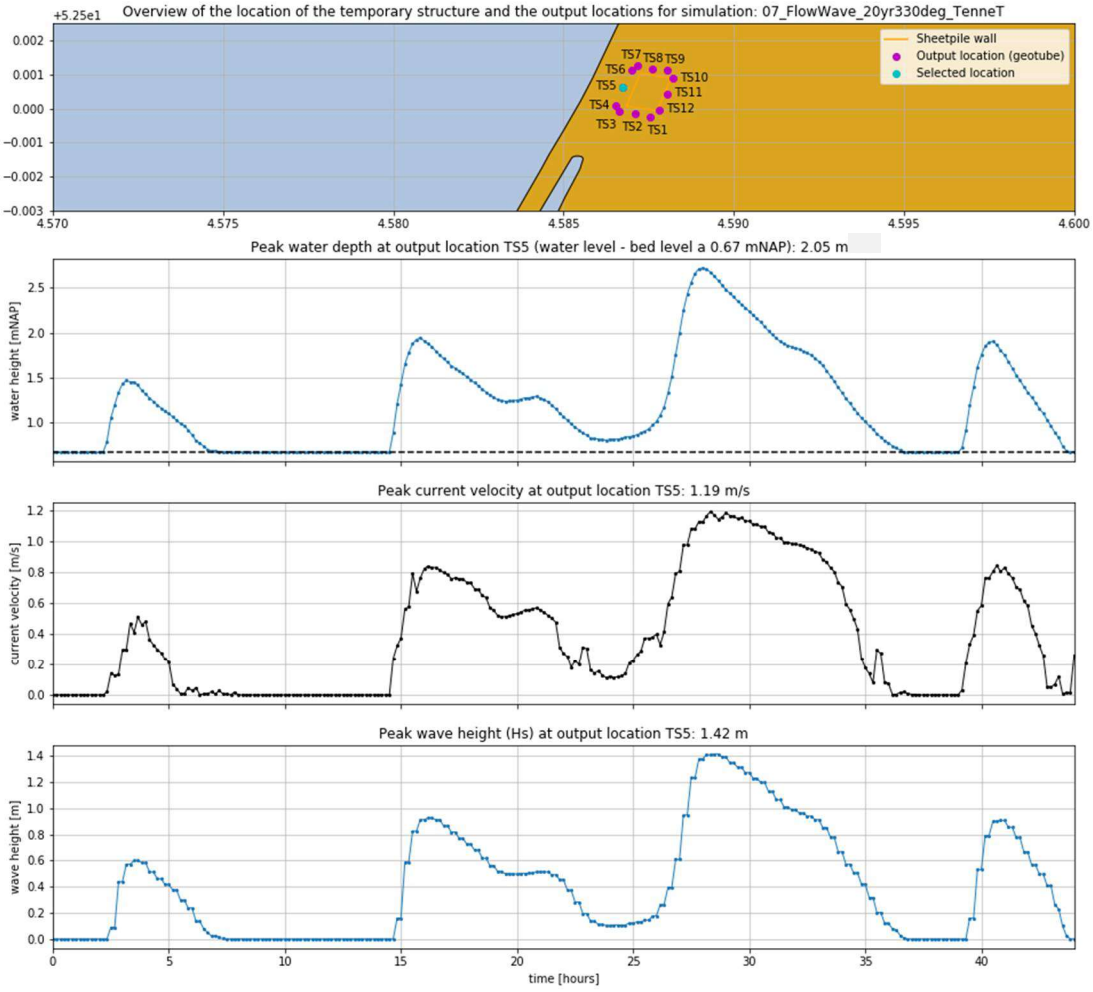

Figuur 3. 4: Locatie en schematisatie van de tijdelijke constructie met (geselecteerde) uitvoerpunt(en) en de geschatte landgrens op de projectlocatie (bovenste paneel), de tijdsserie van de waterhoogte (in m t.o.v. NAP, tweede paneel), de stroomsnelheid (derde paneel) en de golfhoogte (vierde paneel) voor de vierde simulatie (FW_20yr_TenneT); een storm van 20 jaar en de TenneT bathymetrie uit 2018.

3.2.1 Waterdiepten

Vergelijkbaar met de berekende maximale waterdiepte zoals weergegeven in Figuur 3. 4 voor locatie TS5 voor simulatie FW_20yr_TenneT, geeft Tabel 3.1 geeft een overzicht van alle berekende maxima voor alle simulaties en uitvoerlocaties.

Zoals te zien is in Tabel 3.1, blijven de punten TS10, 11 en 12 droog voor alle simulaties. Dit geeft aan dat er geen stroming tussen de damwand en de duinen wordt verwacht. Echter, het moet worden gezegd dat dit afhankelijk is van de exacte locatie en configuratie van de damwanden, alsmede het ontwerp van de tijdelijke aanlandingsconstructie. In het geval van een (milde) storm zullen de locaties TS1 en TS9 onderwater staan (die het landwaartse uiteinde van de Geotubes vertegenwoordigen). Deze punten liggen zeer dicht bij de achterkant van de aanlandingsconstructie, wat aangeeft dat water dicht bij het punt komt waar er wel stroming tussen de damwand en de duinen kan plaatsvinden. De F_TenneT simulatie laat zien dat de verwachting is dat een waterdiepte van tenminste 0,5 m aanwezig zal zijn aan de voorzijde van de aanlandingsconstructie (TS3 tot TS7) tijdens zeer rustige omstandigheden en hoog water (d.w.z. bij afwezigheid van golven). De rest van de zijkanten van de constructie en het aangrenzende strand blijft droog in het geval van deze bodemschematisatie. De maximale waterdiepten in Tabel 3.1 zijn groen gemarkeerd. Men kan zien dat dit voor alle uitvoerlocaties betreft voor de simulatie met de Vaklodingen bathymetrie. De meer realistische resultaten voor

de te verwachten maximale waterdiepten zijn lichtblauw gemarkeerd, deze zijn gebaseerd op de meest recente TenneT bathymetrie.

Tabel 3.1: Maximale waterdiepten in m op verschillende uitvoerlocaties rond de aanlandingsconstructie.

Simulatie / Observatiepunt	TS1 TS1	TS2 TS2	TS3 TS3	TS4 TS4	TS5 TS5	TS6 TS6	TS7 TS7	TS8 TS8	TS9 TS9	TS10 TS10	TS11	TS12 TS12
F_TenneT	0.0	0.0	0.25	0.36	0.56	0.74	0.59	0.0	0.0	0.0	0.0	0.0
FW_1yr_TenneT	0.29	1.18	1.63	1.73	1.92	2.1	1.97	1.26	0.75	0.0	0.0	0.0
FW_5yr_TenneT	0.38	1.26	1.72	1.81	2.0	2.18	2.05	1.36	0.85	0.0	0.0	0.0
FW_20yr_TenneT	0.42	1.31	1.76	1.86	2.05	2.22	2.1	1.4	0.9	0.0	0.0	0.0
FW_20yr_Vakl	0.55	1.78	2.6	2.88	2.89	2.82	2.81	2.24	1.33	0.0	0.0	0.0

3.2.2 Stroomsnelheden

De maximale stroomsnelheden voor alle uitvoerlocaties voor alle simulaties worden samengevat in Tabel 3.2. Stroomsnelheden zijn afwezig als er op geen enkel moment tijdens de simulatie water op een uitvoerlocatie aanwezig is. De maximale stroomsnelheden zijn groen gemarkeerd in Tabel 3.2. Deze komen niet altijd voor bij de grootste waterdiepten, aangezien de FW_20yr_TenneT simulatie ook groen gemarkeerde cellen bevat. In het geval dat de groene cell aanwezig is in de FW_20yr_Vakl simulatie, bevat de tabel lichtblauwe cellen die meer realistische maxima aangeven (gebaseerd op de meer recente bathymetrie) op de betreffende uitvoerlocaties. Door numerieke waarden op verschillende uitvoerlocaties van de FW_TenneT simulaties te vergelijken, kan men zien dat bij een kleinere terugkeerperiode de stroomsnelheden niet zo veel verschillen. Dit geeft een indicatie dat de maximaal voorkomende stroomsnelheden meer afhankelijk zijn van het ontwerp van de tijdelijke aanlandingsconstructie (de locatie en configuratie) dan de terugkeerperiode van geanalyseerde stormen.

Tabel 3.2: Maximale stroomsnelheden in m/s op verschillende uitvoerlocaties rond de aanlandingsconstructie.

Simulatie / Observatiepunt	TS1 TS1	TS2 TS2	TS3 TS3	TS4 TS4	TS5 TS5	TS6 TS6	TS7 TS7	TS8 TS8	TS9 TS9	TS10 TS10	TS11	TS12 TS12
F_TenneT	0.0	0.0	0.13	0.15	0.17	0.2	0.19	0.0	0.0	0.0	0.0	0.0
FW_1yr_TenneT	0.18	0.25	0.92	1.09	1.08	1.14	0.99	0.51	0.25	0.0	0.0	0.0
FW_5yr_TenneT	0.21	0.23	0.99	1.17	1.16	1.24	1.07	0.53	0.25	0.0	0.0	0.0
FW_20yr_TenneT	0.32	0.23	1.0	1.18	1.19	1.29	1.12	0.57	0.26	0.0	0.0	0.0
FW_20yr_Vakl	0.51	0.39	0.83	0.99	1.17	1.31	1.11	0.75	0.37	0.0	0.0	0.0

3.2.3 Golven

In het geval van een getijde simulatie worden er helemaal geen golven beschouwd. Dit wordt weergegeven met behulp van grijze cellen in Tabel 3.3. Houd er rekening mee dat de toepassing van SWAN voor golfhoogten in waterdiepten die aanwezig zijn aan de voet van de aaanlandingsconstructie niet bijzonder nauwkeurig zijn, terwijl SWAN wel bijdraagt aan de nauwkeurige berekening van hydrodynamische processen op grotere schaal (zoals waterdiepten en golfgedreven stroomsnelheden). Daarom moet men de golfhoogten die in Tabel 3.3 zijn gepresenteerd met zorgvuldigheid behandelen. Het geeft slechts een indicatie van wat kan worden verwacht terwijl we, in theorie, golfhoogten iets lager dan aangegeven in de onderstaande tabel verwachten. Dit is verder uitgewerkt in het volgende hoofdstuk over golfbelastingen, waar een andere aanpak wordt gebruikt om representatieve spectrale golfhoogten te schematiseren voor deze ondiepte kustzone.

Tabel 3.3: Maximale golfhoogten in m op verschillende uitvoerlocaties rond de aanlandingsconstructie.

Simulatie / Observatiepunt	TS1 TS1	TS2 TS2	TS3 TS3	TS4 TS4	TS5 TS5	TS6 TS6	TS7 TS7	TS8 TS8	TS9 TS9	TS10 TS10	TS11	TS12 TS12
F_TenneT	0.0	0.0	0.0	0.0	0.0	0.0	0.0	0.0	0.0	0.0	0.0	0.0
FW_1yr_TenneT	0.17	0.75	1.03	1.14	1.26	1.36	1.26	0.79	0.47	0.0	0.0	0.0
FW_5yr_TenneT	0.23	0.83	1.13	1.25	1.38	1.49	1.38	0.9	0.56	0.0	0.0	0.0
FW_20yr_TenneT	0.24	0.87	1.17	1.29	1.42	1.53	1.43	0.94	0.6	0.0	0.0	0.0
FW_20yr_Vakl	0.34	1.21	1.64	1.72	1.69	1.68	1.6	1.42	0.94	0.0	0.0	0.0

3.3 Aandachtspunten voor het ontwerp van de aanlandingsconstructie

Op basis van de resultaten in hoofdstuk 3.4 hierboven, willen we een aantal belangrijke punten aan de orde brengen, welke tijdens het ontwerpen van de aanlandingsconstructie in beschouwing dienen te worden genomen:

- **Seizoensgebonden strandprofiel veranderingen**: het strand bij Wijk aan Zee zal naar verwachting een strandprofiel laten zien dat afhankelijk is van het seizoen.
- **Impact van de constructie op het duinsysteem**: de tijdelijke aanlandingsconstructie kan morfologische veranderingen in het duinsysteem veroorzaken.
- **Grootschalige morfodynamische impact**: het ontbreken van een morfodynamische simulatie zorgt voor een extra onzekerheid over de impact van de tijdelijke aanlandingsconstructie op de grootschaligere stranddynamiek. Aangezien de constructie het langstransport van sediment tijdens hogere getijden en stormen bijna een jaar zal blokkeren, kan dit ook de bodemniveaus en de kustlijnpositie van de aangrenzende stranden in de orde van honderden meters langs de kust beïnvloeden.
- **Variabiliteit in bodemniveaus door de jaren heen**: het bodemniveau op de locatie van de tijdelijke aanlandingsconstructie bleek de laatste jaren vrij variabel te zijn, er wordt aangeraden een nieuwe gebiedsdekkende meetcampagne uit te voeren om zodoende het niveau van het bodem goed in kaart te brengen. Zo kunnen betere schattingen gemaakt worden over de belastingen op de damwand aan de zeezijde.
- **Verticale hoogte van de plaatsing van de Geotubes**: het bodemniveau waarop de Geotubes worden geïnstalleerd is een belangrijke ontwerpoverweging. Voordat wordt besloten of een enkele Geotube of een combinatie van twee gestapelde Geotubes zal worden gebruikt, kan de mogelijkheid worden overwogen om de bodemniveaus aan te passen (verlagen of verhogen).
- **Afwezigheid van lange (golf-groep gebonden) golven ('infra-gravity waves') binnen model simulaties**: met name tijdens stormen kunnen zeer lange golven het waterlevel nog enkele tientallen cm's verhogen. Op dit moment zijn deze lange golven niet in de analyse is opgenomen, waardoor het waterniveau onderschat kan zijn.
- **Toegankelijkheid van de hellingbaan**: tijdens modelsimulaties bereikte het waterpeil de punten TS1 en TS9 (zie Figuur 3.2 en Figuur 3.3), welke het einde van de Geotubes markeren. Dit geeft aan dat de hellingbaan onbeschermd is tegen stijgende waterstanden en dus onderhevig kan zijn aan erosie, wat kan leiden tot een lastige toegankelijkheid van de tijdelijke aanlandingsconstructie.

4 Golfbelastingen

De geëvalueerde belastingen voor alle mogelijke inputvariabelen worden gekwantificeerd voor drie terugkeerperioden (RP01yr, RP05yr en RP20yr). De relevante golfperiodes zijn 12-16 s, de relevante hellingen zijn 1:25 tot 1:45, en de relevante waterdiepten zijn 1,5-3,0 m. Een reeks van inkomende, individuele golven ($H_{n\%}$) tot een overschrijdingswaarde van 0,1% is opgenomen in de evaluatie van de golfbelasting.

4.1 Golfbelasting op de Geotube

De stabiliteit van de Geotube (zie Figuur 4.1) moet worden beoordeeld op golfbelastingen. De huidige evaluatie is beperkt tot (i) horizontale golfbelastingen aan de zeewaartse kant van de Geotube en (ii) verticale golfbelastingen aan de onderkant van de Geotube. De verticale (en herstel)belastingen als gevolg van overslaand water worden verwaarloosd.

De huidige berekeningen zijn beperkt tot golven die haaks op de Geotube binnenkomen. Dit betekent ook dat dezelfde belastingen moeten worden toegepast langs de geotubes loodrecht op de kustlijn.

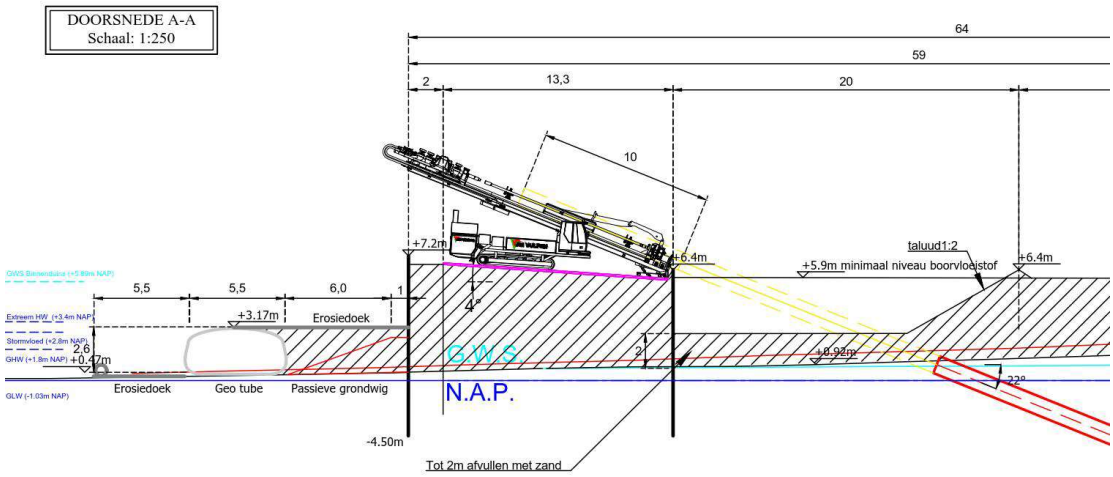

Figuur 4.1 Dwarsdoorsnede van de Geotube zeewaarts van de damwand van de tijdelijke aanlandingsconstructie.

4.1.1 Horizontale belasting aan de zeewaartse zijde van de Geotube

Voor de horizontale belasting aan de zeewaartse zijde wordt de Geotube beschouwd als een volledig reflecterende muur, zodanig dat de kamhoogte van de zeebodem nog steeds waterpeil plus $H_{n\%}$ wordt. De totale kracht is geïntegreerd over de hoogte van de Geotube. Dit wordt afgebeeld door de blauwe polygonen in Figuur 4.2.

De golfperiodes zijn lang (in het bereik van 12-16 s) en de waterdiepte is relatief klein (minder dan 3,0 m), zodat de individuele, extreme golven kunnen worden behandeld als in het ondiepe water regime, waardoor de drukverdeling hydrostatisch is.

De belastingen zijn onafhankelijk van de periode van de inkomende golf. De maximale belasting op land is sterk afhankelijk van de werkelijke waterdiepte voor de constructie, wat betekent dat de werkelijke bathymetrie op het punt van installatie belangrijk is.

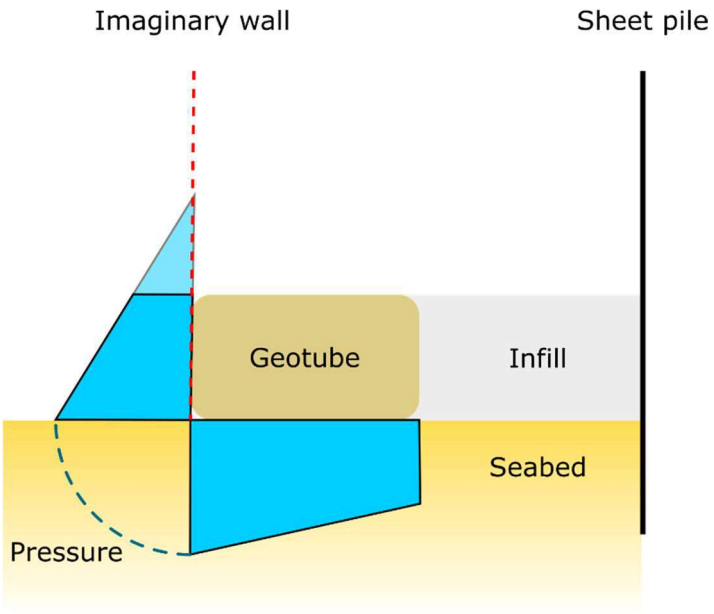

Figuur 4.2 Schets van het opvul- en Geotube systeem aan de zeewaartse zijde van de damwand. De blauwe polygonen tonen de drukverdeling aan de zeewaartse zijde van de Geotube en langs de bodem.

4.1.2 Verticale belastingen op de onderkant van de Geotube

De druk op de bodem van de Geotube volgt uit de hydrostatische druk aan weerszijden van de Geotube, met een lineaire relatie tussen deze twee uiteinden (Figuur 4.2). Opgemerkt wordt dat elke overdruk aan de oeverzijde wordt verwaarloosd, wat conservatief is onder de veronderstelling dat het gewicht van de Geotube geen rekening houdt met een laag water bovenop de Geotube zelf.

4.1.3 Overdruk in het poriewater op het land

Er kan een overdruk optreden in het poriewater in het opvulmateriaal, omdat er water bovenop het geotextiel aanwezig is. De overdruk is een combinatie van het stilstaande waterniveau dat groter is dan de hoogte van de Geotube en het feit dat er overslaand water is.

Er wordt benadrukt dat de overdruk representatief is voor de overdruk tijdens individuele overslaande golven. Deze individuele overslaande golven bewerkstelligen een dynamische gebied op de top van Geotube en het opvulmateriaal, dus het is belangrijk om te beseffen dat de overdruk niet moet worden toegepast als een gemiddelde, statische overdruk.

4.1.4 Golfbelastingen door ‘slamming’

De golfbelasting als gevolg van het breken van golven voor de Geotube is een stochastisch proces dat sterk afhankelijk is van de interactie tussen individuele golven en de diepte van de trog in de voorkant van de brekende golf.

4.2 Golfbelasting op de damwand

De golfbelasting op de damwand treedt op, wanneer de bovenkant van de inkomende golf aan de bovenkant van de Geotube wordt ‘afgesneden' en als kleinere golf over de Geotube en het opvulmateriaal erachter reist. In Chen et al. (2015) is dit gedrag in meer detail bestudeerd.

In Figuur 4.3 zijn de belastingen voor de grootste waterdiepte van 2,87 m voor de Geotube afgebeeld. De initiële waterdiepte op de bovenkant van de Geotube wordt genomen als $\eta_+ - h_G$. Men ziet dat hoe groter de golfperiode, hoe groter de golfbelasting. De resultaten zijn nog steeds een sterke functie van de waterdiepte voor de geotube, wat betekent dat de werkelijke

bathymetrie op het punt van installatie belangrijk is. Daarnaast wordt geadviseerd om een gedeeltelijke belastingscoëfficiënt toe te passen op de voorspelde belastingen.

De impact locatie van de resulterende krachten is niet vermeld in Chen et al. (2015). Deze is benaderd als $.d_0/2$.

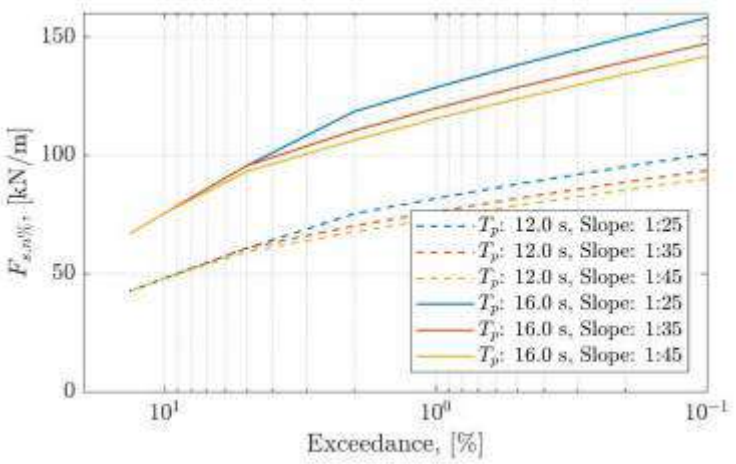

Figuur 4.3 De belasting op de damwand als gevolg van afgesneden golven die als kleinere golf op de damwand slaan.

4.3 Overzicht van belastingen

De voorspelde belastingen voor de twee bathymetrieën en de terugkeerperioden van één jaar (alleen TenneT), vijf jaar (alleen TenneT) en twintig jaar zijn te zien in Tabel 4.1. Opvallend is dat de belastingen als gevolg van de vijf en twintig jarige terugkeerperiode vrijwel identiek zijn voor de TenneT bathymetrie, terwijl er zijn grote verschillen tussen de belastingen voor de TenneT en Vaklodingen bathymetrieën voor een terugkeerperiode van twintig jaar zijn. Deze zijn volledig toegeschreven aan het verschil in waterdiepte. De spreiding in belastingen voor elk van de terugkeerperioden en bathymetrieën zijn toe te schrijven aan spreidingen in de strandhelling (1:25 tot 1:45), de golfperiode (12.0 s tot 16.0 s) en de waterdiepte langs de Geotube (d.w.z. variatie in de lokale bathymetrie).

De locatie van de belastingen is geschematiseerd in Figuur 4.4, waar $F_{+,n\%}$, $F_{-,n\%}$ en $F_{h,n\%}$ allemaal werken aan de buitenkant van de Geotube. Alle belastingen zijn positief langs de getrokken pijlen.

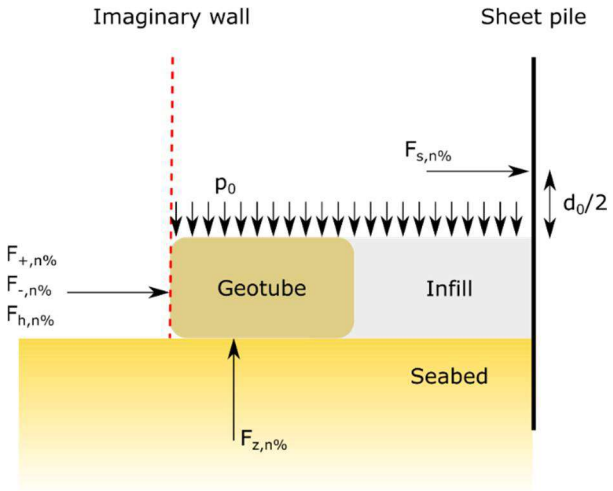

Figuur 4.4 Schets van de plaats van de belastingen zoals gekwantificeerd in Tabel 4.1 (niet op schaal).

Tabel 4.1 Overzicht van de golfbelastingen voor verschillende terugkeerperioden en overschrijdingspercentages. De spreidingen zijn voor strandhellingen van 1:25 tot en met 1:45 en golfperiodes van 12 tot 16 seconden.

		RP01yr	RP05yr	RP20yr	
Bathymetrie		Tennet	Tennet	Tennet	Vakl.
Waterdiepte [m]		1.73-2.10	1.81-2.18	1.86-2.22	2.60-2.87
$H_{n\%}$, [m]	2%	1.1 – 1.4	1.2 – 1.5	1.2 – 1.5	1.8 – 2.0
	1%	1.2 – 1.5	1.2 – 1.6	1.3 – 1.6	1.9 – 2.1
	0.1%	1.3 – 1.7	1.4 – 1.8	1.4 – 1.8	2.1 – 2.3
$F_{+,n\%}$, [kN/m]	2%	41 - 60	45 - 64	47 - 66	90 - 97
	1%	42 - 62	46 - 66	48 - 68	92 - 100
	0.1%	46 - 67	50 - 71	52 - 73	99 - 106
$F_{-,n\%}$, [kN/m]	2%	1 - 3	2 - 3	2 - 3	4 - 5
	1%	1 - 2	1 - 2	1 - 3	3 - 4
	0.1%	1 - 1	1 - 1	1 - 1	1 - 2
$F_{h,n\%}$, [kN/m]	2%	18 - 31	20 - 33	21 - 34	49 - 58
	1%	20 - 33	22 - 36	23 - 38	53 - 63
	0.1%	25 - 42	28 - 45	29 - 47	67 - 79
$F_{z,n\%}$, [kN/m]	2%	155 - 174	159 - 178	161 - 180	204 - 211
	1%	156 - 176	160 - 180	162 - 182	207 - 214
	0.1%	160 - 181	164 - 185	167 - 187	213 - 221
p_0, [kPa]	2%	1.0 - 8.0	2.4 - 9.4	3.1 - 10.1	18.9 - 21.4
	1%	1.5 - 8.7	2.9 - 10.1	3.7 - 10.8	19.8 - 22.4
	0.1%	2.9 - 10.5	4.4 - 12.0	5.2 - 12.7	22.1 - 24.9
$F_{s,n\%}$, [kN/m]	2%	0 - 13	1 - 19	1 - 22	59 - 120
	1%	0 - 16	1 - 22	1 - 26	64 - 131
	0.1%	1 - 23	2 - 31	3 - 36	80 - 162
$d_0/2$, [m]	2%	0.1 - 0.4	0.1 - 0.5	0.2 - 0.5	0.9 - 1.1
	1%	0.1 - 0.4	0.1 - 0.5	0.2 - 0.5	1.0 - 1.1
	0.1%	0.1 - 0.5	0.2 - 0.6	0.3 - 0.6	1.1 - 1.2

4.4 Aandachtspunten voor het ontwerp van de aanlandingsconstructie

Er bestaat een risico dat de gecombineerde afbuiging en convergentie van de stroming langs de kust rond de constructie een zeewaarts gerichte kracht op de hoek van het Geotube systeem zal geven. Daarom wordt het belangrijk geacht om enige verbinding te garanderen tussen de Geotubes zeewaarts van de constructie en de Geotubes aan de zijkant hiervan; het dubbelgevouwen geotextiel op de hoek, dat op 25 november in een online vergadering werd gepresenteerd, zou voldoende kunnen zijn.

De stabiliteit van de Geotube vereist een geotechnisch model, waarbij de gecombineerde bodem- en hydrostatische belasting van het opvulmateriaal wordt verwerkt. Hier is het belangrijk op te merken dat de voorspelde verticale kracht samenvalt met de maximale horizontale kracht ($F_{+,n\%}$).

De huidige berekeningen gaan ervan uit dat de Geotube op zijn plaats blijft tijdens de levensduur van de constructie. Echter, als gevolg van het risico van ontgronding en de golf belastingen, kan de Geotube mogelijk zeewaarts glijden. Het is ook mogelijk dat een verplaatsing van de Geotube de golfhoogte (zowel toename als afname) voor de damwand kan veranderen, deze kan bijvoorbeeld fungeren als een golfbreker (afnemende golven) of als trechter door een combinatie van breking en diffractie rondom de verplaatste geotube (toenemende golven).

Tot slot, mocht de ontwerper kiezen voor een ontwerp met twee Geotubes op elkaar, vereist dit extra aandacht met betrekking tot de golfbelasting. Deze extra aandacht heeft vooral betrekking op de verticale en horizontale belastingen voor elk van de Geotubes. Met name de verticale belasting op de interface tussen de Geotubes is belangrijk, deze kan leiden tot destabilisatie van de bovenste Geotube.

5 Lokale beoordeling van de ontgronding

Golven en stromingen rond de aanlandingsconstructie zullen resulteren in lokale erosie van zand, wat resulteert in ontgrondingskuilen. De ontgrondingskuilen worden voor de buitenste damwand voorkomen door middel van een geotextiel en een Geotube. Echter, ontgrondingskuilen aan de voorkant van de Geotube kunnen wel ontwikkelen. Als deze kuilen aanzienlijk zijn, kan dit leiden tot ondermijning van de Geotube waardoor deze in de ontgrondingskuil kan glijden. Dit kan vervolgens weer leiden tot een onbeschermde damwand. Om de noodzaak en de vereiste afmetingen van het geotextiel te beoordelen, is deze studie gericht op het schatten van het potentieel voor de ontgrondingskuil rond de Geotube (alsof er geen geotextiel was).

Gezien de hydrodynamische condities langs de kust verwachten we dat de ontgronding rond de Geotube zich op de volgende locaties en condities kan ontwikkelen:

- Ontgronding als gevolg van gereflecteerde golven; dit type ontgronding zal voornamelijk plaatsvinden aan de zeezijde van de damwand/Geotube.
- Ontgronding als gevolg van stroming langs de kust; dit type ontgronding zal het grootst zijn rond de hoeken van de damwandconstructie/Geotube.
- Afgezien van de ontgronding, kan een verlaging van het bodemniveau bij de damwandconstructie ook het gevolg zijn van grootschalige veranderingen in het strandprofiel die zich voordoen loodrecht op of langs de kust.

De eerste twee punten worden afzonderlijk besproken in respectievelijk sectie 5.2 en sectie 5.3. De laatste vorm van profielverlaging wordt in het vervolg niet meer op terug gekomen.

5.1 Ontgronding als gevolg van gereflecteerde golven

Om de ontgronding als gevolg van golven en de mogelijke bandbreedte daarin te beoordelen, houden we rekening met in totaal vijf verschillende gevallen.

1. Maximale/piek storm condities
2. Gemiddelde storm condities
3. Minimale storm condities
4. Maximale golfhoogten, minimale golfperiode en maximale stormvloed
5. Maximale golfhoogten, minimale golfperiode en gemiddelde stormvloed

In het algemeen zijn de condities voor éénjarige, vijfjarige en twintigjarige terugkeerperioden stormen redelijk vergelijkbaar. De belangrijkste verschillen in, bijvoorbeeld, de waterdiepte voor de aanlandingsconstructie zijn te wijten aan de geselecteerde bathymetrie. Op basis hiervan is een redelijke schatting voor de verwachte golf-gerelateerde ontgrondingsdiepte tijdens een twintigjarige terugkeerperiode storm om en nabij de 1-2 m, hoewel het niet kan worden uitgesloten dat de golf-gerelateerde ontgrondingsdiepte ook tussen de 0,5 - 3 m zou kunnen liggen.

5.2 Ontgronding als gevolg van langsstroming

Net als hierboven uiteengezet, worden voor de ontgronding door langsstroming ook een aantal verschillende gevallen in overweging genomen. Het gaat hier om storm condities en operationele (dagelijkse) condities.

1. (storm) Hoge golf-geïnduceerde langsstroming, hoge stormvloed
2. (storm) Hoge golf-geïnduceerde langsstroming, gemiddelde stormvloed
3. (storm) Matige golf-geïnduceerde langsstroming, lage stormvloed

4. (getij) Piek getijde snelheid, grote lokale waterdiepte
5. (getij) Piek getijde snelheid, kleine lokale waterdiepte

Op basis van het hierboven gepresenteerde lijstje wordt gesteld dat wanneer er geen storm optreedt voor de levensduur van de aanlandingsconstructie, dat wil zeggen dat de constructie alleen is onderworpen aan stroming door getijden, de verwachtte ontgrondingsdiepte ongeveer 0,5-1 m is. Voor een enkele storm, zoals gesimuleerd in de numerieke modellering van Hoofstuk 3, is het niet onwaarschijnlijk dat een ontgrondingskuil van 3-6 m kan ontwikkelen. Dit hangt uiteindelijk af van de werkelijke lokale bathymetrie na de installatie van de Geotube.

5.3 Synthese

Op basis het bovenstaande verwachten we dat de ontgronding zich aan de buitenzijde van de Geotube zal ontwikkelen. Aan de zeekant (blauw gebied in Figuur 5.1) zal de ontgronding voornamelijk het resultaat zijn van gereflecteerde golven en daarom zal deze zich ontwikkelen tijdens stormen. In dit gebied verwachten we een ontgrondingskuil in de orde van 1-2 m, die zich kan ontwikkelen tijdens één enkele storm. Op de hoeken (rode gebieden in Figuur 5.1) zal de ontgronding het resultaat zijn van langsstroming. Door normale getijdebeweging zal deze ontgrondingskuil ruwweg in de orde van 0.5-1 m zijn. Echter, in combinatie met storm-geïnduceerde langsstroming kunnen ontgrondingsdiepten van 3-6 m bereikt worden. Hoewel de Geotube iets kan vervormen naarmate de ontgronding voor de Geotube toeneemt, vindt de ontwikkeling van de gepresenteerde 3-6 m ontgronding plaats binnen ongeveer 12 uur. In dit geval is de verwachtte vervorming van de Geotube zo groot dat de functie van de bescherming van de passieve grondwig voor de damwand volledig in het gedrang komt. Hierdoor wordt de grondwig voor de damwand snel weggespoeld, wat een onaanvaardbaar risico vormt voor de stabiliteit van de damwand. Maatregelen zijn nodig om ondermijning van de Geotube te voorkomen.

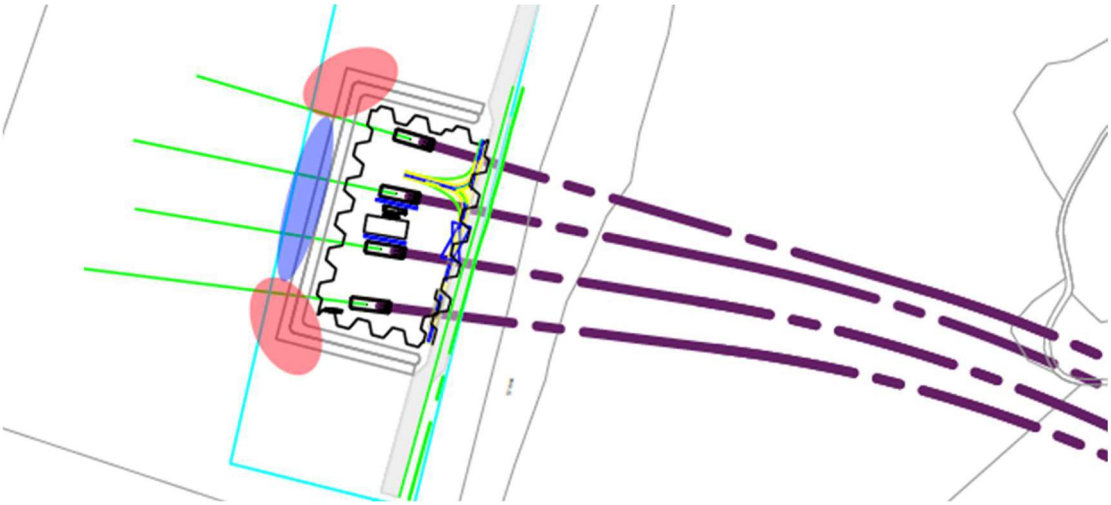

Figuur 5.1 Lokale ontgronding rond de Geotube en damwandconstructie

5.4 Aandachtspunten voor het ontwerp van de aanlandingsconstructie

Op basis van de beoordeling van de ontgrondingsontwikkeling rond de Geotube, raden we aan ondermijning van de Geotube te voorkomen door een ontgrondingsbescherming toe te passen aan de buitenzijde van de Geotube. Voor de omvang van deze bescherming is ten minste 10 m afstand van de Geotube aan te raden. Houd er rekening mee dat een dergelijke extra bescherming niet zal voorkomen dat ontgrondingskuilen zich ontwikkelen, maar het zal deze verder weg van de Geotube houden (en zo ondermijning van de Geotube voorkomen). Golf-

gerelateerde ontgronding zal naar verwachting ontwikkelen binnen 1 / 4 golf lengte uit de buurt van de Geotube. Daarom, natuurlijk afhankelijk van de werkelijke golflengtes, is het minder waarschijnlijk dat golf-gerelateerde ontgronding ontwikkelt binnen 10 m afstand van de Geotube. We kunnen wel verwachten dat sommige stromings-gerelateerde ontgronding zal ontwikkelen aan de rand van het geotextiel, maar dit zal waarschijnlijk aanzienlijk minder dan de verwachtte 3-6 m.

Dit deel van de ontgrondingsbescherming moet flexibel zijn, zodat het zich (in vorm) kan aanpassen aan de ontgrondingskuilen die zich aan de randen gaan ontwikkelen. Bovendien moet deze zanddicht en stabiel zijn binnen de ontwerp condities. Wanneer dit deel van de ontgrondingsberscherming uit een geotextiel bestaat, is er waarschijnlijk extra gewicht nodig (verankering van Geotubes) om het op zijn plaats te houden. Als alternatief kunnen de randen van het geotextiel in het zand worden begraven.

Zoals aangegeven in Figuur 5.1 wordt de grootste ontgrondingsdiepte verwacht rond de zeewaartse hoeken van aanlandingsconstructie, welke een gevolg is van langsstromingen. Een meer gestroomlijnde vorm van de aanlandingsconstructie zou de huidige snelheden rond de hoeken kunnen verminderen, wat op zijn beurt de ontgrondingsontwikkeling op deze locaties zou kunnen verminderen. In dit stadium kan dit effect niet worden gekwantificeerd. Het is echter niet te verwachten dat een gunstigere vorm de eis van een extra ontgrondingsbescherming voor de Geotube helemaal zal wegnemen. Installatieoverwegingen kunnen daarom bindend zijn voor de geselecteerde vorm van de aanlandingsconstructie.

De waargenomen spreiding in bathymetrie (zie hoofdstuk 3) is reeds opgenomen in de onderhavige beoordeling van de ontgronding. Als bijgevolg zijn de gepresenteerde verwachtte ontgrondingsdiepten geldig voor de volledige spreiding in de bodemniveaus. We willen echter opmerken dat bij het tegenkomen van een relatief lage bathymetrie mogelijk twee Geotubes op elkaar moeten worden geplaatst om de vereiste hoogte van de bodemmassa voor de damwand te verkrijgen. In dit geval raden we aan de Geotubes toe te passen in een overlappende of gespreide configuratie, om eventuele gaten zoveel mogelijk te voorkomen. Dit zelfde aandachtspunt geldt voor aangrenzende Geotubes.

Bovendien, wanneer een relatief lage bathymetrie wordt aangetroffen bij de installatie, kan het water de achterzijde (landwaartse kant) van de aanlandingsconstructie bereiken, wat ook aan deze kant kan leiden tot ontgrondingskuilen. Dit kan worden voorkomen door Geotubes te installeren tot een niveau boven het te verwachten maximale waterniveau.

6 Conclusies

Dit Nederlandstalige rapport betreft een vertaling van een samenvattende uitsnede van de uitgebreidere Engelstalige versie (opgenomen als bijlage) om zodoende de vergunningsverlening te vergemakkelijken.

Taak 1: Bepaling van de extreme metocean condities op zee

Op basis van een extreme waarde analyse van hindcast gegevens beschikbaar voor dit gebied zijn offshore extreme metocean condities met terugkeerperioden van één, vijf en twintig jaar (RP1jr, RP5jr & RP20jr) afgeleid.

Taak 2: Bepaling van de metocean condities langs de kust

Een vertaling van de offshore metocean condities naar de aanlandingsconstructie wordt gemaakt door middel van een numeriek model. In deze vertaling hebben we verschillende hydrodynamische condities onderscheiden (enkel getij, RP1jr, RP5jr en RP20jr conditie). De beschikbare bathymetrische gegevens toonden aanzienlijke verschillen van het strandprofiel in de afgelopen jaren. Aangezien a-priori niet bekend is welke bathymetrie tijdens de installatie zal worden aangetroffen, zijn twee verschillende bathymetrieën in deze beoordeling opgenomen. Houd er rekening mee dat wanneer een relatief lage bathymetrie wordt aangetroffen, mogelijk twee Geotubes op elkaar moeten worden geplaatst om de vereiste hoogte van de passieve grondwig voor de damwand te stabiel te krijgen. We willen ook opmerken dat de actuele bathymetrie ten tijde van constructie ook zal bepalen of het waterpeil naar verwachting de landzijde van de constructie zal bereiken tijdens stormcondities. Lokale erosie-effecten aan deze kant van de constructie kunnen daarom in het huidige stadium niet worden uitgesloten.

Taak 3: Beoordeling van de golfbelastingen op de Geotubes en damwand

Op basis van de uitkomst van Taak 2, gecombineerd met empirische en analytische kennis en expertise, worden golfbelastingen die op de Geotube en damwand werken afgeleid voor drie terugkeerperioden (RP1jr, RP5jr en RP20jr), twee bathymetrieën en drie overschrijdingskansen (2%, 1% en 0,1%), zie Tabel 4.1. In alle gevallen zijn we uitgegaan van een situatie waarin de hoogte van één Geotube voldoende is om de vereiste hoogte van de passieve grondwig voor de damwand te stabiel te krijgen.

Taak 4: Beoordeling van de ontgrondingsontwikkeling rond de aanlandingsconstructie

Op basis van de uitkomst van Taak 2, gecombineerd met empirische en analytische kennis en expertise, verwachten we binnen een enkele storm een ontgrondingsontwikkeling in de orde van 1-2 m aan de voorkant en 3-6 m in de hoeken van de zeezijde van de constructie (voor de Geotube). Op basis van deze verwachte ontgrondingsontwikkeling (zowel de diepte als de snelle ontwikkeling) rond de Geotube, raden we aan ondermijning van de Geotube te voorkomen door een ontgrondingsbescherming toe te passen aan de buitenzijde van de Geotube. Houd er rekening mee dat we geen grootschalige veranderingen in dwarsprofiel (van het strand en duin) wijzigingen hebben opgenomen in deze beoordeling.

Bijlage: Engelstalig rapport

Deltares

Assesment of seaside loads on landfall support structure Wijk aan Zee

Assesment of seaside loads on landfall support structure Wijk aan Zee

Client	Van Vulpen
Contact	
Reference	
Keywords	Wave-loads, scour, near-shore, beach, landfall, Wijk aan Zee, HKN

Document control	
Version	1.0
Date	17-12-2020
Project nr.	11206427-000
Document ID	11206427-000-HYE-0001
Pages	87
Classification	
Status	Final

Author(s)		

Doc. version	**Author**	**Reviewer**	**Approver**	**Publish**
1.0				

Summary

The NRG-Group is in the process of preparing a design for the cable-landfall structure of Hollandse Kust Noord Offshore Wind Farm (OWF). To further detail this design of the temporary support structure, Deltares is asked to provide input on the wave loads acting on both the geotubes and the sheet pile wall. Moreover, information of the expected scour development around the structure is required.

To determine the wave loads and scour development around the landfall structure, an extreme value analysis, a numerical model and an analytical model have been used to derive the relevant hydrodynamic conditions close to the structure. It was observed that different sources and different years show a relatively large spread in the bathymetry at the landfall structure (with vertical differences in the bed level up to 0.9 m). Based on this observation we recommend assessing possibly required design adaptations that fit the bathymetry encountered upon installation. Possible effects of the bathymetry that are identified so far include: a two layered-geotube solution might be necessary to obtain the required height, since the implementation of a single geotube layer leads to limitations of geotube system margins; water will be reaching the landward side of the structure and it has a considerable effect on the waves loads on the geotubes and sheet pile wall.

Wave loads acting on the geotubes and sheet pile wall are derived for three return periods (RP1yr, RP5yr and RP20yr), two bathymetries and three exceedance values (2%, 1% and 0.1%).

We expect a scour development within a single RP20yr storm event in the order of 1-2 m at the seaward side of the structure (in front of the geotubes) and 3-6 m at the seaward corners. Based on this expected scour development (both the depth and rapid development) around the geotubes, we strongly recommend preventing undermining of the geotubes by applying a scour protection at the outer side of the geotubes.

Contents

1 Introduction

1.1 Background

The NRG-Group is in the process of preparing a design for the cable-landfall structure of Hollandse Kust Noord Offshore Wind Farm (OWF). At the start of this study the design of this temporary structure consisted of a sheet pile wall placed in a rectangular shape within the intertidal area, see Figure 1.1. For the stability of this sheet pile wall a soil mass will be applied on the seaside. The minimum required level of the infilled soil mass is increased up to a level of approx. 3.17 m NAP to align the level with the elevation of the geotubes. In turn erosion of this soil mass is prevented by surrounding geotubes, as well as an overlaying geotextile ("erosiedoek"), see Figure 1.2.

To further detail this design of the temporary support structure, Deltares is asked to provide input on the wave loads acting on both the geotubes and the sheet pile wall. Moreover, information of the expected scour development around the structure is required. To assess these wave loads and the scour development Deltares has combined numerical studies on the hydrodynamic conditions with empirical and analytical analyses on the wave loads and erosion patterns. The present document describes the outcome of this assessment.

Figure 1.1 Top view of the landfall support structure (extracted from 2200611032NDT_G-A1.pdf)

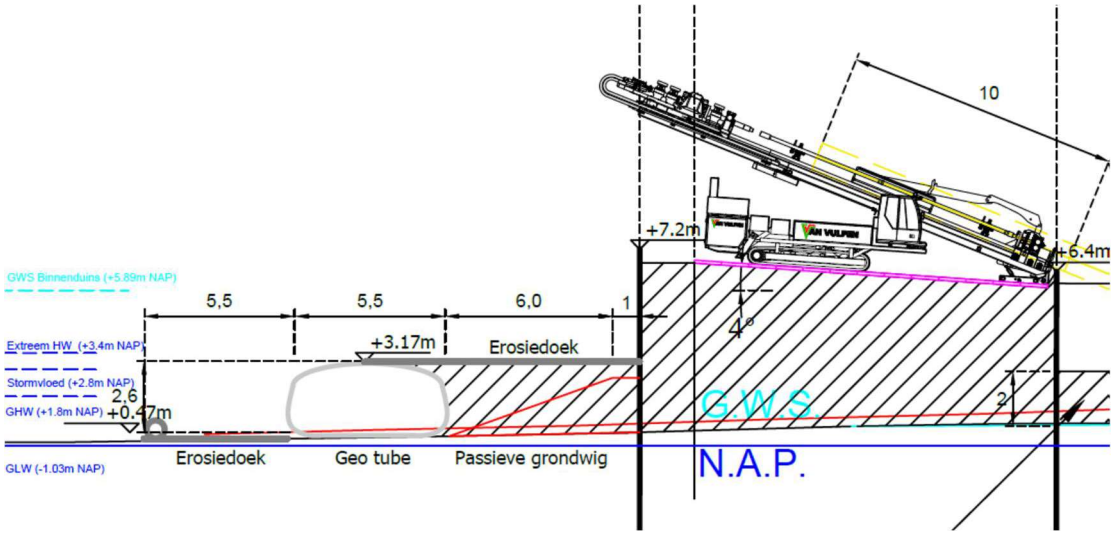

Figure 1.2 Side view of the landfall support structure (extracted from 2200611032NDT_G-A1.pdf)

1.2 Objectives

The objectives of the study are twofold:

- Assess the wave loads on the geotubes and the sheet pile wall
- Assess the scour development around the structure.

All information provided in this report is based on the design provided by NRG at the start of this project, see Figure 1.1 and Figure 1.2. Based on preliminary results discussed during the project, possible adaptations to the design are considered by NRG. Apart from the above-mentioned objectives, we therefore also include attention points regarding an (updated) design of the temporary landfall structure in this report.

1.3 Methodology and Reader guide

To meet the objectives of this study, the following stepwise approach is followed:

Task 1: Determination of the offshore extreme metocean conditions

To assess the local wave loads and scour development, information on the local hydrodynamic conditions around the structure is required. To obtain the required information, we first derived the offshore extreme conditions (for this study we focus on the RP1yr, RP5yr and RP20yr condition). This derivation is based on an Extreme Value analysis of hindcast data available for this area. This part of the study is described in Chapter 2.

Task 2: Determination of the nearshore metocean conditions

Based on the offshore extreme conditions, we have determined the hydrodynamic conditions at the temporary landfall structure. This translation is done by means of a numerical model (DELFT3D-FLOW/FM and SWAN). This part of the study is described in Chapter 3.

Task 3: Assessment of the wave loads on the geotubes and sheet pile wall

The information obtained from the numerical model is combined with empirical and analytical knowledge and expertise to assess the wave loads on the sheet pile wall and the geotubes. This part of the study is described in Chapter 4.

Task 4: Assessment of the scour development around the structure

The information obtained from the numerical model is combined with empirical and analytical knowledge and expertise to assess scour development around the landfall structure. This part of the study is described in Chapter 5.

Task 5: Address attention points for the design of the temporary landfall structure

During intermediate meetings attention points regarding the design of the landfall structure were discussed. These attention points are included separately for Tasks 2-4 within the corresponding chapters.

Conclusions and recommendations are provided in the final chapter of this report, Chapter 6.

2 Offshore extreme metocean conditions

2.1 Introduction

To assess the local wave loads and scour development, information on the local hydrodynamic conditions around the structure is required. To obtain the required information first the offshore extreme conditions were derived based on extreme value analyses (EVA) of hindcast data available from the Deltares in-house North Sea metocean database.

2.2 North Sea database

For the determination of the offshore extreme metocean conditions (water levels, storm surge, waves and winds), data was collected from the Deltares in-house North Sea metocean database. This database contains high resolution (varying spatial resolution from 3x3 km to 0.5x0.5 km) metocean data for a 39-year period (1980-2018) and has been extensively validated and calibrated against long-term observations of multiple measurement platforms throughout the North Sea.

The basis data for the set-up of the North Sea metocean database were the ERA5[1] data in combination with local detailed hydrodynamic and wave modelling, see Figure 2.1.

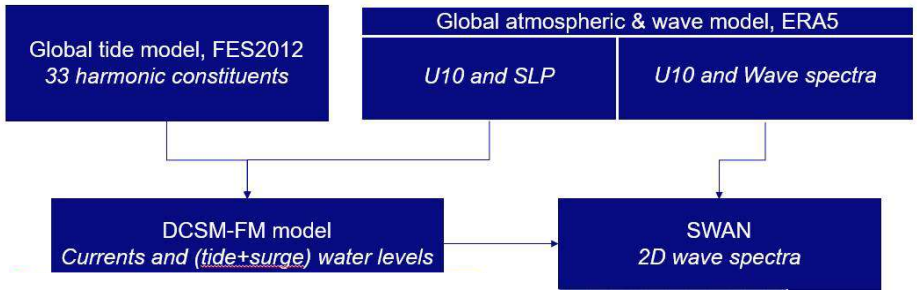

Figure 2.1 Overview of hydrodynamic and wave modelling approach.

The strength of the ERA5 reanalysis dataset is that it has been derived from the combination of one of the leading numerical weather prediction models (the model of the European Centre for Medium-range Weather Forecasts, ECMWF) with an advanced data assimilation system. The ERA5 dataset currently covers the period from 1979 until now on a global grid of 0.25° x 0.25° (~30 km) at an hourly interval and has unprecedented accuracy in terms of global atmospheric and wave data.

Some examples of the validation of the database with data from measurement platform K13a (wind and water levels: 01-1980 – 12-2018, waves: 06-2006 – 12-2017) are given in Figure 2.2 to Figure 2.6 for respectively wind speeds, wind directions, significant wave heights, peak wave periods and mean wave directions, and water levels.

In conclusion of the data validation, the data from the database are considered to be very reliable, with very high correlations with the observations and are considered to form a solid basis for the derivation of metocean conditions in the North Sea. For determination of reliable normal and extreme conditions, the ERA5 1-hour averaged 10 m wind speeds need to be calibrated using a fixed 1.08 (8%) factor, while there is no need to calibrate the ERA5 wind directions. The wave data need to be calibrated using a fixed 1.11 (11%) factor to the significant

[1] https://www.ecmwf.int/en/newsletter/159/meteorology/global-reanalysis-goodbye-era-interim-hello-era5

wave height (H_s) data and by applying a fixed 1.055 (5.5%) factor to the wave period (e.g. peak wave period, T_p) data; there is no need to calibrate the wave directions. Last, no correction is deemed necessary for the water levels.

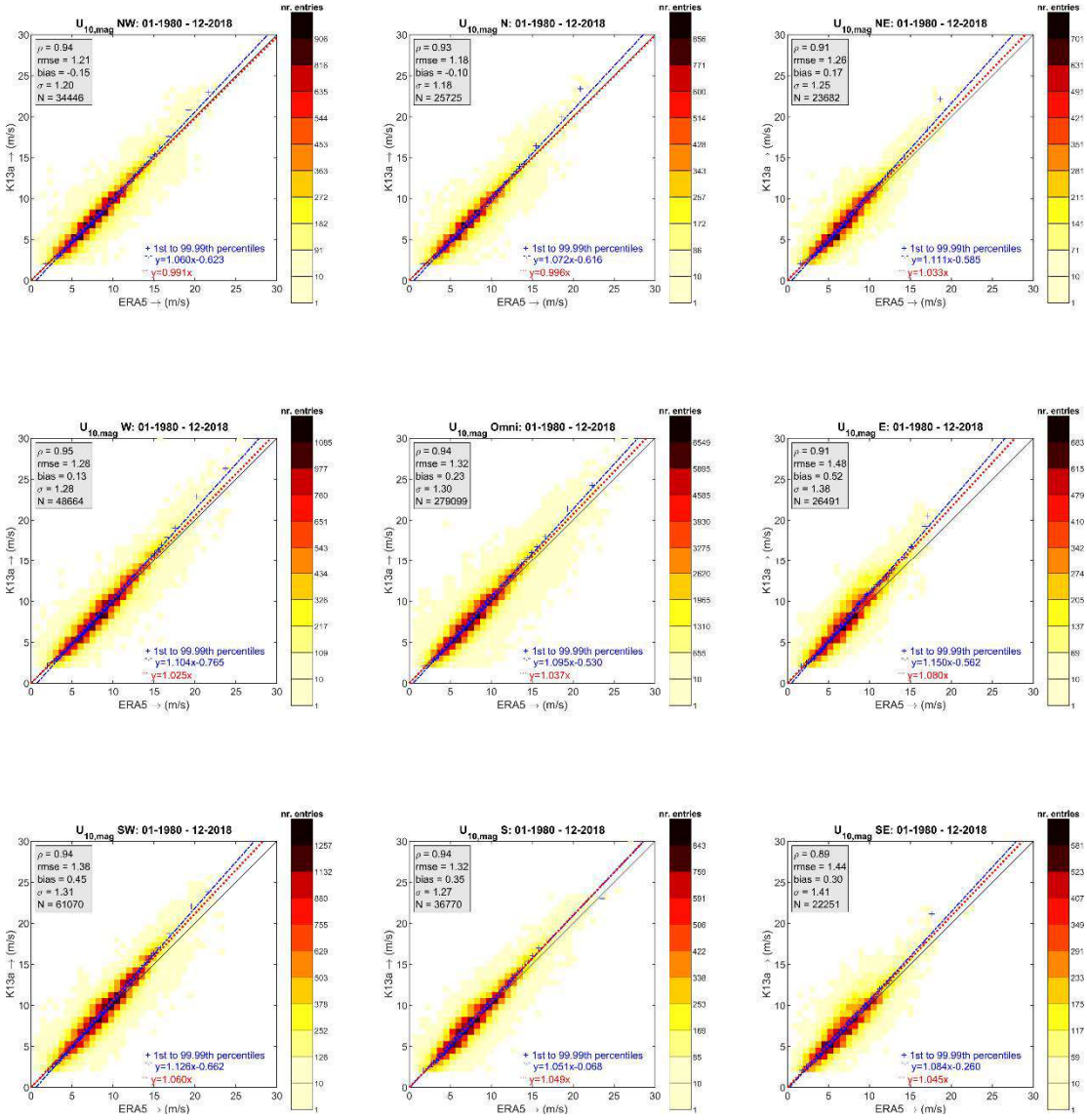

Figure 2.2 Wind speed density scatter comparisons between the K13a observations and the ERA5 data. The panel in the middle shows the omni-directional comparisons and the panels surrounding it show the comparisons for the corresponding directional sectors (from top left, clockwise: NW, N, NE, E, SE, S, SW and W). The symmetric fit to the data is given by the red dotted line and the linear fits through the data percentiles (blue pluses) is given by the dashed blue line. The statistics of the comparisons are printed in the panels.

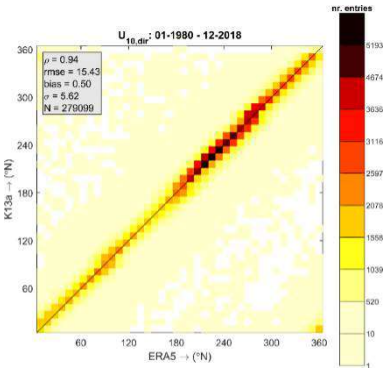

Figure 2.3 Wind direction density scatter comparisons between the K13a observations and the ERA5 data. The statistics of the comparisons are printed in the top left box.

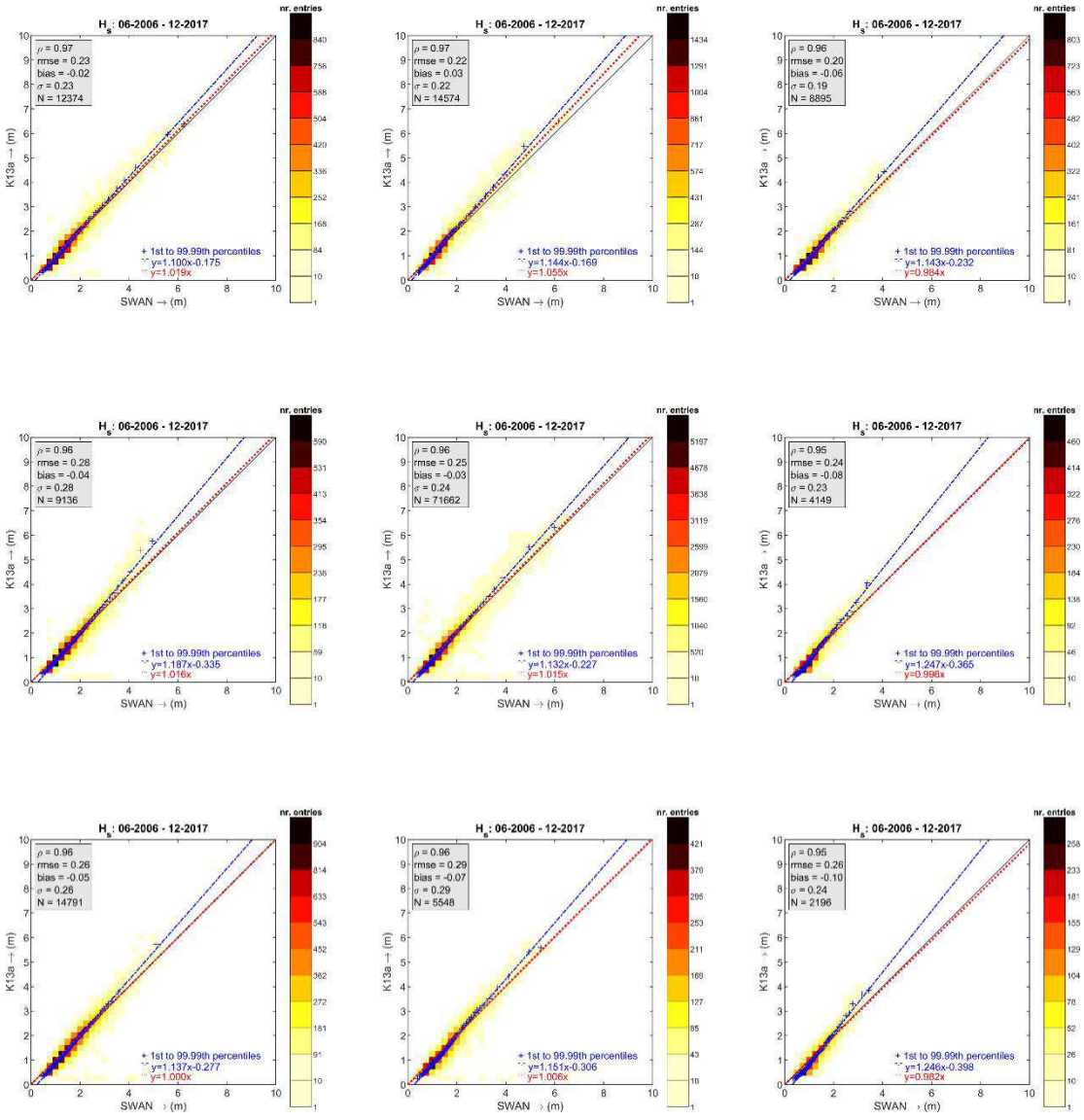

Figure 2.4 Significant wave height density scatter comparisons between the (3-hr averaged) K13a buoy observations and the (raw) SWAN results at K13a. The panel in the middle shows the omni-directional comparisons and the panels surrounding it show the comparisons for the corresponding directional sectors (from top left, clockwise: NW, N, NE, E, SE, S, SW and W). The symmetric fit to the data is given by the red dotted line and the linear fit through the data percentiles (blue pluses) is given by the dashed blue line. The statistics of the comparisons are printed in the panels.

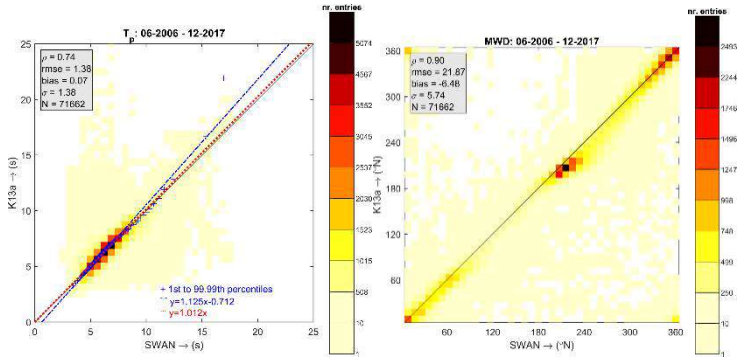

Figure 2.5 Peak wave period (left) and mean wave direction (right) density scatter comparisons between the (3-hr averaged) K13a buoy observations and the (raw) SWAN results at K13a.

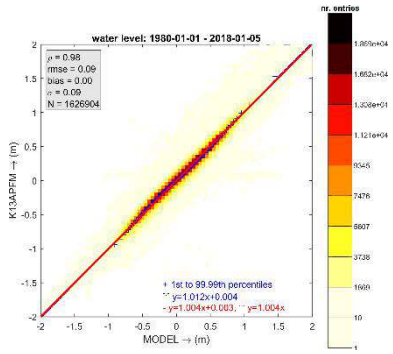

Figure 2.6 Water level density scatter comparisons at observation station K13a and the model data (10-minute interval). The symmetric fit to the data is given by the red dotted line and the linear fits through the data percentiles (blue pluses) is given by the dashed blue line. The statistics of the comparisons are printed in the panels.

2.3 The Wijk aan Zee dataset

Extreme wind, wave (H_s and associated T_p) and water level (total water level and surge) conditions were derived based on calibrated 39-year timeseries (1980-2018) at a total of 6 output locations along the outer edges of the foreseen numerical modelling domains (see Figure 2.7 and Table 2.1). Locations WS, WC and WN represented the boundary wave conditions for respectively the southern corner, central edge and northern corner of the wave model (red polygon in Figure 2.7). Locations FS, FC and FM represented the boundary water level conditions for respectively the southern corner, central edge and northern corner of the flow model (blue polygon in Figure 2.7).

Figure 2.7 Considered output locations for the derivation of extreme conditions. The project location is marked by the white dot.

Table 2.1 Coordinates of considered output locations.

Location	Longitude (°E)	Latitude (°N)
WS	4.363605	52.372179
WC	4.425550	52.493114
WN	4.473526	52.618254
FS	4.445410	52.416842
FN	4.475197	52.484835
FC	4.504632	52.551648

The wind speed timeseries were defined as the calibrated ERA5 timeseries from the closest ERA5 grid point which was not influenced by land effects (i.e. higher drag). The coordinates of the ERA5 grid point from which the wind speed data were considered to be representative for all considered output locations were 4.25ºE and 52.5ºN. For the wind directions, which were considered not to be significantly influenced by land effects, the data from the more nearshore grid point 4.50ºE and 52.5ºN were used.

For the determination of the representative water level and wave-related timeseries, data from the nearest database grid points (spatial resolution of 0.5x0.5 km) were used.

Please note that the surge timeseries were not directly obtained from the North Sea database but were derived by subtracting the tide-only water level timeseries (no wind or atmospheric forcing) from timeseries of a complete simulation (tide + wind and atmospheric forcing).

2.4 Methodology

2.4.1 Extreme value analyses

Extreme value analyses (EVA) of the 39-year long (1980-2018) timeseries of the water levels (total and surge), wave parameters and 1-hour averaged 10 m winds at the considered output locations were carried out using the peaks-over-threshold (POT) method, see Appendix A. The EVAs of the data included omni-directional analyses and directional analyses over four 30º sectors. The sectors considered are: 225ºN-255ºN (240), 255ºN-285ºN (270), 285ºN-315ºN (300) and 315ºN-345ºN (330). In the omni-directional analysis all data are considered. In the directional analysis only the data falling in the sector of interest are taken into account. The data are stratified into sectors before the EVA is carried out (for the water levels the concomitant wind directions were used), meaning that a given storm may be considered in more than one sector. The stratification into sectors before the analysis is necessary because we are interested in the return value for the above enumerated fixed sectors. If only storm peaks were to be stratified, the return values obtained for a given sector could have been underestimated. For more details on the applied methods for the EVAs, please refer to Appendix A.

2.4.2 Associated peak wave periods

For the extreme offshore significant wave heights also associated (conditional) values of the peak wave periods have been determined For this, the associated peak period T_p was computed by means of a power relation fit to the H_s and corresponding T_p values in the POT sample (i.e. the sample of H_s peak values to which the extreme value distribution, the GPD, was fitted and the associated values of the other variables). For a given H_s value the relation is used to compute the associated T_p value. Please refer to the figures in Appendix B.2 for the resulting fits per location and per sector.

2.5 Results locations WS, WC and WN

In Table 2.2, Table 2.3 and Table 2.4, the return value estimates for the significant wave heights (H_s, column 3) and 1-hour average wind speeds at 10 m (U_{10}, column 5) are presented for respectively locations WS, WC and WN. The fourth columns of the tables also present the peak wave periods (T_p) associated to the extreme significant wave heights (see Section 2.4). The return value plots for H_s (including associated 95% confidence intervals) can be found in the sub-sections of Appendix B.2. The return value plots for U_{10} (including associated 95% confidence intervals) can be found in Appendix B.1.

Table 2.2 Waves (H_s and associated T_p) and wind extremes for location WS.

Sector	RP	H_s (m)	T_p (s)	U_{10} (m/s)
Omni	1	5.2	10.5	21.5
	2	5.6	11.1	22.4
	5	6.1	11.7	23.5
	10	6.5	12.1	24.4
	20	6.8	12.6	25.2
	50	7.2	13.1	26.4
	100	7.5	13.4	27.2
240	1	4.4	9.4	20.3
	2	4.8	9.7	21.5
	5	5.3	10.2	23.0
	10	5.7	10.5	24.1
	20	6.0	10.8	25.1
	50	6.4	11.1	26.3
	100	6.8	11.4	27.2
270	1	4.5	9.2	19.8
	2	5.0	9.5	21.0
	5	5.5	10.0	22.4
	10	6.0	10.3	23.4
	20	6.4	10.6	24.3
	50	7.0	11.0	25.3
	100	7.4	11.2	26.1
300	1	4.7	9.9	18.7
	2	5.1	10.3	19.6
	5	5.6	10.8	20.8
	10	5.9	11.0	21.7
	20	6.2	11.2	22.6
	50	6.4	11.5	23.8
	100	6.6	11.6	24.6
330	1	4.6	10.8	17.3
	2	5.2	11.5	18.6
	5	5.9	12.2	20.2
	10	6.4	12.7	21.2
	20	6.7	13.1	22.2
	50	7.2	13.5	23.4
	100	7.5	13.8	24.3

Table 2.3 Waves (H_s and associated T_p) and wind extremes for location WC.

Sector	RP	H_s (m)	T_p (s)	U_{10} (m/s)
Omni	1	5.4	10.7	21.5
	2	5.8	11.3	22.4
	5	6.4	11.9	23.5
	10	6.8	12.3	24.4
	20	7.1	12.7	25.2
	50	7.6	13.2	26.4
	100	7.9	13.5	27.2
240	1	4.5	9.5	20.3
	2	4.9	9.9	21.5
	5	5.4	10.3	23.0
	10	5.8	10.6	24.1
	20	6.1	10.9	25.1
	50	6.5	11.2	26.3
	100	6.8	11.5	27.2
270	1	4.7	9.3	19.8
	2	5.1	9.7	21.0
	5	5.7	10.2	22.4
	10	6.1	10.5	23.4
	20	6.5	10.8	24.3
	50	7.0	11.1	25.3
	100	7.3	11.4	26.1
300	1	4.9	10.1	18.7
	2	5.4	10.5	19.6
	5	5.8	11.0	20.8
	10	6.1	11.3	21.7
	20	6.4	11.5	22.6
	50	6.7	11.7	23.8
	100	6.8	11.9	24.6
330	1	4.8	10.9	17.3
	2	5.4	11.6	18.6
	5	6.2	12.4	20.2
	10	6.6	12.9	21.2
	20	7.1	13.3	22.2
	50	7.5	13.8	23.4
	100	7.9	14.1	24.3

Table 2.4 Waves (H_s and associated T_p) and wind extremes for location WN.

Sector	RP	H_s (m)	T_p (s)	U_{10} (m/s)
Omni	1	5.5	10.8	21.5
	2	6.0	11.3	22.4
	5	6.5	11.9	23.5
	10	6.9	12.3	24.4
	20	7.3	12.7	25.2
	50	7.7	13.1	26.4
	100	8.0	13.4	27.2
240	1	4.7	9.5	20.3
	2	5.1	9.9	21.5
	5	5.6	10.4	23.0
	10	6.0	10.7	24.1
	20	6.4	10.9	25.1
	50	6.8	11.3	26.3
	100	7.1	11.5	27.2
270	1	4.8	9.3	19.8
	2	5.2	9.7	21.0
	5	5.8	10.2	22.4
	10	6.2	10.5	23.4
	20	6.6	10.8	24.3
	50	7.1	11.1	25.3
	100	7.5	11.4	26.1
300	1	5.0	10.0	18.7
	2	5.4	10.4	19.6
	5	5.9	10.8	20.8
	10	6.2	11.0	21.7
	20	6.5	11.3	22.6
	50	6.9	11.5	23.8
	100	7.1	11.7	24.6
330	1	5.0	11.0	17.3
	2	5.6	11.6	18.6
	5	6.3	12.4	20.2
	10	6.8	12.8	21.2
	20	7.2	13.2	22.2
	50	7.7	13.6	23.4
	100	8.0	13.9	24.3

2.6 Results locations FS, FC and FN

2.6.1 Tidal water levels

The tidal levels at locations FS, FC and FN are given in respectively Table 2.5, Table 2.6 and Table 2.7.

Table 2.5 Tidal levels for location FS.

Tidal levels	Reference level	
	m MSL	m LAT
Highest Astronomical Tide, HAT	1.32	2.27
Mean High High Water, MHHW	1.00	1.95
Mean Low High Water, MLHW	0.46	1.41
Mean Sea Level, MSL	0.00	0.95
Mean High Low Water, MHLW	-0.45	0.51
Mean Low Low Water, MLLW	-0.73	0.23
Lowest Astronomical Tide	-0.95	0.00

Table 2.6 Tidal levels for location FC.

Tidal levels	Reference level	
	m MSL	m LAT
Highest Astronomical Tide, HAT	1.29	2.24
Mean High High Water, MHHW	0.98	1.94
Mean Low High Water, MLHW	0.61	1.57
Mean Sea Level, MSL	0.00	0.96
Mean High Low Water, MHLW	-0.49	0.47
Mean Low Low Water, MLLW	-0.73	0.22
Lowest Astronomical Tide	-0.96	0.00

Table 2.7 Tidal levels for location FN.

Tidal levels	Reference level	
	m MSL	m LAT
Highest Astronomical Tide, HAT	1.24	2.20
Mean High High Water, MHHW	0.95	1.91
Mean Low High Water, MLHW	0.68	1.63
Mean Sea Level, MSL	0.00	0.96
Mean High Low Water, MHLW	-0.53	0.43
Mean Low Low Water, MLLW	-0.74	0.22
Lowest Astronomical Tide	-0.96	0.00

2.6.2 Extreme water levels, surge and winds

In Table 2.8, Table 2.9 and Table 2.10, the return value estimates for the total water levels (tide + surge, column 3), the surge levels (column 4) and the 1-hour average wind speeds at 10 m height (U_{10}, column 5) are presented for respectively locations FS, FC and FN. The return value plots for the total water levels and surge levels (including associated 95% confidence intervals) can be found in the sub-sections of respectively Appendix B.3 and B.4. The return value plots for U_{10} (including associated 95% confidence intervals) can be found in Appendix B.1.

Table 2.8 Total water level (WL), surge and wind extremes for location FS.

Sector	RP	Total WL (mMSL)	Surge (m)	U_{10} (m/s)
Omni	1	2.1	1.6	21.5
	2	2.2	1.8	22.4
	5	2.4	2.0	23.5
	10	2.6	2.1	24.4
	20	2.7	2.2	25.2
	50	2.9	2.4	26.4
	100	3.1	2.5	27.2
240	1	1.6	1.2	20.3
	2	1.7	1.3	21.5
	5	1.8	1.4	23.0
	10	1.8	1.5	24.1
	20	1.9	1.6	25.1
	50	2.0	1.6	26.3
	100	2.0	1.7	27.2
270	1	1.9	1.4	19.8
	2	2.1	1.6	21.0
	5	2.3	1.8	22.4
	10	2.4	1.9	23.4
	20	2.6	2.0	24.3
	50	2.8	2.2	25.3
	100	2.9	2.3	26.1
300	1	1.9	1.3	18.7
	2	2.1	1.5	19.6
	5	2.3	1.8	20.8
	10	2.5	1.9	21.7
	20	2.6	2.1	22.6
	50	2.8	2.3	23.8
	100	3.0	2.4	24.6
330	1	1.8	1.1	17.3
	2	2.0	1.3	18.6
	5	2.2	1.6	20.2
	10	2.4	1.7	21.2
	20	2.5	1.9	22.2
	50	2.8	2.1	23.4
	100	2.9	2.3	24.3

Table 2.9 Total water level (WL), surge and wind extremes for location FC.

Sector	RP	Total WL (mMSL)	Surge (m)	U_{10} (m/s)
Omni	1	2.1	1.6	21.5
	2	2.2	1.8	22.4
	5	2.4	2.0	23.5
	10	2.6	2.1	24.4
	20	2.7	2.2	25.2
	50	2.9	2.4	26.4
	100	3.0	2.4	27.2
240	1	1.6	1.2	20.3
	2	1.7	1.3	21.5
	5	1.8	1.5	23.0
	10	1.8	1.6	24.1
	20	1.9	1.7	25.1
	50	1.9	1.8	26.3
	100	2.0	1.9	27.2
270	1	1.9	1.4	19.8
	2	2.1	1.6	21.0
	5	2.3	1.8	22.4
	10	2.4	1.9	23.4
	20	2.6	2.0	24.3
	50	2.8	2.2	25.3
	100	2.9	2.3	26.1
300	1	1.9	1.3	18.7
	2	2.1	1.5	19.6
	5	2.3	1.8	20.8
	10	2.5	1.9	21.7
	20	2.6	2.1	22.6
	50	2.8	2.3	23.8
	100	3.0	2.4	24.6
330	1	1.8	1.1	17.3
	2	2.0	1.3	18.6
	5	2.2	1.5	20.2
	10	2.4	1.7	21.2
	20	2.5	1.9	22.2
	50	2.7	2.2	23.4
	100	2.9	2.4	24.3

Table 2.10 Total water level (WL), surge and wind extremes for location FN.

Sector	RP	Total WL (mMSL)	Surge (m)	U_{10} (m/s)
Omni	1	2.1	1.6	21.5
	2	2.2	1.8	22.4
	5	2.4	2.0	23.5
	10	2.6	2.1	24.4
	20	2.7	2.3	25.2
	50	2.9	2.4	26.4
	100	3.1	2.5	27.2
240	1	1.6	1.2	20.3
	2	1.7	1.3	21.5
	5	1.8	1.5	23.0
	10	1.8	1.6	24.1
	20	1.9	1.7	25.1
	50	2.0	1.8	26.3
	100	2.0	1.9	27.2
270	1	1.9	1.4	19.8
	2	2.0	1.6	21.0
	5	2.2	1.8	22.4
	10	2.4	1.9	23.4
	20	2.5	2.0	24.3
	50	2.7	2.2	25.3
	100	2.9	2.3	26.1
300	1	1.9	1.3	18.7
	2	2.1	1.5	19.6
	5	2.3	1.7	20.8
	10	2.5	1.9	21.7
	20	2.6	2.1	22.6
	50	2.8	2.2	23.8
	100	3.0	2.4	24.6
330	1	1.8	1.1	17.3
	2	1.9	1.3	18.6
	5	2.2	1.5	20.2
	10	2.3	1.7	21.2
	20	2.5	1.9	22.2
	50	2.7	2.2	23.4
	100	2.9	2.3	24.3

3 Near shore metocean conditions

3.1 Introduction

To provide accurate flow and wave conditions near the structure, a sufficiently high-resolution numerical model is set up for the project area. Simulations in this model resolve the tide, wind and wave-generated currents and hence allow to compute nearshore timeseries for study-relevant parameters. In this case, water depths, current velocities and wave heights at twelve locations around the structure are provided for different scenarios. These scenarios include a tide-only simulation, a typical wave event for the period the structure is placed on the intertidal beach (storms with a return period of approx. 1 year) and 2 storms with higher return periods.

3.2 Model setup

The numerical model is set up using DELFT3D-FLOW/FM (for the flow grid) as well as SWAN (for the wave grid). The following paragraphs elaborate on important information and decisions that stand at the base of the developed numerical models.

3.2.1 Grids

The numerical grids are set up in line with Figure 2.7. The red rectangle shows the extent of the wave grid, whereas the blue rectangle outlines the extent of the flow grid. The flow grid has a northern boundary approximately 5 km to the north of the project area and a southern boundary around 10 km to the south. The eastern boundary is located 7 km offshore, in 15 m water depth. The red grid boundaries are extended around 7 km to the south and north and 4 km to the east (offshore). This allows to propagate waves into the flow grid without any boundary induced errors. The red grid is used in the SWAN wave model and the blue grid in the DELFT3D-FLOW/FM model. Both grids have a cross shore resolution of 10 m and alongshore resolution of 20 m at the project location.

3.2.2 Bathymetry

To construct the bathymetry of the numerical model, three different 2D sources are incorporated:

1. Vaklodingen (open source, 2017, MSL)
2. MBES Buitenhaven IJmuiden (internal RWS data, 2011, MSL)
3. MBES TenneT (provided by NRG, 2018, LAT)

The conversion between different vertical reference levels in the bathymetry surveys to MSL are based on the Memorie - Noordzee reductiematrix (2006) from the Dienst Hydrografie Geodesie & Getijden. The reductiematrix gives a conversion between MSL, LAT and NAP as follows for the location IJmuiden buitenhaven:

Table 3.1: Conversion matrix for the location IJmuiden buitenhaven according to Noordzee reductiematrix (2006).

LAT to MSL	**MSL** to **NAP**	**LAT to NAP**
-1,07 m	0,04 m	-1,03 m

The conversion between MSL and NAP towards the project side near Wijk aan Zee has been confirmed by the data of MATROOS (Multifunctional Access Tool foR Operational Oceandata Services), which provides 2D maps of the MSL-NAP conversion in the North Sea.

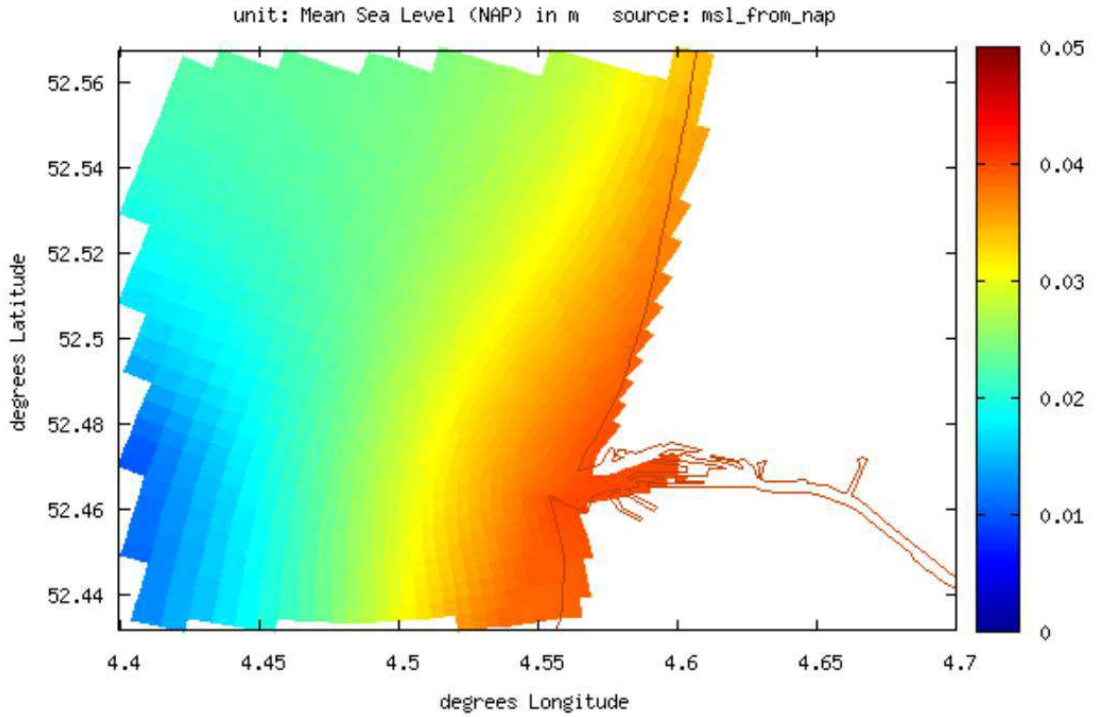

Figure 3.1: Difference plot between MSL and NAP for the area around the project location, derived from MATROOS.

The Vaklodingen data from 2017 covers almost the complete extent of both the red and blue grids (see Figure 2.7), while the harbour of IJmuiden is absent. The bed level in this area is provided by supplementing the Vaklodingen bathymetry with internal Multi-Beam Survey (MBES) data from Rijkswaterstaat (RWS), originating from 2011.

At the project site TenneT performed an additional MBES survey in 2018. This data is incorporated into the bathymetry as well. However, it does not replace the Vaklodingen data in the area. There are substantial differences between the data up to 2017 and the TenneT MBES from 2018. This is visualized in Figure 3.2, which shows the bed level along a transect (AA; orange line) in **Error! Reference source not found.**. Along transect AA, NRG provided bed level data (ground level survey) measured on 06-10-2020. Apart from the Vaklodingen 2017 and TenneT 2018 data, the plot in Figure 3.2 is supplemented with a NRG transect survey from 2020 and JarKus data (open source, RWS) from 2017, 2018 and 2020. The design drawings of the support structure are based on the NRG transect survey from 2020.

As seen in Figure 3.2, the vertical differences in the bed level (comparing Vaklodingen 2017 and TenneT 2018 data) reach up to about 0.9 m at the seaside sheet pile wall and 0.25 cm at the duneside sheet pile wall. It is also seen that the JarKus 2017 transect lays exactly on top of the Vaklodingen 2017 data. One year later, in 2018, the JarKus data shows a significantly elevated profile. According to a publicly available nourishment database from RWS, there was a beach nourishment close to Wijk aan Zee in 2017. Apparently, this nourishment was not yet present in the 2017 survey but did affect the bed level at the project site as seen in the 2018 surveys from JarKus and TenneT. Apart from this, there is also a significant difference in the inclination or slope of the bed level measurements. At the seaside sheet pile wall, the ground level survey from 2020 lays 0.5 m lower than the TenneT 2018 survey while it is the other way around at the duneside sheet pile wall. Here, the TenneT 2018 survey bed level lays 0.5 m lower than the ground level survey from 2020.

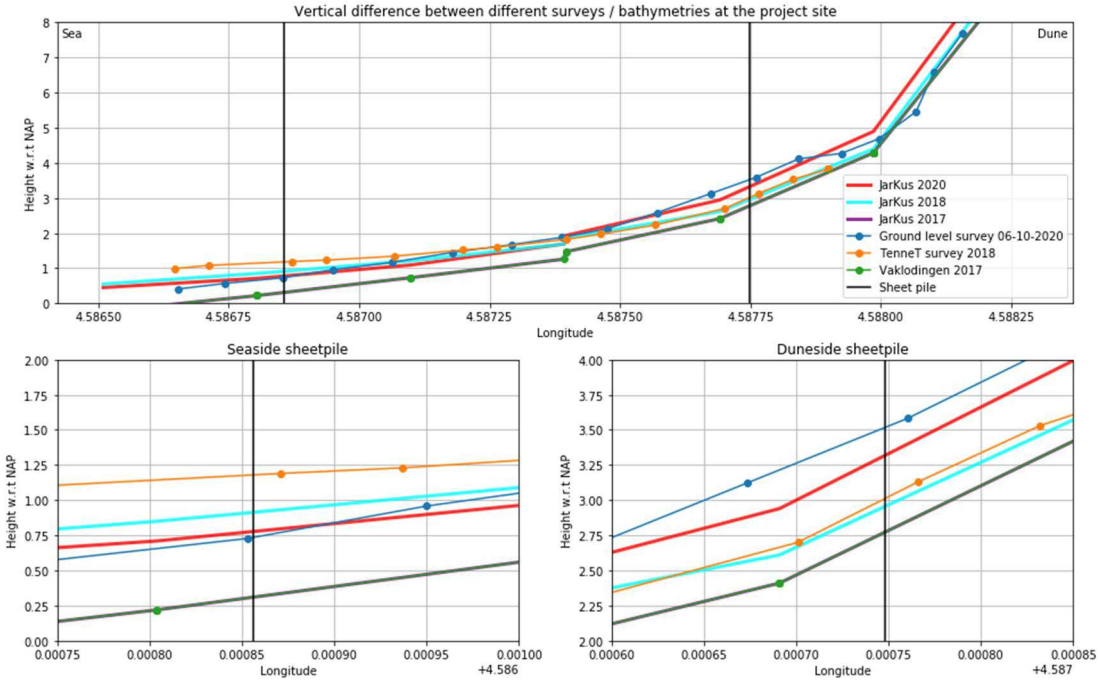

Figure 3.2: Vertical bed level elevations (in mNAP) for different bathymetry sources for different years along transect AA (see *Figure 1.1*). The upper panel shows the complete cross section of transect AA, where the location of the sea- and dune-side sheet pile walls are indicated with vertical black lines. The lower left and lower right plots zoom in on the bed level elevation around the sea- and dune-side sheet pile walls respectively.

The paragraph above indicates that the differences in bathymetry obtained from the compared data sources are substantial and are present in the vertical as well as horizontal (inclination / slope). The latter is an indication that there are seasonal differences in bed level, referred to as the summer and winter beach profiles. As the design of the support structure is dependent on the bed level, it is decided to continue with two bathymetries.

One bathymetry is based on the data up to 2017 (sources 1 and 2 in the list above) and is referred to as the Vaklodingen bathymetry in the remainder of the report. By incorporating the Vaklodingen bathymetry in this study (see Figure 3.3 and green / purple line in Figure 3.2), we are conservative for both the dune and seaside sheet pile wall as we have lower bed levels that might be inundated earlier or subject to higher flow velocities due to larger water depths.

The other bathymetry is composed of the all three sources in the list above and is referred to as the TenneT bathymetry in the remainder of the report. By incorporating the TenneT bathymetry in this study (see Figure 3.4 and orange line in Figure 3.2), we are approximating the most recent bathymetry which will result in the most realistic outcomes. However, it should be noted that this bathymetry leads to an underestimation of the water depths and flow velocities computed at the seaside sheet pile wall as the ground level survey of 06-10-2020 is below the level of the TenneT bathymetry.

By comparing Figure 3.3 and Figure 3.4, one can get an idea of the spatial differences in vertical bed levels between the two different bathymetries at the project site. Besides, the numerical model implementation of the schematisation of the sheet pile walls and the locations of output points are indicated. Location TS1 to 9 are put down right at the seaside of the geotubes, while TS10, 11 and 12 are located at the backside of the sheet pile walls (see Appendix C for more information on output locations). Although the focus in this study will be on the most recent bathymetry (Figure 3.4), the inclusion of the Vaklodingen bathymetry allows to give a bandwidth of results and gives an indication on the uncertainty that comes along with the vertical bed level at the time of construction.

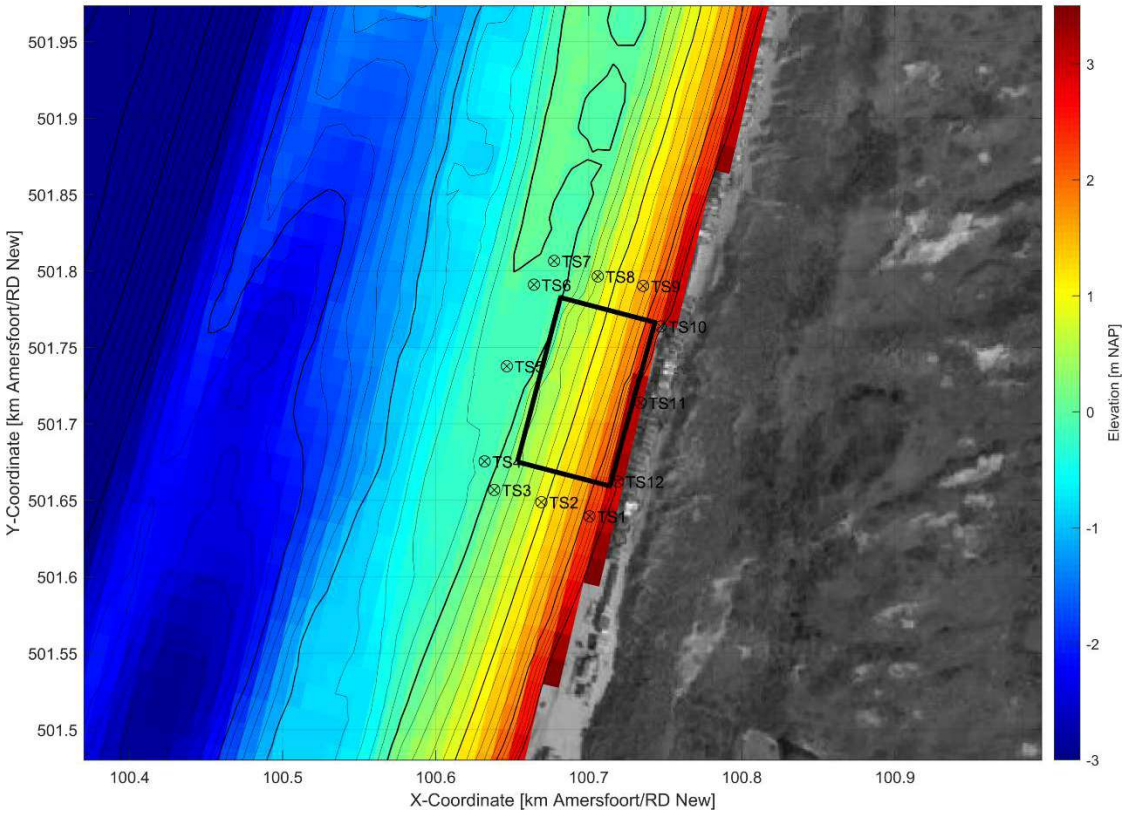

Figure 3.3: The vertical bed levels represented by the Vaklodingen bathymetry (2017) together with the schematised sheet pile walls (black rectangle) and output locations (TS1 to 12) of the numerical model.

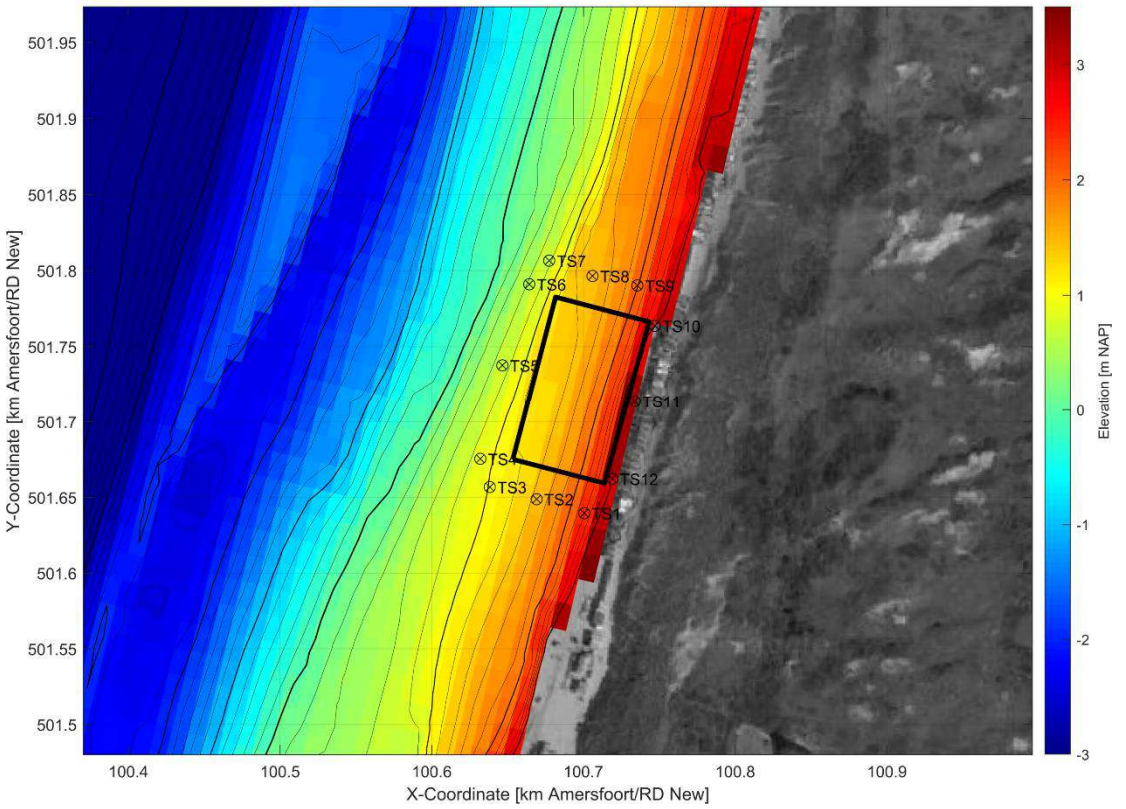

Figure 3.4: The vertical bed levels represented by the TenneT bathymetry (2018) together with the schematised sheet pile walls (black rectangle) and output locations (TS1 to 12) of the numerical model.

3.2.3 Boundary conditions

The numerical model is forced with boundary conditions at the northern, western and southern edges of the grid, while the eastern edge is bounded by land.

For a tide-only simulation, the flow grid contains Neumann (water level gradient) boundaries at the northern and southern edges. These boundaries are derived from the Dutch Continental Shelf Model (DCSM), an extensively validated model with a grid resolution of 0.5 nautical miles used in many of Deltares' studies. On the western boundary, water levels are imposed on the flow grid. This boundary is also derived from the DCSM model.

For storm simulations, the wave (SWAN) and flow grid (DELFT3D-FLOW/FM) are coupled to each other. The western boundary condition of the tide-only simulation is extended to include the surge level that is originating from data derived in Chapter 2. Here, a typical storm of 32 hours is assumed. Furthermore, the storm is schematized to reach its peak storm surge level simultaneously with the occurrence of the highest tide in the tide-only simulation. Wind fields (direction and speed) are added to all grid points on the flow grid. For the wave grid, wave boundaries on the northern, western and eastern grid edges contain the significant wave height, peak wave period, mean wave direction and directional wave spreading characteristics derived in Chapter 2. Besides, the wind fields and water levels (including surge) from the newly imposed flow boundaries are extrapolated and also imposed on the wave grid boundaries.

3.2.4 Scenarios

Together with the client, it is decided to run a total of five numerical simulations as per the list below:

1. A tide-only simulation (flow) with the TenneT bathymetry (reference F_TenneT)
2. A typical wave event (flow-wave) representative for the period (1yr) the structure is placed on the beach with the TenneT bathymetry (reference FW_1yr_TenneT)
3. A storm event (flow-wave) with a higher return period (5yr) with the TenneT bathymetry (reference FW_5yr_TenneT)
4. A storm event (flow-wave) with a higher return period (20yr) with the TenneT bathymetry (reference FW_20yr_TenneT)
5. A storm event (flow-wave) with a higher return period (20yr) with the Vaklodingen bathymetry (reference FW_20yr_Vakl)

Typical daily hydrodynamic conditions for the period the temporary structure is placed on the beach are represented by the bandwidth of outcomes between the tide-only simulation and the typical wave event (point 1 and 2). Wave / storm events coming from North-West (angle > 300 degrees N) typically induce the highest flow velocities along the coastline. Hence, all wave / storm simulations (point 2 to 5) incorporate a wave angle between 315 and 345 degrees N, where the main wave angle equals approximately 330 degrees N. Please note that the angle of the coastline-normal at the project location is approximately 300 degrees N.

3.3 Validation tide-only simulation

The tide-only simulation used in this study should be well capable of producing tide-generated currents and water levels that are comparable to the variables computed by the DCSM model, which is too coarse for this particular application. This is achieved finetuning boundaries and adjusting some small settings in the setup of the numerical model, while checking the water level and current velocity at some validation points as visualized in Figure 3.5.

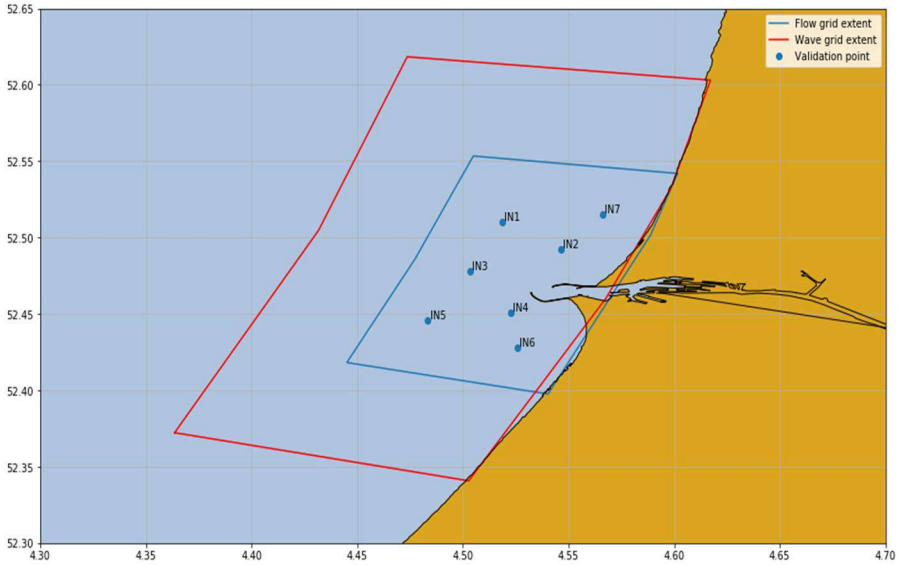

Figure 3.5: Flow and wave grid extents of the numerical models, together with a total of seven points that are used for the validation.

In the figures below (see Figure 3.6 and Figure 3.7), the current velocity (X and Y direction) and water level in validation point 1 (IN1) are shown. Here, it is seen that the flow simulation (named 03_Flow_Blue_cstbnd1, later renamed to F_TenneT) is capable of approximating current velocities correctly. Minor differences in the X and Y current velocities are explained by the differences in bathymetry between the coarser DCSM model and the designed flow and wave models for this specific project. The flow model is also seen to be able to reproduce the water levels from the DCSM model very well.

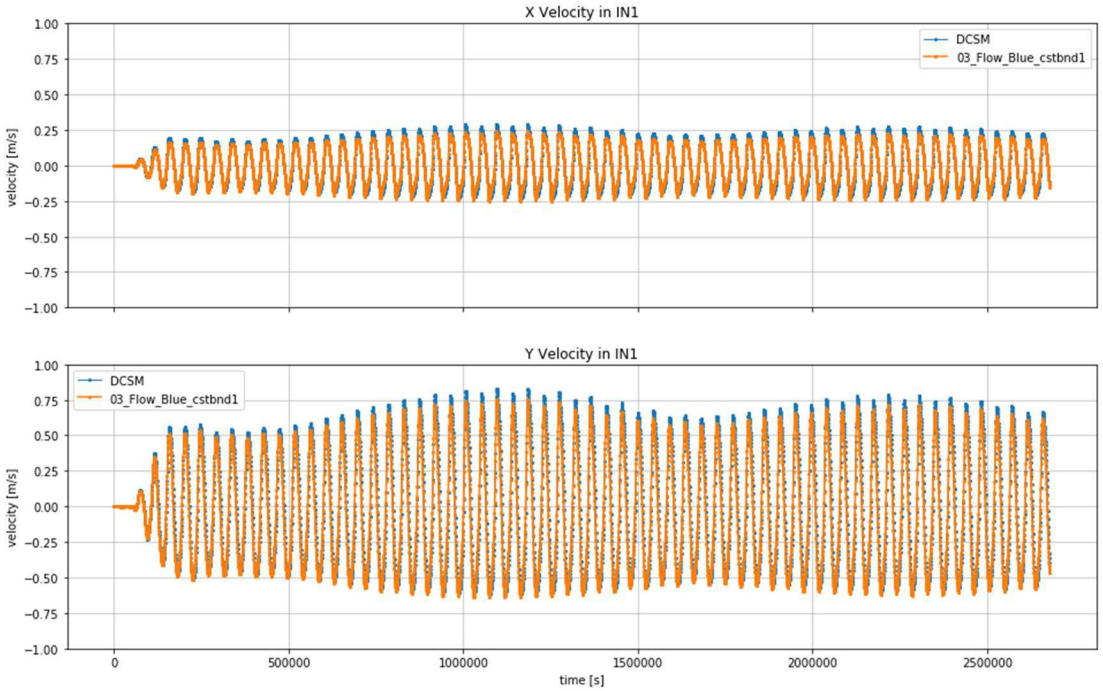

Figure 3.6: Current velocity in X (upper panel) and Y (lower panel) direction for the flow model (orange line; named 03_Flow_Blue_cstbnd1, later renamed to F_TenneT) and the DCSM model (blue line) at validation point IN1.

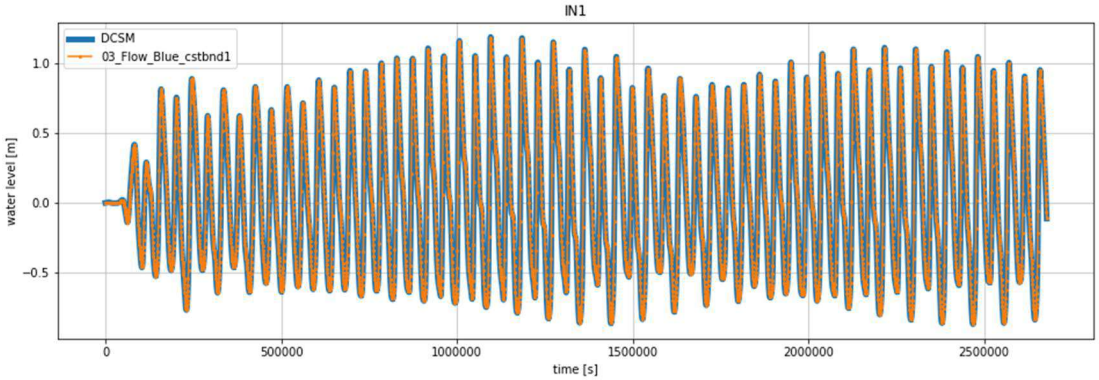

Figure 3.7: Water level variation for the flow model (orange line) and the DCSM model (blue line) at validation point IN1.

3.4 Results

The outcomes of the five run simulations (tide-only, 1yr, 5yr and 20yr storms for the TenneT bathymetry and 20yr storm for the Vaklodingen bathymetry) are presented as shown in Figure 3.8 below for output location TS5. The upper panel shows the location and schematization of the sheet pile walls together with the output locations TS1 to 12 at the front of the geotubes and at the backside of the sheet pile walls. The second panel shows the water height in mNAP together with the bed level at which the output location is situated. The computed maximum water depth at that location is indicated in the title of the panel. The third panel shows the resultant current velocity, which is due to tides, winds and waves for this flow-wave simulation. Similarly to the second panel, the maximum current velocity is indicated in the title of the panel. The last panel contains the wave height timeseries at the output location, where the maximum wave height is again shown in the panel title. Plots for all output locations for all run simulations (in total 60) are given in Appendix C.

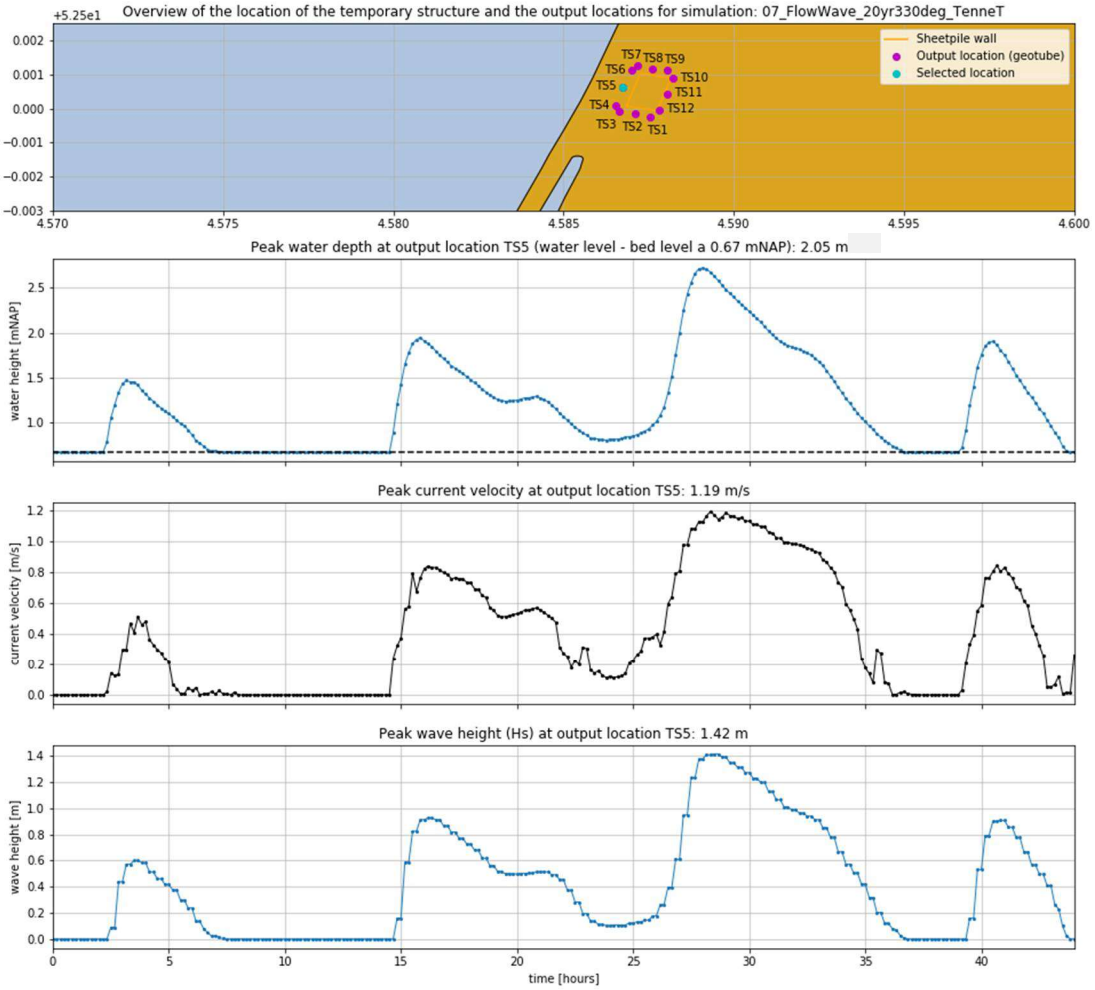

Figure 3.8: Location and schematization of the temporary structure with (selected) output point(s) and the approximate land boundary at the project location (upper panel), the water height timeseries (in mNAP, second panel), the current velocity (third panel) and the wave height (fourth panel) for the fourth simulation (FW_20yr_TenneT); a 20 yr storm with an angle of 330 degrees using the most recent TenneT bathymetry from 2018.

3.4.1 Water depths

Similarly to the computed maximum water depth as shown in Figure 3.8 for location TS5 for simulation FW_20yr_TenneT, Table 3.2: Maximum water depths in m at different output locations around the temporary structure.Table 3.2 gives a summary of all the computed maxima for all scenarios and all output locations for the 59 other figures in Appendix C.

As can be seen from the table, points TS10, 11and 12 remain dry for all simulations. This indicates that there is no backflow (i.e. flow between the dune-side sheet pile wall and the dunes). However, it should be said that this is dependent on the exact location and configuration of the sheet pile walls as well as the design of the temporary structure. In case of a (mild) storm, there will be a water depth at the locations TS1 and TS9 (which represent the landward end of the geotubes). These points are very close to the back of the temporary structure, indicating that water will be close to reaching the point where backflow occurs. The F_TenneT simulation indicates that it is expected that a water depth of at least around 0.5 m will be present at the front side of the structure (TS3 to TS7) during very calm conditions and high tide (i.e. in absence of any waves). The rest of the sides of the structure and the adjacent beach remains dry. In Table 3.2, the maximum water depths are marked green. It is seen that this holds for all locations using the more conservative bed levels of the Vaklodingen

bathymetry. The more realistic results on maximum water depths are marked light blue, as these are based on the most recent bathymetry.

Table 3.2: Maximum water depths in m at different output locations around the temporary structure.

Simulation / Observation point	TS1	TS2	TS3	TS4	TS5	TS6	TS7	TS8	TS9	TS10	TS11	TS12
F_TenneT	0.0	0.0	0.25	0.36	0.56	0.74	0.59	0.0	0.0	0.0	0.0	0.0
FW_1yr_TenneT	0.29	1.18	1.63	1.73	1.92	2.1	1.97	1.26	0.75	0.0	0.0	0.0
FW_5yr_TenneT	0.38	1.26	1.72	1.81	2.0	2.18	2.05	1.36	0.85	0.0	0.0	0.0
FW_20yr_TenneT	0.42	1.31	1.76	1.86	2.05	2.22	2.1	1.4	0.9	0.0	0.0	0.0
FW_20yr_Vakl	0.55	1.78	2.6	2.88	2.89	2.82	2.81	2.24	1.33	0.0	0.0	0.0

3.4.2 Current velocities

The maximum current velocities for all output locations and all simulations are summarized in Table 3.3. Current velocities are absent if there is no water depth in an output location at any time during the simulation. In Table 3.3, the maximum current velocities are marked green. Note that these do not always occur for the highest water depths as the FW_20yr_TenneT simulation also contains greenish boxes. In case the green box is present in the FW_20yr_Vakl simulation, the table contains light blue colours indicating more realistic maxima (based on the more recent bathymetry) at those output locations. By comparing numbers between the FW_TenneT simulations for various output locations, one can see that with a smaller return period, the current velocities are not particularly differing that much. This gives an indication that the maximum occurring flow velocities are more dependent on the design of the temporary structure (its footprint, the location and configuration) than the return period of analysed storms.

Table 3.3: Maximum current velocities in m/s at different output locations around the temporary structure.

Simulation / Observation point	TS1	TS2	TS3	TS4	TS5	TS6	TS7	TS8	TS9	TS10	TS11	TS12
F_TenneT	0.0	0.0	0.13	0.15	0.17	0.2	0.19	0.0	0.0	0.0	0.0	0.0
FW_1yr_TenneT	0.18	0.25	0.92	1.09	1.08	1.14	0.99	0.51	0.25	0.0	0.0	0.0
FW_5yr_TenneT	0.21	0.23	0.99	1.17	1.16	1.24	1.07	0.53	0.25	0.0	0.0	0.0
FW_20yr_TenneT	0.32	0.23	1.0	1.18	1.19	1.29	1.12	0.57	0.26	0.0	0.0	0.0
FW_20yr_Vakl	0.51	0.39	0.83	0.99	1.17	1.31	1.11	0.75	0.37	0.0	0.0	0.0

3.4.3 Waves

The maximum wave height for all output locations and all simulations are summarized in Table 3.4. Here, the maxima are marked green while the more realistic maxima (based on the more recent bathymetry) are marked light blue. In case of a tide-only simulation, there are no waves at all. This is indicated by the greyish boxes in Table 3.4. Please note that the application of SWAN for wave heights in water depths present at the toe of the structure is not particularly accurate, whereas SWAN is required to contribute to accurate assessments on larger-scale hydrodynamic processes (like water depths and current velocities). Hence, one should interpret the maximum wave height outlined in Table 3.4 with great care. It only gives an indication of what can be expected as, in theory, we expect waves somewhat lower than pointed out in the table below. This is elaborated on in the next chapter on wave loads, where a different approach is used to schematize representative spectral wave heights.

Table 3.4: Maximum wave heights in m at different output locations around the temporary structure.

Simulation / Observation point	TS1	TS2	TS3	TS4	TS5	TS6	TS7	TS8	TS9	TS10	TS11	TS12
F_TenneT	0.0	0.0	0.0	0.0	0.0	0.0	0.0	0.0	0.0	0.0	0.0	0.0
FW_1yr_TenneT	0.17	0.75	1.03	1.14	1.26	1.36	1.26	0.79	0.47	0.0	0.0	0.0
FW_5yr_TenneT	0.23	0.83	1.13	1.25	1.38	1.49	1.38	0.9	0.56	0.0	0.0	0.0
FW_20yr_TenneT	0.24	0.87	1.17	1.29	1.42	1.53	1.43	0.94	0.6	0.0	0.0	0.0
FW_20yr_Vakl	0.34	1.21	1.64	1.72	1.69	1.68	1.6	1.42	0.94	0.0	0.0	0.0

3.5 Attention points for the design of the temporary landfall structure

Based on the results shown in Chapter 3.4 above, we want to highlight several important points to consider while designing the temporary support structure:

- **Seasonal beach profile changes**: the beach at Wijk aan Zee is expected to show a beach profile that is dependent on the season. This means that in winter, the profile might show a lower elevation at the land side of the structure (i.e. storms erode dunes and tend to flatten the profile). In summer, the relatively persistent forcing of tide and waves tend to steepen the profile. This might induce a lower elevation at the sea side of the structure. An indication of this behaviour can be seen in Figure 3.2, by looking at the ground level survey of 06-10-2020 (blue line) and the TenneT survey of 2018 (orange line).

- **Impact of the structure on the dune system**: the temporary structure might cause morphological changes in the dune system. Although it is not expected that backflow occurs, we cannot predict the development of the dunes as simulations were run in morphostatic mode. During storm or high wind conditions, the beach profile is likely to be altered (see point above) and this might even be enhanced by the presence of the temporary structure.

- **Large-scale morphodynamic impact**: the absence of a morphodynamic simulation induces an extra uncertainty on the impact of the temporary structure on the larger-scale beach dynamics. As the structure will block longshore transport during higher tides and storms for almost a year, this might affect the bed levels and shoreline position in the adjacent shorelines in the order of hundreds of metres alongshore as well.

- **Variability in bed levels over the years**: the bed level at the location of the temporary structure was found to be quite variable the last few years (see Figure 3.2). The latest area covering bathymetry is from 2018 (performed by TenneT), while this survey shows bed levels much higher than the bathymetry from 2017 (obtained from Vaklodingen). Although this change is expected to be due to a close-by beach nourishment, it is advised to perform another area covering bed level survey to be able to make better estimates on the sea-side loads on the temporary support structure.

- **Vertical height of placement of the geotubes**: the bed level at which the geotubes will be installed is an important design consideration. Before it is decided whether a single geotube or a combination of two stacked geotubes will be used, the possibility of adapting the bed levels can be considered (either lowering or heightening). The information obtained from this assessment can be used to cope with the actual bed

levels at the time the temporary structure will be constructed. At this moment, this is quite uncertain as outlined in the point above. In case of encountering a low bathymetry the margin on top of the single geotube remains limited, applying two stacked geotubes will increase the margin on the design height.

- **Absence of infragravity waves within model simulations**: particularly during storms, very long waves induce additional water level setup not included in the analysis right now. These waves are bounded by the presence of short-wave groups and might add up to tens of cm's to the predicted water level. As it was already stated that the water level nearly reaches the point of inducing back flow, the absence of infragravity waves in the analysis induces an extra uncertainty in the impact of the temporary structure on the dune system.

- **Accessibility of the 'hellingbaan'**: during model simulations, the water level reached the points TS1 and TS9 (see Figure 3.3 and Figure 3.4) which mark the end of the geotubes. This indicates that the 'hellingbaan' is unprotected against rising water levels and hence might be subject to erosion, leading to troublesome access to the temporary structure.

4 Wave loads

4.1 Introduction

The present section addresses the wave loads on the geotubes and on the sheet pile wall. First, a discussion on the choice of wave periods is given, where after the loads on the geotubes and the sheet pile wall is discussed. The evaluated loads over all possible input variables are subsequently quantified for three return periods (RP01yr, RP05yr, and RP20yr). Finally, other considerations are briefly discussed.

4.2 Choice of wave conditions and extreme wave heights

The application of SWAN all the way to the toe of the structure is not accurate, while the large-scale hydrodynamic processes (longshore current and wave-induced setup) requires SWAN for an accurate assessment. For the evaluation of the wave loads, it means that the water depth in front of the structure is accurate, while the applied wave height should come from a different source.

The incident wave height at coasts is studied in the field (Raubenheimer et al., 1996) and they proposed a relationship between the spectral weight height and the water depth as follows:

$$H_s = \gamma_s h \tag{4.1}$$

Where H_s is the spectral wave height, h is the total water depth, and γ_s is an empirical coefficient. Their measured empirical relationship is depicted in Figure 4.1. γ_s is seen to depend on the quantity $\beta/(kh)$, where β is the local slope and k is the linear wave number. This effectively means that H_s depends on water depth, beach slope, and wave period.

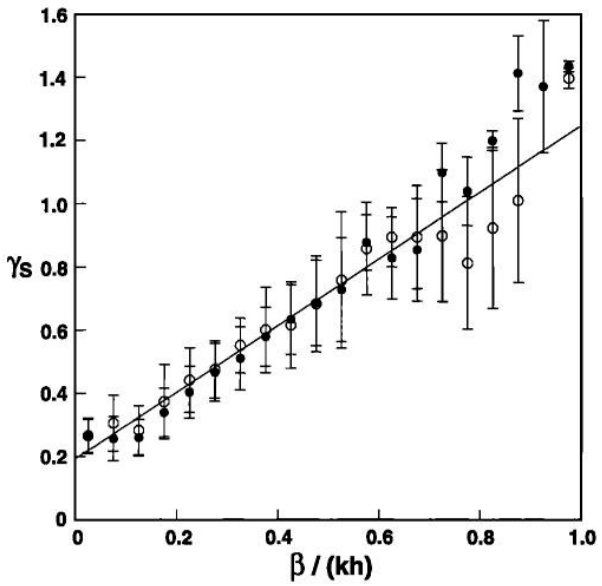

Figure 4.1 The dependency of γ_s on the quantity $\beta/(kh)$.

The relevant wave periods are 12-16 s, the relevant slopes are 1:25 to 1:45, and the relevant water depths are 1.5-3.0 m and this resolves in $\beta/kh \in [0.18, 0.26]$. Inspection of Figure 4.1 gives that a constant value of γ_s of 0.5 is a suitable choice.

The spectral wave height is a representative wave height adjacent to the structure, however, the irregular wave signal means that larger, individual waves are possible. Given the limited water depth, the classical Rayleigh distribution is not valid, which is why the wave height distribution for shallow foreshores by Battjes and Groenendijk (2000) is adopted. The implementation in the toolbox ORCA is applied. A range of incident, individual waves up to an exceedance value of 0.1% is included in the load evaluation. The individual wave height is termed $H_{n\%}$.

4.3 Wave loads on geotube

The stability of the geotube (see Figure 4.2) must be assessed against exerted wave loads. The present evaluation is restricted to (i) horizontal wave loads on the offshore side of the geotube and (ii) vertical wave loads on the bottom of the geotube. The vertical (and restoring) loads due to overtopping water is neglected, since the simplified calculation method in the present work cannot capture the details and conservatism and constraints of this approach are discussed in Section 4.3.2. The combined soil and water pressure on the geotube on its onshore side must be incorporated through the geotechnical calculation.

The present calculations are restricted to waves normal to the geotube, which is conservative as all other combinations will give smaller instantaneous loads on the geotube. This also means that the same loads should be applied along the geotubes perpendicular to the coastline, which is also considered conservative, because the waves diminish shoreward due to depth-induced breaking.

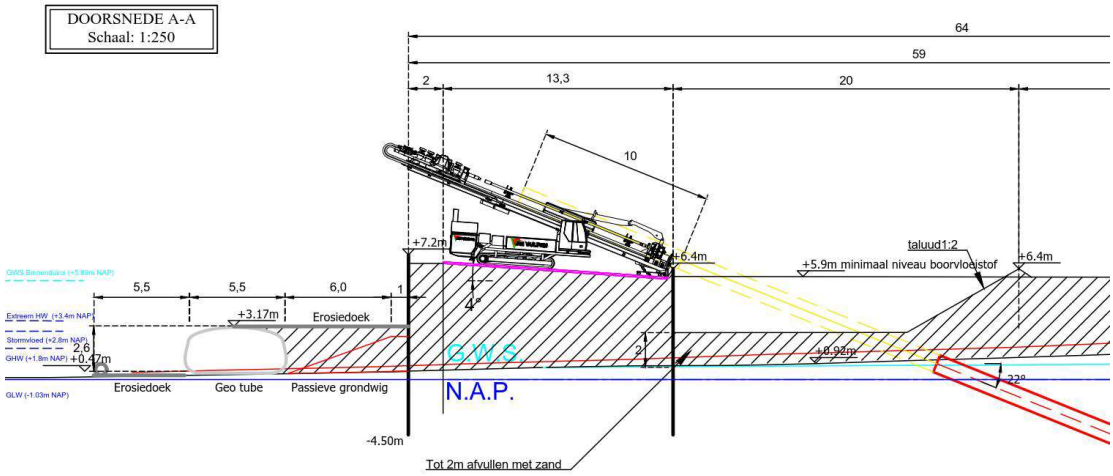

Figure 4.2 Cross section of the geotube offshore of the sheet pile wall of the drilling pit.

The simulated water level reaches to 0.12 m above the crest of the geotube (Section 4.5), while the maximum spectral wave height is almost 1.5 m. This gives a complicated wave pattern in front of the geotube, where the latter works as a partly reflective structure with the adjacent sheet pile wall (12.5 m shoreward) as fully reflective. The partly reflective nature will give rise to deep troughs in front of the geotube and the seabed might be temporarily dry. Starting from the instance of a wave through in front of the geotube, the following sequence of events will take place:

- A (broken) wave will propagate towards the geotube and partly reflect on the structure;
- A part of the wave will reflect offshore, while a part of the wave will propagate over the geotube and infill material and interact with the sheet pile wall;
- After the reflection has occurred, the water will drain off the elevated platform and fall down seaward of the geotube;
- The falling water may impact the seabed directly or fall in a layer of water.

The broken bore in front of the geotube and on top of the sheet pile wall can lead to slamming wave impacts.

The complicated train of events and the irregular nature of irregular waves makes it impossible to make a wave-by-wave evaluation of the wave loads without the use of detailed numerical modelling. Therefore, the following section will rely on simple and conservative assumptions; an approach which is required given the short timeline.

4.3.1 Horizontal loads on offshore side

For the horizontal load on the offshore side, the geotube is considered as a fully reflecting wall, such that the crest elevation from seabed becomes still water level plus $H_{n\%}$. The total force is integrated over the height of the geotube. This is depicted by the blue polygons in Figure 4.3.

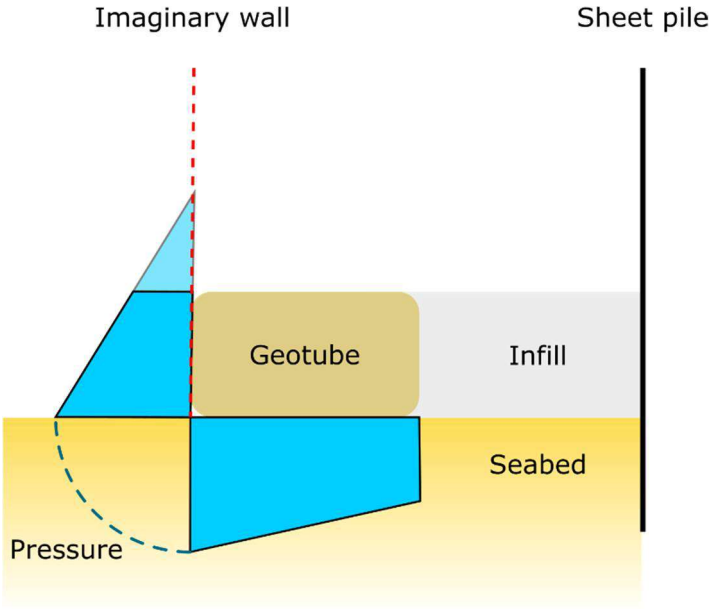

Figure 4.3 Sketch of the infill and geotube system on the seaward side of the sheet pile wall. The blue polygons show the pressure distribution on the seaward side of the geotube and along its bottom.

The wave periods are long (in the range of 12-16 s) and the water depth is relatively small (less than 3.0 m), so the individual, extreme waves can be treated as in the shallow water regime, why the pressure distribution is hydrostatic. The maximum elevation of the surface relative to seabed, η_+, in front of the imaginary wall is given as

$$\eta_+ = SWL + H_{n\%} \tag{4.2}$$

and the corresponding minimum elevation relative to seabed, η_-, in front of the imaginary wall is given as:

$$\eta_- = \max(0, SWL - H_{n\%}) \tag{4.3}$$

The height of the geotube relative to seabed is furthermore specified as h_G and it is set to 2.75 m. The maximum and minimum wave loads on the seaward side of the geotube are specified as

$$F_{+,n\%} = \frac{1}{2}\rho g \eta_+ \left[2 - \min\left(\frac{h_G}{\eta_+}, 1\right)\right] \min(h_G, \eta_+) \quad , \quad F_{-,n\%} = \frac{1}{2}\rho g \eta_-^2 \tag{4.4}$$

The loads for water depths of 1.5 m and 2.8 m, respectively, are depicted in Figure 4.4, for three slopes of 1:25, 1:35, and 1:45. The loads are independent of the incident wave period. The maximum onshore load is highly dependent on the actual water depth in front of the structure, which means that the actual bathymetry at the point of installation is important.

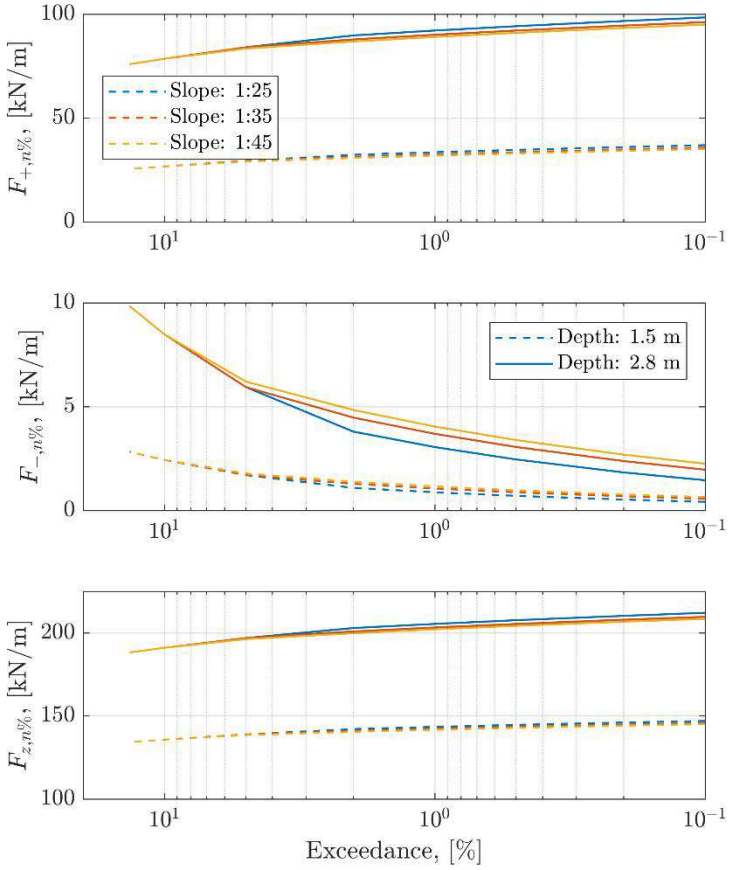

Figure 4.4 Wave loads on the geotube. Top panel: $F_{+,n\%}$. Middle panel: $F_{-,n\%}$. Bottom panel: $F_{z,n\%}$.

4.3.2 Vertical loads on bottom of geotube

The pressure on the bottom of the geotube follows from the hydrostatic pressure on either side of the tube with a linear variation in between (Figure 4.3). It is noted that any overpressure on the shoreward side is neglected, which is conservative under the premise that the weight of the geotube does not account of a layer of water on top of the tube. Hereby, the vertical force reads:

$$F_{z,n\%} = \frac{1}{2}\rho g\left(\eta_{+} + h_G\right) L_G \tag{4.5}$$

where L_G (5.5 m) is the width of the geotube. The loads are depicted as a function of the exceedance probability in Figure 4.4 (bottom panel) for three values of the slope of the shoreface and two water depths. It is seen that the vertical force is mainly a function of the water depth, which means that the actual bathymetry at the point of installation is important.

It is expected that additional overpressure stemming from the pressure distribution below the geotube due to frontal waves is dissipated at the sheet pile. There will, however, be an overpressure from water on top of the infill material.

4.3.3 Overpressure in the pore water on the onshore side

An overpressure in the pore water within the infill material can occur, because there is water on top of the geotextile. The overpressure is a combination of the still water level being larger than the height of the geotube and that there is overtopping water. It is discussed below (Section 4.4) that the initial water depth during overtopping events is defined by d_0. Since there is limited information on how this overtopping propagates towards the sheet pile water, the overpressure on top of the geotextile is simply stated as $p_o = \rho g d_0$. The values are tabulated in Table 4.1.

It is stressed that the overpressure is a representative for the overpressure during individual overtopping events. The overtopping events give a dynamic environment on top of geotube and infill, so it is important to realise that the overpressure should not be applied as a mean, static overpressure. The mean, static overpressure is expected to be smaller than p_0, however, it is hard to quantify given the complex flow behaviour discussed in the beginning of Section 4.3.

4.3.4 Slamming wave loads

The slamming wave load due to breaking waves in front of the geotube is a stochastic process that depends heavily of the interaction between individual waves and the depth of the trough in front of the breaking wave. The case of a broken wave travelling towards and impacting the geotube is considered as follows:

- The previous wave has dried out the seabed;
- The incident wave has a wave height $H_{n\%}$ which travels as a bore with propagation speed $\sqrt{gH_{n\%}}$
- The impact occurs over the height $H_{n\%}$ of the geotube
- The slamming coefficient of 2.9 for horizontal wave in-deck calculations following DNVGL (2017), section 8.3.3.5 is applied.

This gives the following definition of the slamming force on the geotube:

$$F_h = \frac{1}{2}\rho 2.9(\sqrt{gH_{n\%}})^2 H_{n\%} \tag{4.6}$$

The slamming wave load is tabulated in Table 4.1.

4.4 Wave loads on sheet pile wall

The wave loads on the sheet pile wall occurs, when the top of the incident wave is ‘cut off’ at the top of the geotube and travels as a bore over the geotube and the infill material behind it. Chen et al (2015) studied this process for schematic dikes representative for the Belgium coast. Their experimental setup is reproduced in Figure 4.5. They classified the wave loads on the vertical wall at a distance of B from the top of the dike as a function of the initial water depth on the top of the dike, d_0, the horizontal stretch B, and the local wave length, L. The main difference to the present situation is that their study did not have a near-vertical seaward slope, i.e. $\beta = 90°$.

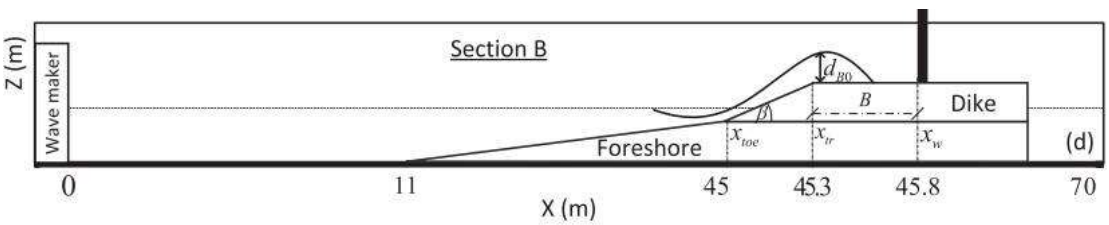

Figure 4.5 The experimental setup in Chen et al. (2015).

Their parameterisation for the total impact force on the wall no top of the dike is depicted in Figure 4.6 and their parameterisation is adopted in the present work. Since their parameterisation depends on the wave length, there will be an impact of the wave period in the results. The loads are depicted in Figure 4.7 for the largest water depth of 2.87 m in front of the geotube. The initial water depth on the top of the geotube is taken as $\eta_+ - h_G$. It is seen that the larger the wave period, the larger the wave load. The results are still a strong function of the water depth in front of the geotube, which means that the actual bathymetry at the point of installation is important.

There is a slight difference between the results from Chen et al. (2015) for a 1:3 and a 1:6 slope, where the 1:3 results give slightly larger loads. This suggests that the applied formulation might be non-conservative, on the other hand η_+ assumes a fully reflecting wall, which will not be the case, so η_+ and thus d_0 are conservative estimates. In any case, it is advised to apply a partial load coefficient on the predicted loads.

The impact location of the resulting forcing is not stated in Chen et al. (2015), so it is approximated as $d_0/2$.

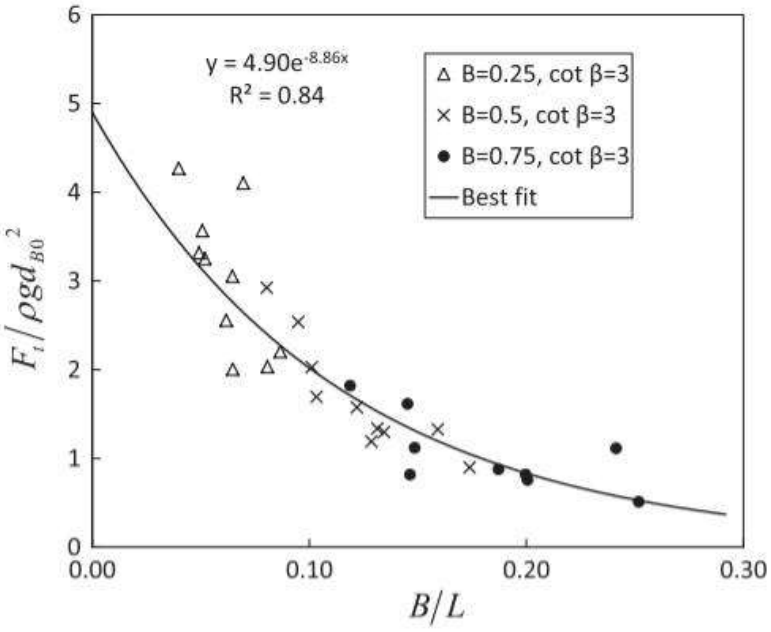

Figure 4.6 The nondimensional force on the wall in the study by Chen et al. (2015), their figure 10.

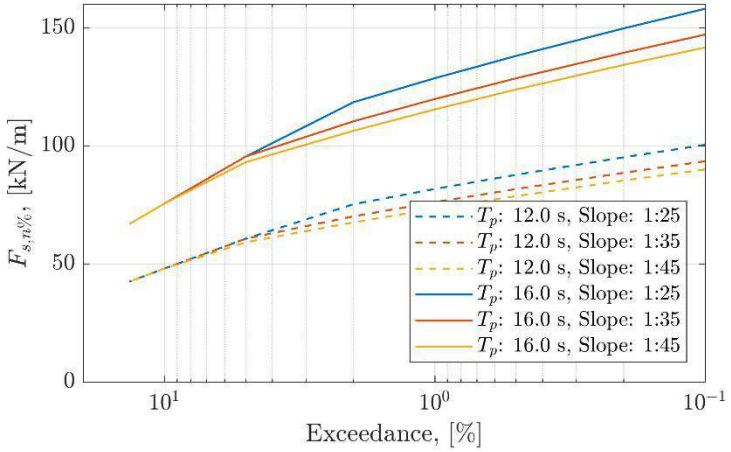

Figure 4.7 The load on the sheet pile wall due to capping waves impacting as a bore.

4.5 Overview of loads

The examples above showed the loads depend on the water depth, slope of the foreshore, and wave period. The predicted loads over the two bathymetries and return period RP01yr (only TenneT), RP05yr (only TenneT), RP20 are shown in Table 4.1. It is noticeable that the loads due to RP05yr and RP20yr are practically identical for the TenneT bathymetry, but there are large differences between the loads for the TenneT and vaklodingen bathymetries (RP20yr), which is ascribed entirely to the difference in water depth. The ranges in loads for each of the return periods and bathymetries are due to ranges in beach slope (1:25 through 1:45), ranges in wave period (12.0 s through 16.0 s), and ranges in water depth along the geotube (i.e. variation in the local bathymetry).

The location of the loads is schematised in Figure 4.8, where $F_{+,n\%}$, $F_{-,n\%}$, and $F_{h,n\%}$ all work on the outside of the geotube. All loads and pressures are positive along the drawn arrows.

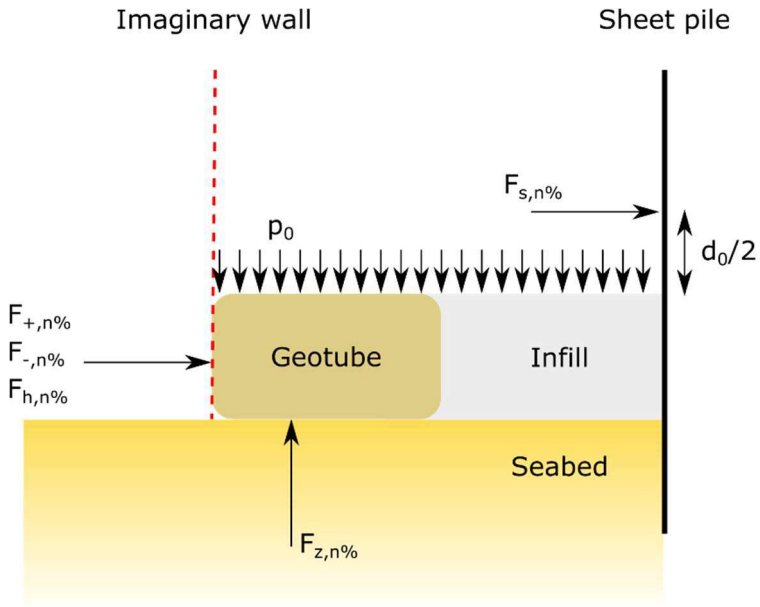

Figure 4.8 Sketch of the location of loads as quantified in Table 4.1. Not to scale.

Table 4.1 Overview of the wave loads for different return periods and exceedance percentages. The intervals are for beach slopes of 1:25 through 1:45 and wave periods of 12. s to 16.0 s.

		RP01yr	RP05yr	RP20yr	
Bathymetry		TenneT	TenneT	TenneT	Vakl.
Water depth, [m]		1.73-2.10	1.81-2.18	1.86-2.22	2.60-2.87
$H_{n\%}$, **[m]**	2%	1.1 – 1.4	1.2 – 1.5	1.2 – 1.5	1.8 – 2.0
	1%	1.2 – 1.5	1.2 – 1.6	1.3 – 1.6	1.9 – 2.1
	0.1%	1.3 – 1.7	1.4 – 1.8	1.4 – 1.8	2.1 – 2.3
$F_{+,n\%}$, [kN/m]	2%	41 - 60	45 - 64	47 - 66	90 - 97
	1%	42 - 62	46 - 66	48 - 68	92 - 100
	0.1%	46 - 67	50 - 71	52 - 73	99 - 106
$F_{-,n\%}$, [kN/m]	2%	1 - 3	2 - 3	2 - 3	4 - 5
	1%	1 - 2	1 - 2	1 - 3	3 - 4
	0.1%	1 - 1	1 - 1	1 - 1	1 - 2
$F_{h,n\%}$, [kN/m]	2%	18 - 31	20 - 33	21 - 34	49 - 58
	1%	20 - 33	22 - 36	23 - 38	53 - 63
	0.1%	25 - 42	28 - 45	29 - 47	67 - 79
$F_{z,n\%}$, [kN/m]	2%	155 - 174	159 - 178	161 - 180	204 - 211
	1%	156 - 176	160 - 180	162 - 182	207 - 214
	0.1%	160 - 181	164 - 185	167 - 187	213 - 221
p_0, [kPa]	2%	1.0 - 8.0	2.4 - 9.4	3.1 - 10.1	18.9 - 21.4
	1%	1.5 - 8.7	2.9 - 10.1	3.7 - 10.8	19.8 - 22.4
	0.1%	2.9 - 10.5	4.4 - 12.0	5.2 - 12.7	22.1 - 24.9
$F_{s,n\%}$, [kN/m]	2%	0 - 13	1 - 19	1 - 22	59 - 120
	1%	0 - 16	1 - 22	1 - 26	64 - 131
	0.1%	1 - 23	2 - 31	3 - 36	80 - 162
$d_0/2$, [m]	2%	0.1 - 0.4	0.1 - 0.5	0.2 - 0.5	0.9 - 1.1
	1%	0.1 - 0.4	0.1 - 0.5	0.2 - 0.5	1.0 - 1.1
	0.1%	0.1 - 0.5	0.2 - 0.6	0.3 - 0.6	1.1 - 1.2

4.6 Attention points for the design of the temporary landfall structure

The combined waves and current loads on the corner of the geotube arrangement cannot be assessed easily with the present simplistic approach and it would require somewhat more advanced techniques that are outside the scope of the present work. There is, however, a risk that the combined deflection and convergence of the longshore current around the structure will give an offshore directed force on the corner of the geotube arrangement. The magnitude of this push might not be critical, because the current interacts the most with the geotube under the wave crest, while the water column almost dries out during the (extreme) wave troughs. Nonetheless, it is deemed important to ensure some connectivity between the geotubes seaward of the structure and the geotubes on the side of the structure; the double-folded geotextile at the corner, which was presented in an online meeting on 25th of November, might be sufficient.

The stability of the geotube requires a geotechnical model, where the combined soil and hydrostatic load from the infill material is incorporated. Here, it is important to note that the predicted vertical force coincides with the maximum horizontal force ($F_{+,n\%}$).

The present calculations assume that the geotube stays in place during the lifetime of the structure. However, due to the risk of scour and the wave loads, the geotube could potentially slide seaward and sink into the scour hole. This would expose the infill material to erosion and subsequently the sheet pile wall to increased wave loads. Initially, the sheet pile wall will be subject to increased loads, because the distance to the sheet pile wall is reduced (see Section 4.4). Once the infill is completely eroded, the sheet pile wall acts as a fully reflecting wall and the loads are expected to exceed the horizontal loads derived for the geotube, because the upper part of the triangle (see Figure 4.3) must be included in the load evaluation. It is also possible that the displacement of the geotube can change the wave height (both increase and decrease) in front of the sheet pile wall, e.g. the geotube works either as an 'offshore' breakwater (decreasing waves) or funnels the waves through a combination of refraction and diffraction around the displaced geotube (increasing waves).

Finally, should the designer choose for a design with two geotubes on top of each other, this requires additional attention with respect to the wave loads. The additional attention especially relates to the vertical and horizontal loads for each of the geotubes. The horizontal loads will be similar to those reported above, however, they need to be split into one force component per geotube. Furthermore, there will be a vertical load at the interface between the geotubes, which can lead to destabilisation of the upper geotube.

5 Local scour assessment

5.1 Introduction

Waves and currents around the landfall structure will result in local erosion. Erosion in front of the outer sheet pile wall is prevented by means of a geotextile and a geotube. However, scour holes at the front side of the geotube can develop. If significantly large, this erosion might result in undermining of the geotube and the geotube might slide into the erosion hole, leaving the sheet pile wall unprotected. To prevent this progressive failure mechanism undermining of the geotube due to erosion must be prevented. The present design of the landfall structure therefore includes a geotextile at the outerside of the geotube. To assess the necessity and required dimensions of this geotextile, the present study is aimed at estimating the potential for erosion around the geotube (as if there was no geotextile).

Given the nearshore hydrodynamic conditions (Chapter 3), we expect that scour around the geotube can develop in the following locations and conditions:

- Scour due to reflected waves; this type of scour will mainly occur at the front of the sheet pile wall/geotube (seaside).
- Scour due to alongshore currents; this type of scour will be largest around the tip of the cofferdam/geotube.
- Apart from scour, a lowering of the bed level at the cofferdam can also result from large-scale beach profile changes that occur in either the cross-shore or alongshore direction.

The first two items are discussed separately in respectively Section 5.2 and Section 5.3. The latter type of lowering is not considered in the present assessment.

5.2 Scour due to reflected waves

5.2.1 Theoretical background

No explicit formulations for scour development due to waves at cofferdams exist, especially cofferdams that are partially protected by a geotube and an erosion fabric. Nevertheless, comparable situations do exist. To assess the wave induced scour development in front of the geotube, use is made of empirical relations for scour at vertical seawalls. This is likely a conservative estimate, due to both the shape and flexibility of the geotube. For the situation of a vertical seawall, there is general consensus that the scour in front of the wall is proportional to the (reflected) wave height in front of the wall. Formulations like those from the Shore Protection Manual (1984), Steetzel (1988) or Kraus and McDougal (1996) relate the scour to local quantities such as the water depth or wave height just in front of the structure. Of these, the SPM (1984) formulation also includes the current velocity. Experiments performed by Deltares (2007) show a good correlation between the scour depth and near-structure parameters. Nevertheless, these are not always straightforwardly determined. Therefore, other formulations exist that use the deep water wave parameters such as deep water significant wave height and period (e.g. Fowler, 1992).

Not much information on time-development of toe scour in front of seawalls is available, since these constructions are usually placed for a long time. Therefore, temporal development of the scour hole is less important than the total scour depth. Observations from Deltares (2007) did however show that the initial development of toe scour occurs rapidly, where almost 90% of the scour depth is reached in the initial phase of the design condition. After this initial rapid growth of the scour depth, the scour hole mostly developed in total extent. It is therefore

assumed in the present study that for the design conditions the corresponding equilibrium scour depth is reached within the storm duration.

5.2.2 Considered input parameters

For this analysis, the input parameters considered are:

- Water depth (tidal water level + storm surge set-up) in front of the structure
- Maximum unbroken wave height in front of the structure
- Alongshore current velocity in front of the structure
- Significant deep-water wave height
- Peak period corresponding to the wave field

For this analysis, both empirical relations using near-structure parameters as well as relations using the deep-water parameters are used to assess the scour depth. The near-structure formulations make use of maximum unbroken wave height, whereas the formulation by Fowler (1992) that makes use of the deep-water wave height also was designed whilst also considering the effect of waves breaking in front of the structure.

Simulations were performed with a bathymetry only consisting of data from 'Vaklodingen', as well as with a bathymetry that is a combination between the 'Vaklodingen' data and a local measurement provided by Tennet. There are significant differences between these bathymetries (see Section 3.2.2), but these differences are considered to be within the order of the natural beach dynamics. As such, the actual bathymetry could be different from the most recent site investigation, but likely within the bandwidth presented by the measurements. Therefore, a variety of parameter combinations is considered belonging to results from simulations with an older bathymetric survey (the 'Vaklodingen') and to results from simulations with the most recent bathymetric survey. The bandwidth in input to the scour model is considered to govern the intrinsic uncertainty associated with scour predictions.

5.2.3 Expected scour development

To assess the scour due to waves, and the possible bandwidth therein, we consider a total of five different cases. The bandwidth in input conditions for the cases is selected as discussed in Section 5.2.2, and thus governs conditions associated with the vaklodingen bathymetry (larger water depth) and conditions associated with the updated bathymetry (smaller water depth). The model output provides the time-development of the storm, from which representative maximum, mean and minimum storm characteristics can be derived as input for the cases. For each of these cases, the scour depth is computed with empirical equations from Fowler (1992), the Shore Protection Manual (1984), Kraus and McDougal (1996) and the data of Deltares (2007). The five cases are as follows:

- Case 1: Maximum (peak) storm conditions
- Case 2: Average (mean) storm conditions
- Case 3: Minimum (low end) storm conditions
- Case 4: Maximum wave heights, minimum period, maximum storm surge (overload)
- Case 5: Maximum wave heights, minimum period, medium storm surge

The conditions for each respective case are shown in Table 5.1. The selected unbroken wave height in front of the structure was determined based on the water depth (following the approach as in the wave loads section). In this section, a breaker parameter of 0.5 was selected for the significant wave height. The maximum unbroken wave height in this section was (conservatively) derived to be 0.78 times the local water depth in front of the structure. All conditions in Table 5.1 are based on the numerical model results, and they span the range in parameters presented in Chapter 3. In general, the conditions of the RP1yr, RP5yr and RP20yr

storm are quite similar, and the main differences in, for example, the water depth in front of the structure are due to the selected bathymetry. For example, Case 1 is representative of a RP20yr storm for the Vaklodingen bathymetry, whereas Case 2 is representative of a RP20yr storm for the TenneT bathymetry. Similarly, Case 2 can also be representative for a storm with a shorter return period for the Vaklodingen bathymetry (although these were not explicitly simulated). Cases 3 is a 'mild' condition case more resembling of daily conditions. Cases 4 and 5 are overload conditions based on Cases 1 and 2. This is how the below table, and the variation in the cases, should be interpreted.

Table 5.1 Definition of the cases for which the wave-related scour depth was assessed.

Parameter	Parameter value				
	Case 1	Case 2	Case 3	Case 4	Case 5
Water depth in front of structure	3.0 m	2.0 m	0.5 m	3.0 m	2.0 m
Unbroken wave height in front of structure	2.34 m	1.56 m	0.39 m	2.34 m	1.56 m
Current velocity in front of structure	1.10 m/s	0.75 m/s	0.30 m/s	1.10 m/s	1.10 m/s
Deep water significant wave height	6.3 m	5.5 m	4.0 m	6.3 m	6.3 m
Deep water peak period	14.00 s	12.50 s	10.00 s	9.00 s	9.00 s

The results of the scour assessment using the various formulae is shown in Table 5.2.

Table 5.2 Wave-related scour depth according to the various formulae

Formulation	Scour depth [m]				
	Case 1	Case 2	Case 3	Case 4	Case 5
Fowler (1992)	5.0	4.4	3.2	6.3	6.3
SPM (1984)	2.3	1.6	0.4	2.3	1.6
SPM incl. Current (1984)	2.7	1.8	0.4	2.7	1.8
Kraus & McDougal (1996)	1.8	1.2	0.3	1.8	1.2
Deltares (2007)	2.5	2.2	1.6	2.7	2.5

It is noted that, in general, the scour depths as predicted by the lower four formulae are of the same order of magnitude. The formulation of Fowler (1992) leads, in all cases, to significantly larger scour depths than the other formulations. As mentioned in the previous section, the formulation by Fowler includes breaking waves, which might explain this difference. However, since breaking waves were observed during the experiment from Deltares (2007), this difference cannot be fully attributed to breaking waves. Another argument to dismiss the formulae by Fowler is that it does not include site-specific wave propagation, while the other formulae do make use of local nearshore conditions. Thus, the lower four formulae are considered to provide the most realistic bandwidth for the present scour assessment.

The results in Table 5.2 can be interpreted as follows. Case 1 involves the maximum modelled wave heights and periods, as well as the maximum storm surge level. These maxima are only occurring for a relatively short time, whereas in this assessment it is assumed that they occur sufficiently long for equilibrium to be reached. Hence, the results of Case 1 can be seen as an upper limit. Likewise, to account for uncertainty in the input and/or uncertainty in the empirical relations, an overload case is defined with a combination of the most unfavourable conditions; Case 4. In a similar fashion a minimum case is defined (Case 3). These minimum conditions do occur during a storm, but most of the time they are exceeded. The predicted scour depth for this case can therefore be interpreted as a lower limit. The most likely cases seem to be

Cases 2 and 5, whereas uncertainty in the input, bathymetry and the formulae is covered by considering the other cases. As such, a reasonable estimate for the expected wave-related scour depth during an RP20yr storm is 1-2 m, although it cannot be excluded that the wave-related scour depth could be between 0.5 – 3 m.

5.3 Scour due to alongshore currents

5.3.1 Theoretical background

As mentioned in Section 5.2.1, no explicit relations exist for determining cofferdam scour, let alone for scour around a sheet pile wall protected with a geotube. As for the wave-related scour, a similar useful reference situation exists in the form of scour around abutments placed in rivers. River abutments have a similar shape as the present structure and are situated in a steady current. Empirical formulae for the scour depth around abutments were derived by Melville (1997). In a later study, Coleman et al. (2003) further developed those formulae specifically for clear-water scour situations, where also time development was assessed.

Scour development around an abutment is, besides the current velocity, dependent on abutment dimensions like size and shape, as well as the median grain diameter, alignment of the abutment, channel geometry and time. For the situation as considered in the present study, correction factors for the cofferdam shape, median grain diameter w.r.t. the cofferdam size and alignment are all 1. Essentially, the equilibrium depth of the scour hole is in this case a function of the abutment blockage area, the intensity of the flow and the duration of the condition.

First, the influence of the abutment area is considered. The formulae of Melville (1997) were derived for a rectangular channel, whereas in this study a beach profile is considered. Therefore, the effective blockage area of a cofferdam sticking out a certain length is less than that of a similarly sized abutment placed in a rectangular channel. To correct for this, we assume a linear increase in bed level at the cofferdam between its most seaward edge towards the land boundary. By doing so, a correction factor of 0.7 is derived for the blockage area. Furthermore, the relation between the scour depth and abutment geometry was also shown to be a function of the relative shallowness of the flow by Melville (1997), a feature that is thus also taken into account.

In the clear water regime, the influence of the flow velocity is most generally captured by the ratio of the flow velocity with the critical flow velocity needed to entrain sediment. If the flow velocity is larger than the critical flow velocity, the influence of the flow velocity on the depth of the scour hole is minimal, and thus for those cases the equilibrium depth is solely dependent on the dimensions of the cofferdam. More precisely, on the effective flow blocking area of the cofferdam.

Time development is assessed with two different methods. Firstly, the formulations of Coleman et al. (2003) are used. These are however only applicable to the clear-water scour regime, whereas it is expected that during storm conditions the flow velocities exceed the critical velocity. Therefore, an in-house formulation for time development of scour is used as well. This formulation was applied for use around monopiles but can be calibrated for different structures as well by varying an entrainment parameter. This parameter was varied such that the time-scale found is of the same order of magnitude as the validated formulation of Coleman et al. (2003), and with those settings applied to conditions outside the clear-water regime.

5.3.2 Considered input parameters

For this analysis, the input parameters considered are:

- The depth-averaged current velocity
- Flow depth at the seaward edge of the cofferdam
- Protrusion of the cofferdam into the flow (“wet length of the cofferdam”)
- Median grain diameter at the structure (assumed 150 µm)
- Duration of the peak flow condition

We make use of the Melville (1997) equations for abutment scour, in combination with in-house developed knowledge of time development of scour holes. As with the wave-induced scour, we define a number of cases based on the output of the different model runs. The cases are selected such that the range of parameter variability found in the model simulations is well represented in the scour assessment.

5.3.3 Expected scour development

As with the scour assessment for wave-related scour, a number of different cases are considered. These involve storm conditions, as well as operational (daily) conditions. For the storm conditions, the peak flow condition is a nominal flow condition representative for that storm, and the duration of that condition is based on the numerical model output. Based on this output, a duration of the peak condition of 12 hours is deemed representative. Although for the ‘vaklodingen’ bathymetry the duration of the peak condition can be slightly longer, it is assumed that the wave-induced current is a steady current. This is an over-simplification, since also wave action is present at the geotube during storm conditions, which changes the dynamics. Therefore, a steady current with a duration of 12 hours is likely a conservative choice.

For the tidal flow conditions, the peak condition is the nominal peak tidal flow velocity. It is assumed that this peak flow velocity occurs 20 minutes every tidal cycle, and that the construction is subject to approximately half a year of tides (roughly 365 tidal cycles). For the time development of the scour depth, it is then assumed that the peak condition occurs constantly for a duration of 20 minutes times the number of tidal cycles. In the present assessment, three storm conditions and two tidal conditions are considered:

- Storm 1: High wave-induced longshore current, high storm surge
- Storm 2: High wave-induced longshore current, medium storm surge
- Storm 3: Moderate wave-induced longshore current, low storm surge
- Tidal 1: Peak tidal velocity, large local water depth
- Tidal 2: Peak tidal velocity, small local water depth

The conditions belonging to those cases are shown in Table 5.3. The interpretation of the case conditions is similar as described in Section 5.3.2, that is, the conditions spanning those cases span the variety of the simulated cases such that the outcome of the scour assessment can be applied depending on the actual bathymetry at the time of construction.

Table 5.3 Definition of the cases for which the current-related scour depth was assessed.

Parameter	Parameter value				
	Storm 1	Storm 2	Storm 3	Tidal 1	Tidal 2
Water depth in front of structure	3.0 m	2.0 m	1.5 m	1.0 m	0.5 m
Depth-averaged approach flow velocity	1.10 m/s	0.90 m/s	0.70 m/s	0.30 m/s	0.25 m/s
Cofferdam protrusion length	40 m	30 m	20 m	20 m	15 m
Duration of the peak flow condition	12 hrs	12 hrs	12 hrs	20 min	20 min

The results of the scour assessment using the Melville/Coleman approach and Deltares’ approach is shown in Table 5.4.

Table 5.4 Wave-related scour depth according to the various formulae

Formulation	Scour depth [m]				
	Case 1	Case 2	Case 3	Case 4	Case 5
Melville/Coleman (2003)	11.9	8.5	5.7	0.5	0.3
Deltares (2020)	5.8	4.1	2.4	0.6	0.3

As can be seen in Table 5.4, for the tidal conditions both formulations predict a scour depth that is of the same order of magnitude. However, large differences can be seen for the storm cases. For one, this is explained by the fact that the Melville/Coleman timescale formulation was developed and validated for clear-water conditions only. For the storm conditions, the occurring flow velocity is larger than the critical flow velocity, thus the scour is not in the clear-water regime anymore. For Case 3, a flow velocity of 0.70 m/s is imposed for a time duration of 12 hours, whereas in Case 4 a flow velocity of 0.3 m/s is imposed for a duration of 240 hours. The jump from a scour depth of 0.5 m for Case 4 towards a scour depth of 5.7 m for Case 3 seems excessive based on a comparison of the conditions. A scour depth as predicted by Deltares' time scale relation therefore seems more realistic. The Melville/Coleman predictions for storm conditions are considered overly conservative.

Therefore, it is stated that in the case that no storm occurs for the lifetime of the landfall structure, that is, the landfall is only subject to tidal flow, the expected scour depth is roughly 0.5-1 m. For a storm as simulated in the numerical modelling study, it is not unlikely to expect a scour depth of 3-6 m to develop during the storm. This ultimately depends on the actual local bathymetry implementation of the geotube.

5.4 Synthesis

Based on the above assessment we expect scour to develop at the outer side of the geotube. At the seaside (blue area in Figure 5.1) the scour will mainly be the result of reflected waves and will therefore develop during storms. In this area we expect scour in the order of 1-2 m, which can develop in a single storm event. Around the corners (red areas in Figure 5.1) the scour will be the result of alongshore currents. In tidal-only condition this scour development is roughly expected to be in the order of 0.5-1 m. However, when combined with storm-induced alongshore currents, scour depths of 3-6 m are expected to develop within a single storm event. Although the geotube is a flexible structure that can deform slightly along with the formation of scour in front of the tube, the development of the presented 3-6 m of scour occurs within roughly 12 hours. In that case the expected deformation of the geotube is so large that it's function of protecting the soil wedge in front of the sheet pile wall is completely compromised. As a result, the soil wedge in front of the sheet pile wall will be rapidly washed away by the storm conditions, posing an unacceptable risk to the stability of the sheet pile wall. Mitigating measures to prevent undermining of the geotube are therefore required.

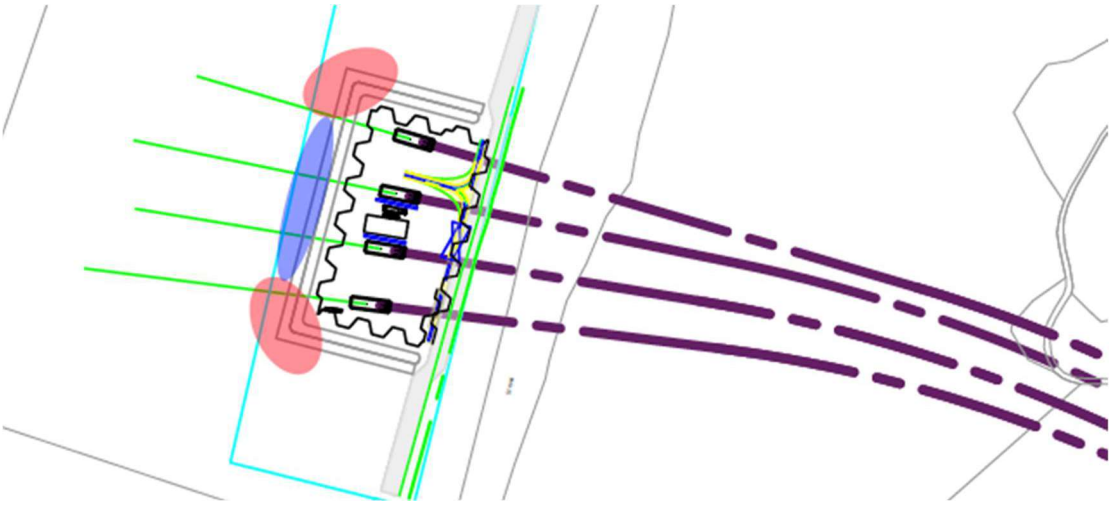

Figure 5.1 Local scour around the geotube and cofferdam

5.5 Attention points for the design of the temporary landfall structure

Based on the assessment of the scour development around the geotube, we recommend preventing undermining of the geotube by applying a scour protection at the outer side of the geotube. We recommend an extent of this protection of 10 m away from the geotube. Please note that such an additional protection will not prevent scour from developing, but it will keep it further away from the geotube (and prevent undermining of the geotube). Wave-related scour is expected to develop within 1/4 wave length away from the geotube. Therefore, depending of course on the actual wave lengths, it is less likely that wave-related scour develops 10 m away from the geotube. We can expect some current-related scour to develop at the edge of the geotextile, but this will likely be significantly less than the anticipated 3-6 m.
This part of the scour protection should be flexible, so that it can adapt (in shape) to the scour holes that will develop at the edges. Moreover, it should be sand-tight and it should be stable within the design conditions. When this part of the scour protection consists of a geotextile, it likely requires additional weight (anchoring geotubes) to keep it in place. Alternatively, the edges of the geotextile might be buried in the sand.

As indicated in Figure 5.1 the largest scour depth is expected around the seaward corners of landfall structure and related to alongshore currents. A more “streamlined” shape of the structure might decrease the current velocities around the corners, which in turn might decrease the scour development at these locations. At this stage this effect cannot be quantified. However, it is not expected that a more favourable shape will dismiss the requirement of an additional scour protection in front of the geotube altogether. Installation considerations might therefore be governing for the selected shape of the landfall structure.

The observed range in bathymetry (see Section 3.2.2 and Section 3.5) is already included in the present scour assessment. Consequently, the presented expected scour depths are valid for this full range of the bathymetry. We would like to note however, that when encountering a relatively low bathymetry, possibly two geotubes should be placed on top of each other to obtain the required height of the soil mass in front of the sheet pile wall. In this case, we recommend applying the geotubes in an overlapping or staggered configuration, to prevent any gaps between the individual tubes as much as possible. This same attention point holds for adjacent geotubes.

Moreover, when a relatively low bathymetry is encountered upon installation, the water might reach the backside (landward side) of the landfall structure, which might induce scour at this

side as well. This might be prevented by installing geotubes up to a level above the expected maximum water level.

6 Conclusions and recommendations

6.1 Conclusions

Below we have described the main findings per task.

Task 1: Determination of the offshore extreme metocean conditions

Based on an Extreme Value Analysis of hindcast data available for this area, offshore extreme conditions (RP1yr, RP5yr and RP20yr condition) are derived.

Task 2: Determination of the nearshore metocean conditions

A translation of the offshore metocean conditions towards the landfall structure is made by means of a numerical model. In this translation we have distinguished several hydrodynamic conditions (tidal, RP1yr, RP5yr and RP20yr condition). The available bathymetrical data showed significant differences of the beach profile in the last years. As it is not known a-priori what bathymetry will be encountered during installation, two different bathymetries are included in this assessment. Please note that when a relatively low bathymetry is encountered, possibly two geotubes need to be placed on top of each other to obtain the required height of the soil mass in front of the sheet pile wall. We would also like to note that the encountered bathymetry will also determine if the water level is expected to reach the landward side of the structure during storm events. Local erosion effects at this side of the structure can therefore not be excluded at the present stage.

Task 3: Assessment of the wave loads on the geotubes and sheet pile wall

Based on the outcome of Task 2, combined with empirical and analytical knowledge and expertise, wave loads acting on the geotube and sheet pile wall are derived for three return periods (RP1yr, RP5yr and RP20yr), two bathymetries and three exceedance values (2%, 1% and 0.1%), see Table 4.1. In all cases we have assumed a situation where the height of one geotube is sufficient to obtain the required height of the soil mass in front of the sheet pile wall.

Task 4: Assessment of the scour development around the structure

Based on the outcome of Task 2, combined with empirical and analytical knowledge and expertise, we expect a scour development within a single storm event in the order of 1-2 m at the seaward side of the structure (in front of the geotube) and 3-6 m at the seaward corners. Based on this expected scour development (both the depth and rapid development) around the geotube, we recommend preventing undermining of the geotube by applying a scour protection at the outer side of the geotube. Please note that we have not included any large scale profile changes in this assessment.

6.2 Recommendations

For the recommendation we refer to the attention point provided in the separate chapters/tasks; Section 3.5, Section 4.6 and Section 5.5.

References

Battjes, J.A. and Groenendijk, H.W. (2000). Wave height distributions on shallow foreshores. *Coastal Engineering*, **40**, 161-182.

Chen, X., Hofland, B., Altomare, C., Suzuki, T., and Uijttewaal, W. (2015). Forces on a vertical wall on a dike crest due to overtopping flow. *Coastal Engineering*, **95**, 94-104.

Coleman, S.E., Lauchlan, C.S. and Melville, B.W., 2003. Clear-water scour development at bridge abutments, p. 521-531. Journal of Hydraulic Research, Vol. 41, No. 5

Delft Hydraulics, 2007. Influence of collapsed revetments on dune erosion. Large-scale model tests, Report H4731.

Dienst Hydrografie - Geodesie & Getijden (2006): Memorie - Noordzee reductiematrix, Link: https://www.defensie.nl/onderwerpen/hydrografie/downloads/rapporten/2007/04/27/memorie-noordzeereductiematrix-2006

Fowler, J.E., 1992. Scour problems and methods for prediction of maximum scour at vertical seawalls. T.R. CERC 92-16. U.S.W.E.S., Vicksburg, USA

Kraus, N.C. and McDougal, W.G., 1996. The effects of seawalls on the beach: Part I and Part II, p. 691-701 and p. 702-713. Journal of Coastal Research, Vol. 12, No. 3

Melville, B.W., 1997. Pier and abutment scour: integrated approach. Journal of Hydraulic Engineering, Vol. 123, No. 2

Raubenheimer, B., Guza, R.T., and Elgar, S. (1996). Wave transformation across the inner surf zone. *Journal of Geophysical Research*, **101**(C10), 25589-25597.

Shore protection manual, 1984. Volume I and II, Coastal Engineering Research Center, Dep. of the Army, Waterways Exp. Station, Vicksburg, Mississippi, USA

Steetzel, H., 1988. Scour holes near seawalls (in Dutch), Report H298 part 4, Delft Hydraulics, Delft, The Netherlands

Appendices

A Extreme value analysis

The extreme value analysis approach applied in this study is based on the Peaks-Over-Threshold (POT) method, e.g. (Coles, 2001). It consists of fitting the Generalized Pareto Distribution (GPD) to the peaks of clustered excesses over a threshold, the excesses being the observations in a cluster minus the threshold, and calculating return values by taking into account the rate of occurrence of clusters. Under very general conditions this procedure ensures that the data can have only three possible, albeit asymptotic, distributions (the three forms of the GPD) and, moreover, that observations belonging to different peak clusters are (approximately) independent. More precisely, the peaks of clustered excesses over a high threshold *u*, $y = z - u$, are assumed to occur in time according to a Poisson process with rate λ_u and to be independently distributed with a GPD, whose distribution function is given by

$$F_u(y) = \begin{cases} 1 - \left(1 + \xi \frac{y}{\sigma_u}\right)^{-1/\xi}, & \text{for } \xi \neq 0 \\ 1 - \exp\left(-\frac{y}{\sigma_u}\right), & \text{for } \xi = 0, \end{cases},$$

where $0 < y < \infty$, $\sigma_u > 0$ and $-\infty < \xi < \infty$. The two parameters of the GPD are called scale (σ_u) and shape (ξ) parameters. When $\xi = 0$ the GPD is said to have a type I tail and amounts to the exponential distribution with mean σ_u; when $\xi > 0$ it has a type II tail and it is the Pareto distribution; and when $\xi < 0$ it has a type III tail and it is a special case of the beta distribution. If $\xi < 0$, just as with the GEV distribution, the support of the GPD has an upper bound, $-\sigma_u / \xi$, which is called the *upper end-point* of the GPD and is to be thought of as the upper-limit of the excesses, the upper limit of the variable of interest being then $u - \sigma_u / \xi$.

One of the main applications of extreme value theory is the estimation of the *m year (m-yr) return value*, the value which is exceeded on average once every *m* years. The *m*-yr return value based on a POT/GPD analysis, z_m, is given by[2]

$$z_m = \begin{cases} u + \frac{\sigma_u}{\xi}\{(\lambda_u \mathrm{m})^{\xi} - 1\}, & \text{for } \xi \neq 0 \\ u + \sigma_u \ln(\lambda_u \mathrm{m}), & \text{for } \xi = 0. \end{cases}$$

Note that this expression is obtained by solving $(1 - F_u(y)) = \frac{1}{\lambda_u m}$ for *y* and then adding the threshold *u* to the result.

The choice of threshold represents a trade-off between bias and variance: choosing too low a threshold is likely to violate the asymptotic basis of the model, leading to bias; a threshold which is too high will generate fewer excesses with which to estimate the model, leading to high variance. An important property of the POT/GPD approach is the threshold stability property: if a GPD is a reasonable model for excesses of a threshold u_0, then for a higher threshold u a GPD should also

2. In this report the natural logarithm of x is written as ln(x).

apply; the two GPD's have identical shape parameter and their scale parameters bear a simple relation. This property of the GPD was used to find the optimal threshold to fit a GPD model to the data.

The sample to be used in the POT method has to be extracted from the original time series in such a way that the data can be modelled as independent observations. This is done by a process of declustering in which only the peak (highest) observations in clusters of successive exceedances of a specified threshold are retained and, of these, only those which in some sense are sufficiently apart (so that they belong to more or less 'independent storms') are considered as belonging to the collection of POT points. Specifically, in the present application we have treated cluster maxima at a distance of less than 48 h apart as belonging to the same cluster (storm).

There are several methods available for the estimation of the parameters of the GPD. For the type of data we are concerned with in this report the method of Probability-Weighted Moments (PWM) represents an adequate choice (for details, see Hosking and Wallis, 1987, Hosking et al., 1985 and Caires, 2016). In order to provide reliable asymmetric confidence bands, the method of PWM has been combined with adjusted bootstrap estimates (see Coles and Simiu, 2003 and Caires, 2007) for computing confidence intervals.

To recap, the extreme value analysis procedure applied here consist of the following steps:

1 POT samples of storm maxima are collected from the original time series using different thresholds.
2 For each POT sample the GPD parameters and their uncertainties are estimated.
3 Based on the variation of the shape parameter estimates with the threshold, the optimal threshold is chosen.
4 Fixing this threshold, the definite return values estimates and confidence intervals are computed.

A.1 References

Caires, S., 2007: Extreme wave statistics. Confidence Intervals. WL | Delft Hydraulics Report H4803.30.

Caires, S., 2016: A comparative simulation study of the annual maxima and the peaks-over-threshold methods. J. Offshore Mech. Arct. Eng., 138(5), doi:10.1115/1.4033563.

Coles, S., 2001: An Introduction to the Statistical Modelling of Extreme Values. Springer Texts in Statistics, Springer-Verlag: London.

Coles, S. and E. Simiu, 2003: Estimating uncertainty in the extreme value analysis of data generated by a hurricane simulation model. J. Engrg. Mech., 129 (11), 1288-1294.

Hosking, J. R. M. and J. R. Wallis, 1987: Parameter and quantile estimation for the Generalized Pareto Distribution. Technometrics, 29, 339–349.

Hosking, J.R.M., J.R. Wallis, and E.F. Wood, 1985: Estimation of the generalized extreme-value distribution by the method of probability-weighted moments. Technometrics, 27, 251-261.

B Offshore extreme conditions

B.1 Return value plots wind

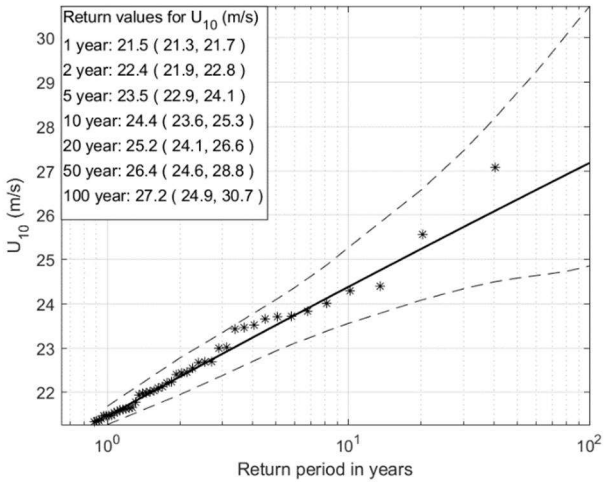

Figure B.1 Omni-directional U_{10} return value plot for all locations. The dashed lines are the associated 95% confidence intervals. The POT data are represented by the asterisks, with as plotting position (xi, (n+1)/(l_u(n+1-i)), where n is the sample size, i the order and l_u the Poisson rate.

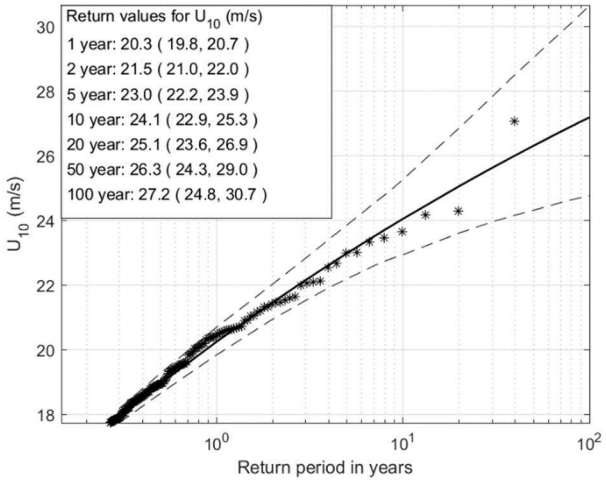

Figure B.2 As Figure B.1, now for Sector 240.

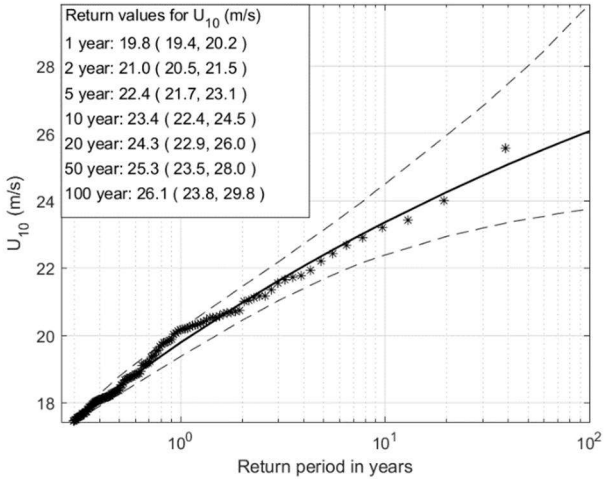

Figure B.3 As Figure B.1, now for Sector 270.

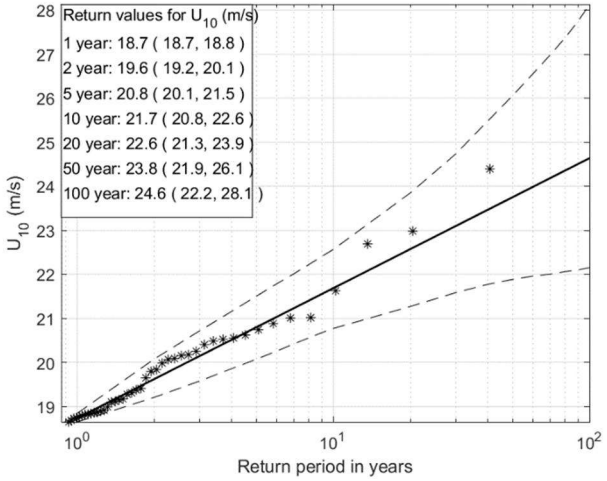

Figure B.4 As Figure B.1, now for Sector 300.

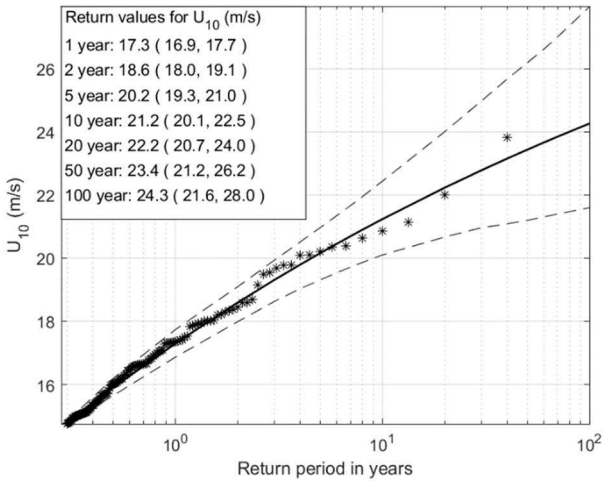

Figure B.5 As Figure B.1, now for Sector 330.

B.2 Return value plots waves

B.2.1 Location WS

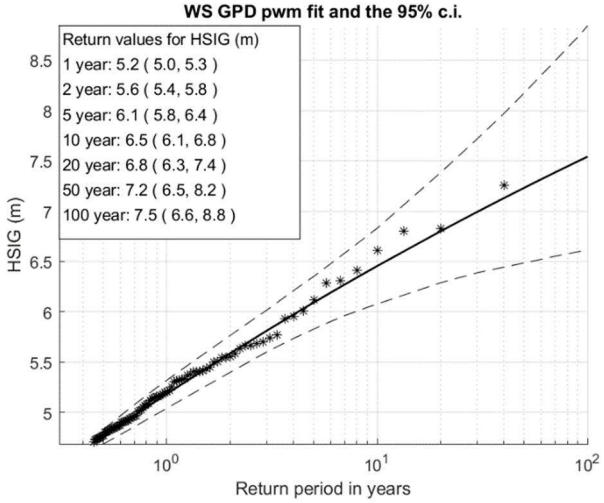

Figure B.6 WS omni-directional H_s return value plot. The dashed lines are the associated 95% confidence intervals. The POT data are represented by the asterisks, with as plotting position (xi, (n+1)/(l_u(n+1-i)), where n is the sample size, i the order and l_u the Poisson rate.

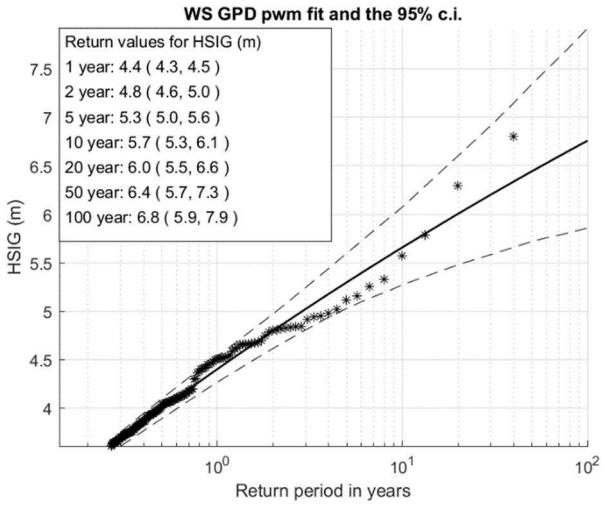

Figure B.7 As Figure B.6, now for Sector 240.

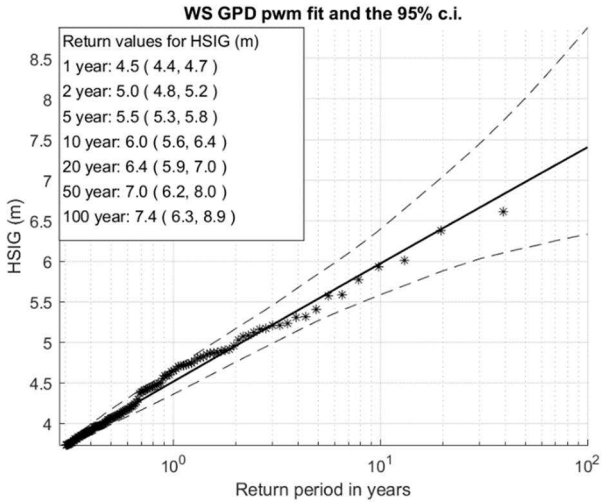

Figure B.8 As Figure B.6, now for Sector 270.

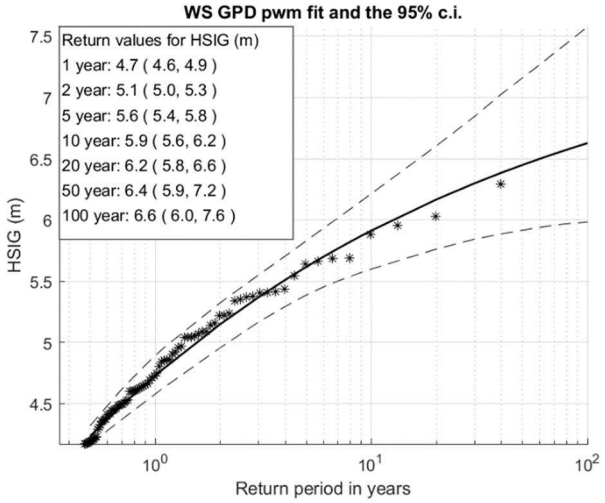

Figure B.9 As Figure B.6, now for Sector 300.

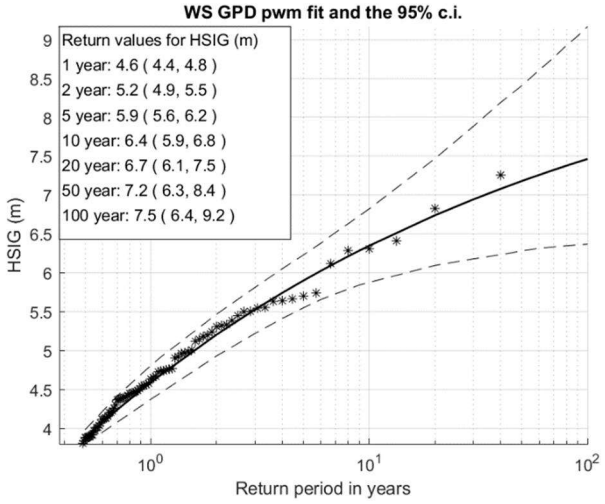

Figure B.10 As Figure B.6, now for Sector 330.

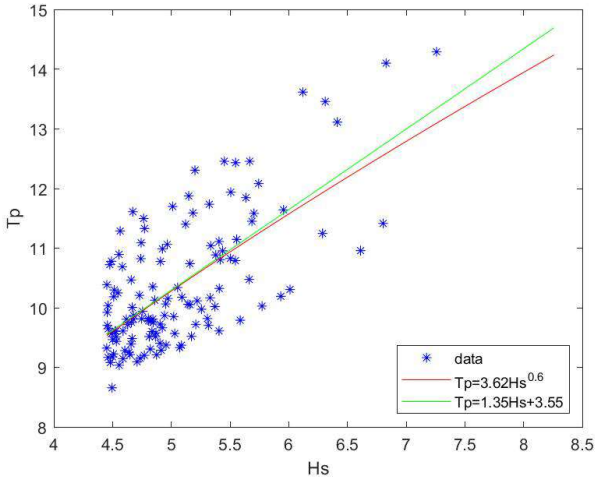

Figure B.11 WS linear and power fit through omni-directional wave height peaks and concomitant peak wave periods.

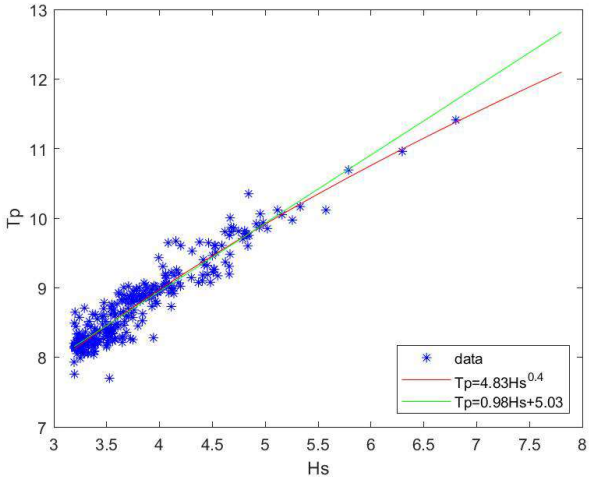

Figure B.12 As Figure B.11, now for Sector 240.

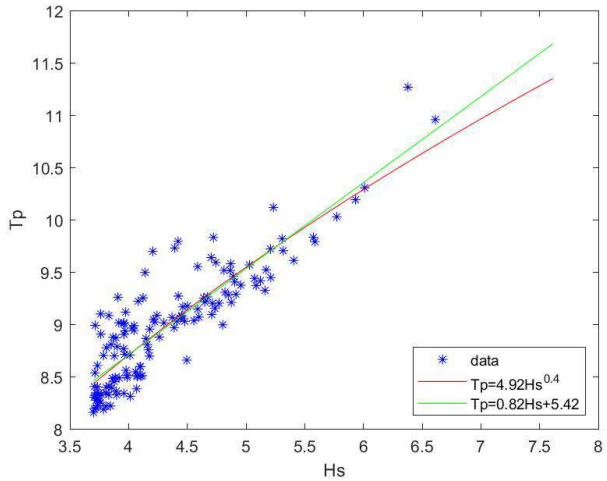

Figure B.13 As Figure B.11, now for Sector 270.

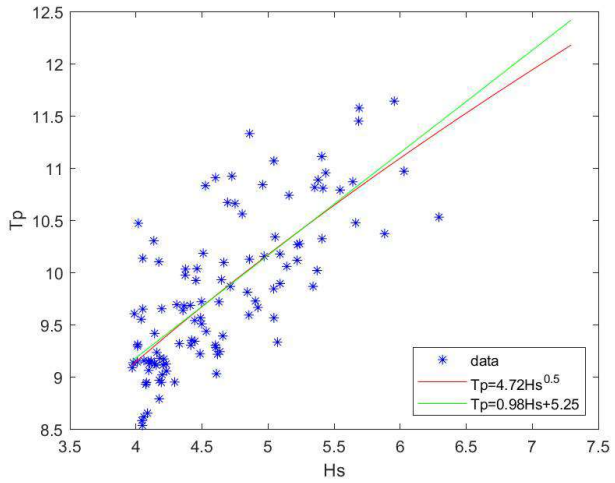

Figure B.14 As Figure B.11, now for Sector 300.

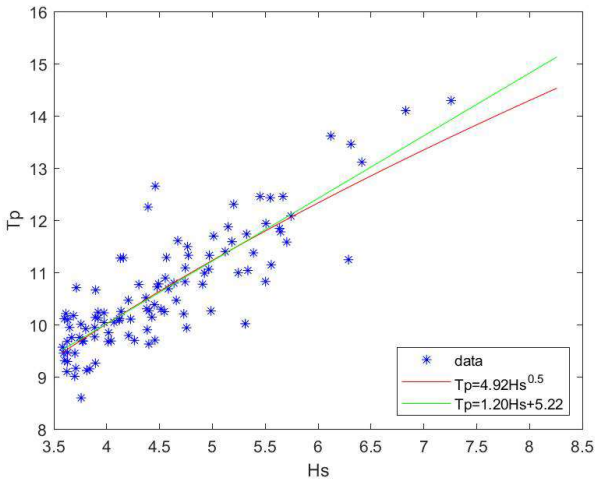

Figure B.15 As Figure B.11, now for Sector 330.

B.2.2 Location WC

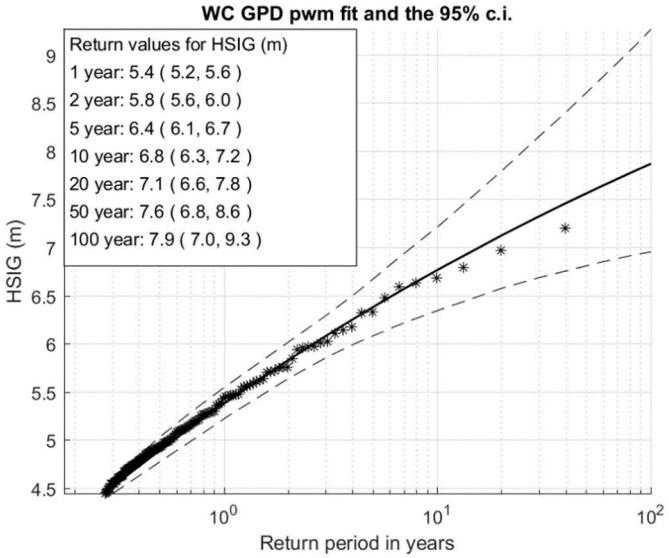

Figure B.16 WC omni-directional H_s return value plot. The dashed lines are the associated 95% confidence intervals. The POT data are represented by the asterisks, with as plotting position (xi, (n+1)/(l_u(n+1-i)), where n is the sample size, i the order and l_u the Poisson rate.

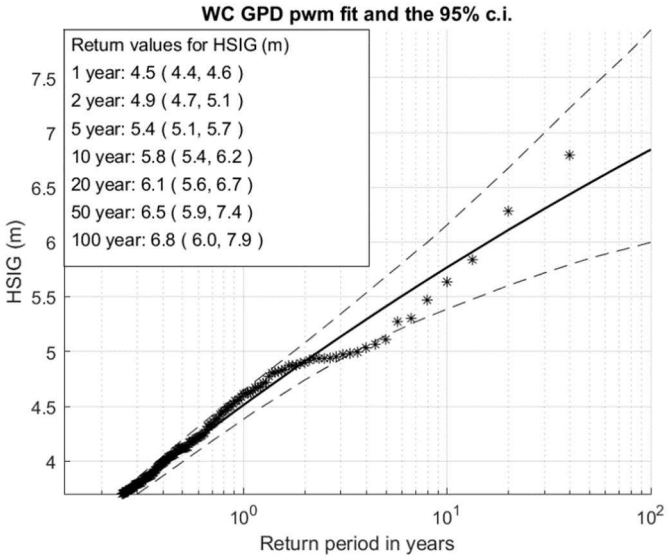

Figure B.17 As Figure B.16, now for Sector 240.

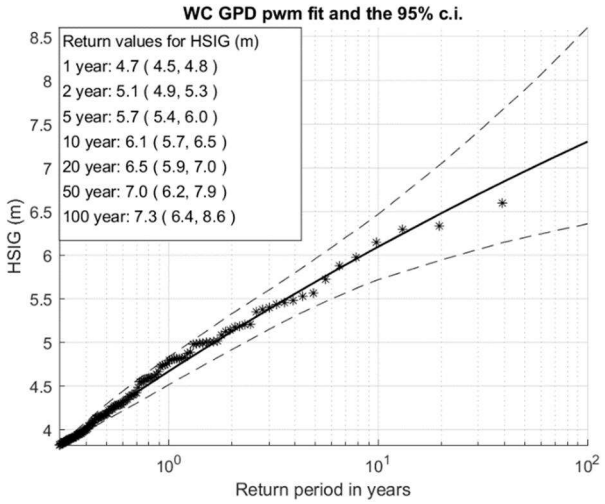

Figure B.18 As Figure B.16, now for Sector 270.

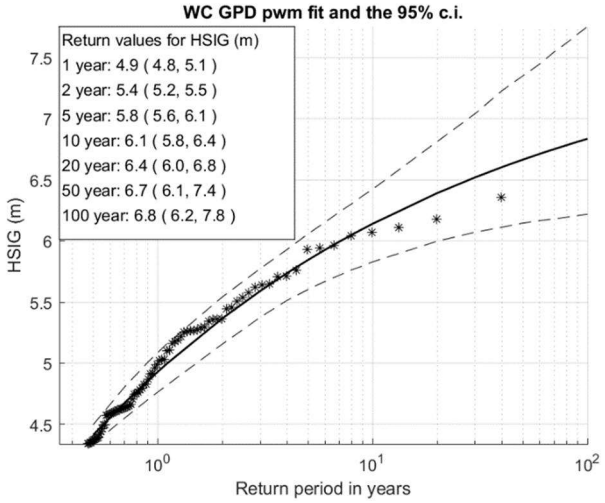

Figure B.19 As Figure B.16, now for Sector 300.

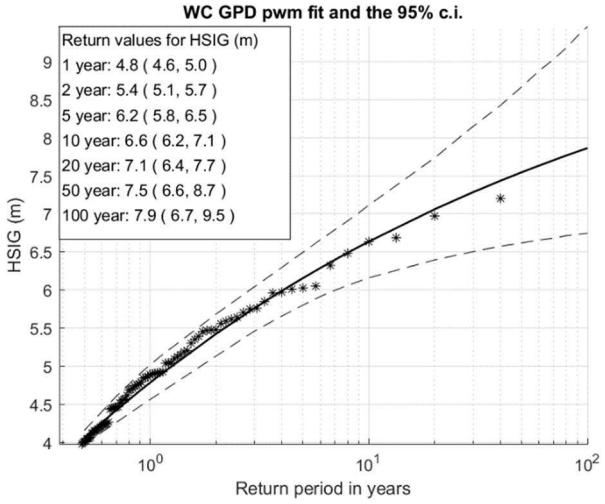

Figure B.20 As Figure B.16, now for Sector 330.

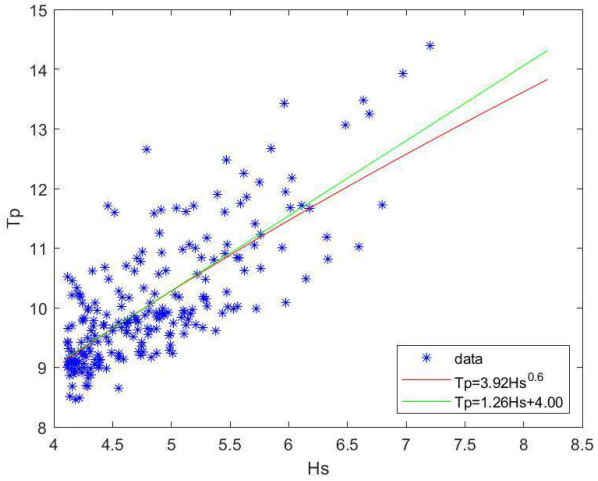

Figure B.21 WC linear and power fit through omni-directional wave height peaks and concomitant peak wave periods.

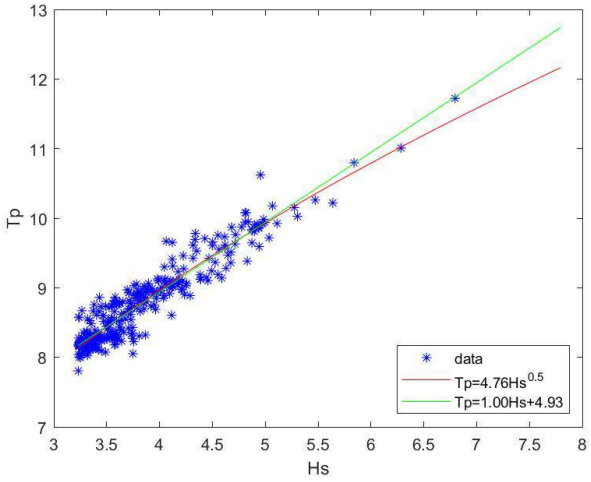

Figure B.22 As Figure B.21, now for Sector 240.

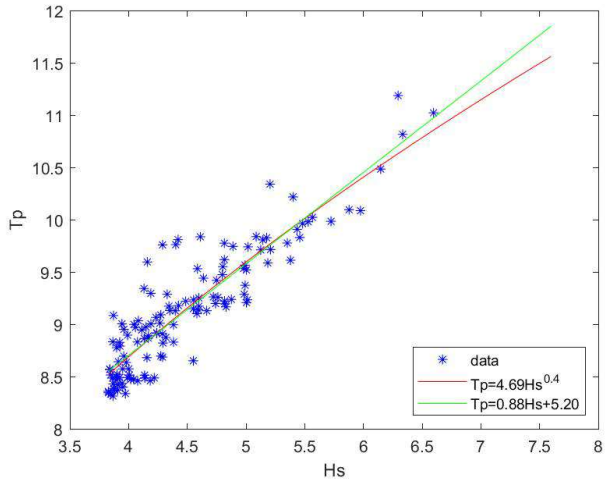

Figure B.23 As Figure B.21, now for Sector 270.

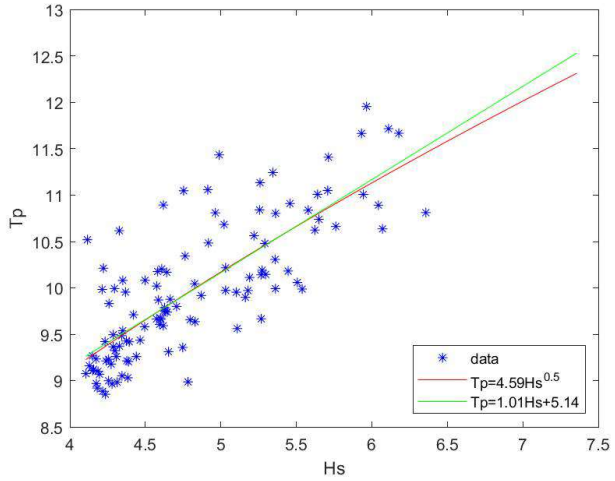

Figure B.24 As Figure B.21, now for Sector 300.

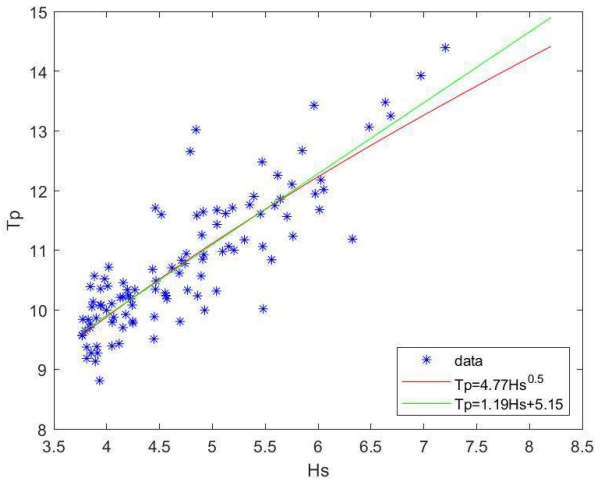

Figure B.25 As Figure B.21, now for Sector 330.

B.2.3 Location WN

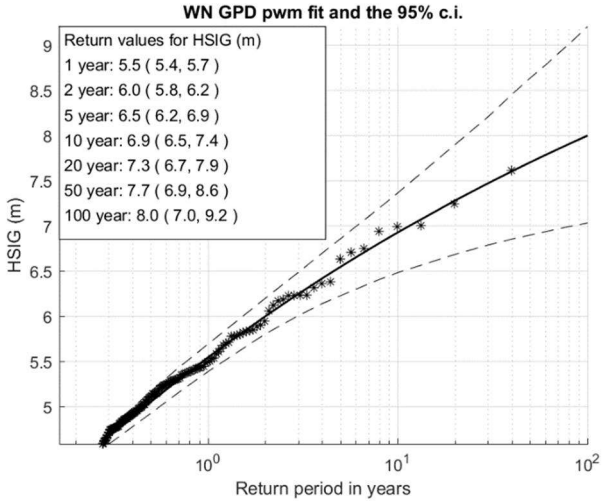

Figure B.26 WN omni-directional H_s return value plot. The dashed lines are the associated 95% confidence intervals. The POT data are represented by the asterisks, with as plotting position (xi, (n+1)/(l_u(n+1-i)), where n is the sample size, i the order and l_u the Poisson rate.

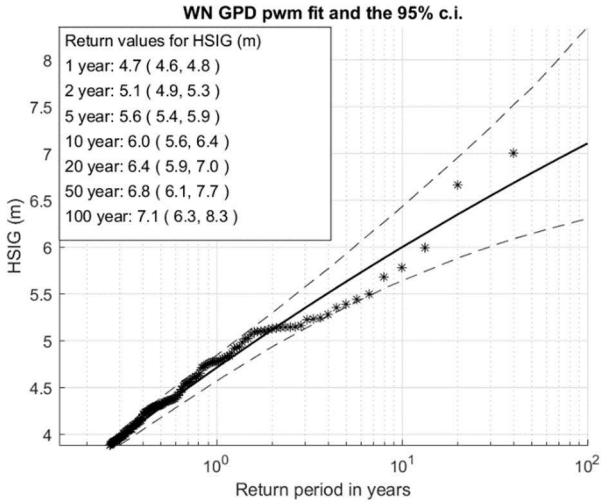

Figure B.27 As Figure B.26, now for Sector 240.

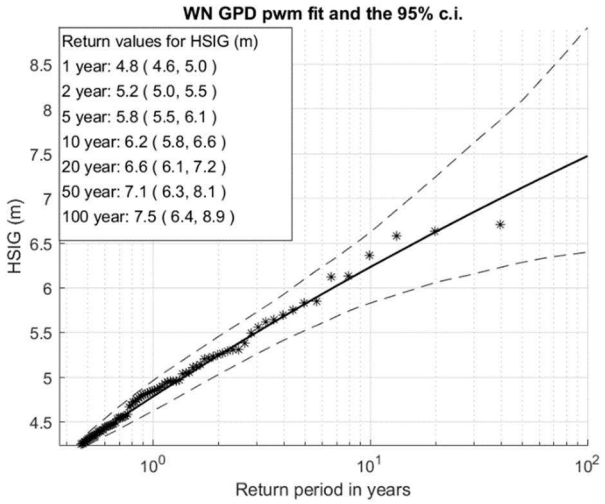

Figure B.28 As Figure B.26, now for Sector 270.

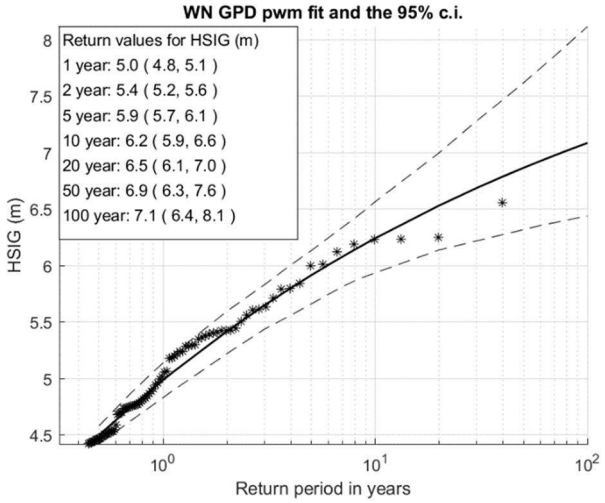

Figure B.29 As Figure B.26, now for Sector 300.

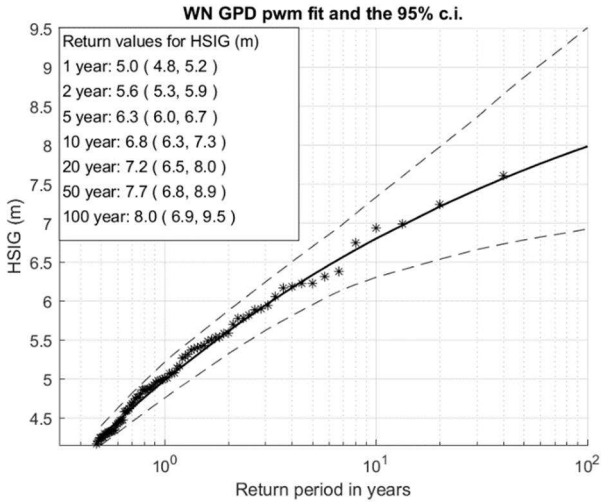

Figure B.30 As Figure B.26, now for Sector 330.

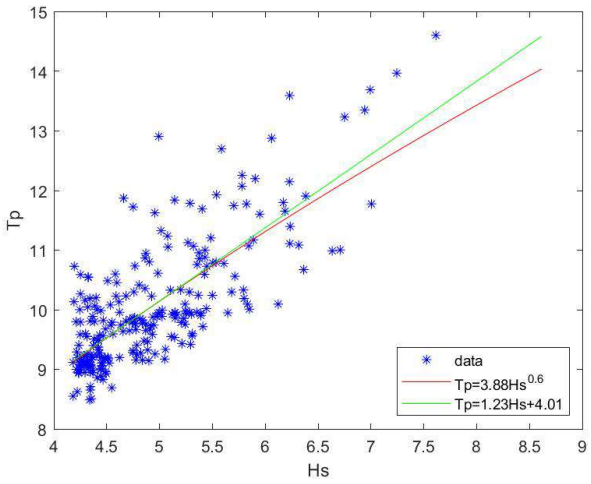

Figure B.31 WN linear and power fit through omni-directional wave height peaks and concomitant peak wave periods.

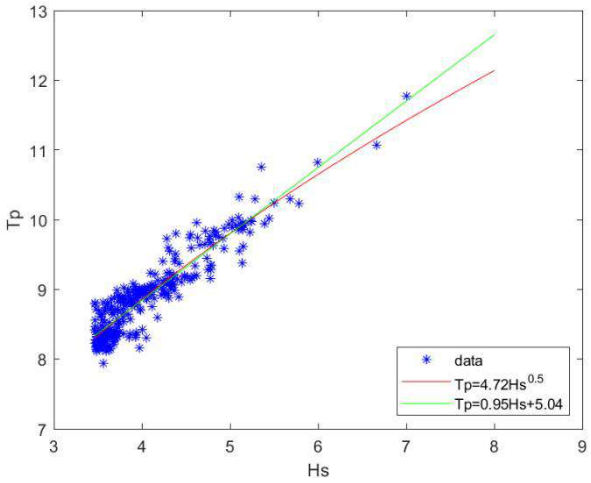

Figure B.32 As Figure B.31, now for Sector 240.

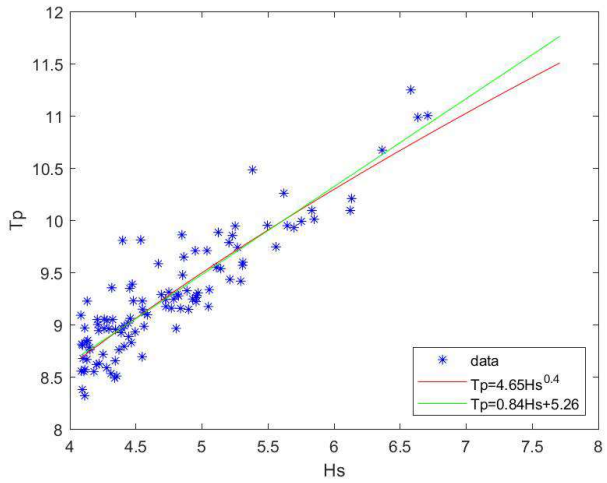

Figure B.33 As Figure B.31, now for Sector 270.

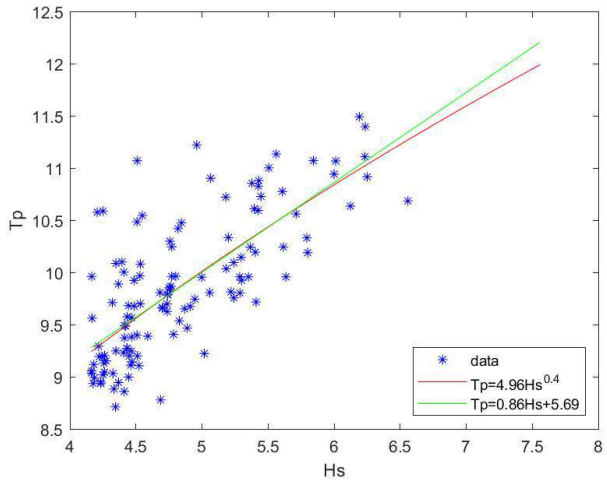

Figure B.34 As Figure B.31, now for Sector 300.

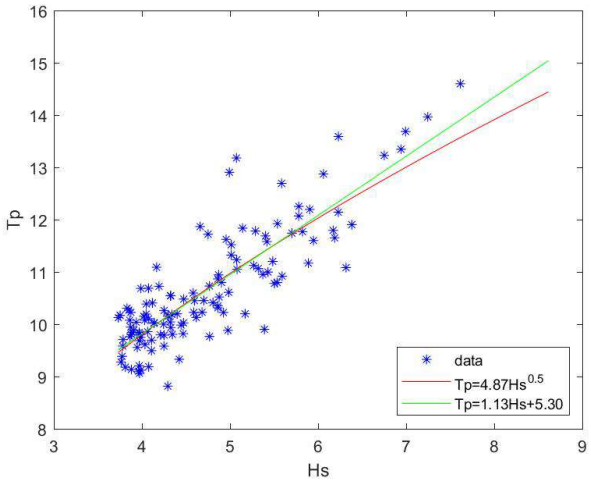

Figure B.35 As Figure B.31, now for Sector 330.

B.3 Return value plots total water levels

B.3.1 Location FS

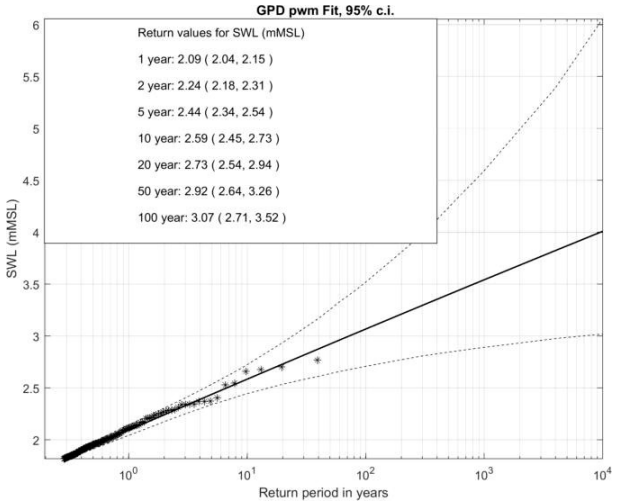

Figure B.36 FS omni-directional total water level return value plot. The dashed lines are the associated 95% confidence intervals. The POT data are represented by the asterisks, with as plotting position (xi, (n+1)/(l_u(n+1-i)), where n is the sample size, i the order and l_u the Poisson rate.

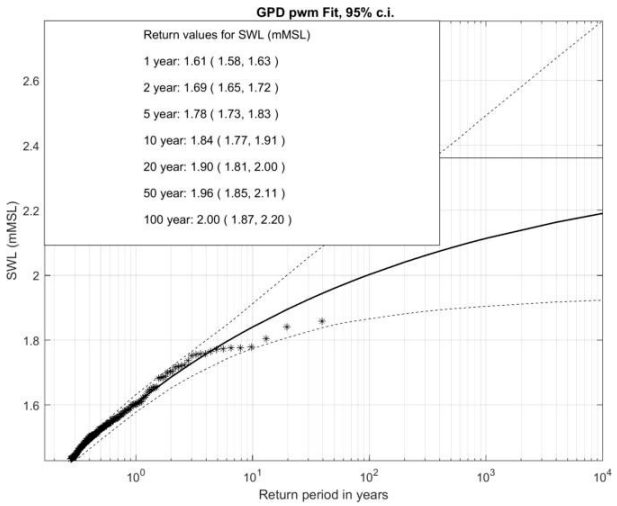

Figure B.37 As Figure B.36, now for Sector 240.

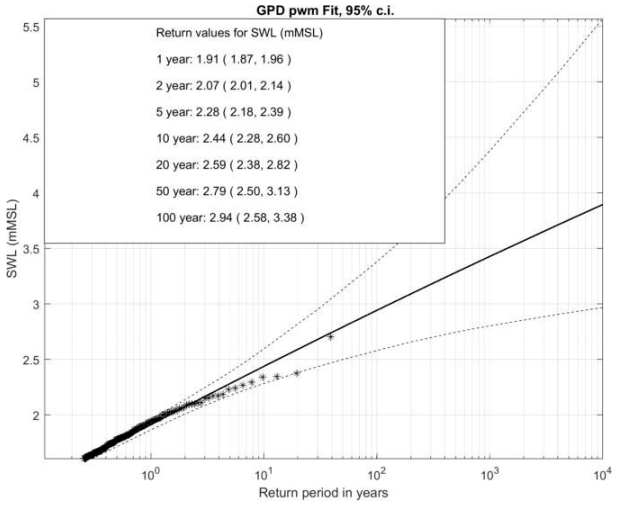

Figure B.38 As Figure B.36, now for Sector 270.

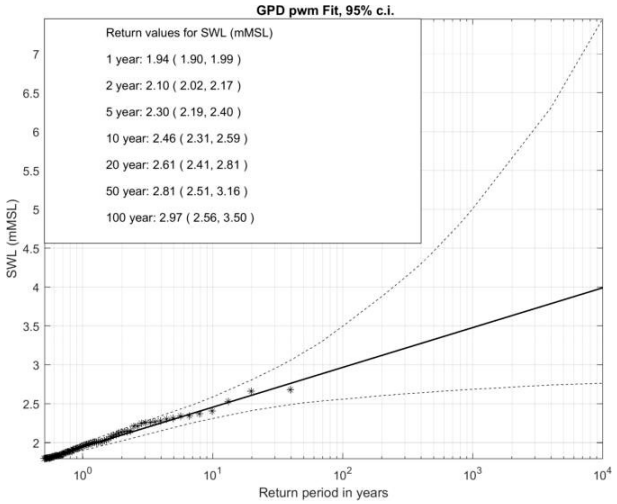

Figure B.39 As Figure B.36, now for Sector 300.

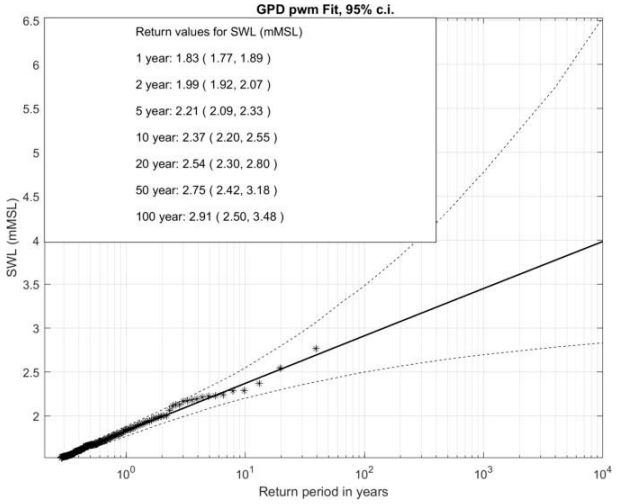

Figure B.40 As Figure B.36, now for Sector 330.

B.3.2 Location FC

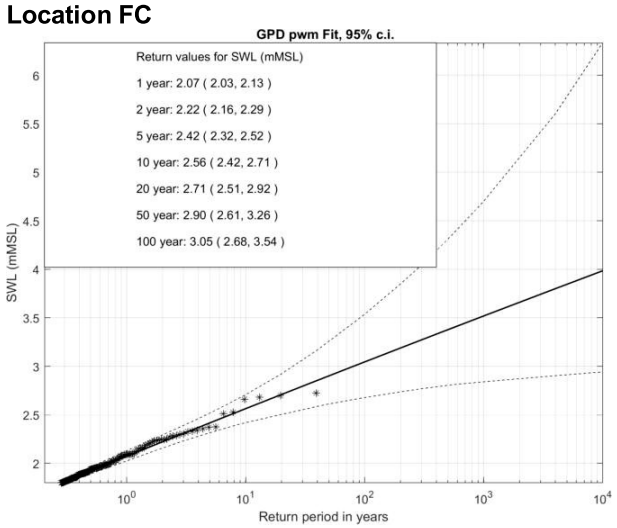

Figure B.41 FC omni-directional total water level return value plot. The dashed lines are the associated 95% confidence intervals. The POT data are represented by the asterisks, with as plotting position (xi, (n+1)/(l_u(n+1-i)), where n is the sample size, i the order and l_u the Poisson rate.

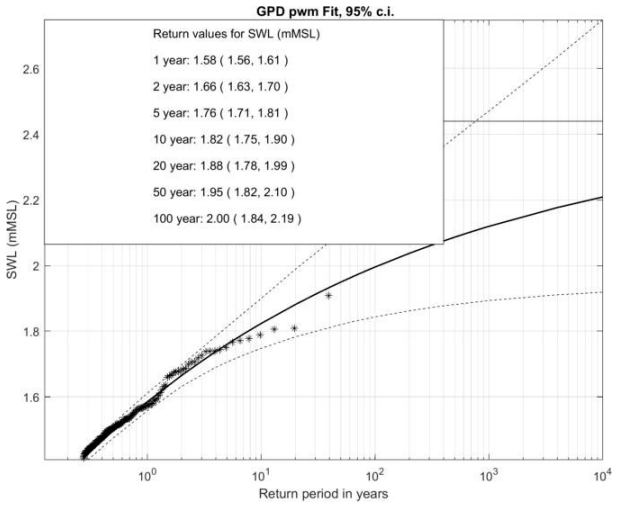

Figure B.42 As Figure B.41, now for Sector 240.

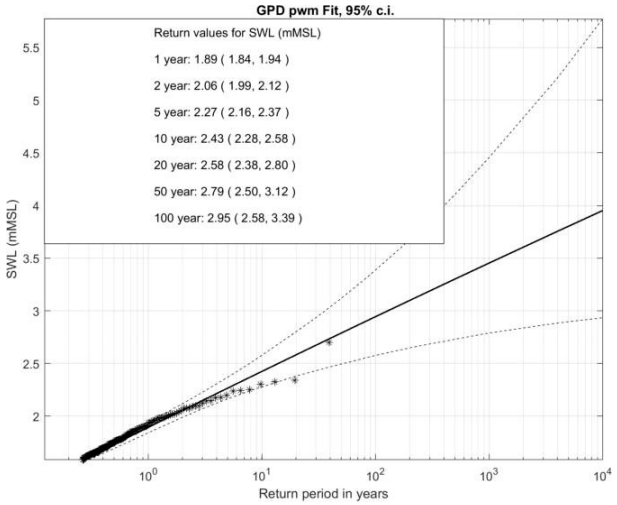

Figure B.43 As Figure B.41, now for Sector 270.

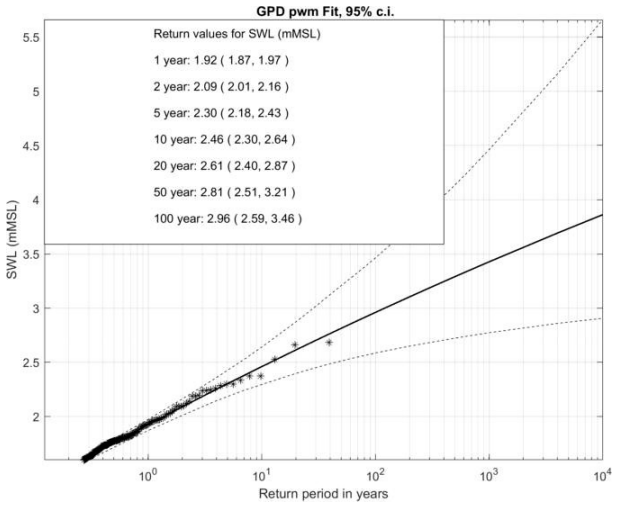

Figure B.44 As Figure B.41, now for Sector 300.

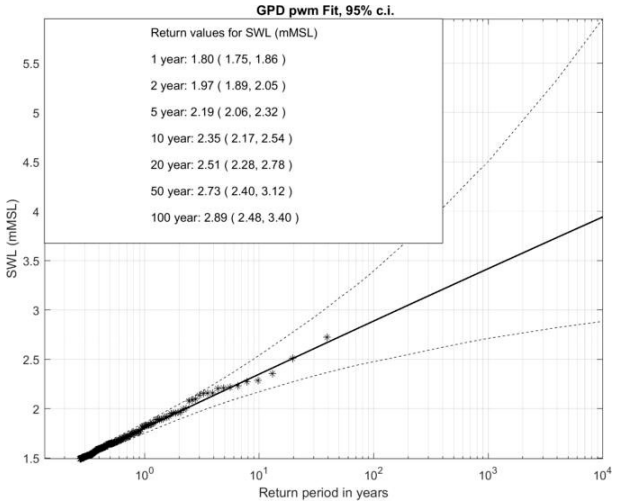

Figure B.45 As Figure B.41, now for Sector 330.

B.3.3 Location FN

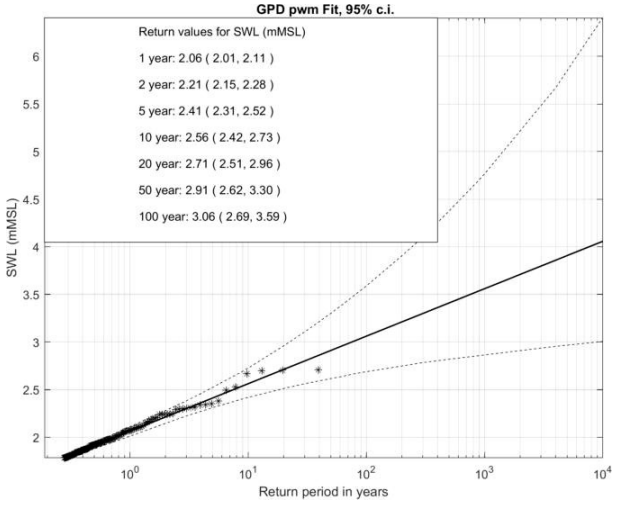

Figure B.46 FN omni-directional total water level return value plot. The dashed lines are the associated 95% confidence intervals. The POT data are represented by the asterisks, with as plotting position (xi, (n+1)/(l_u(n+1-i)), where n is the sample size, i the order and l_u the Poisson rate.

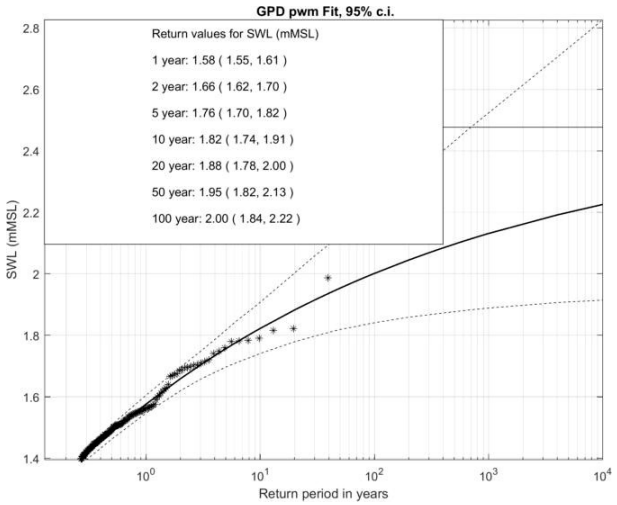

Figure B.47 As Figure B.46, now for Sector 240.

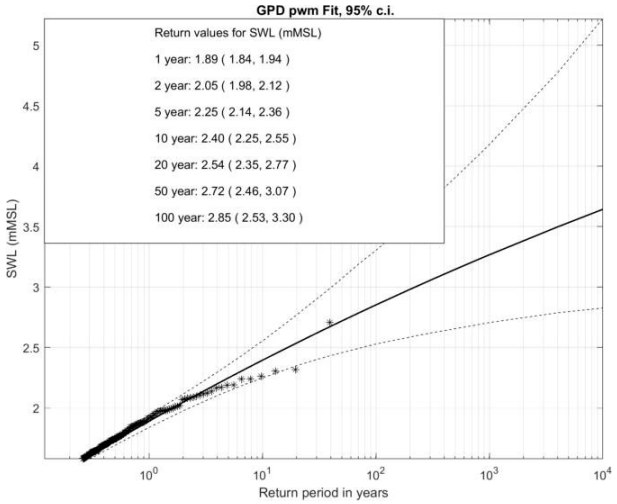

Figure B.48 As Figure B.46, now for Sector 270.

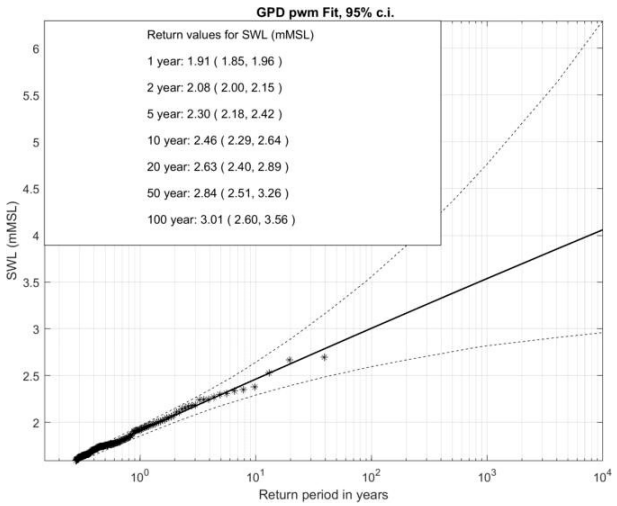

Figure B.49 As Figure B.46, now for Sector 300.

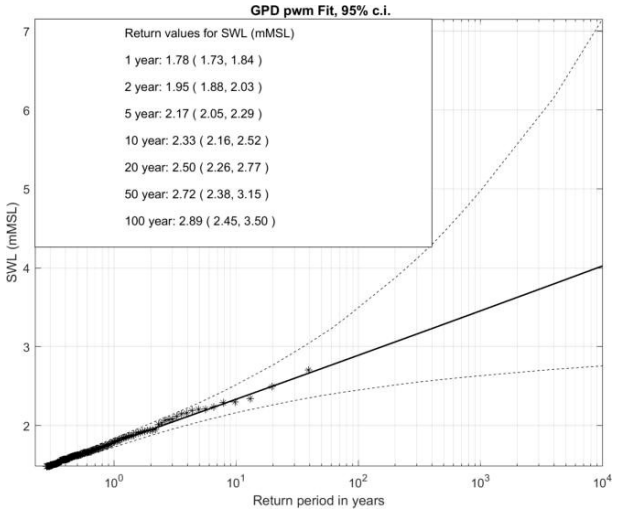

Figure B.50 As Figure B.46, now for Sector 330.

B.4 Return value plots surge levels

B.4.1 Location FS

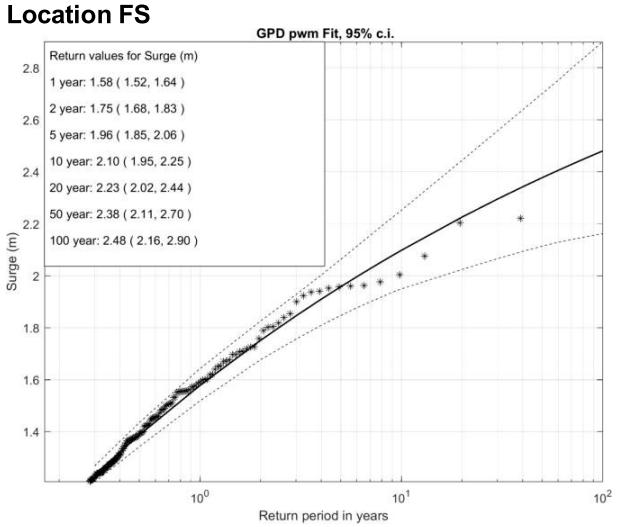

Figure B.51 FS omni-directional surge level return value plot. The dashed lines are the associated 95% confidence intervals. The POT data are represented by the asterisks, with as plotting position (xi, (n+1)/(l_u(n+1-i)), where n is the sample size, i the order and l_u the Poisson rate.

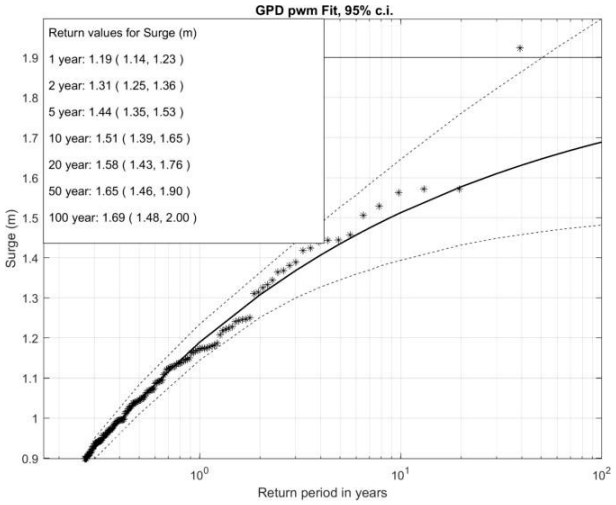

Figure B.52 As Figure B.51, now for Sector 240.

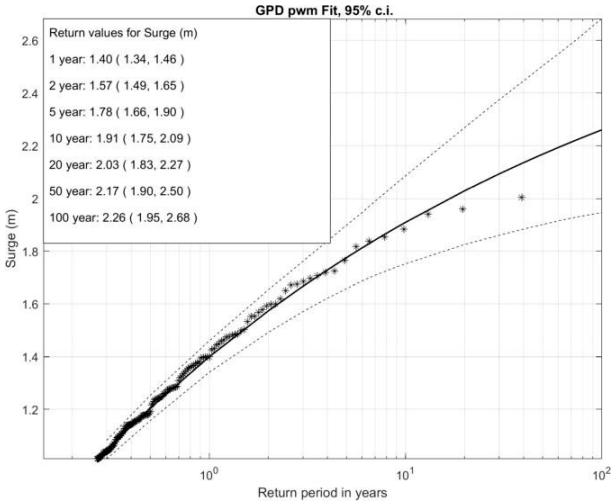

Figure B.53 As Figure B.51, now for Sector 270.

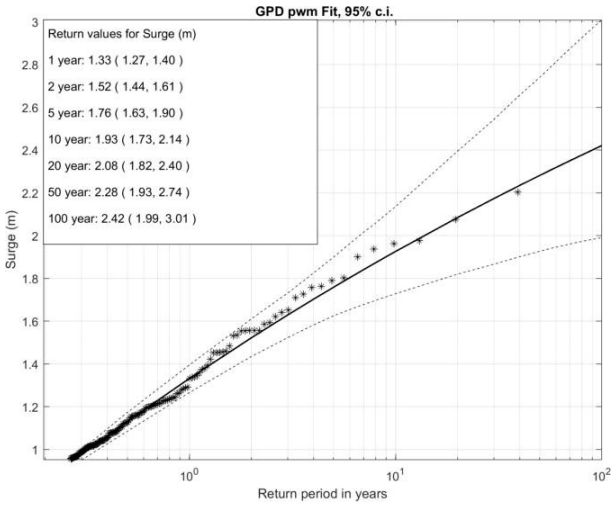

Figure B.54 As Figure B.51, now for Sector 300.

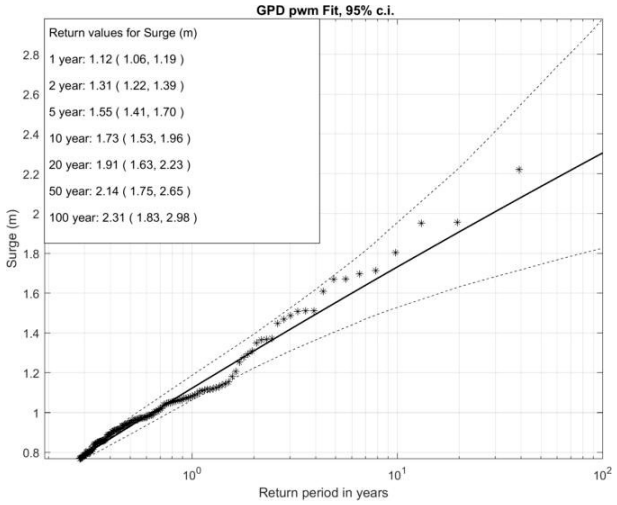

Figure B.55 As Figure B.51, now for Sector 330.

B.4.2 Location FC

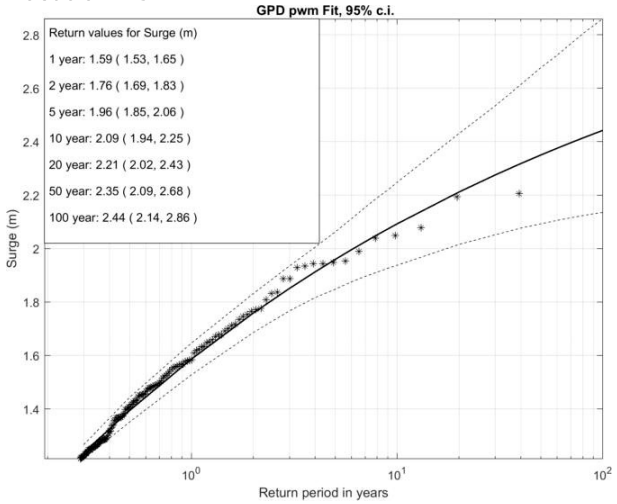

Figure B.56 FC omni-directional surge level return value plot. The dashed lines are the associated 95% confidence intervals. The POT data are represented by the asterisks, with as plotting position (xi, (n+1)/(l_u(n+1-i)), where n is the sample size, i the order and l_u the Poisson rate.

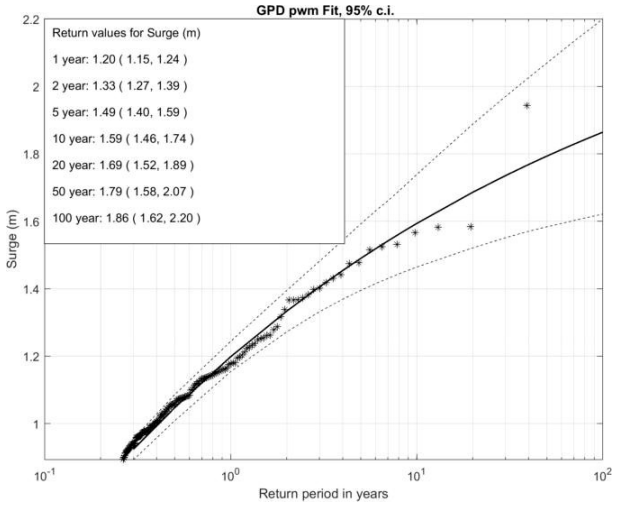

Figure B.57 As Figure B.56, now for Sector 240.

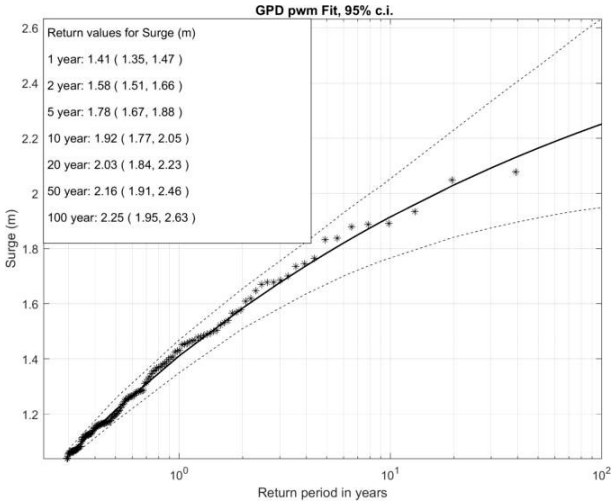

Figure B.58 As Figure B.56, now for Sector 270.

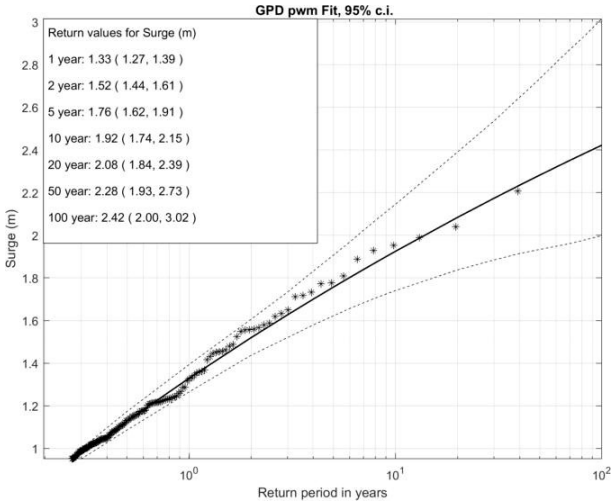

Figure B.59 As Figure B.56, now for Sector 300.

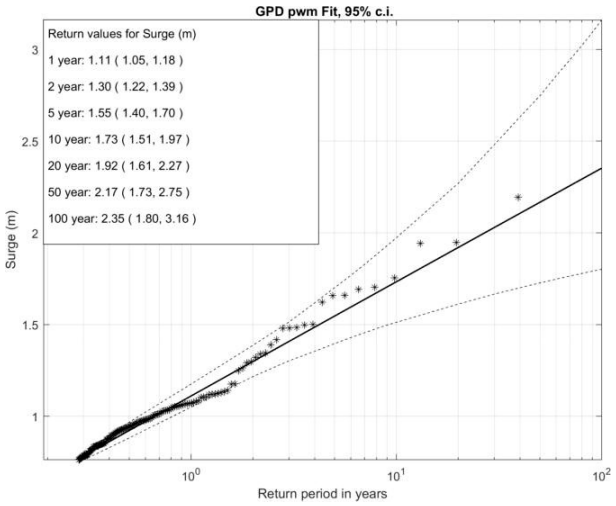

Figure B.60 As Figure B.56, now for Sector 330.

B.4.3 Location FN

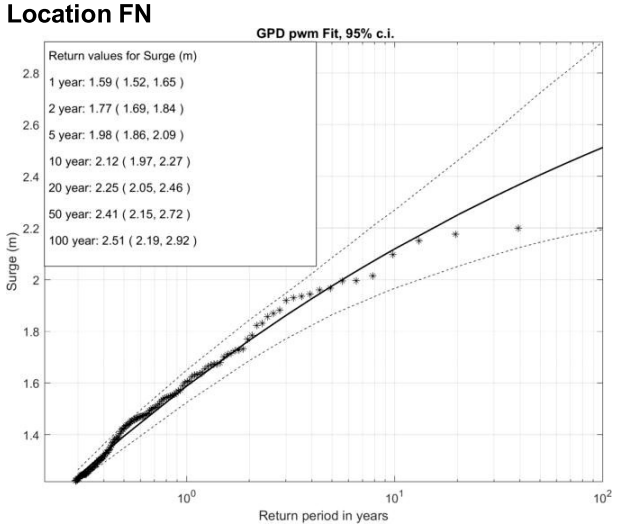

Figure B.61 FN omni-directional surge level return value plot. The dashed lines are the associated 95% confidence intervals. The POT data are represented by the asterisks, with as plotting position (xi, (n+1)/(l_u(n+1-i)), where n is the sample size, i the order and l_u the Poisson rate.

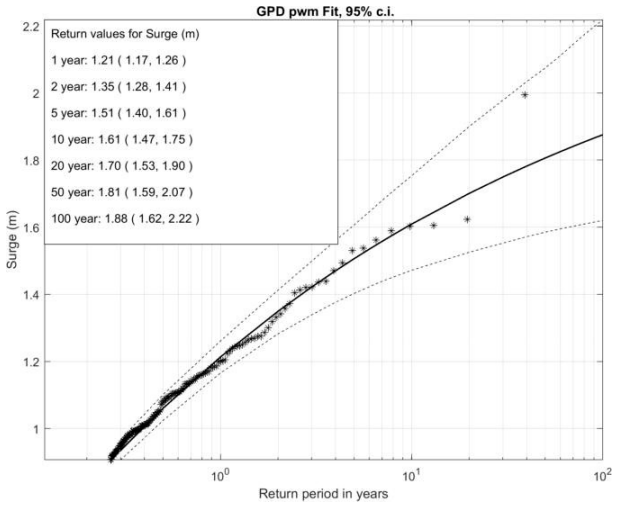

Figure B.62 As Figure B.61, now for Sector 240.

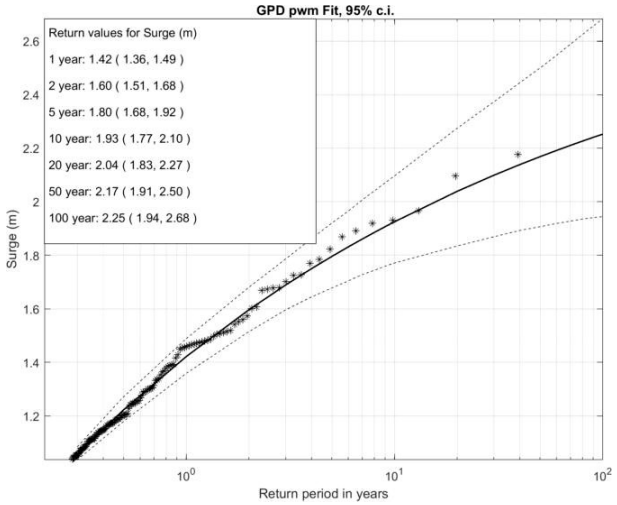

Figure B.63 As Figure B.61, now for Sector 270.

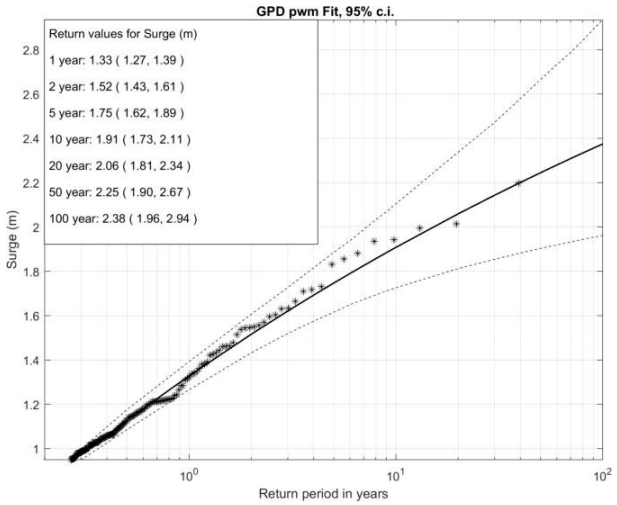

Figure B.64 As Figure B.61, now for Sector 300.

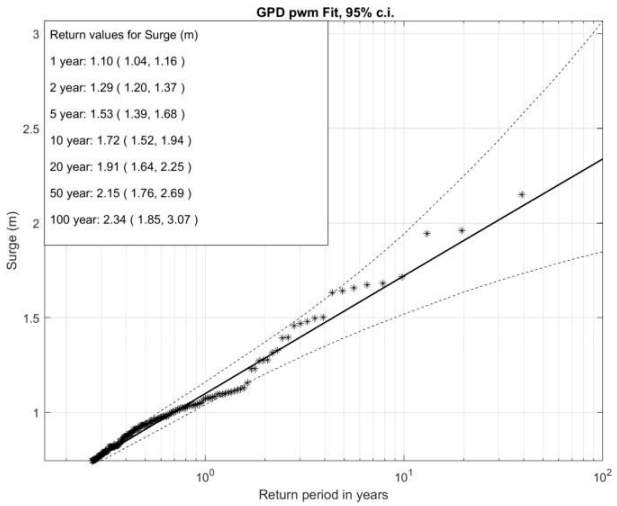

Figure B.65 As Figure B.61, now for Sector 330.

C Numerical model output at the structure

C.1 Output location information

Location name	X [m] (EPSG:28992)	Y [m] (EPSG:28992)	TenneT bathymetry [mNAP]	Vaklodingen bathymetry [mNAP]
TS1	100700.502	501639.547	2.37	2.22
TS2	100669.094	501648.796	1.45	0.93
TS3	100638.215	501656.816	0.98	0.08
TS4	100631.97	501675.468	0.87	-0.2
TS5	100646.512	501737.734	0.67	-0.22
TS6	100664.215	501791.062	0.5	-0.13
TS7	100677.357	501806.607	0.65	-0.09
TS8	100705.903	501796.499	1.43	0.52
TS9	100735.51	501790.275	1.97	1.5
TS10	100746.966	501763.776	3.95	3.95
TS11	100733.852	501713.846	3.24	3.03
TS12	100719.021	501662.266	2.83	2.83

C.2 FIow – TenneT bathymetry

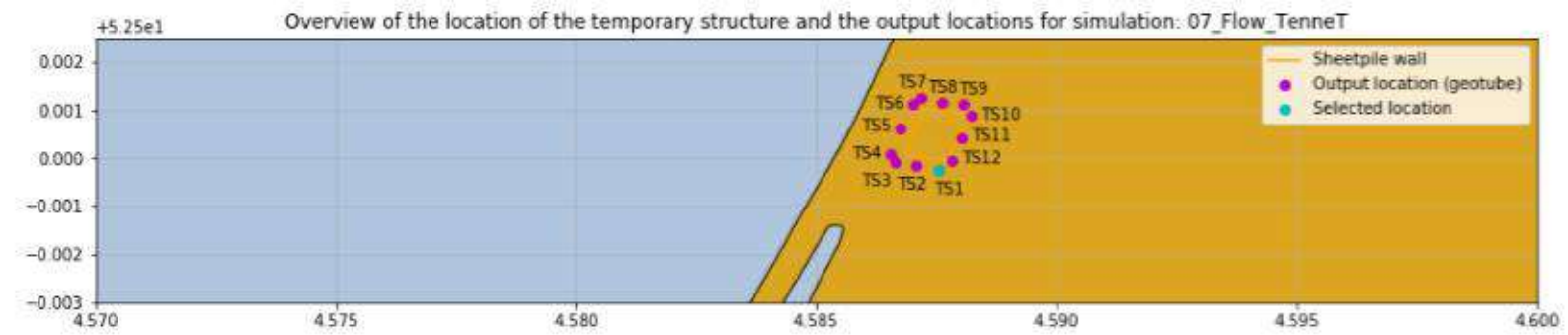
Overview of the location of the temporary structure and the output locations for simulation: 07_Flow_TenneT
+5.25e1
Sheetpile wall
Output location (geotube)
Selected location
TS1
TS2
TS3
TS4
TS5
TS6
TS7
TS8
TS9
TS10
TS11
TS12
0.002
0.001
0.000
−0.001
−0.002
−0.003
4.570
4.575
4.580
4.585
4.590
4.595
4.600

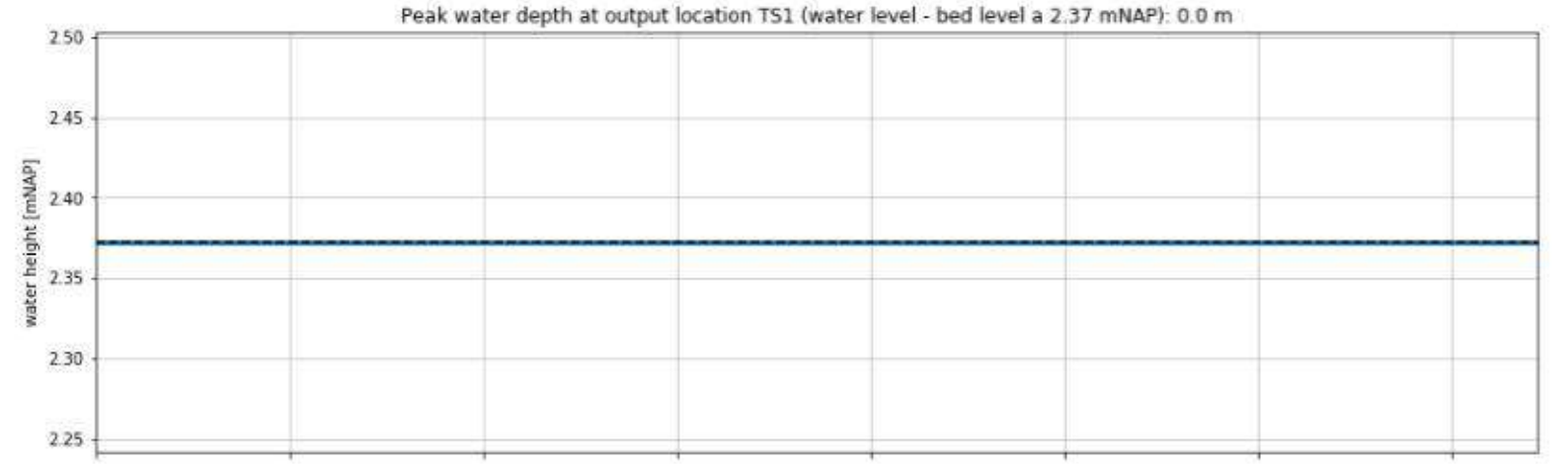
Peak water depth at output location TS1 (water level - bed level a 2.37 mNAP): 0.0 m
water height [mNAP]
2.50
2.45
2.40
2.35
2.30
2.25

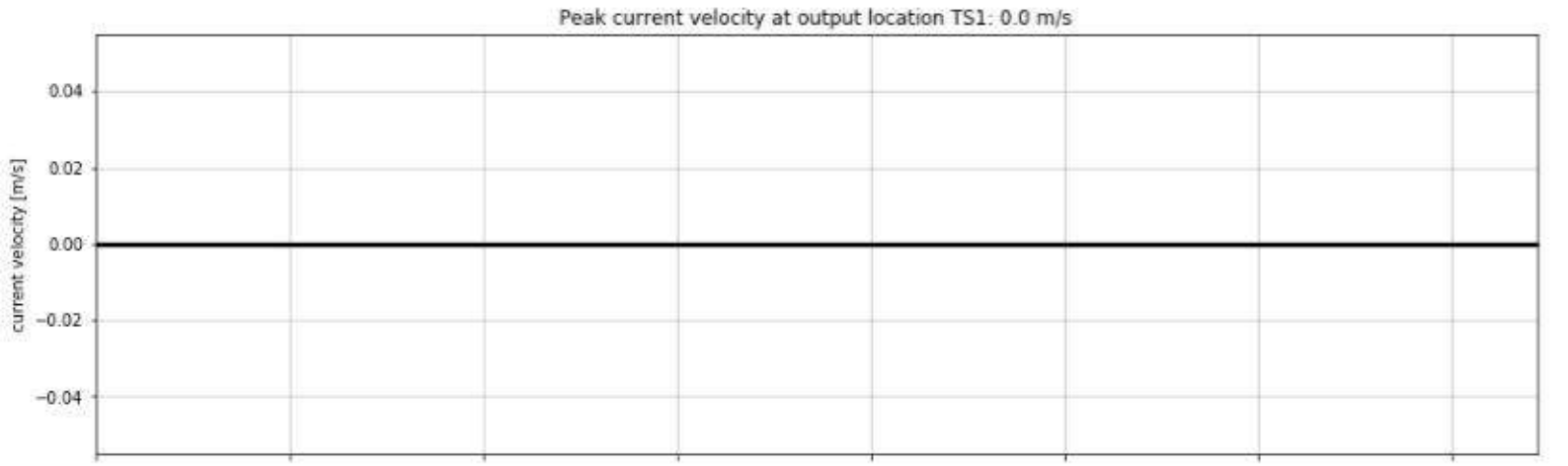
Peak current velocity at output location TS1: 0.0 m/s
current velocity [m/s]
0.04
0.02
0.00
−0.02
−0.04

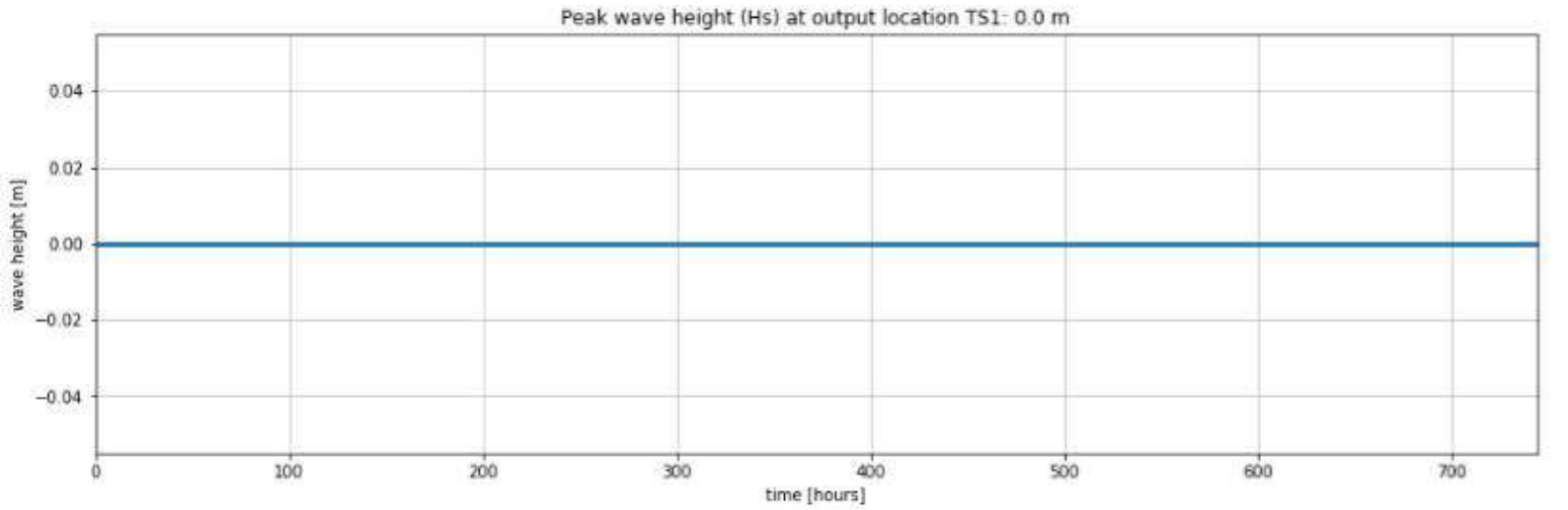
Peak wave height (Hs) at output location TS1: 0.0 m
wave height [m]
0.04
0.02
0.00
−0.02
−0.04
0
100
200
300
400
500
600
700
time [hours]

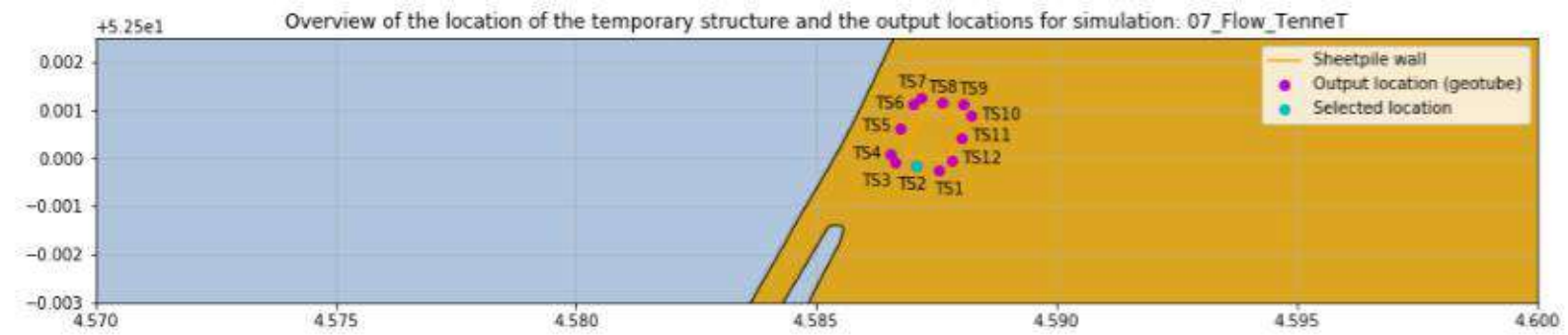
Overview of the location of the temporary structure and the output locations for simulation: 07_Flow_TenneT
+5.25e1
Sheetpile wall
Output location (geotube)
Selected location
TS1
TS2
TS3
TS4
TS5
TS6
TS7
TS8
TS9
TS10
TS11
TS12
0.002
0.001
0.000
−0.001
−0.002
−0.003
4.570
4.575
4.580
4.585
4.590
4.595
4.600

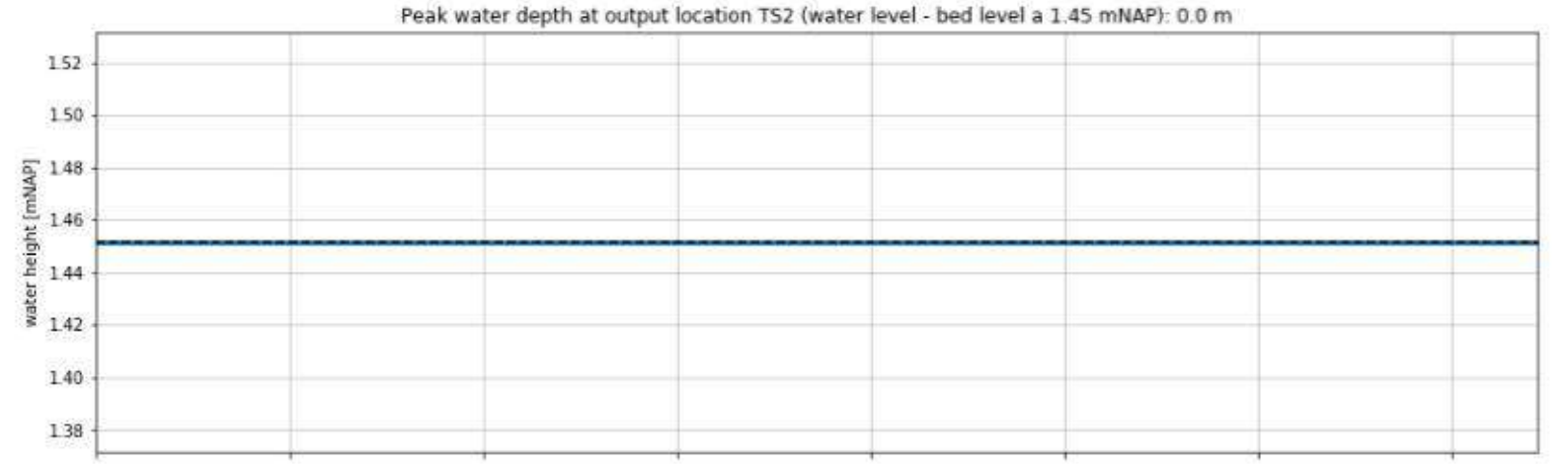
Peak water depth at output location TS2 (water level - bed level a 1.45 mNAP): 0.0 m
water height [mNAP]
1.52
1.50
1.48
1.46
1.44
1.42
1.40
1.38

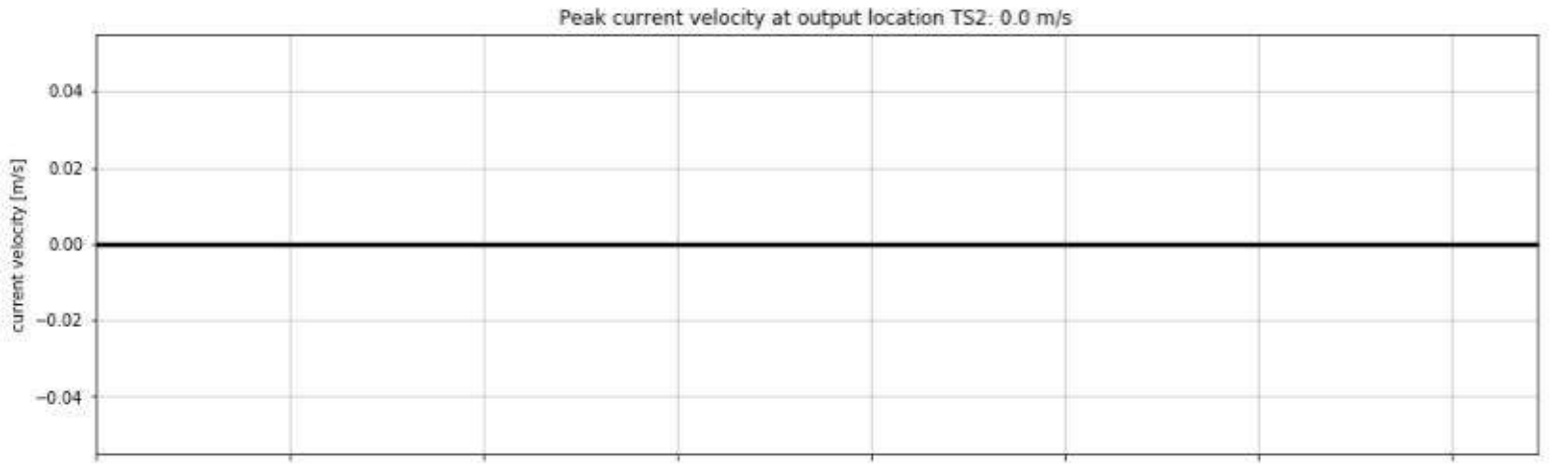
Peak current velocity at output location TS2: 0.0 m/s
current velocity [m/s]
0.04
0.02
0.00
−0.02
−0.04

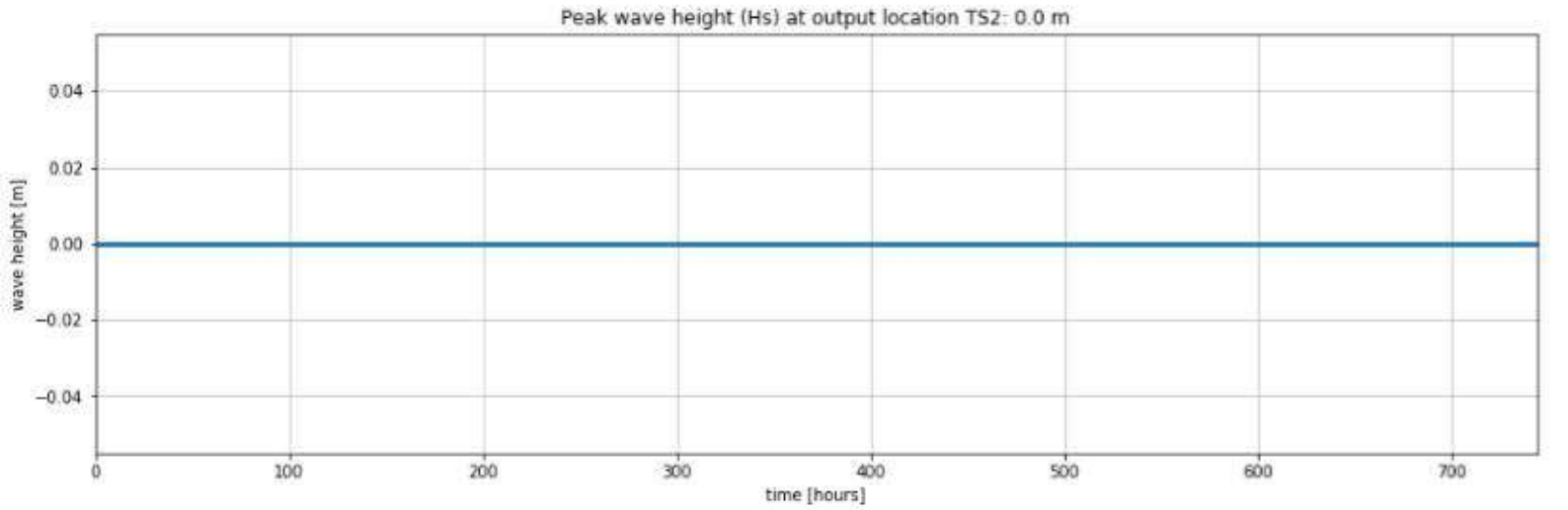
Peak wave height (Hs) at output location TS2: 0.0 m
wave height [m]
0.04
0.02
0.00
−0.02
−0.04
0
100
200
300
400
500
600
700
time [hours]

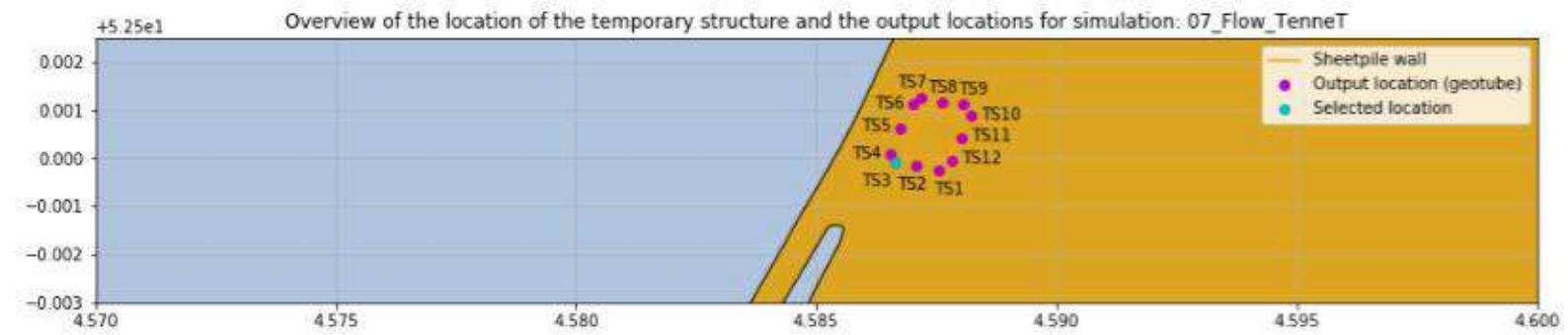
Overview of the location of the temporary structure and the output locations for simulation: 07_Flow_TenneT
+5.25e1
Sheetpile wall
Output location (geotube)
Selected location
TS1
TS2
TS3
TS4
TS5
TS6
TS7
TS8
TS9
TS10
TS11
TS12

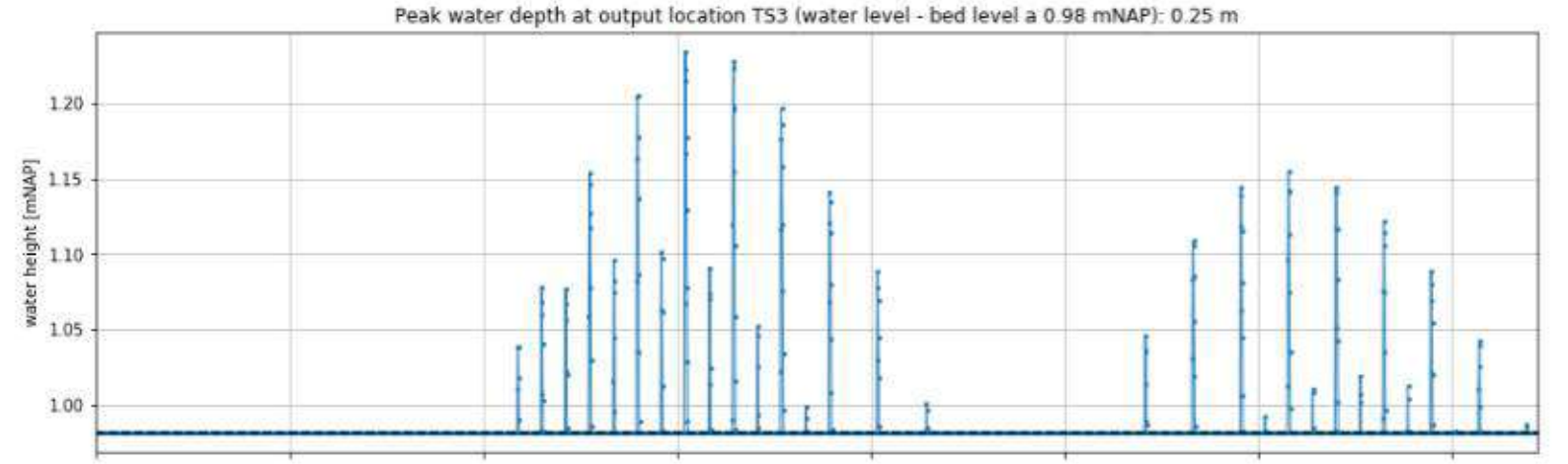
Peak water depth at output location TS3 (water level - bed level a 0.98 mNAP): 0.25 m
water height [mNAP]

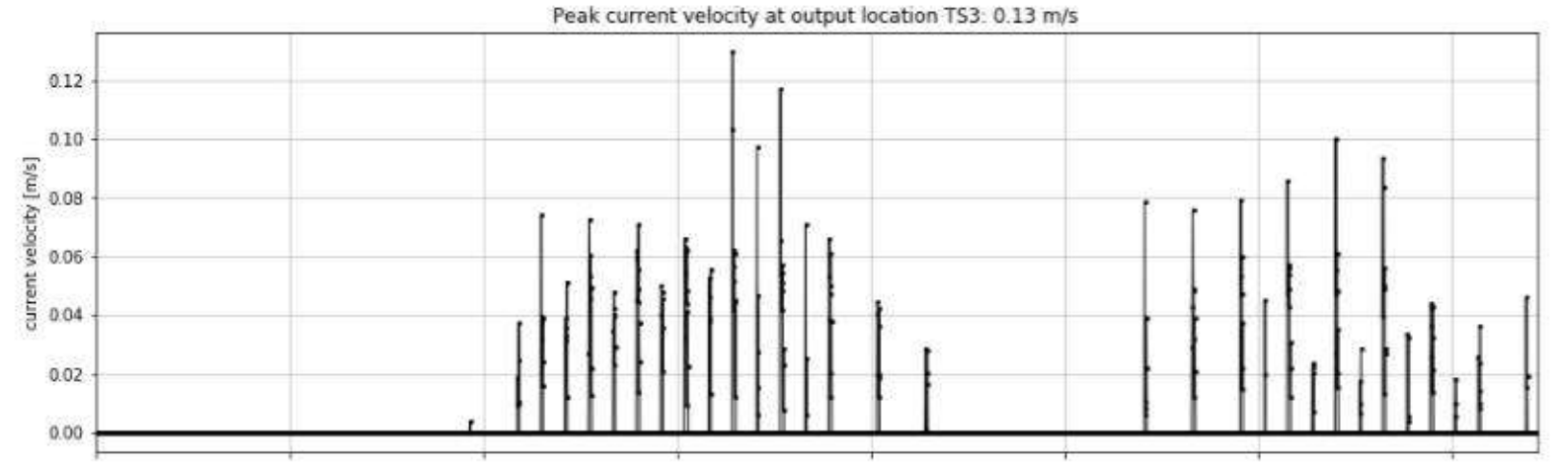
Peak current velocity at output location TS3: 0.13 m/s
current velocity [m/s]

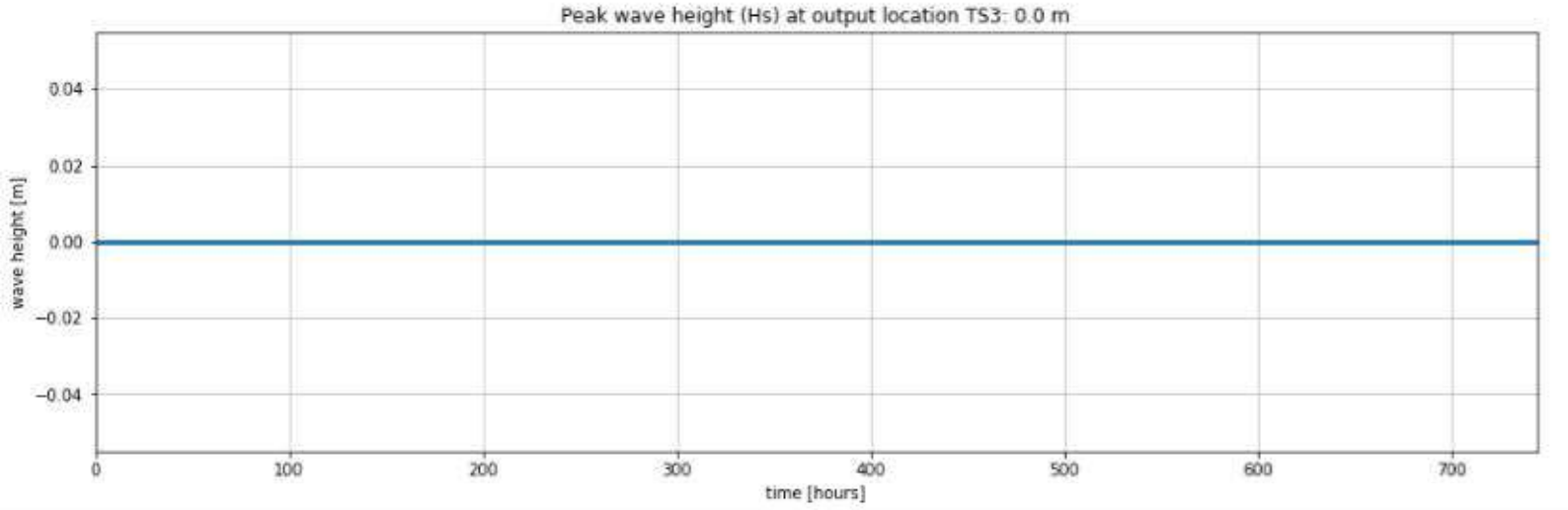
Peak wave height (Hs) at output location TS3: 0.0 m
wave height [m]
time [hours]

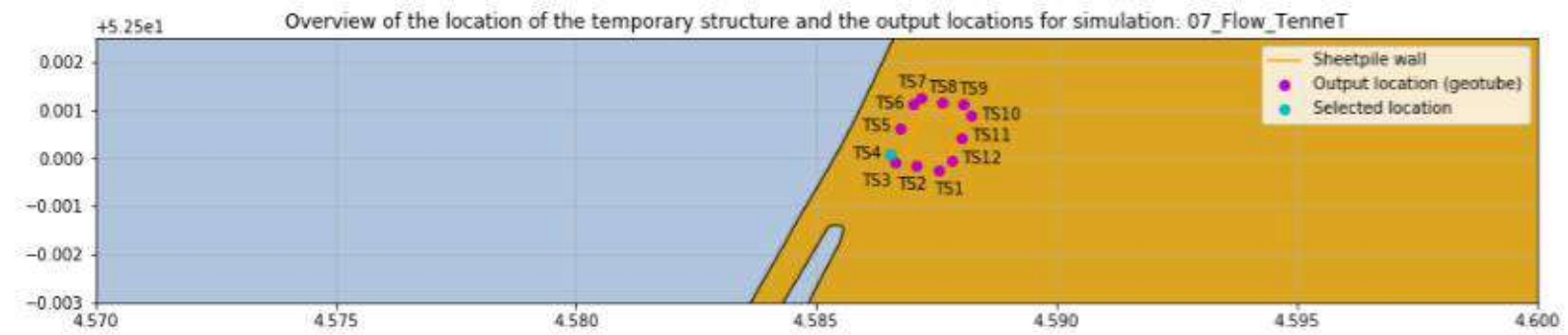
Overview of the location of the temporary structure and the output locations for simulation: 07_Flow_TenneT
+5.25e1
Sheetpile wall
Output location (geotube)
Selected location
TS1
TS2
TS3
TS4
TS5
TS6
TS7
TS8
TS9
TS10
TS11
TS12

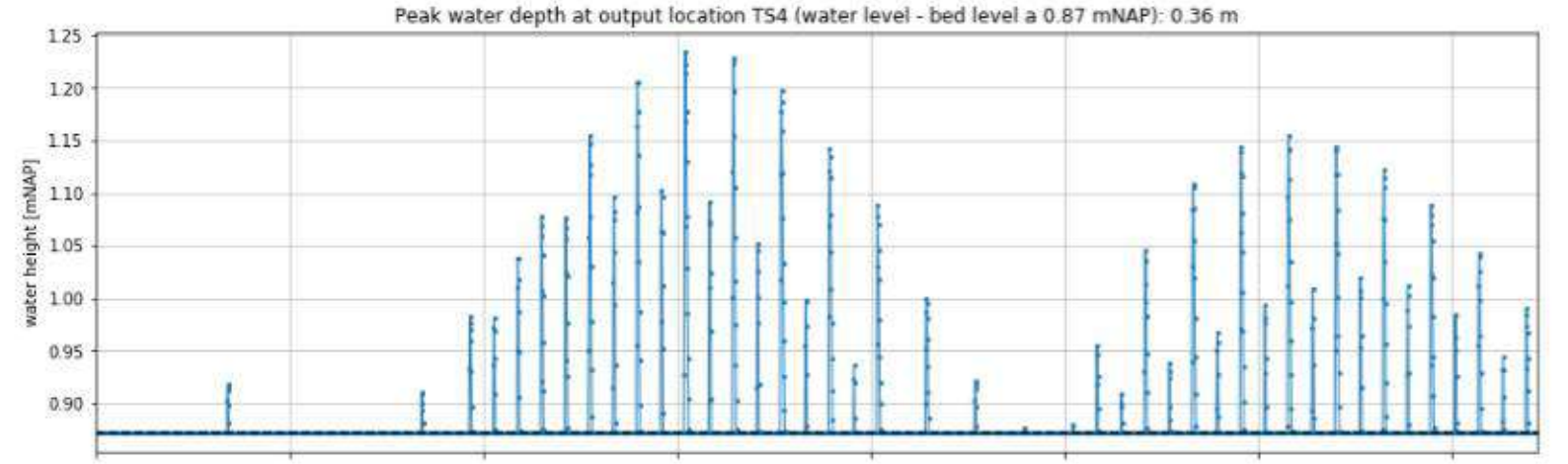
Peak water depth at output location TS4 (water level - bed level a 0.87 mNAP): 0.36 m
water height [mNAP]

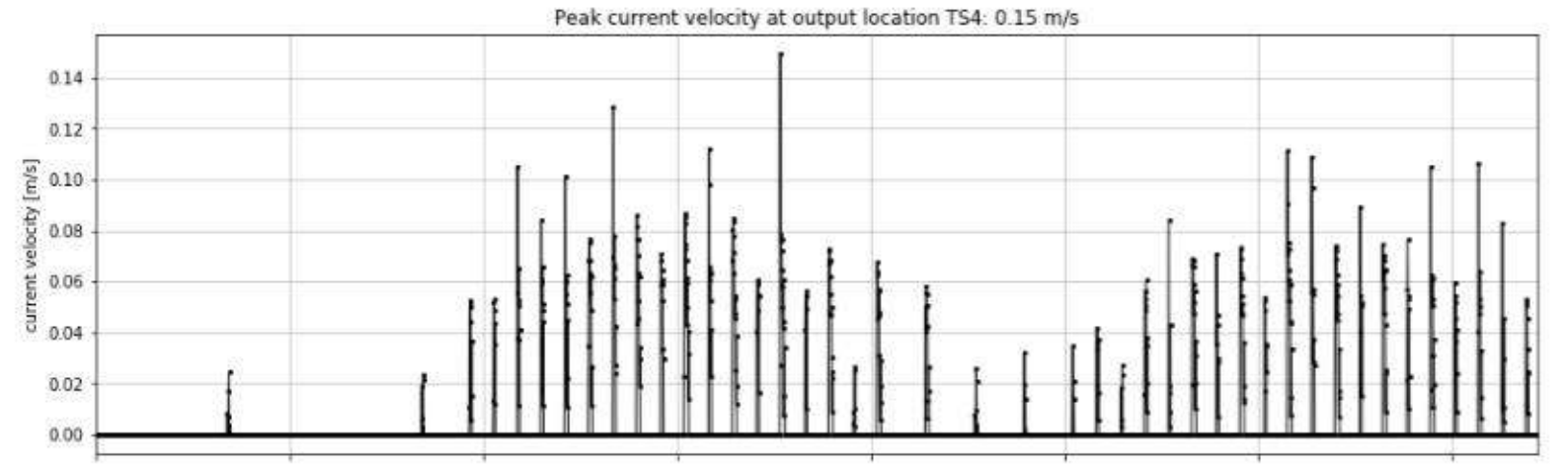
Peak current velocity at output location TS4: 0.15 m/s
current velocity [m/s]

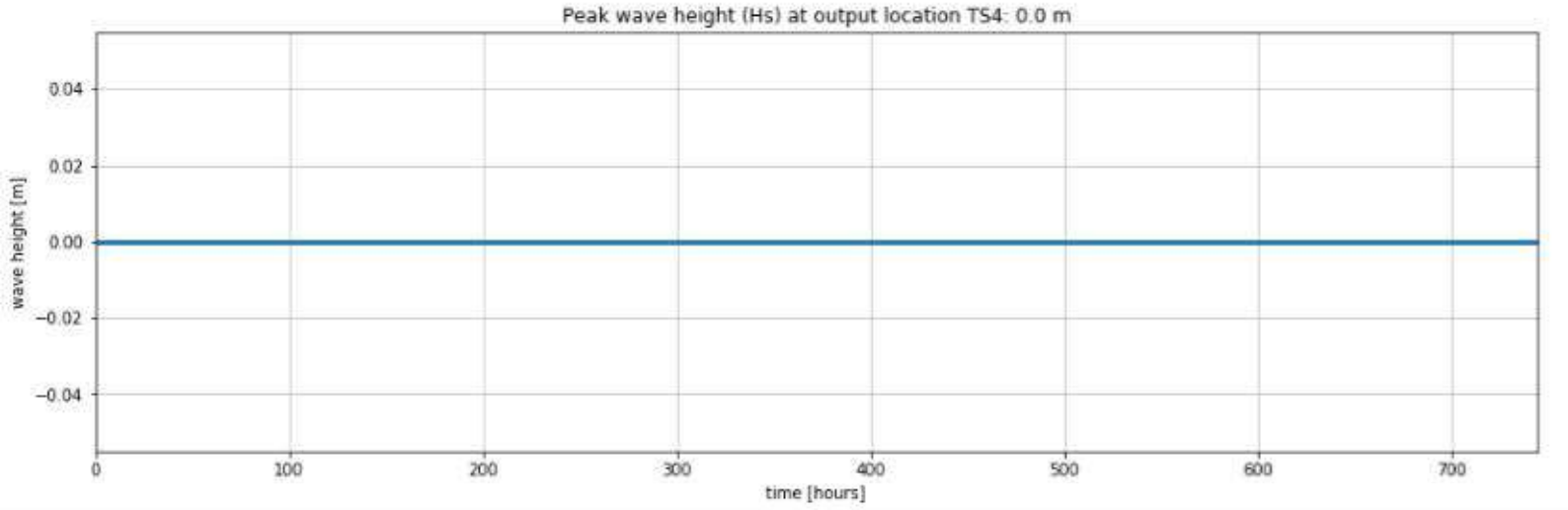
Peak wave height (Hs) at output location TS4: 0.0 m
wave height [m]
time [hours]

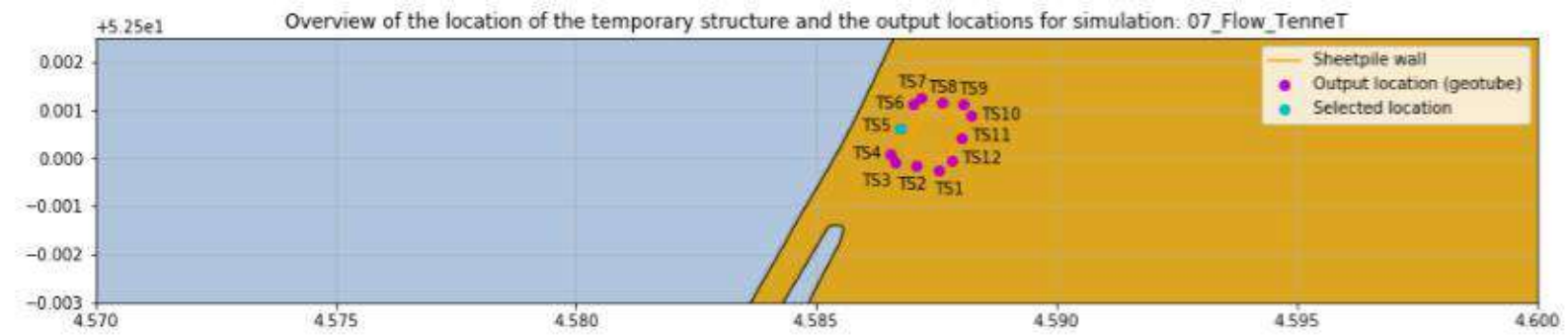
Overview of the location of the temporary structure and the output locations for simulation: 07_Flow_TenneT
+5.25e1
Sheetpile wall
Output location (geotube)
Selected location
TS1
TS2
TS3
TS4
TS5
TS6
TS7
TS8
TS9
TS10
TS11
TS12

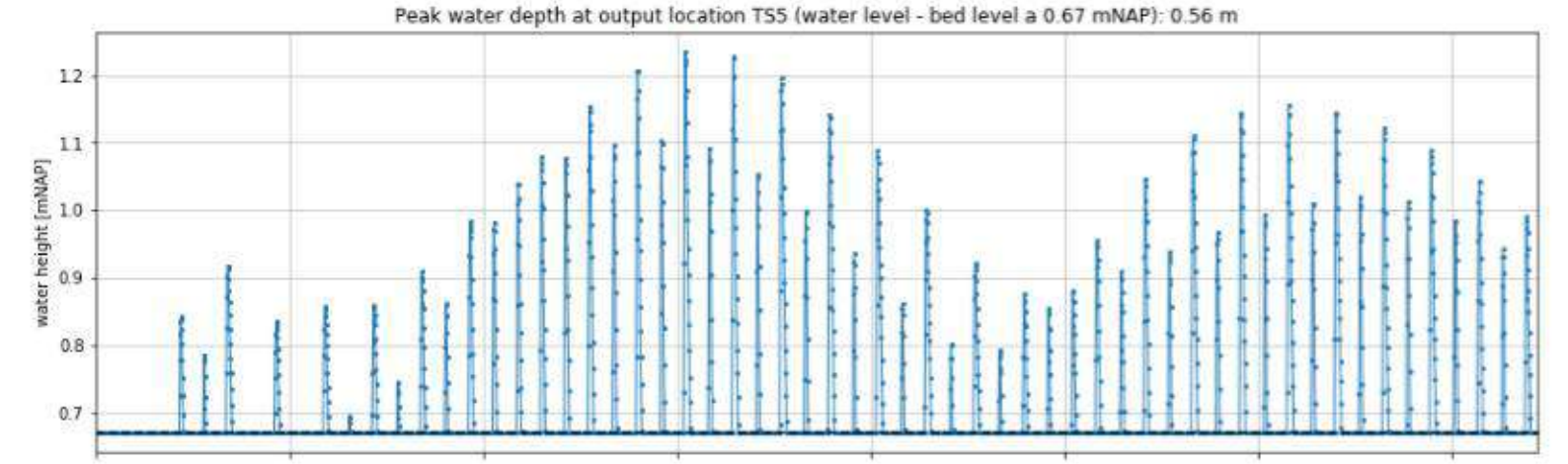
Peak water depth at output location TS5 (water level - bed level a 0.67 mNAP): 0.56 m
water height [mNAP]

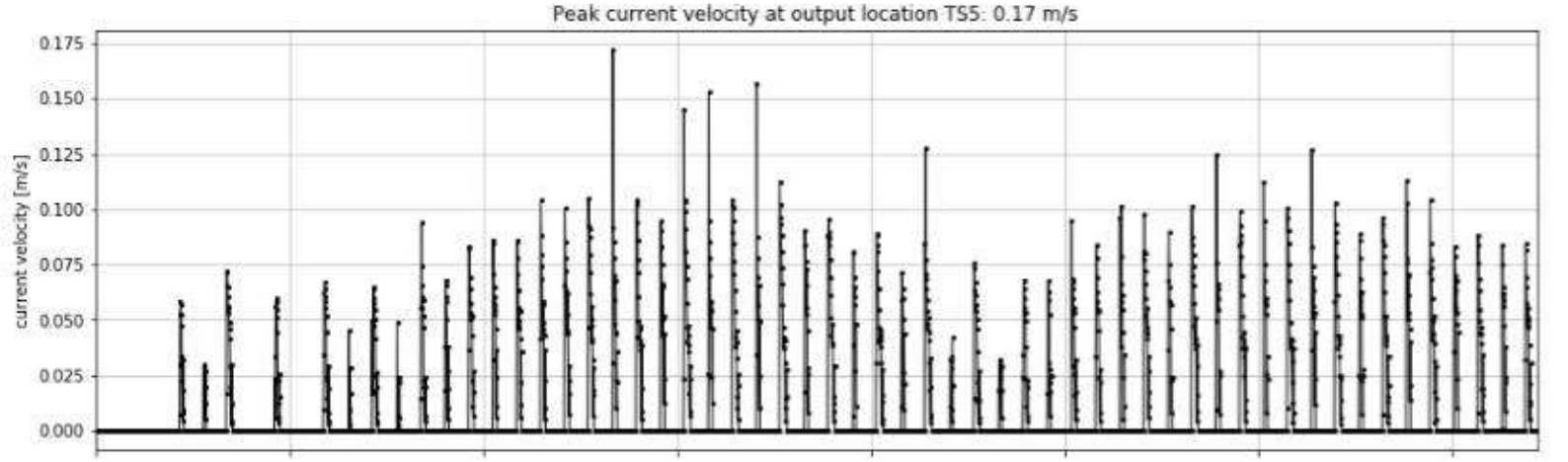
Peak current velocity at output location TS5: 0.17 m/s
current velocity [m/s]

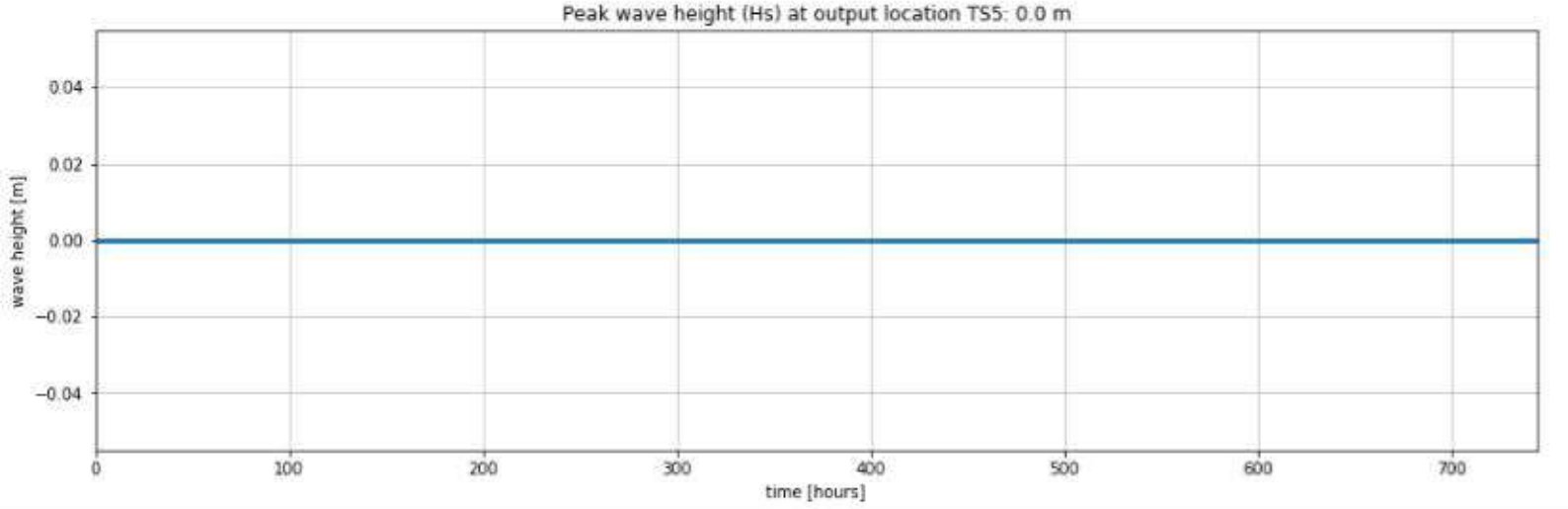
Peak wave height (Hs) at output location TS5: 0.0 m
wave height [m]
time [hours]

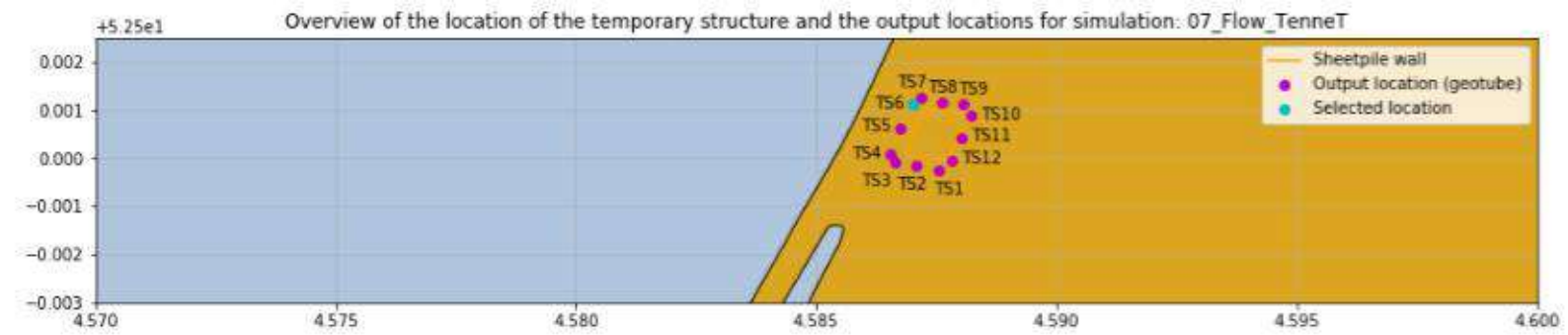
Overview of the location of the temporary structure and the output locations for simulation: 07_Flow_TenneT
+5.25e1
Sheetpile wall
Output location (geotube)
Selected location
TS1
TS2
TS3
TS4
TS5
TS6
TS7
TS8
TS9
TS10
TS11
TS12

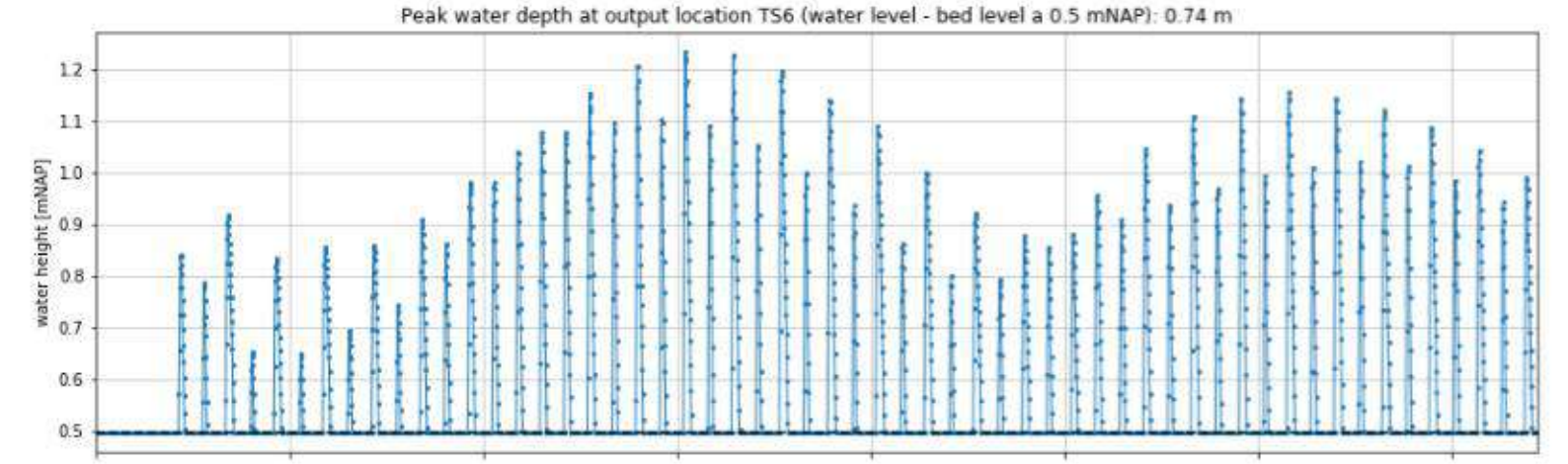
Peak water depth at output location TS6 (water level - bed level a 0.5 mNAP): 0.74 m
water height [mNAP]

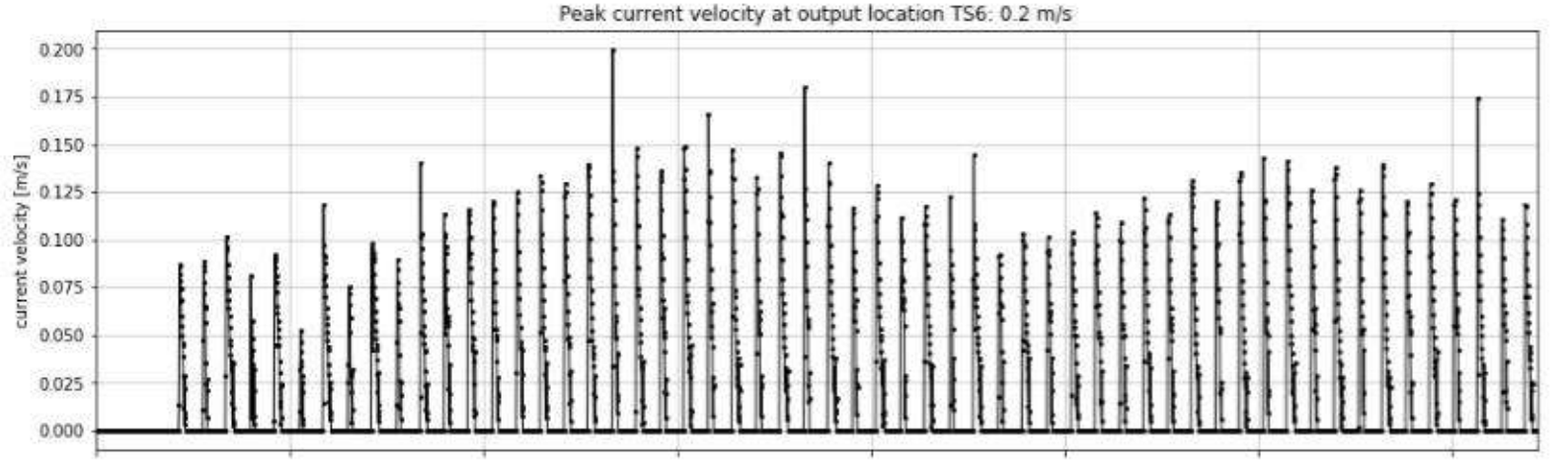
Peak current velocity at output location TS6: 0.2 m/s
current velocity [m/s]

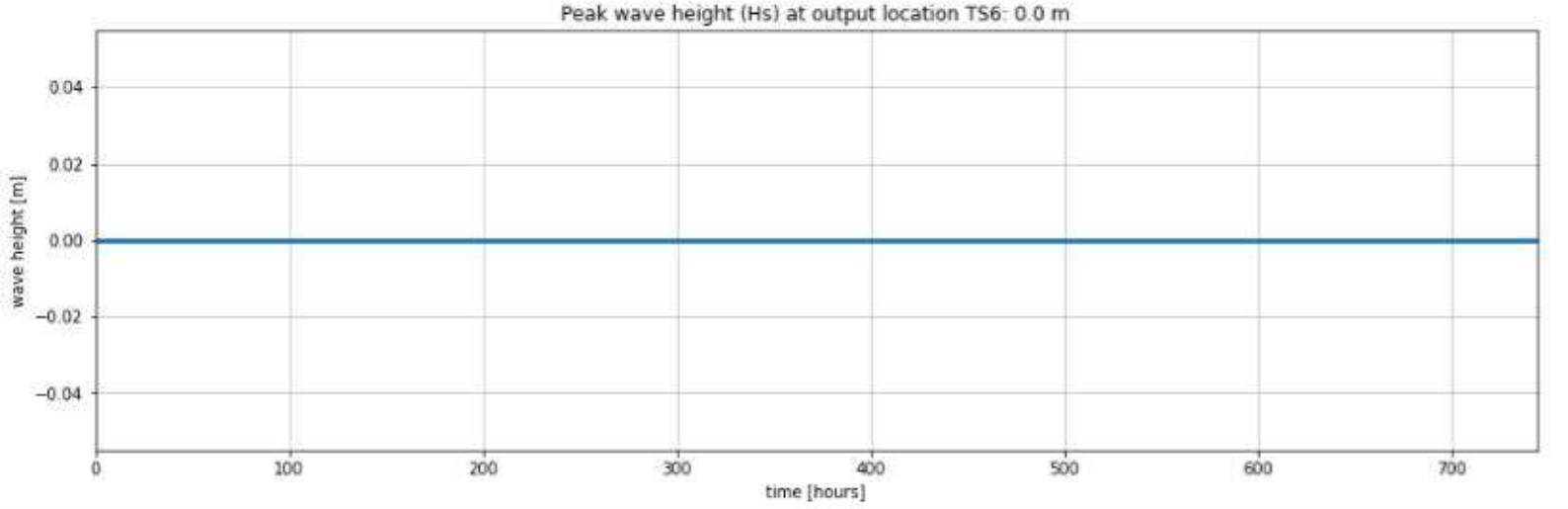
Peak wave height (Hs) at output location TS6: 0.0 m
wave height [m]
time [hours]

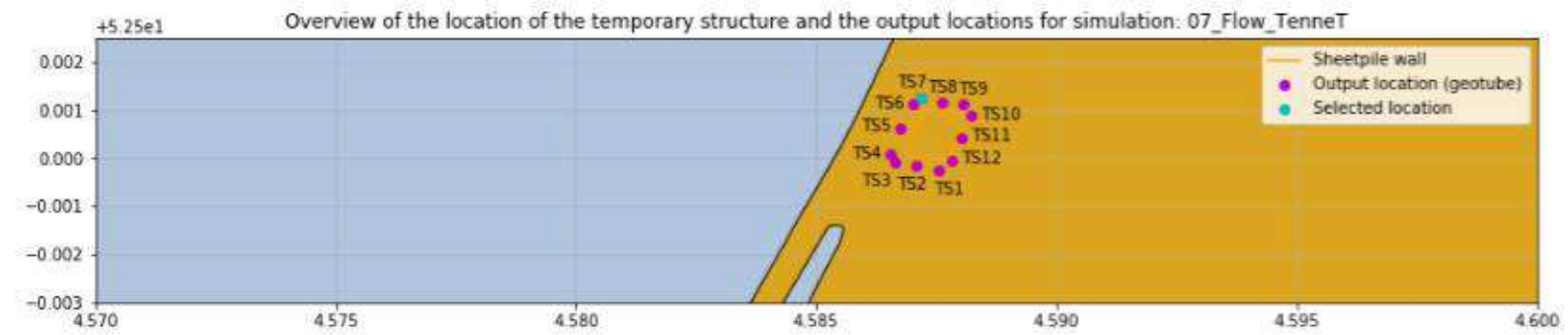
Overview of the location of the temporary structure and the output locations for simulation: 07_Flow_TenneT
+5.25e1
Sheetpile wall
Output location (geotube)
Selected location
TS1
TS2
TS3
TS4
TS5
TS6
TS7
TS8
TS9
TS10
TS11
TS12

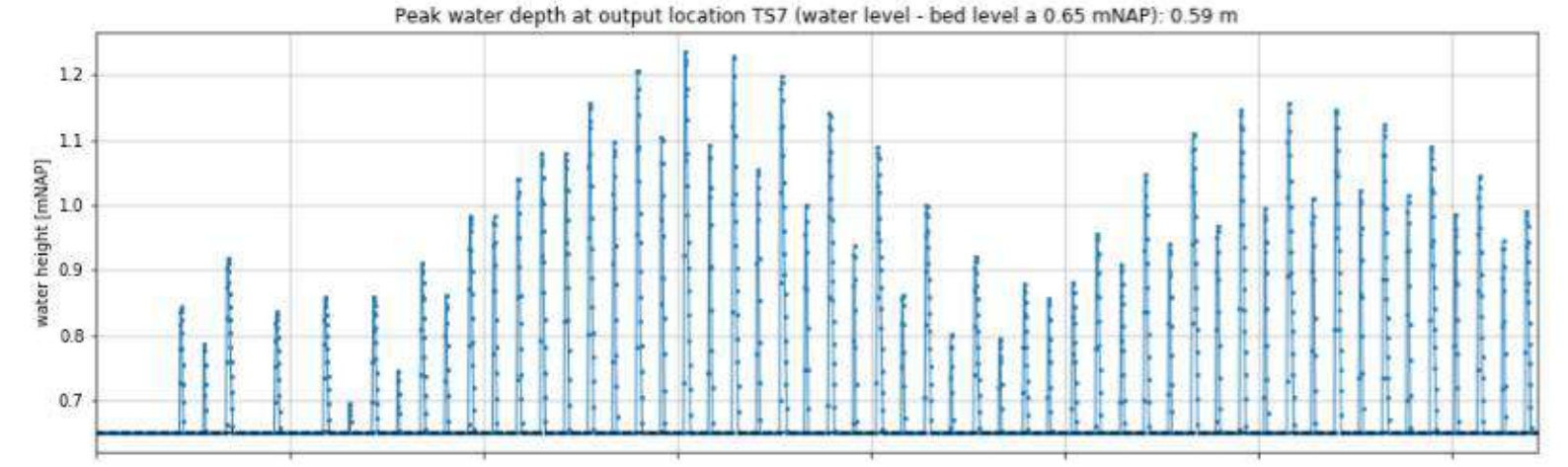
Peak water depth at output location TS7 (water level - bed level a 0.65 mNAP): 0.59 m
water height [mNAP]

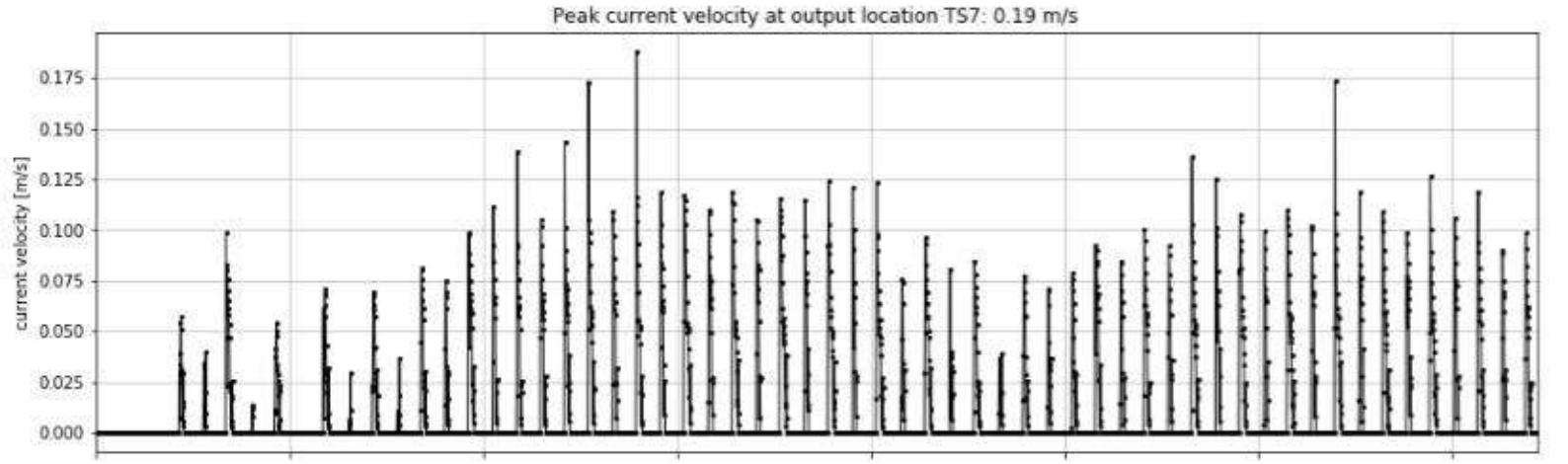
Peak current velocity at output location TS7: 0.19 m/s
current velocity [m/s]

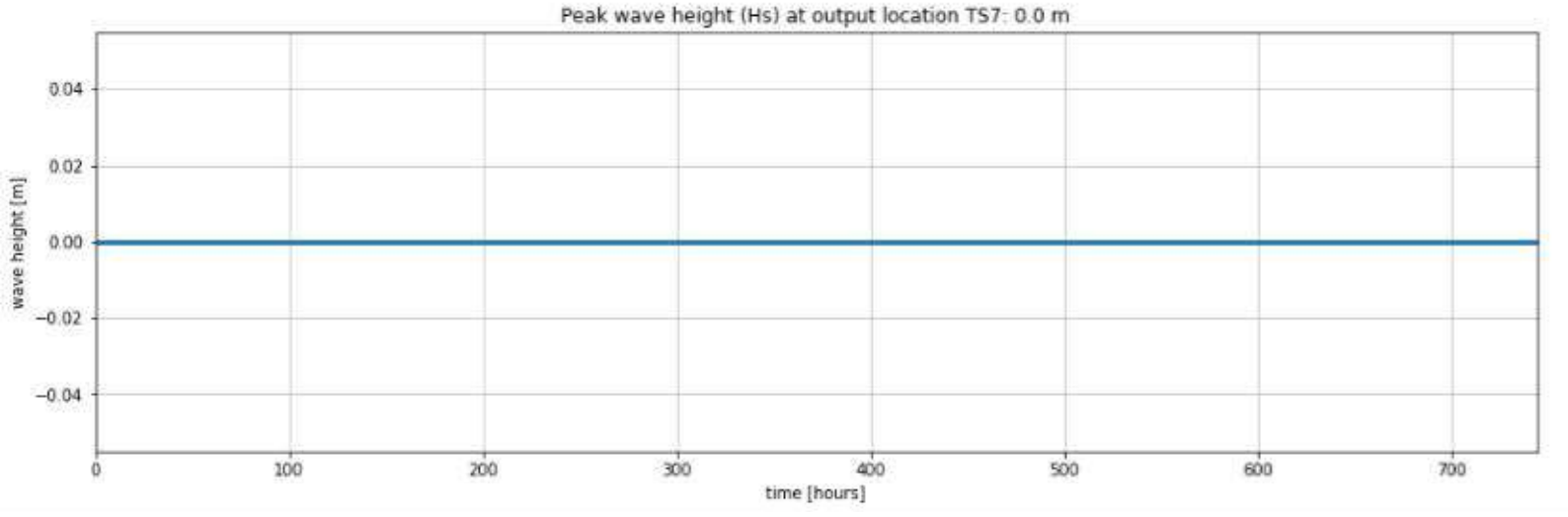
Peak wave height (Hs) at output location TS7: 0.0 m
wave height [m]
time [hours]

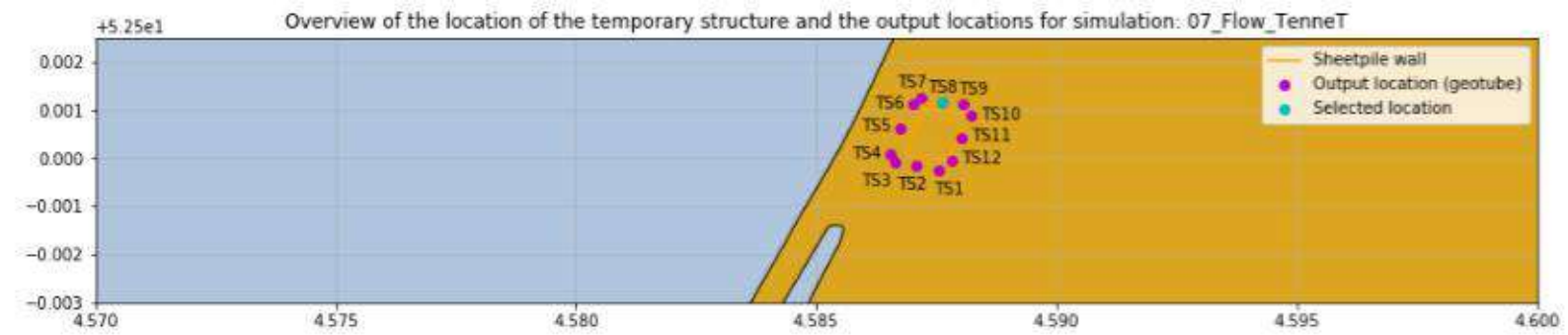
Overview of the location of the temporary structure and the output locations for simulation: 07_Flow_TenneT
+5.25e1
Sheetpile wall
Output location (geotube)
Selected location
TS1
TS2
TS3
TS4
TS5
TS6
TS7
TS8
TS9
TS10
TS11
TS12
0.002
0.001
0.000
−0.001
−0.002
−0.003
4.570
4.575
4.580
4.585
4.590
4.595
4.600

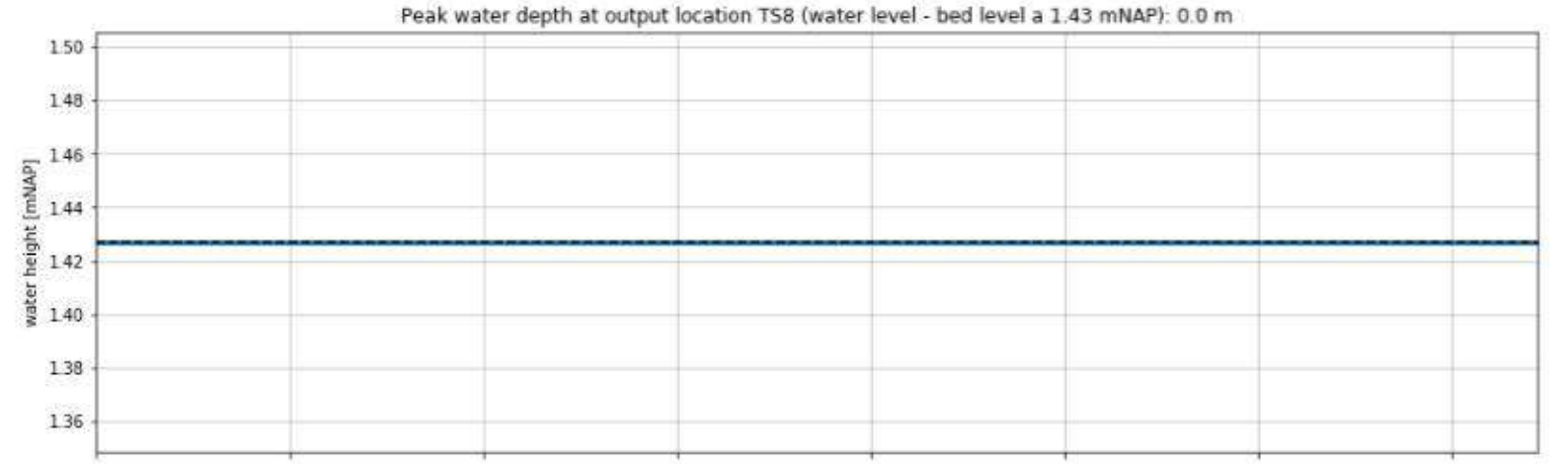
Peak water depth at output location TS8 (water level - bed level a 1.43 mNAP): 0.0 m
water height [mNAP]
1.50
1.48
1.46
1.44
1.42
1.40
1.38
1.36

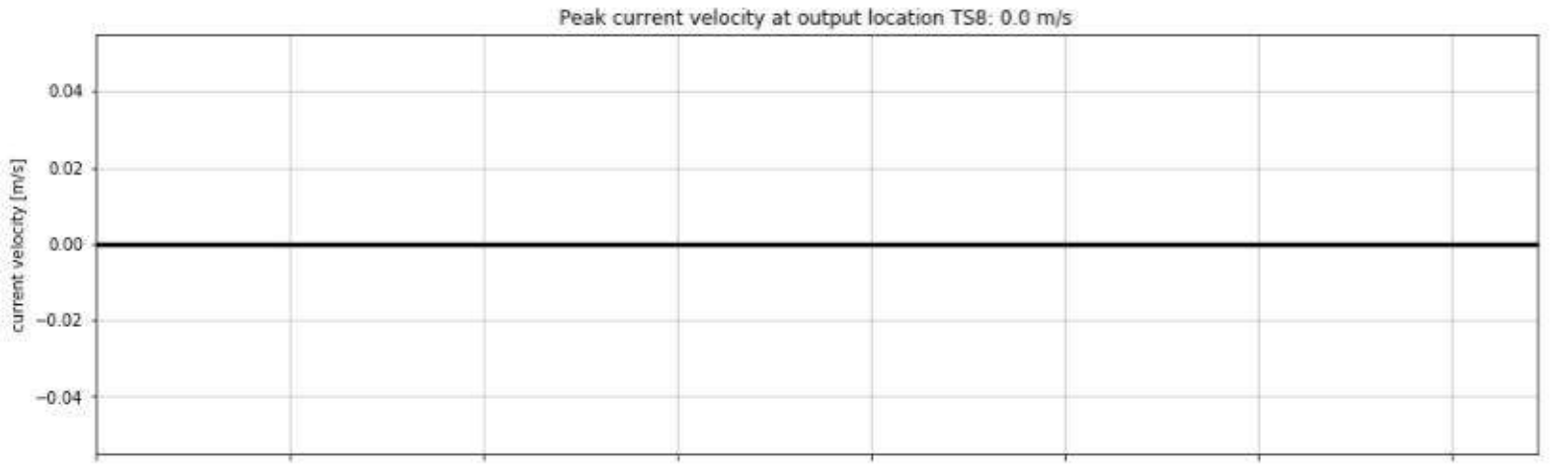
Peak current velocity at output location TS8: 0.0 m/s
current velocity [m/s]
0.04
0.02
0.00
−0.02
−0.04

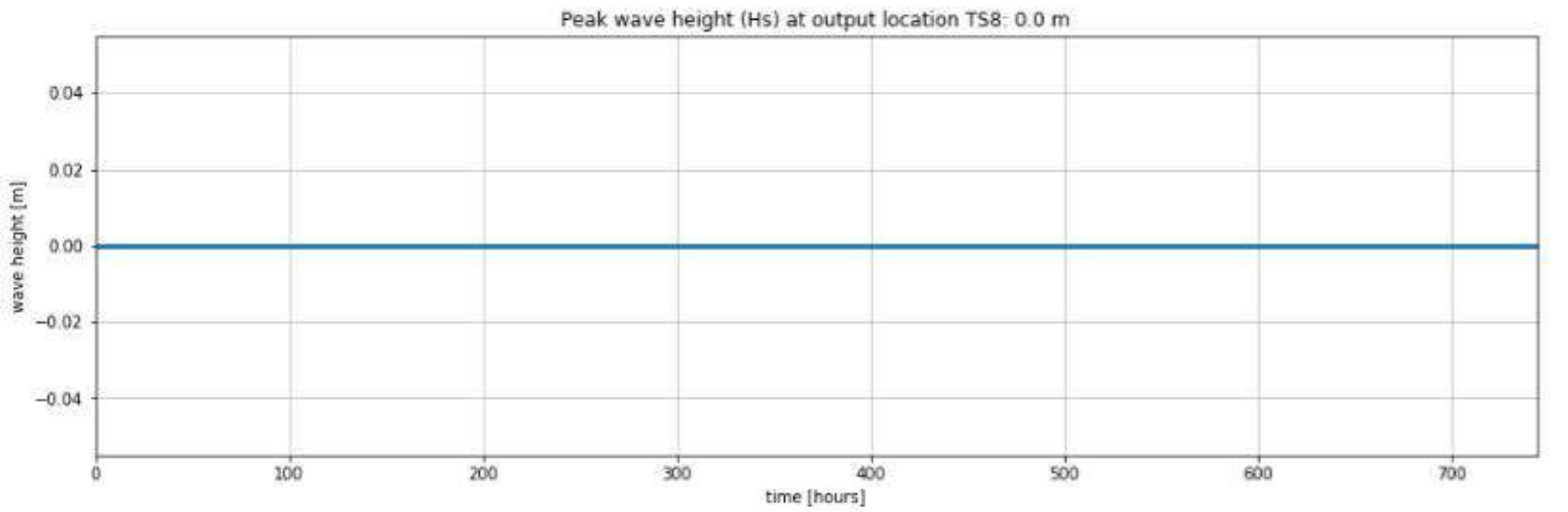
Peak wave height (Hs) at output location TS8: 0.0 m
wave height [m]
0.04
0.02
0.00
−0.02
−0.04
0
100
200
300
400
500
600
700
time [hours]

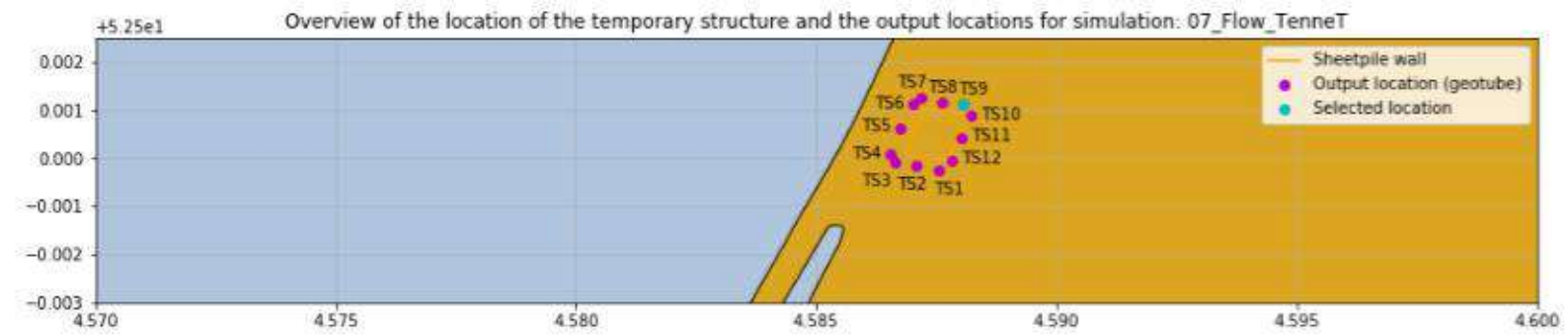
Overview of the location of the temporary structure and the output locations for simulation: 07_Flow_TenneT
+5.25e1
Sheetpile wall
Output location (geotube)
Selected location
TS1
TS2
TS3
TS4
TS5
TS6
TS7
TS8
TS9
TS10
TS11
TS12

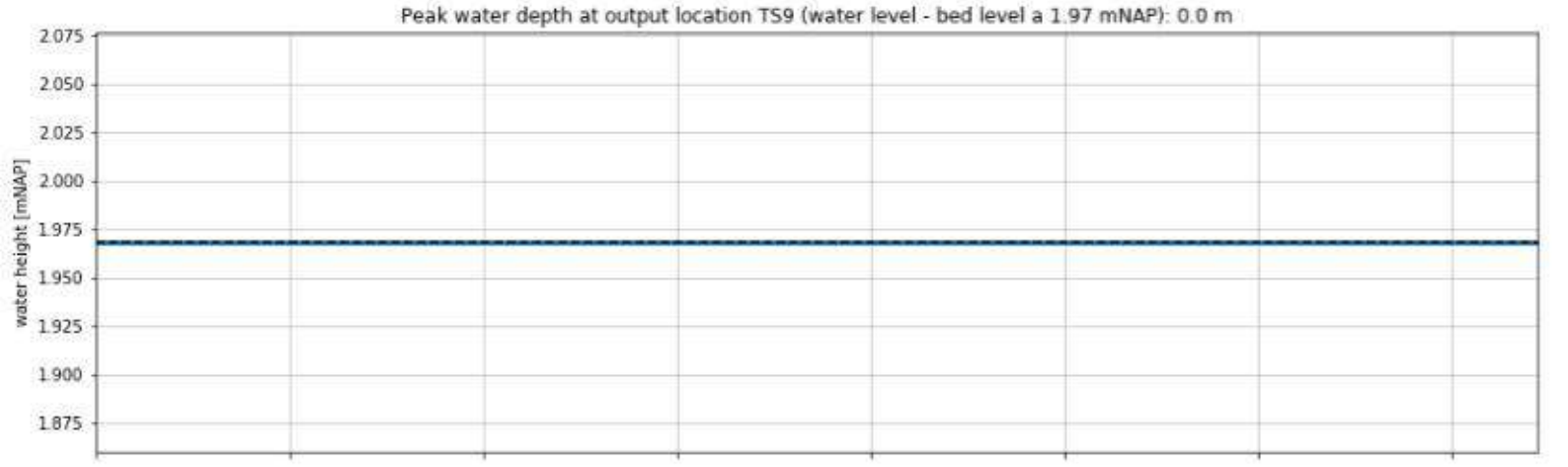
Peak water depth at output location TS9 (water level - bed level a 1.97 mNAP): 0.0 m
water height [mNAP]

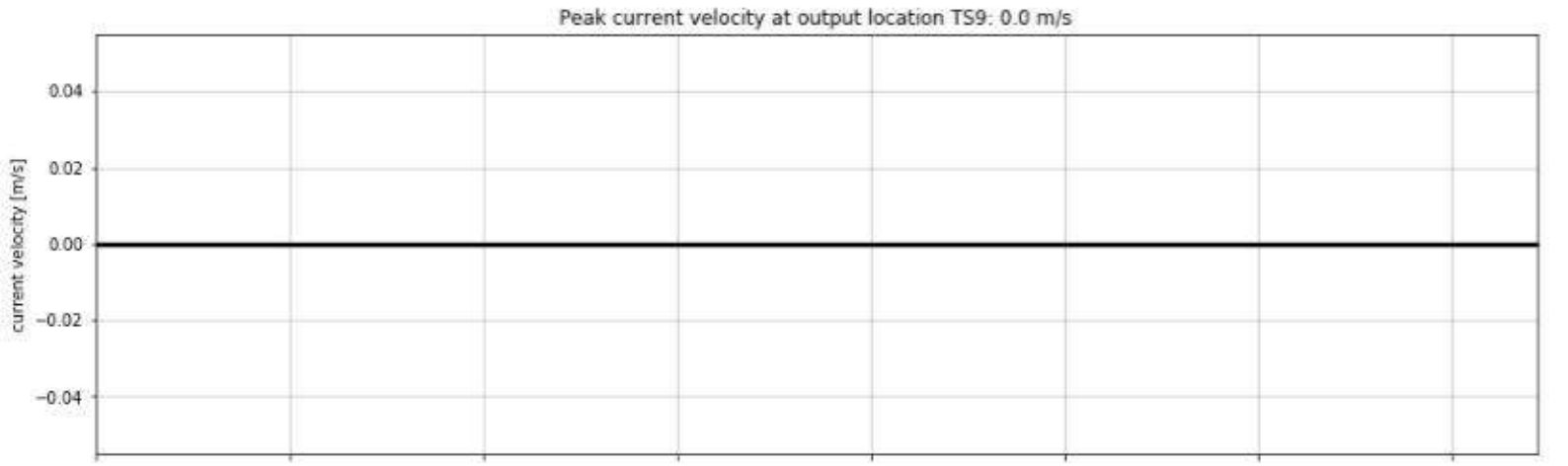
Peak current velocity at output location TS9: 0.0 m/s
current velocity [m/s]

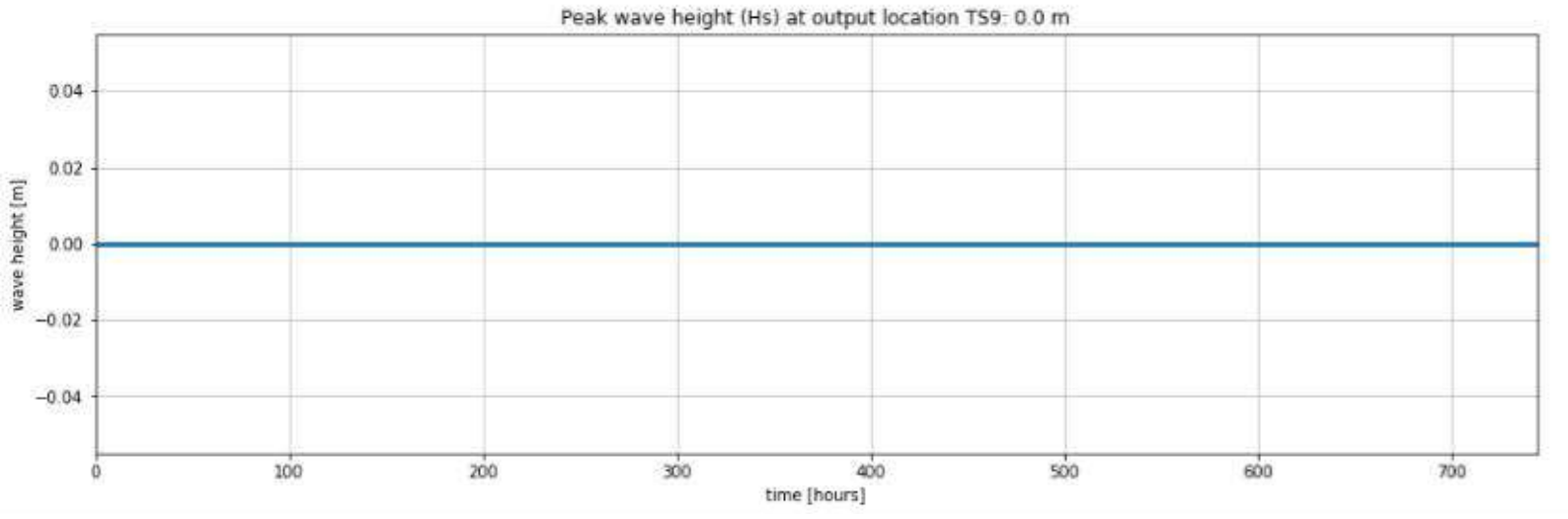
Peak wave height (Hs) at output location TS9: 0.0 m
wave height [m]
time [hours]

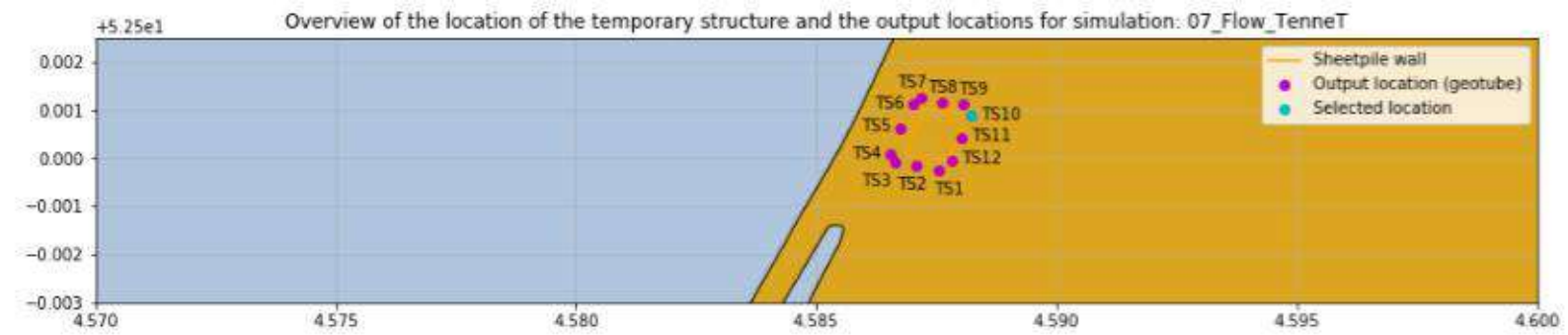
Overview of the location of the temporary structure and the output locations for simulation: 07_Flow_TenneT
+5.25e1
Sheetpile wall
Output location (geotube)
Selected location
TS1
TS2
TS3
TS4
TS5
TS6
TS7
TS8
TS9
TS10
TS11
TS12
0.002
0.001
0.000
−0.001
−0.002
−0.003
4.570
4.575
4.580
4.585
4.590
4.595
4.600

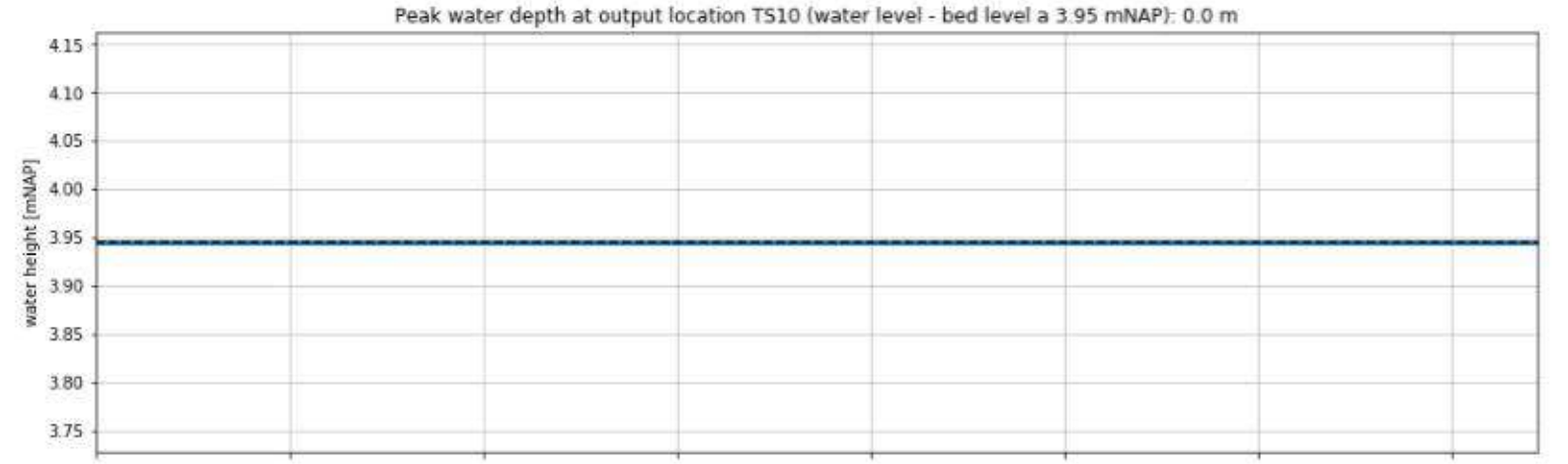
Peak water depth at output location TS10 (water level - bed level a 3.95 mNAP): 0.0 m
water height [mNAP]
4.15
4.10
4.05
4.00
3.95
3.90
3.85
3.80
3.75

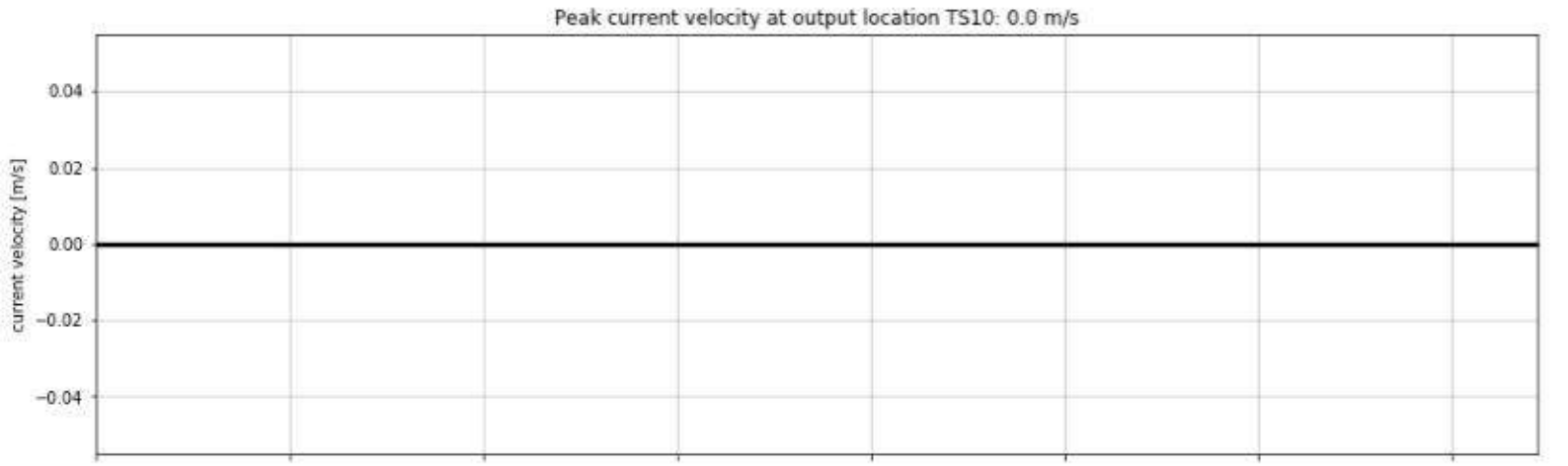
Peak current velocity at output location TS10: 0.0 m/s
current velocity [m/s]
0.04
0.02
0.00
−0.02
−0.04

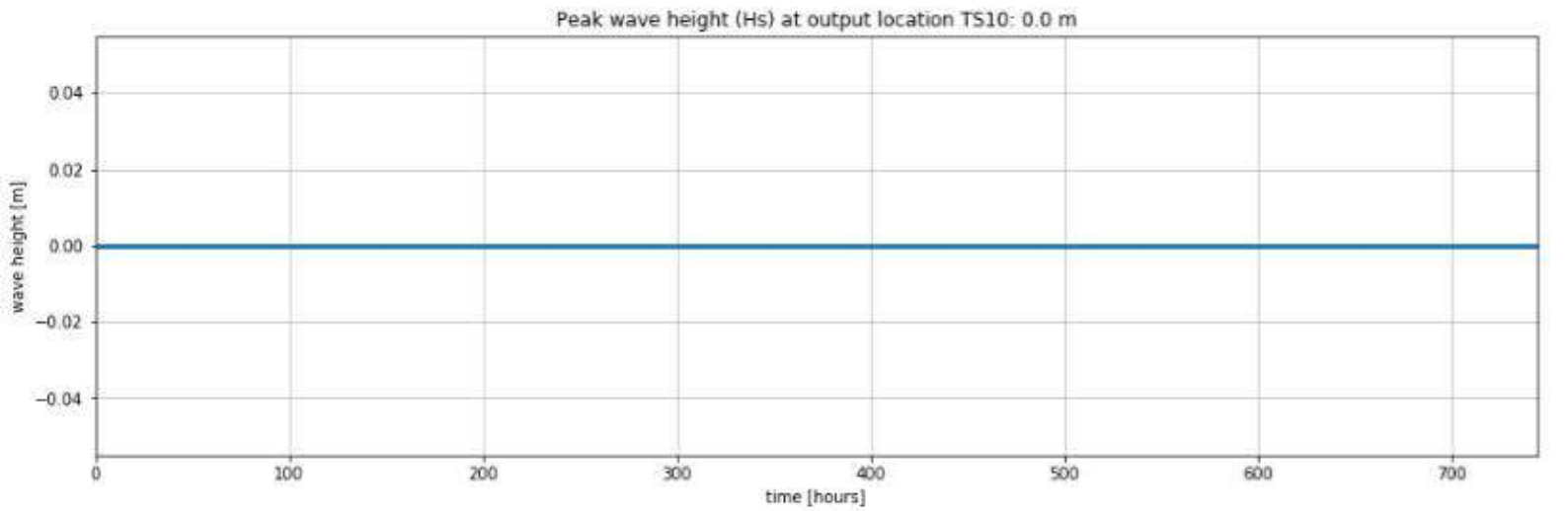
Peak wave height (Hs) at output location TS10: 0.0 m
wave height [m]
0.04
0.02
0.00
−0.02
−0.04
0
100
200
300
400
500
600
700
time [hours]

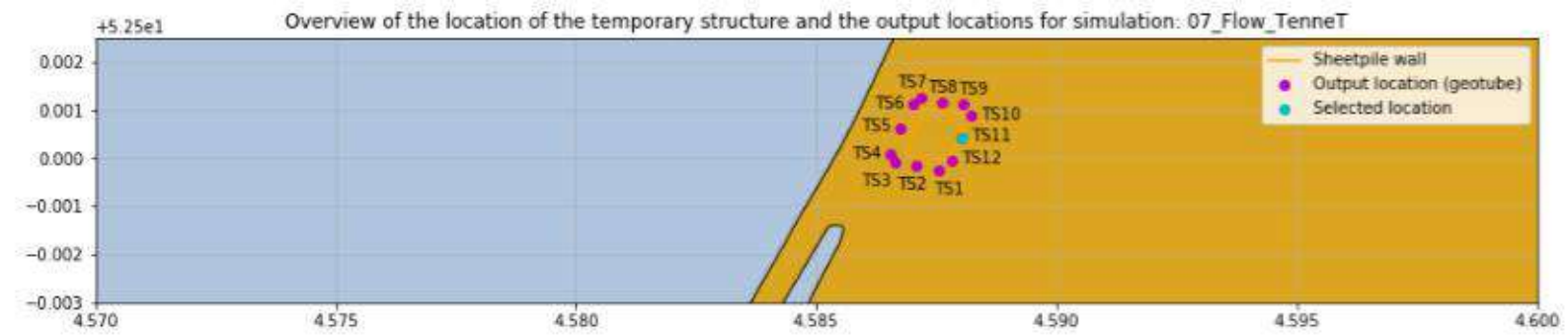
Overview of the location of the temporary structure and the output locations for simulation: 07_Flow_TenneT
+5.25e1
Sheetpile wall
Output location (geotube)
Selected location
TS1
TS2
TS3
TS4
TS5
TS6
TS7
TS8
TS9
TS10
TS11
TS12
0.002
0.001
0.000
−0.001
−0.002
−0.003
4.570
4.575
4.580
4.585
4.590
4.595
4.600

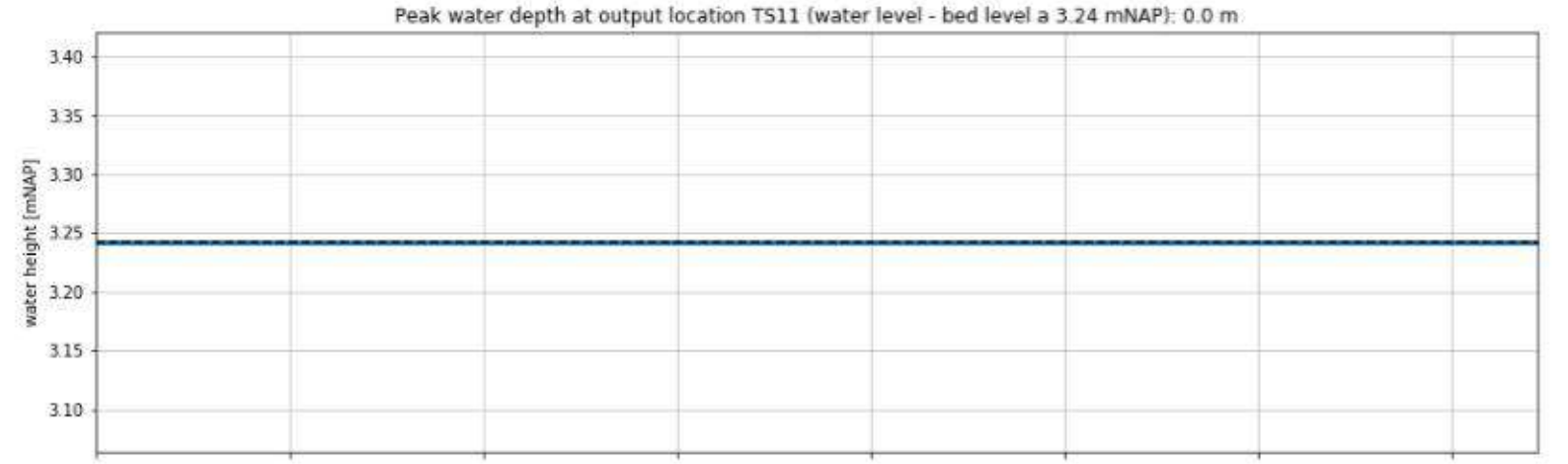
Peak water depth at output location TS11 (water level - bed level a 3.24 mNAP): 0.0 m
water height [mNAP]
3.40
3.35
3.30
3.25
3.20
3.15
3.10

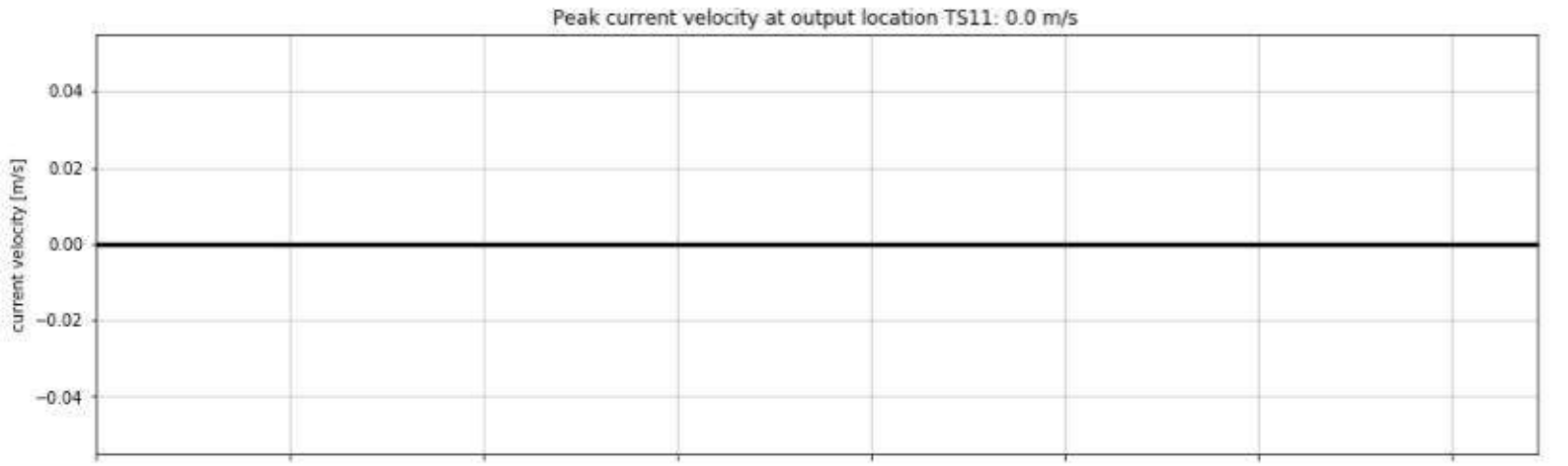
Peak current velocity at output location TS11: 0.0 m/s
current velocity [m/s]
0.04
0.02
0.00
−0.02
−0.04

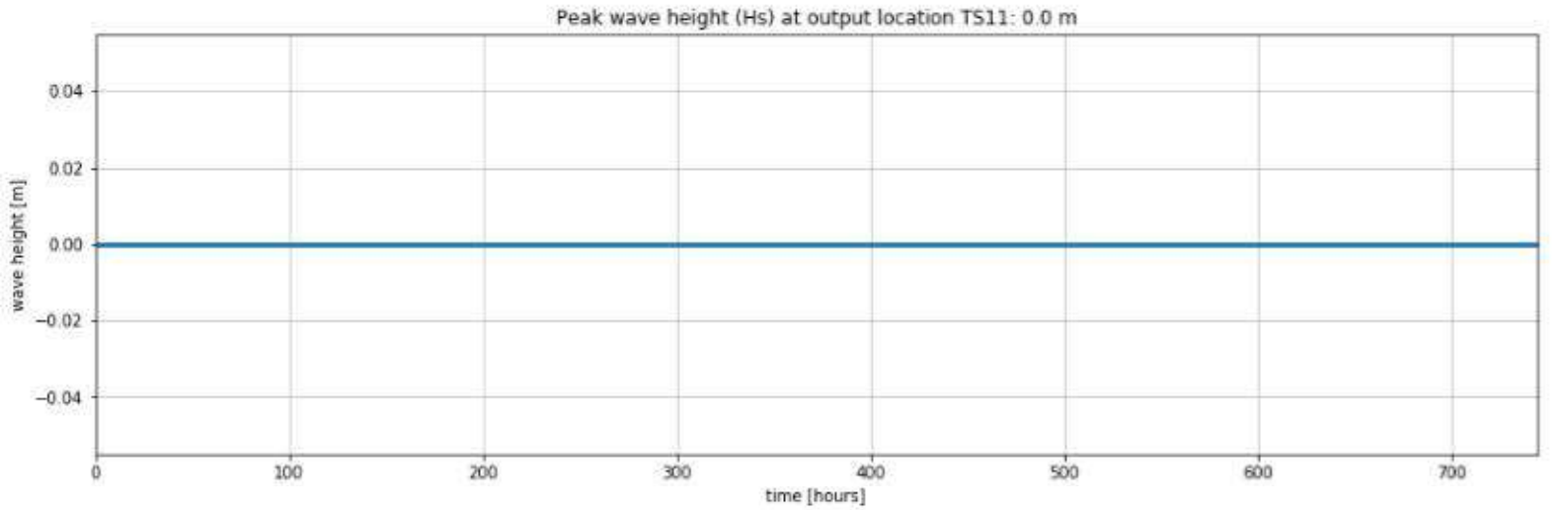
Peak wave height (Hs) at output location TS11: 0.0 m
wave height [m]
0.04
0.02
0.00
−0.02
−0.04
0
100
200
300
400
500
600
700
time [hours]

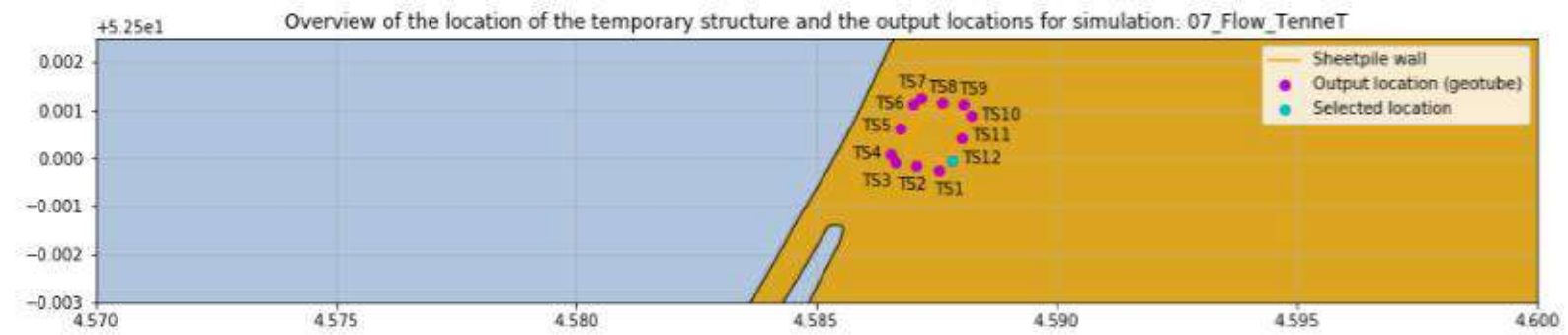
Overview of the location of the temporary structure and the output locations for simulation: 07_Flow_TenneT
+5.25e1
Sheetpile wall
Output location (geotube)
Selected location
TS1
TS2
TS3
TS4
TS5
TS6
TS7
TS8
TS9
TS10
TS11
TS12

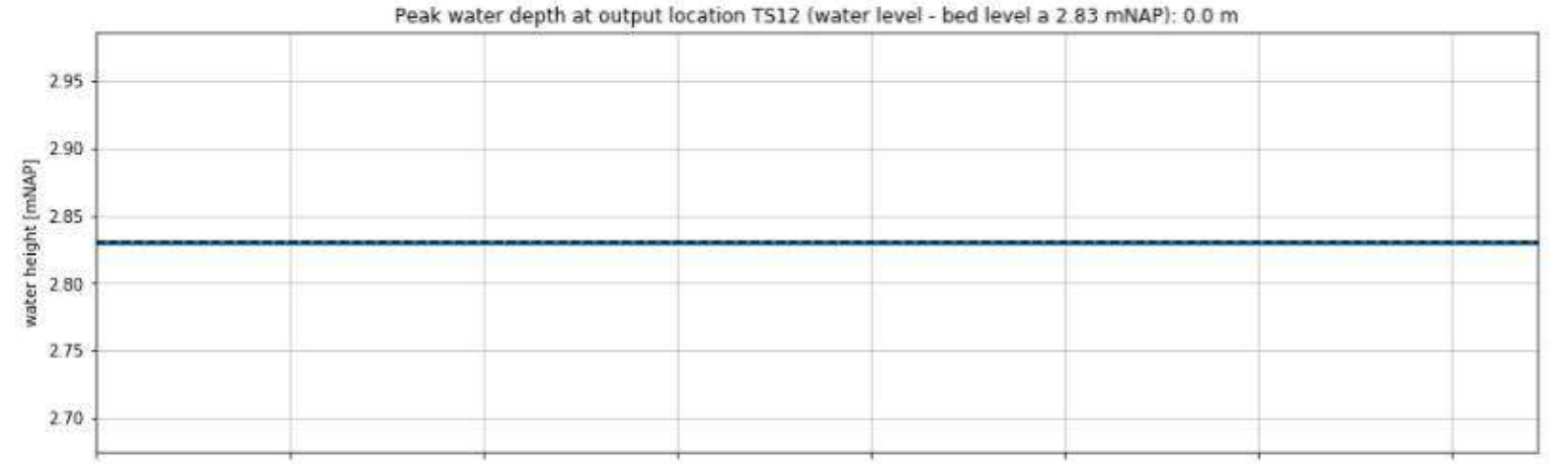
Peak water depth at output location TS12 (water level - bed level a 2.83 mNAP): 0.0 m
water height [mNAP]

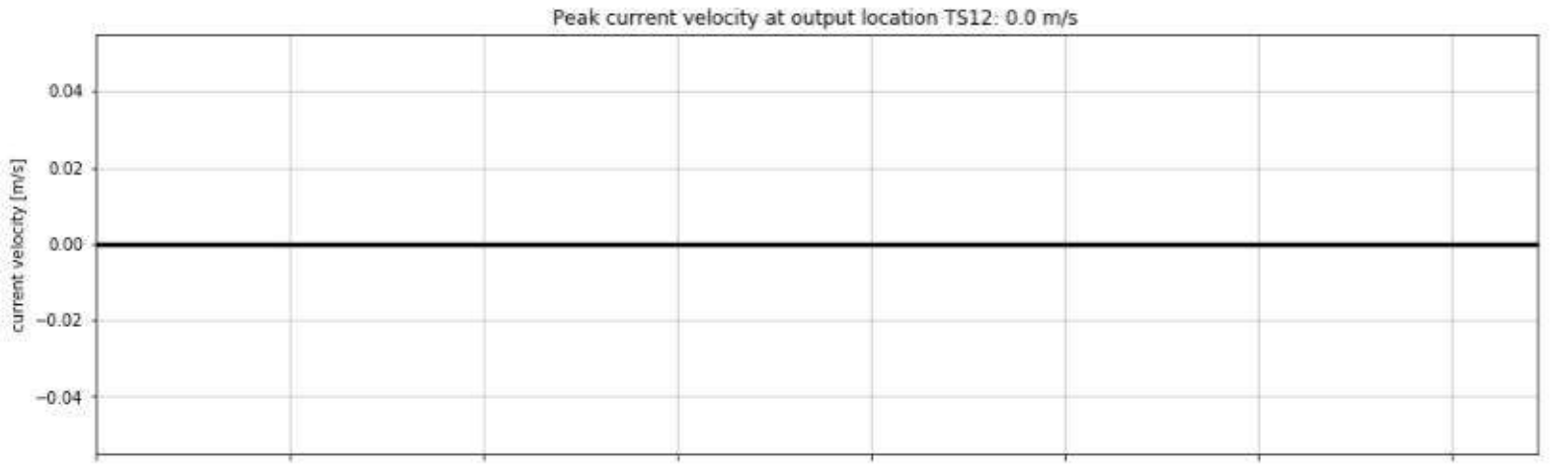
Peak current velocity at output location TS12: 0.0 m/s
current velocity [m/s]

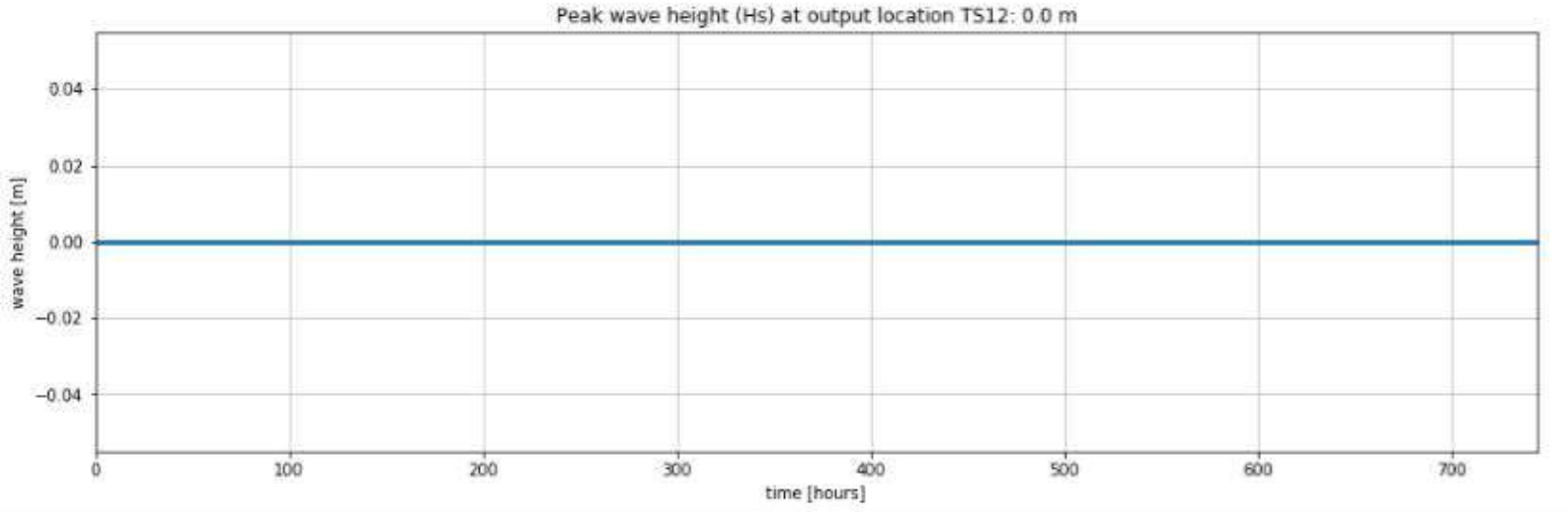
Peak wave height (Hs) at output location TS12: 0.0 m
wave height [m]
time [hours]

C.3 Flow-Wave 1yr storm 330 degrees – TenneT bathymetry

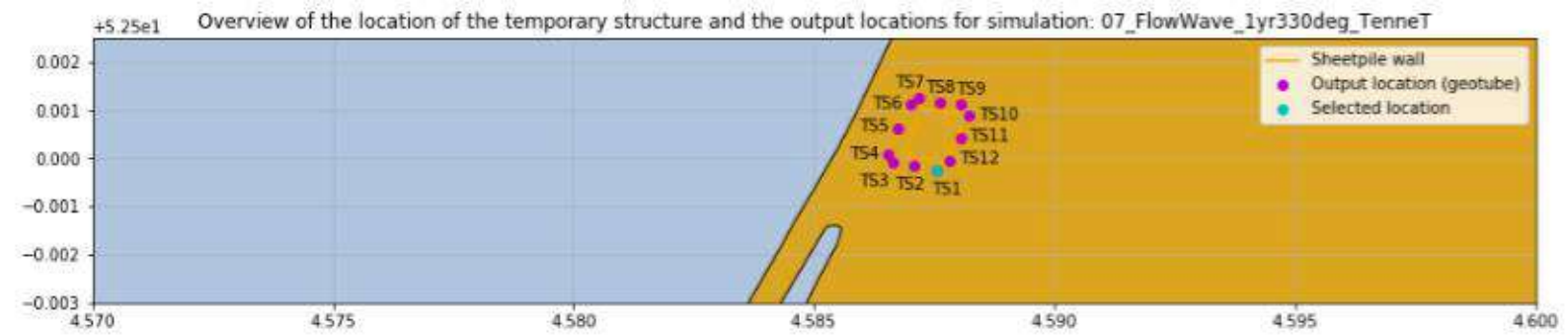
Overview of the location of the temporary structure and the output locations for simulation: 07_FlowWave_1yr330deg_TenneT
+5.25e1
Sheetpile wall
Output location (geotube)
Selected location
TS1
TS2
TS3
TS4
TS5
TS6
TS7
TS8
TS9
TS10
TS11
TS12
0.002
0.001
0.000
−0.001
−0.002
−0.003
4.570
4.575
4.580
4.585
4.590
4.595
4.600

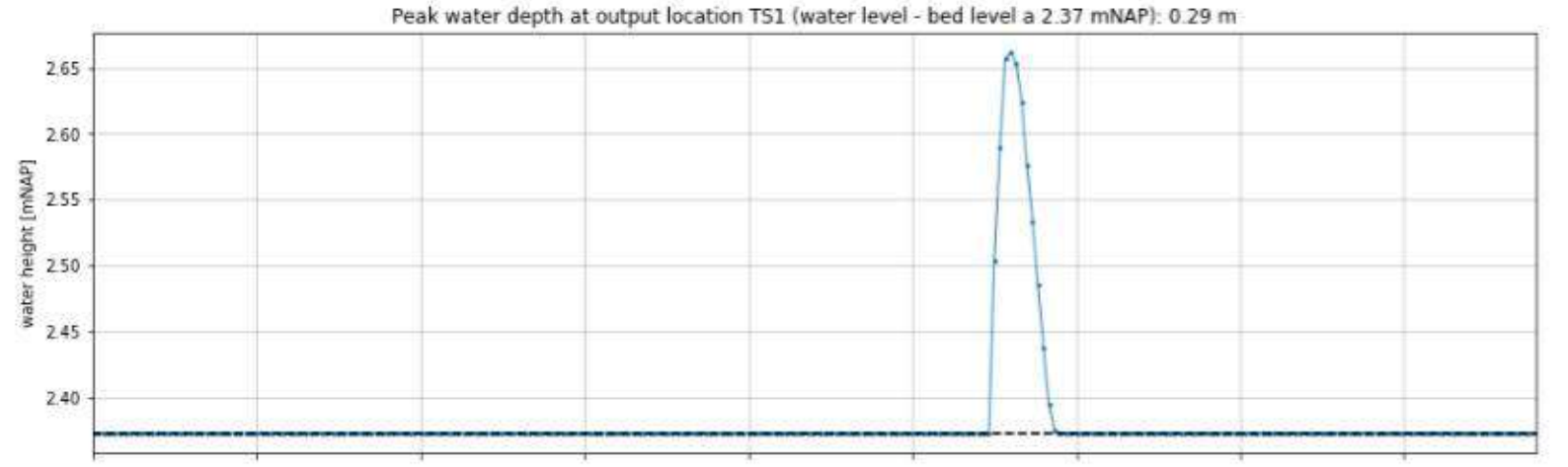
Peak water depth at output location TS1 (water level - bed level a 2.37 mNAP): 0.29 m
water height [mNAP]
2.65
2.60
2.55
2.50
2.45
2.40

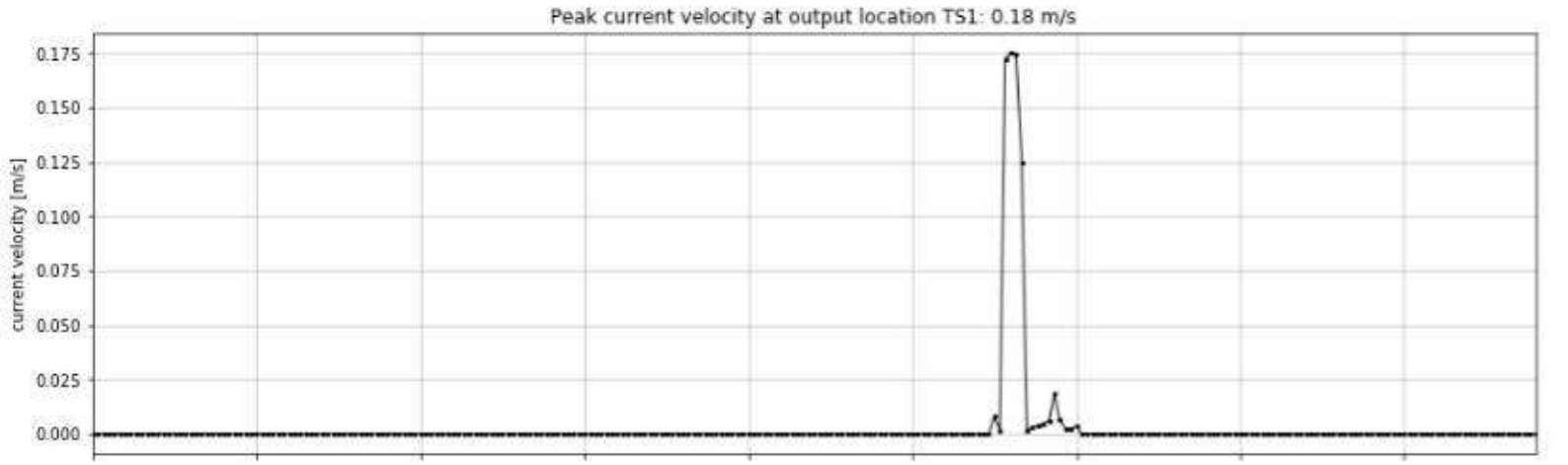
Peak current velocity at output location TS1: 0.18 m/s
current velocity [m/s]
0.175
0.150
0.125
0.100
0.075
0.050
0.025
0.000

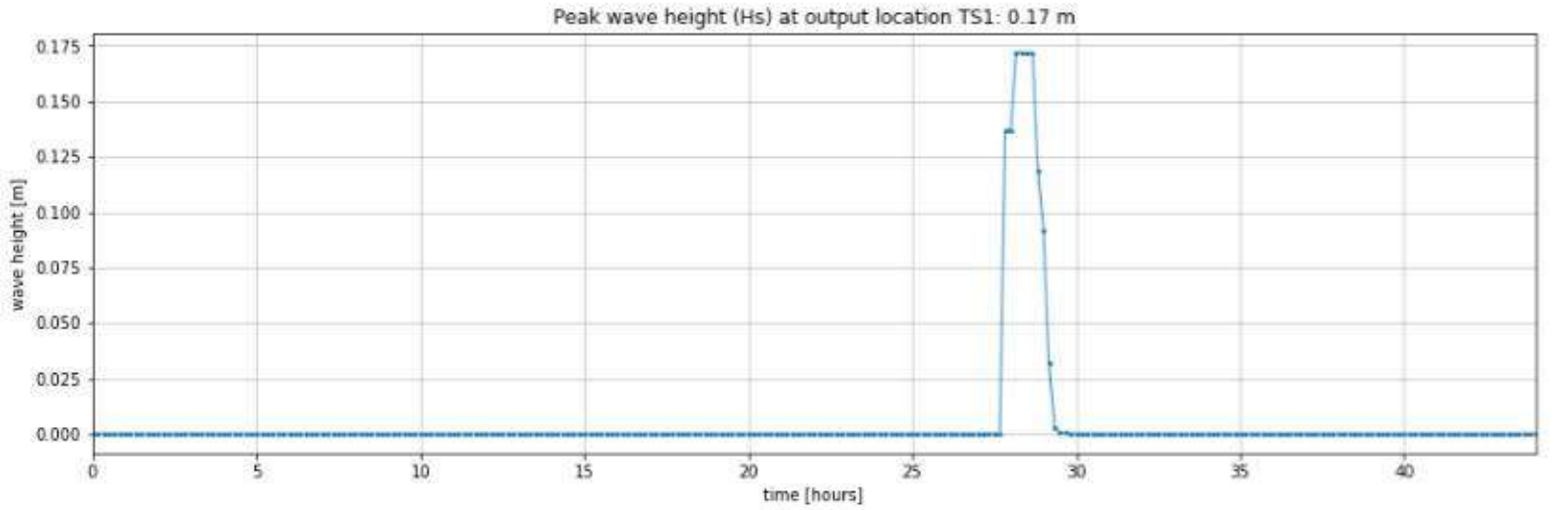
Peak wave height (Hs) at output location TS1: 0.17 m
wave height [m]
0.175
0.150
0.125
0.100
0.075
0.050
0.025
0.000
0
5
10
15
20
25
30
35
40
time [hours]

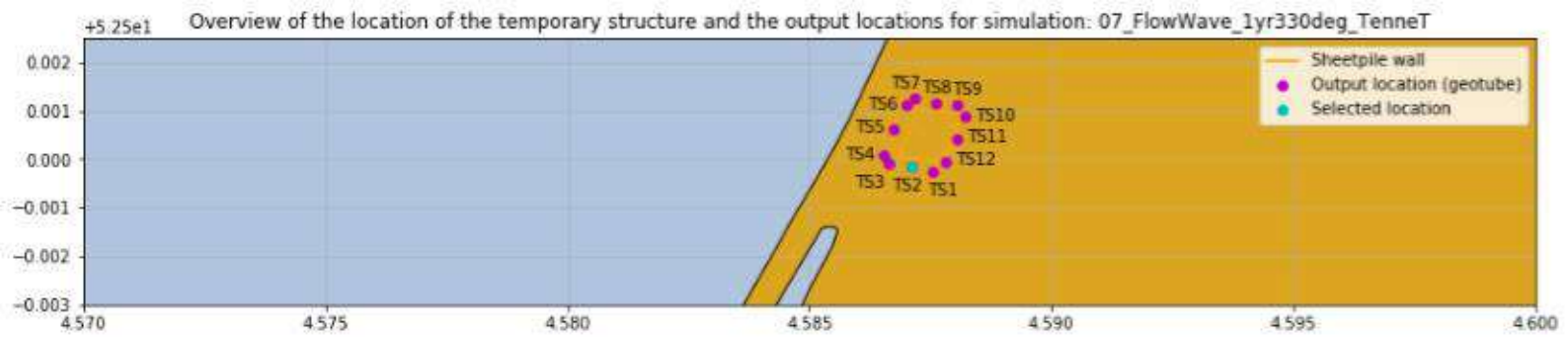
Overview of the location of the temporary structure and the output locations for simulation: 07_FlowWave_1yr330deg_TenneT
+5.25e1
Sheetpile wall
Output location (geotube)
Selected location
TS1
TS2
TS3
TS4
TS5
TS6
TS7
TS8
TS9
TS10
TS11
TS12
0.002
0.001
0.000
−0.001
−0.002
−0.003
4.570
4.575
4.580
4.585
4.590
4.595
4.600

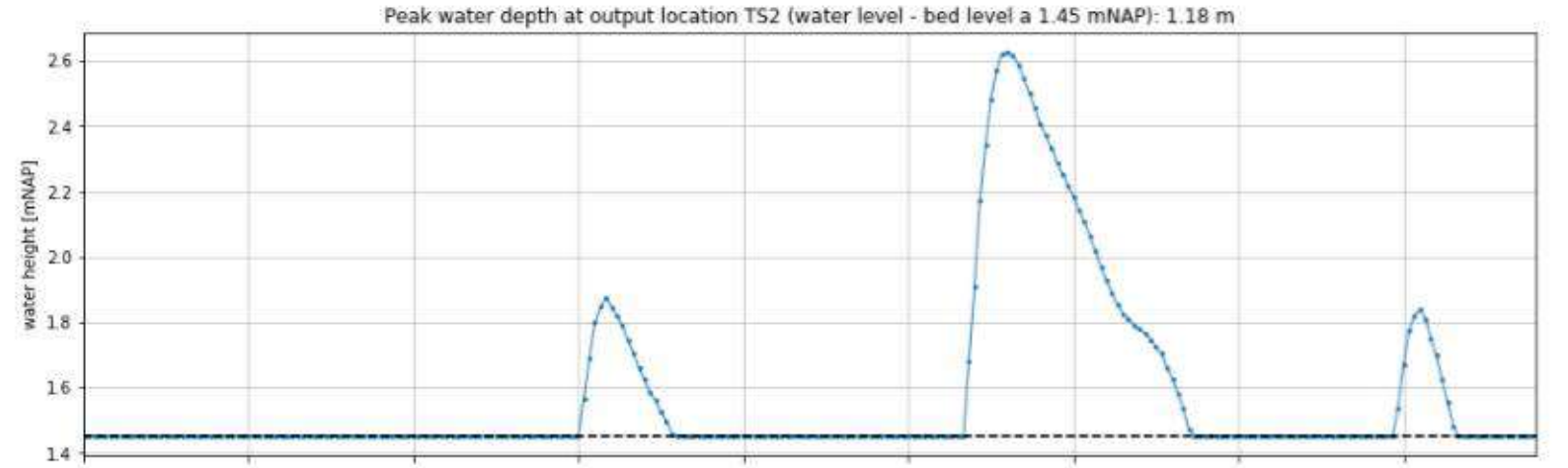
Peak water depth at output location TS2 (water level - bed level a 1.45 mNAP): 1.18 m
water height [mNAP]
2.6
2.4
2.2
2.0
1.8
1.6
1.4

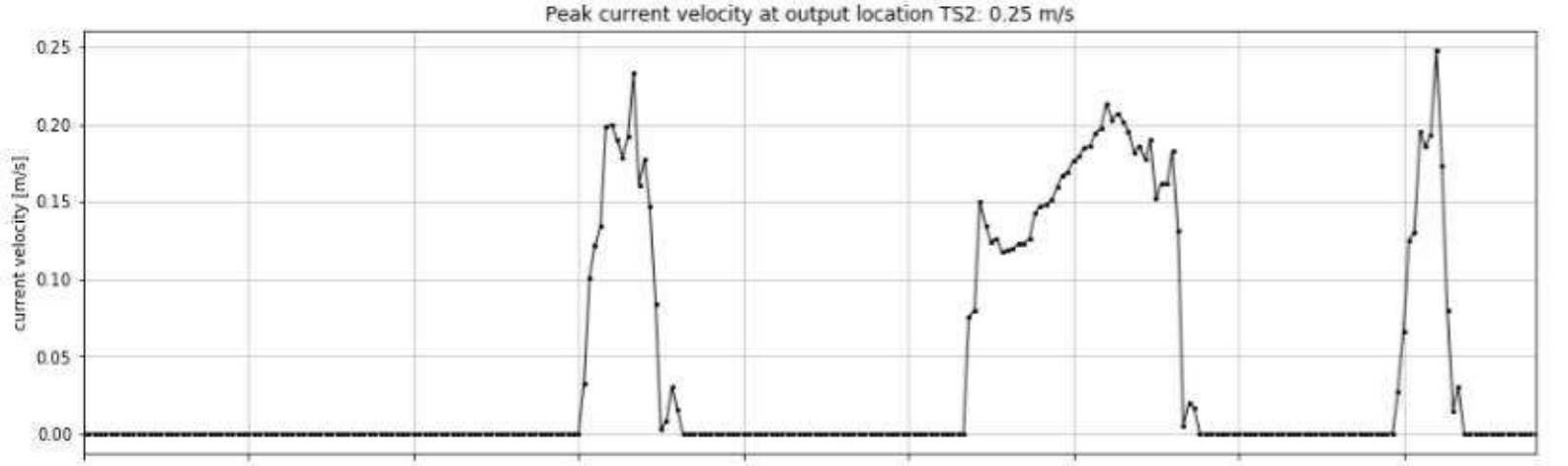
Peak current velocity at output location TS2: 0.25 m/s
current velocity [m/s]
0.25
0.20
0.15
0.10
0.05
0.00

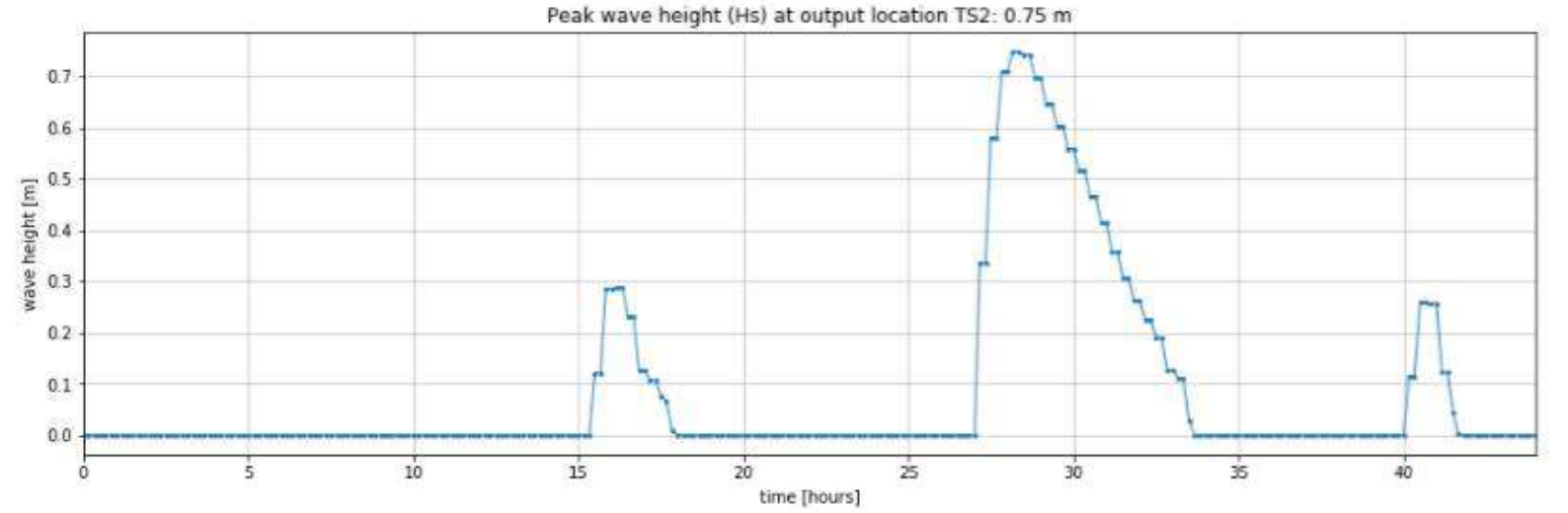
Peak wave height (Hs) at output location TS2: 0.75 m
wave height [m]
0.7
0.6
0.5
0.4
0.3
0.2
0.1
0.0
0
5
10
15
20
25
30
35
40
time [hours]

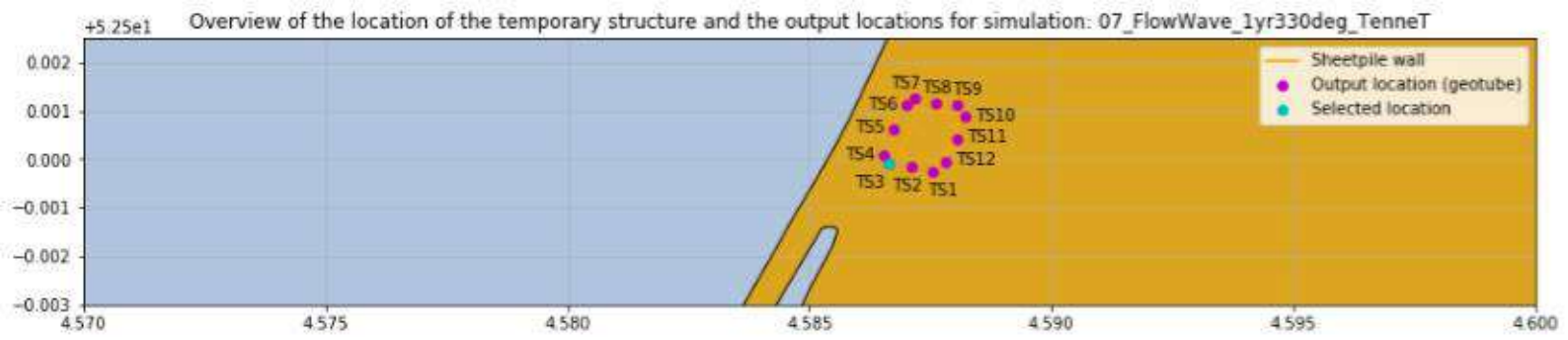
Overview of the location of the temporary structure and the output locations for simulation: 07_FlowWave_1yr330deg_TenneT
+5.25e1
Sheetpile wall
Output location (geotube)
Selected location
TS1
TS2
TS3
TS4
TS5
TS6
TS7
TS8
TS9
TS10
TS11
TS12
0.002
0.001
0.000
−0.001
−0.002
−0.003
4.570
4.575
4.580
4.585
4.590
4.595
4.600

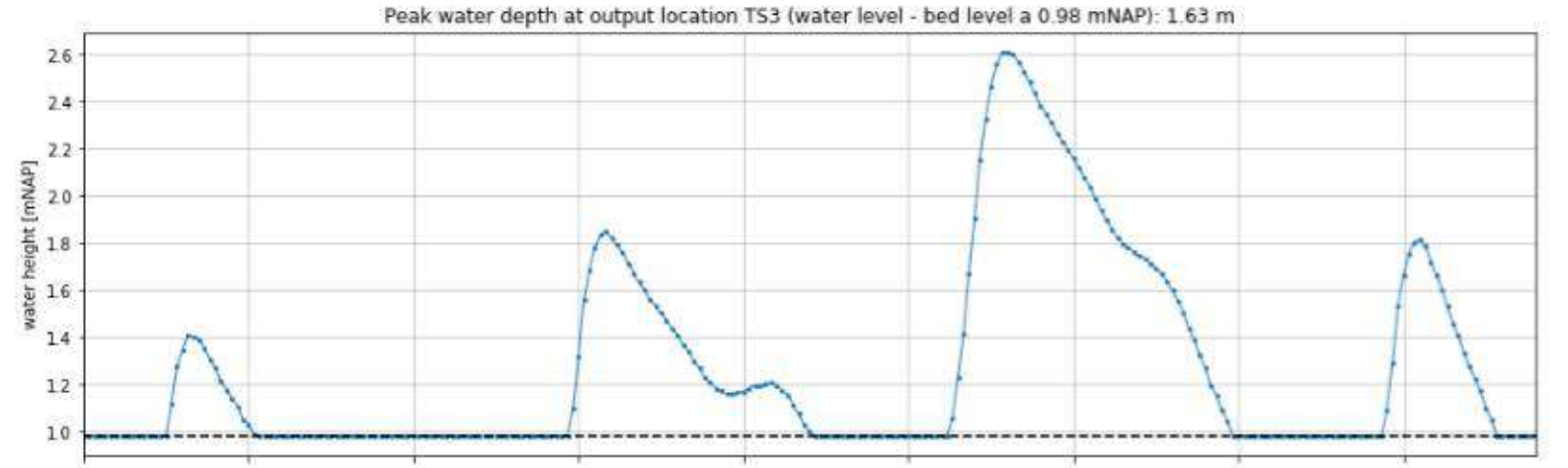
Peak water depth at output location TS3 (water level - bed level a 0.98 mNAP): 1.63 m
water height [mNAP]
2.6
2.4
2.2
2.0
1.8
1.6
1.4
1.2
1.0

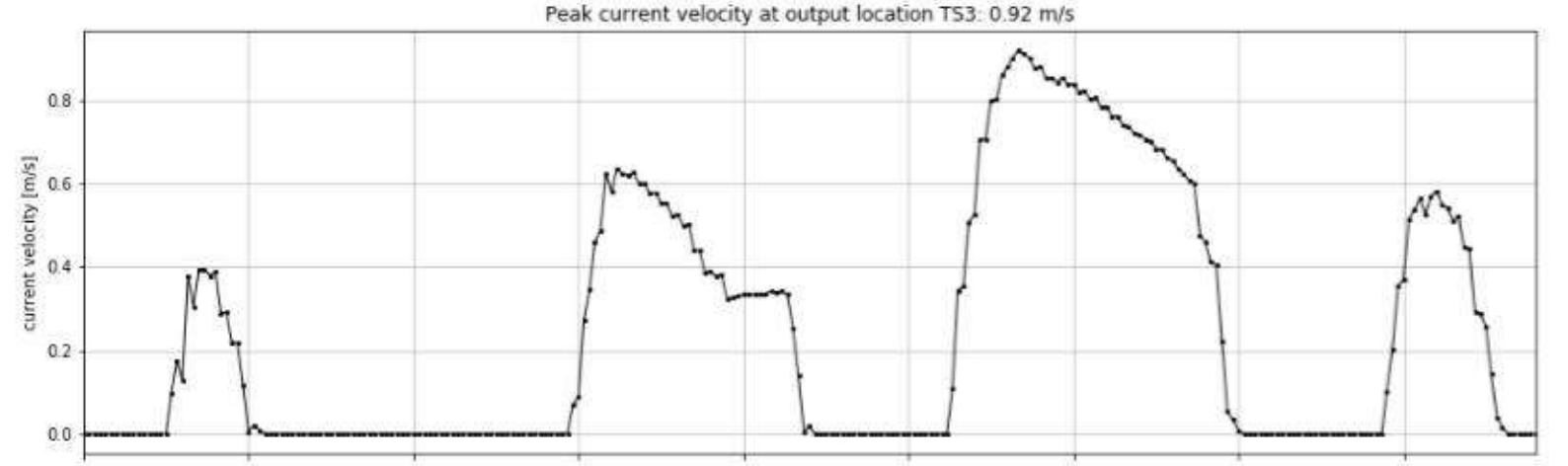
Peak current velocity at output location TS3: 0.92 m/s
current velocity [m/s]
0.8
0.6
0.4
0.2
0.0

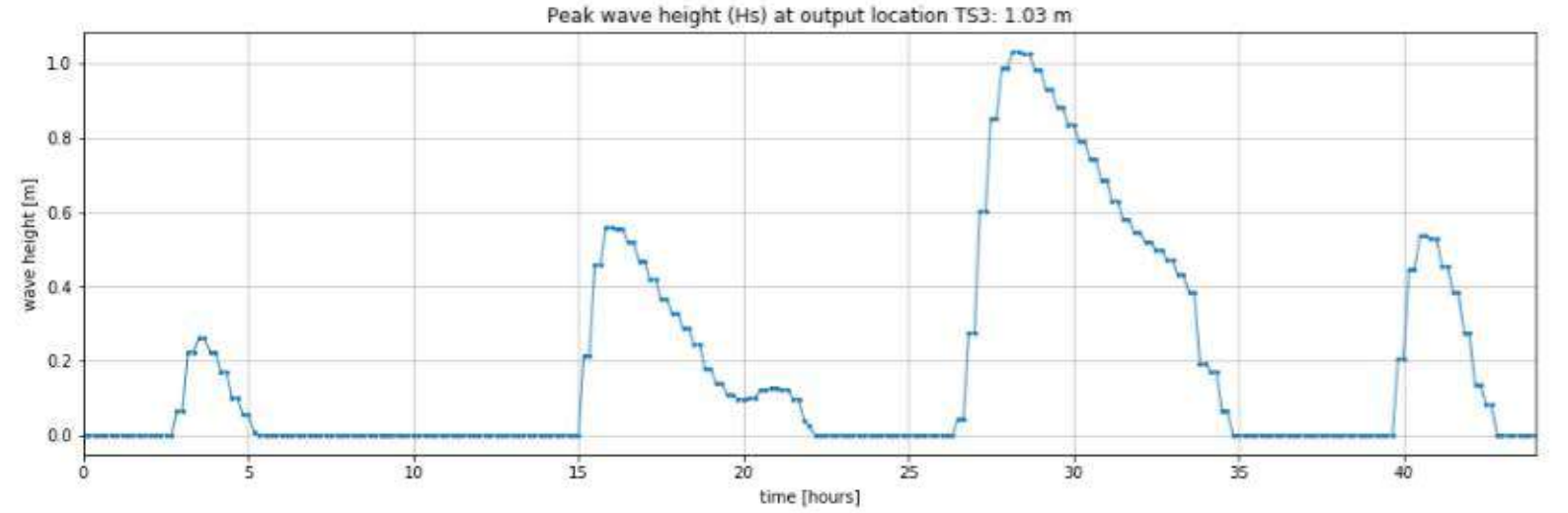
Peak wave height (Hs) at output location TS3: 1.03 m
wave height [m]
1.0
0.8
0.6
0.4
0.2
0.0
0
5
10
15
20
25
30
35
40
time [hours]

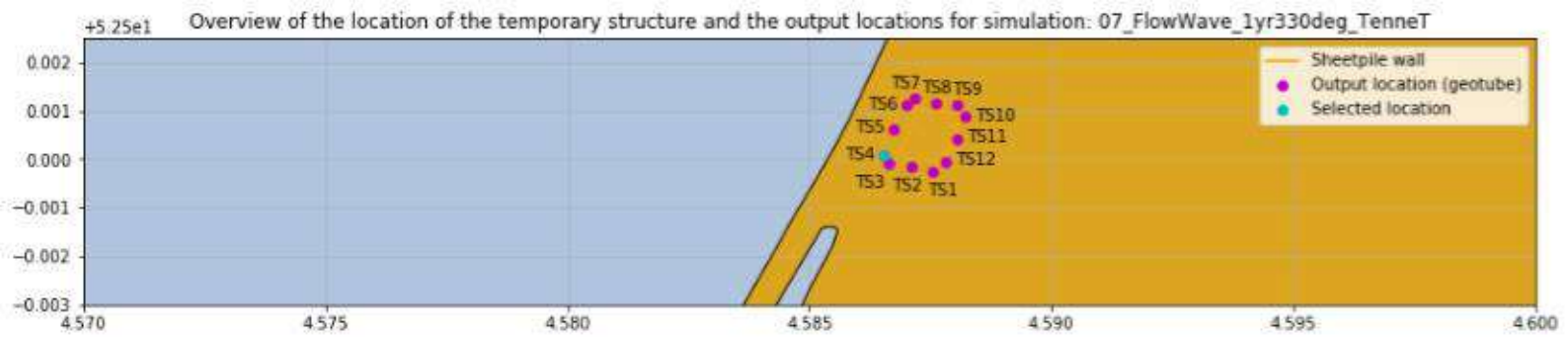
Overview of the location of the temporary structure and the output locations for simulation: 07_FlowWave_1yr330deg_TenneT
+5.25e1
Sheetpile wall
Output location (geotube)
Selected location
TS1
TS2
TS3
TS4
TS5
TS6
TS7
TS8
TS9
TS10
TS11
TS12
0.002
0.001
0.000
−0.001
−0.002
−0.003
4.570
4.575
4.580
4.585
4.590
4.595
4.600

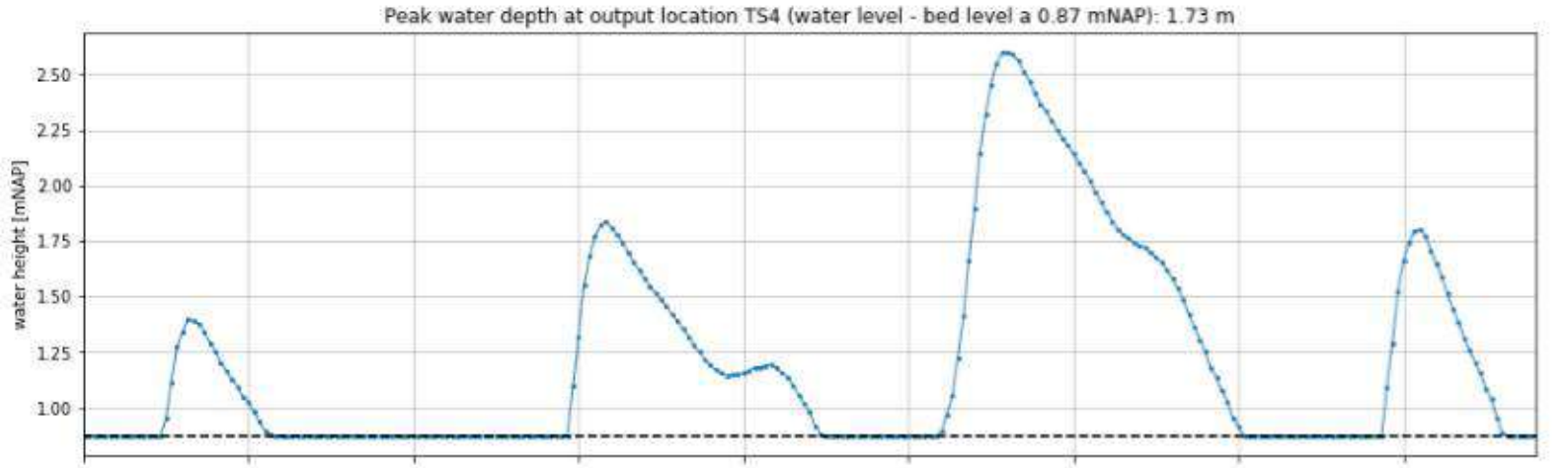
Peak water depth at output location TS4 (water level - bed level a 0.87 mNAP): 1.73 m
water height [mNAP]
2.50
2.25
2.00
1.75
1.50
1.25
1.00

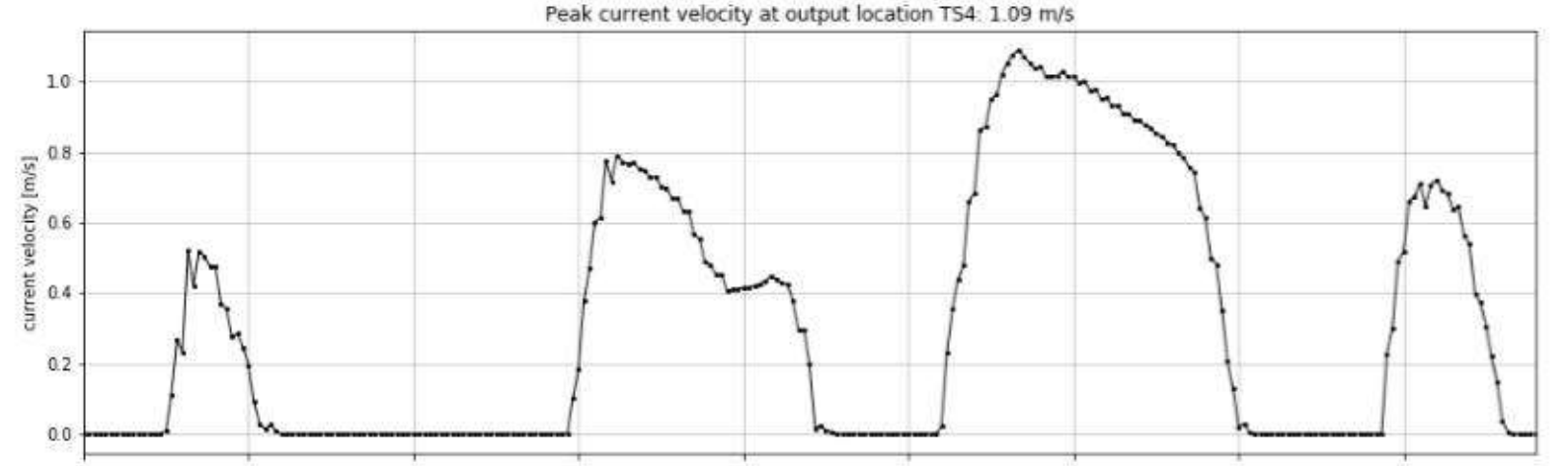
Peak current velocity at output location TS4: 1.09 m/s
current velocity [m/s]
1.0
0.8
0.6
0.4
0.2
0.0

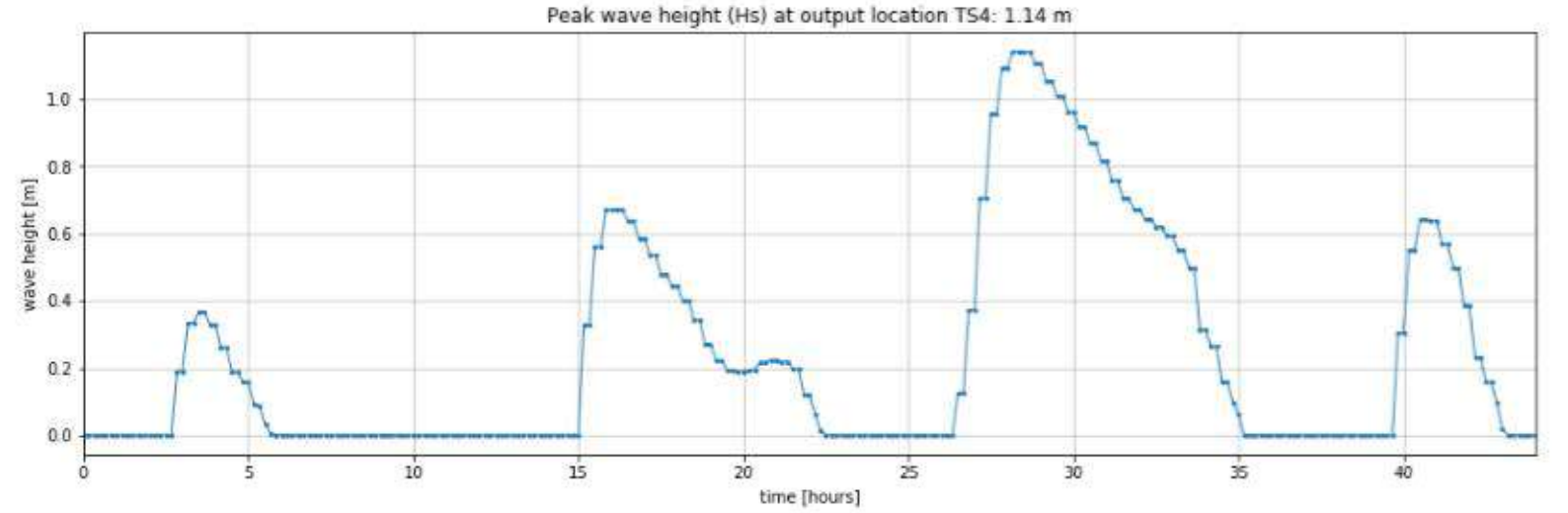
Peak wave height (Hs) at output location TS4: 1.14 m
wave height [m]
1.0
0.8
0.6
0.4
0.2
0.0
0
5
10
15
20
25
30
35
40
time [hours]

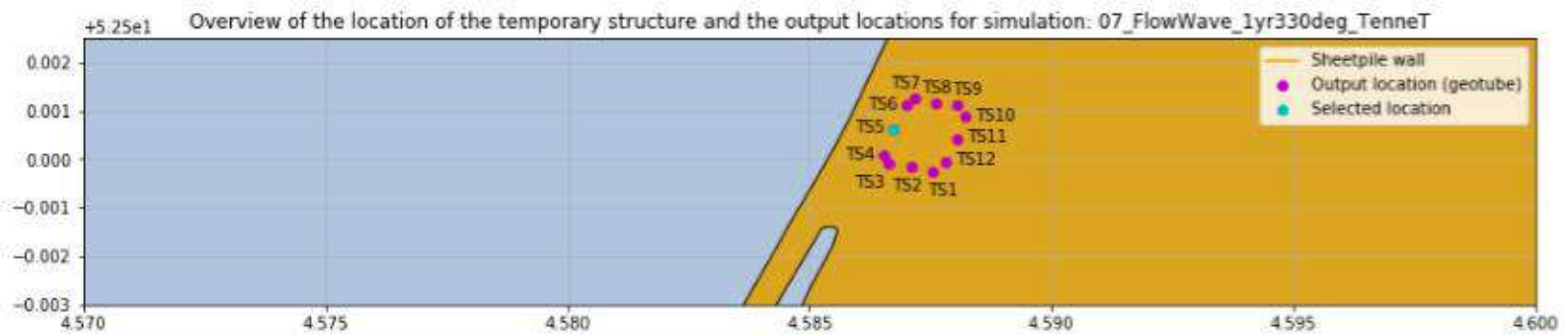
Overview of the location of the temporary structure and the output locations for simulation: 07_FlowWave_1yr330deg_TenneT
+5.25e1
Sheetpile wall
Output location (geotube)
Selected location
TS1
TS2
TS3
TS4
TS5
TS6
TS7
TS8
TS9
TS10
TS11
TS12
0.002
0.001
0.000
−0.001
−0.002
−0.003
4.570
4.575
4.580
4.585
4.590
4.595
4.600

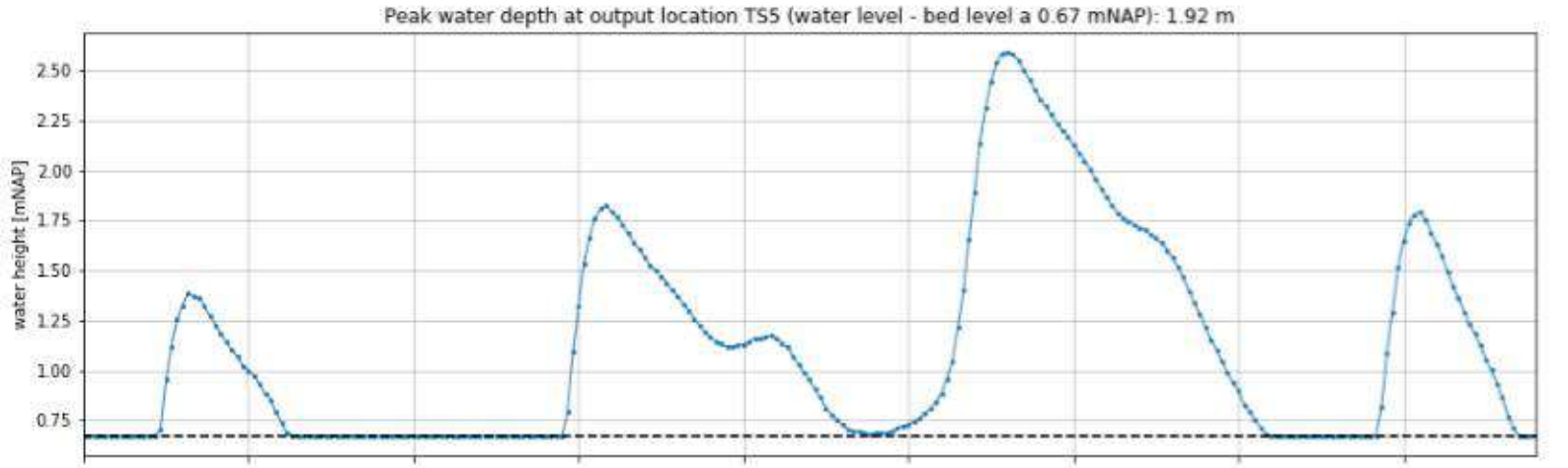
Peak water depth at output location TS5 (water level - bed level a 0.67 mNAP): 1.92 m
water height [mNAP]
2.50
2.25
2.00
1.75
1.50
1.25
1.00
0.75

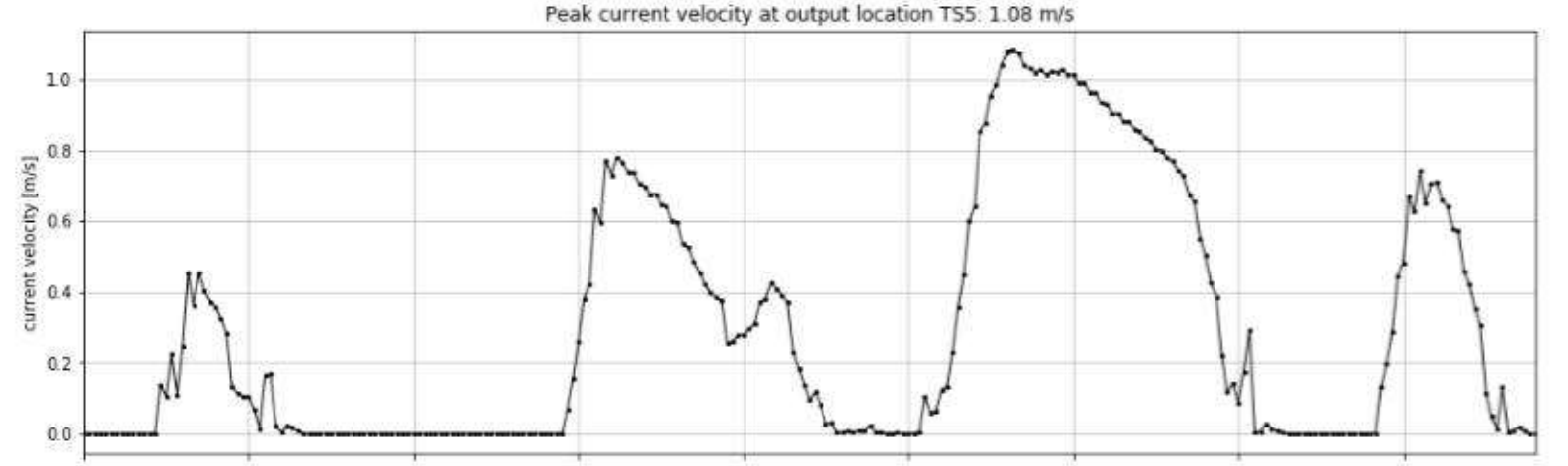
Peak current velocity at output location TS5: 1.08 m/s
current velocity [m/s]
1.0
0.8
0.6
0.4
0.2
0.0

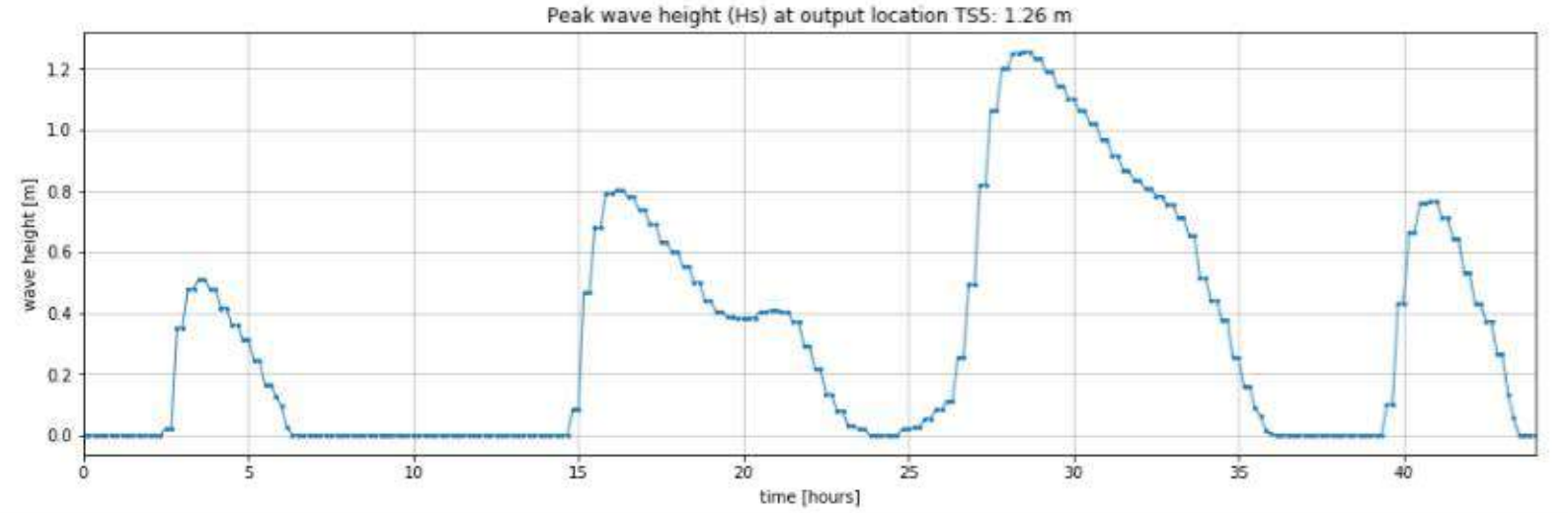
Peak wave height (Hs) at output location TS5: 1.26 m
wave height [m]
1.2
1.0
0.8
0.6
0.4
0.2
0.0
0
5
10
15
20
25
30
35
40
time [hours]

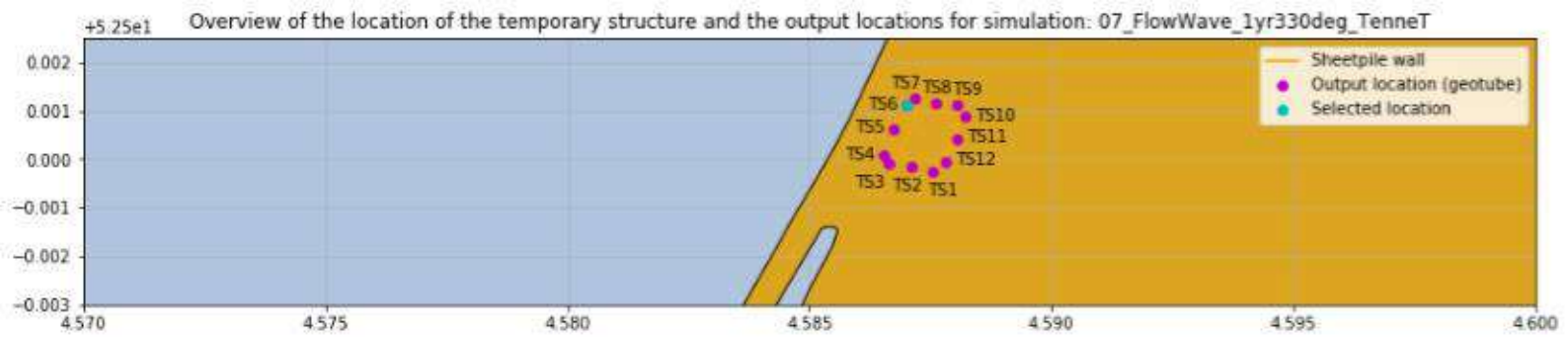
Overview of the location of the temporary structure and the output locations for simulation: 07_FlowWave_1yr330deg_TenneT
+5.25e1
Sheetpile wall
Output location (geotube)
Selected location
TS1
TS2
TS3
TS4
TS5
TS6
TS7
TS8
TS9
TS10
TS11
TS12
0.002
0.001
0.000
−0.001
−0.002
−0.003
4.570
4.575
4.580
4.585
4.590
4.595
4.600

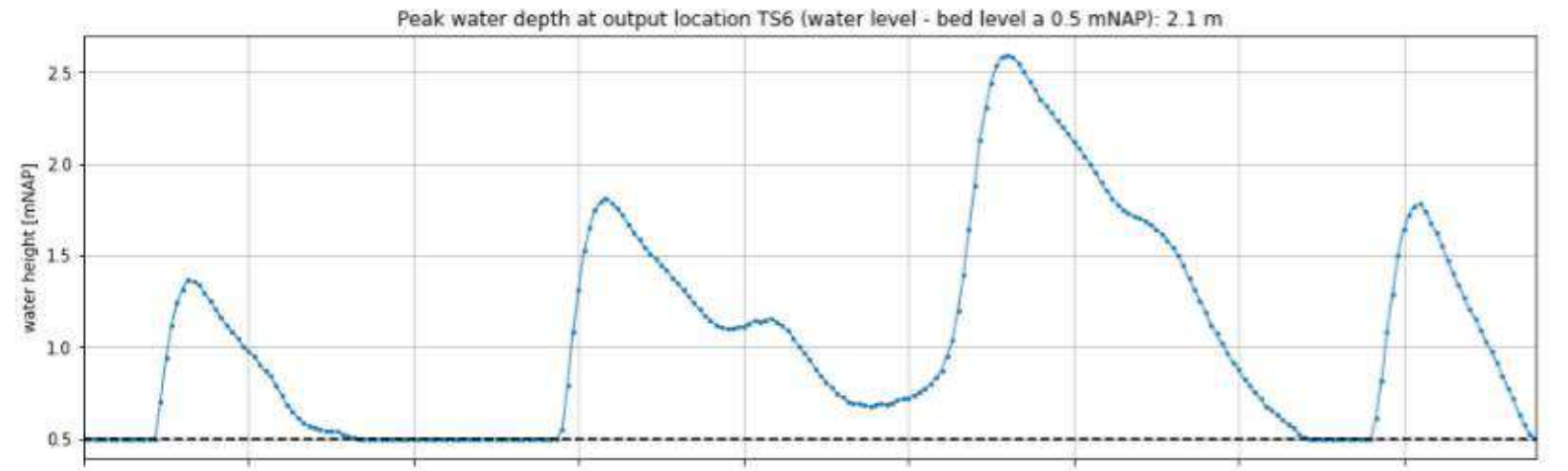
Peak water depth at output location TS6 (water level - bed level a 0.5 mNAP): 2.1 m
water height [mNAP]
2.5
2.0
1.5
1.0
0.5

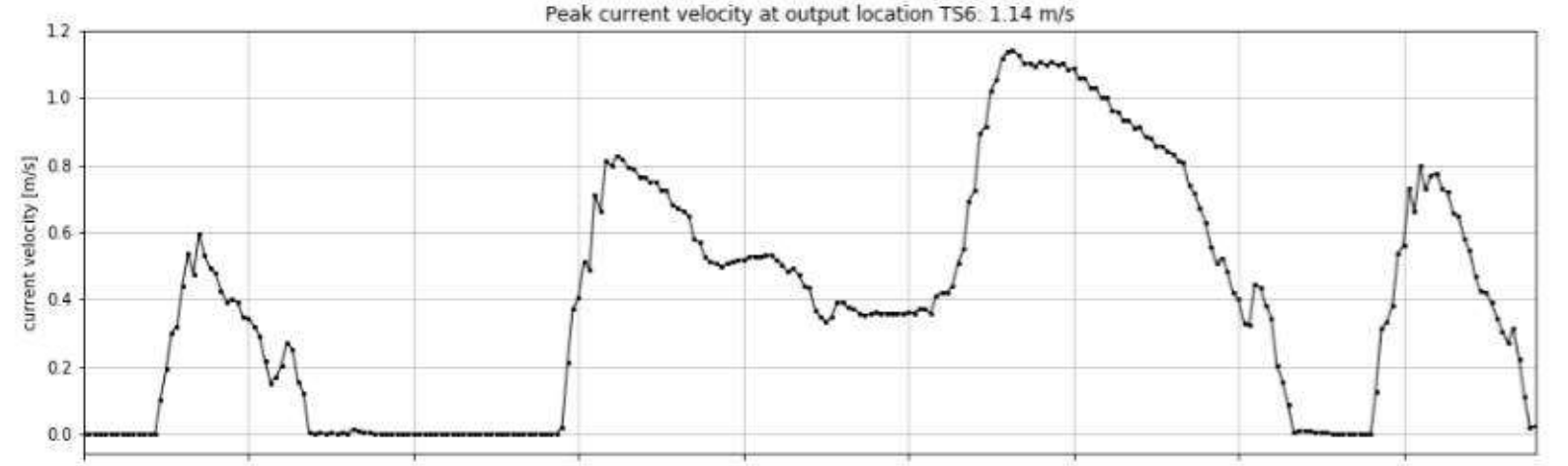
Peak current velocity at output location TS6: 1.14 m/s
current velocity [m/s]
1.2
1.0
0.8
0.6
0.4
0.2
0.0

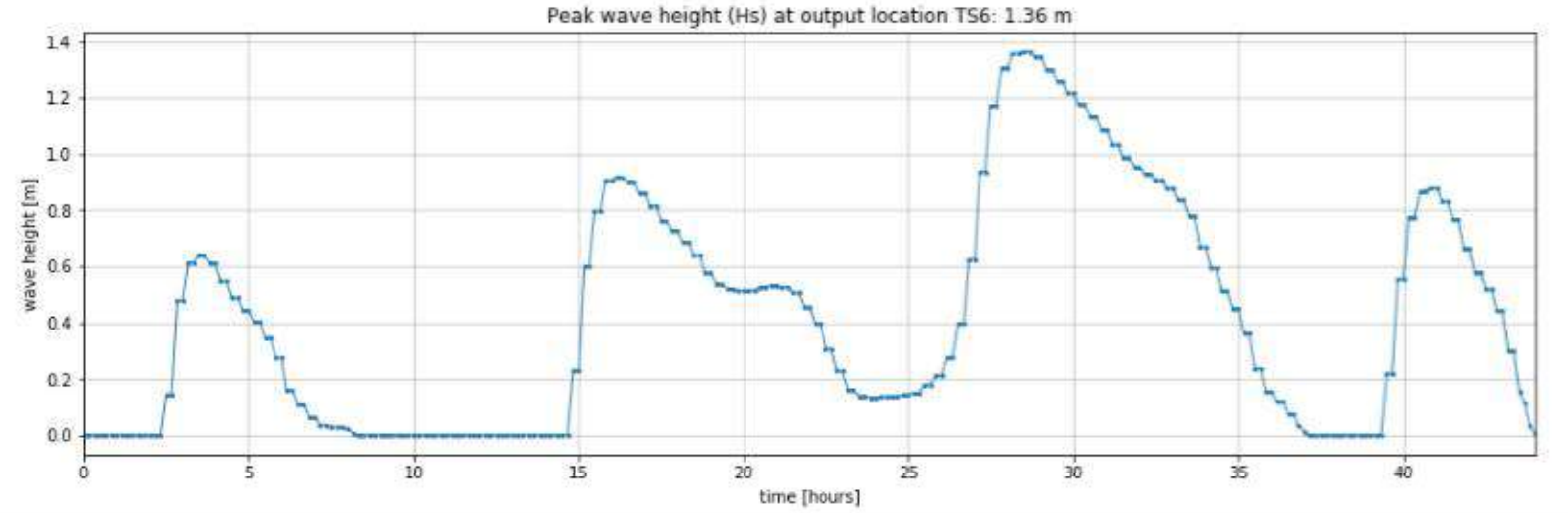
Peak wave height (Hs) at output location TS6: 1.36 m
wave height [m]
1.4
1.2
1.0
0.8
0.6
0.4
0.2
0.0
0
5
10
15
20
25
30
35
40
time [hours]

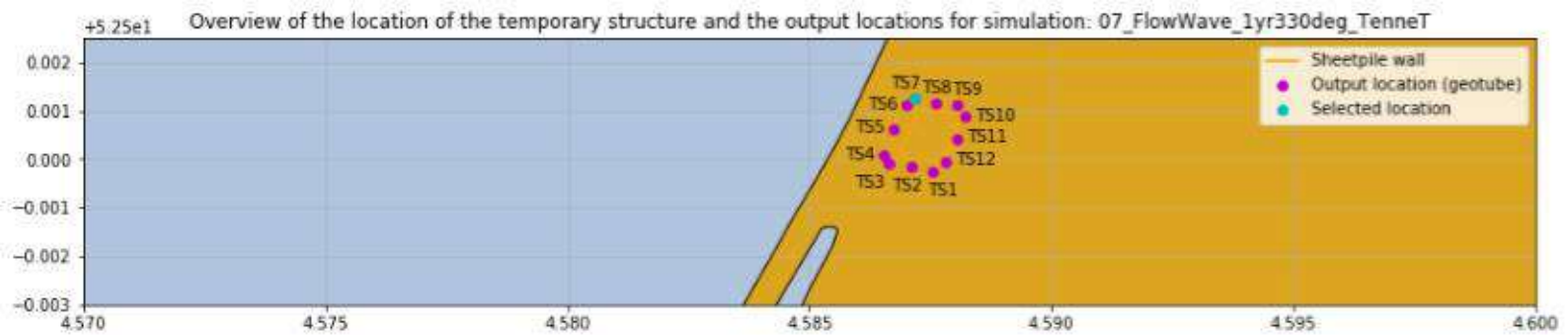
Overview of the location of the temporary structure and the output locations for simulation: 07_FlowWave_1yr330deg_TenneT
+5.25e1
Sheetpile wall
Output location (geotube)
Selected location
TS1
TS2
TS3
TS4
TS5
TS6
TS7
TS8
TS9
TS10
TS11
TS12
0.002
0.001
0.000
−0.001
−0.002
−0.003
4.570
4.575
4.580
4.585
4.590
4.595
4.600

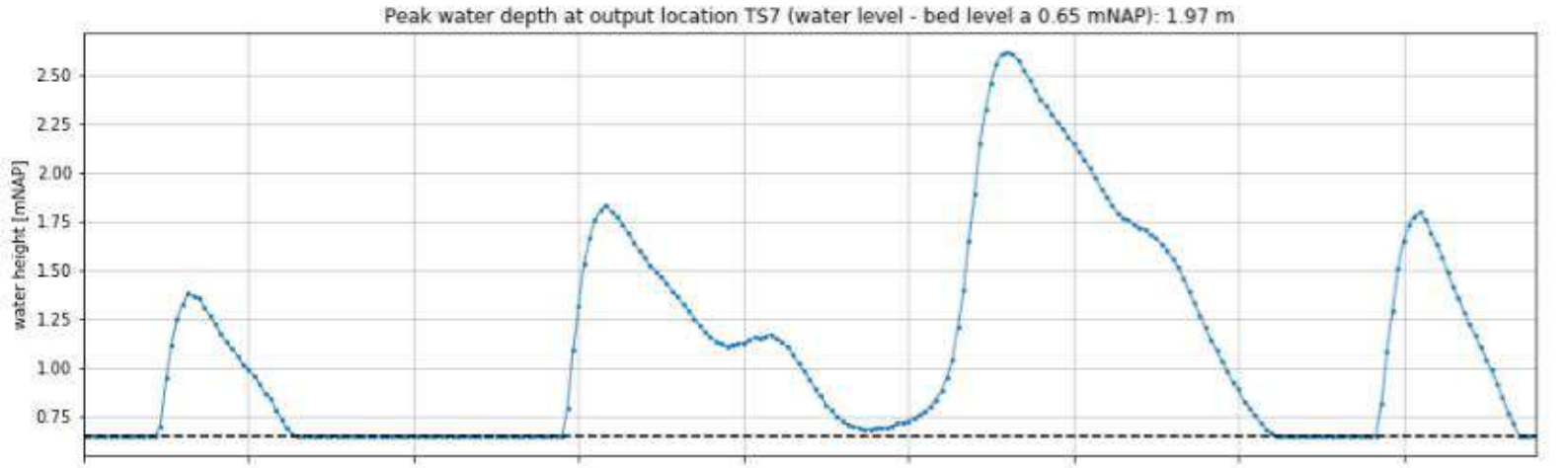
Peak water depth at output location TS7 (water level - bed level a 0.65 mNAP): 1.97 m
water height [mNAP]
2.50
2.25
2.00
1.75
1.50
1.25
1.00
0.75

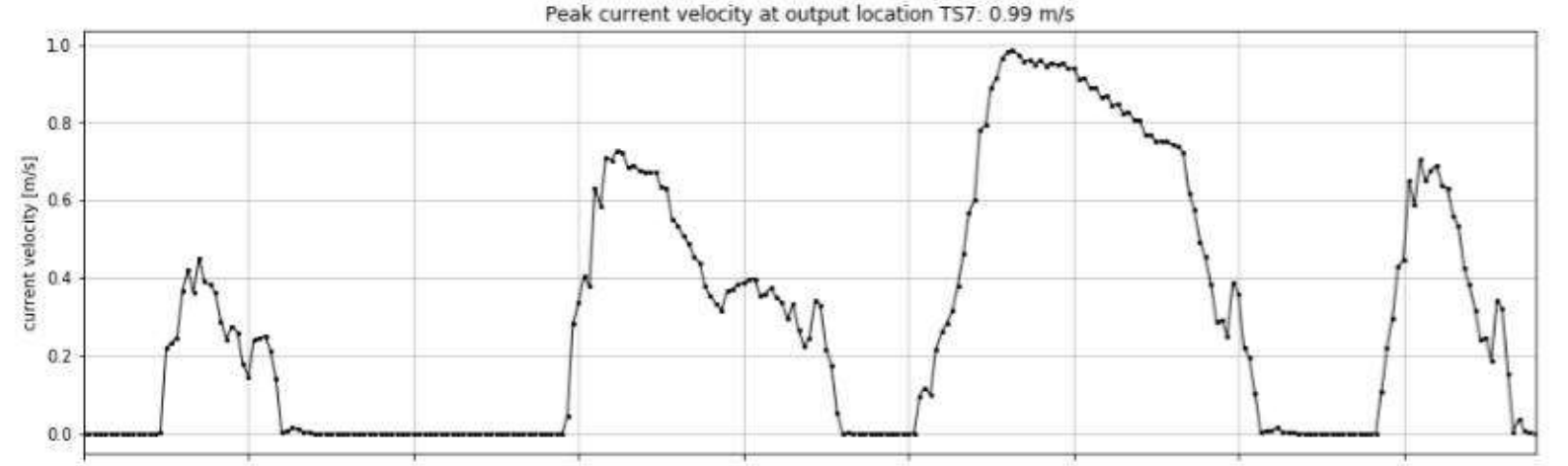
Peak current velocity at output location TS7: 0.99 m/s
current velocity [m/s]
1.0
0.8
0.6
0.4
0.2
0.0

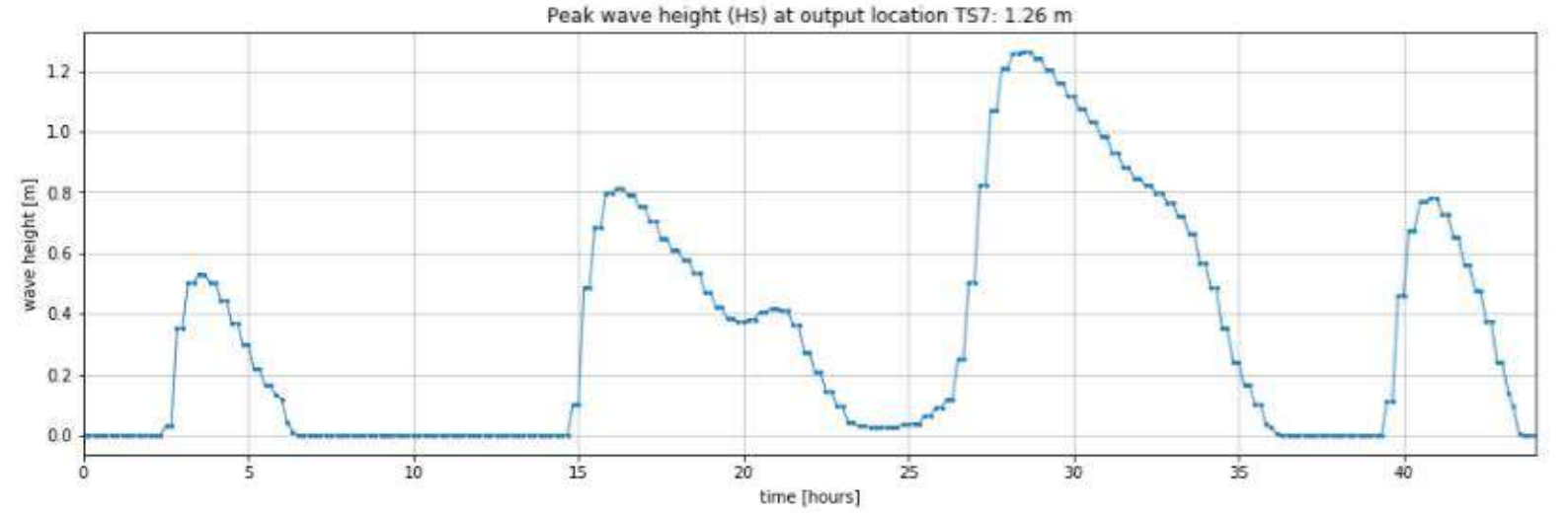
Peak wave height (Hs) at output location TS7: 1.26 m
wave height [m]
1.2
1.0
0.8
0.6
0.4
0.2
0.0
0
5
10
15
20
25
30
35
40
time [hours]

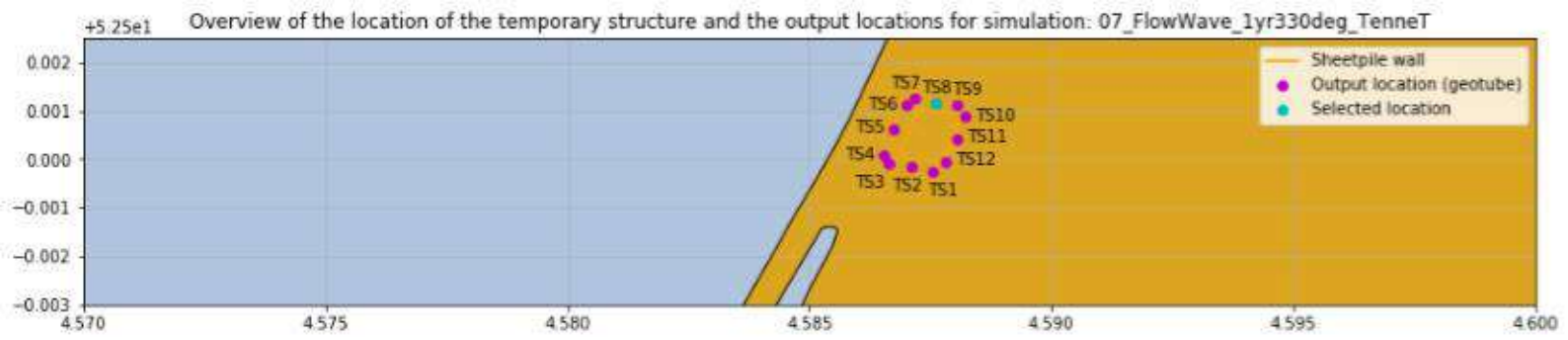
Overview of the location of the temporary structure and the output locations for simulation: 07_FlowWave_1yr330deg_TenneT
+5.25e1
Sheetpile wall
Output location (geotube)
Selected location
TS1
TS2
TS3
TS4
TS5
TS6
TS7
TS8
TS9
TS10
TS11
TS12
0.002
0.001
0.000
−0.001
−0.002
−0.003
4.570
4.575
4.580
4.585
4.590
4.595
4.600

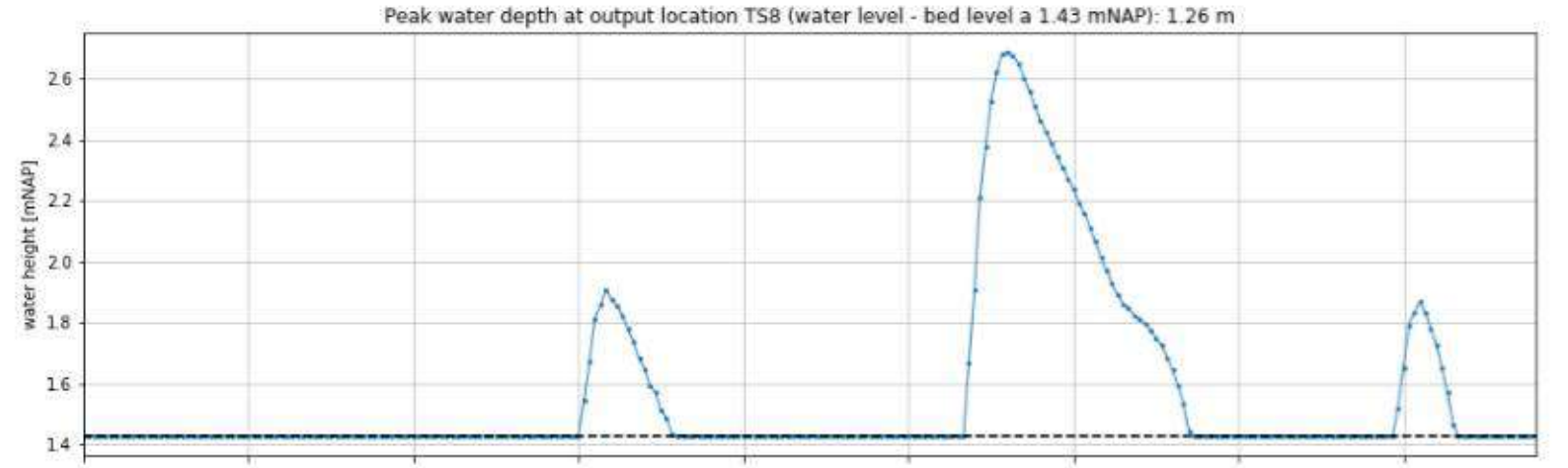
Peak water depth at output location TS8 (water level - bed level a 1.43 mNAP): 1.26 m
water height [mNAP]
2.6
2.4
2.2
2.0
1.8
1.6
1.4

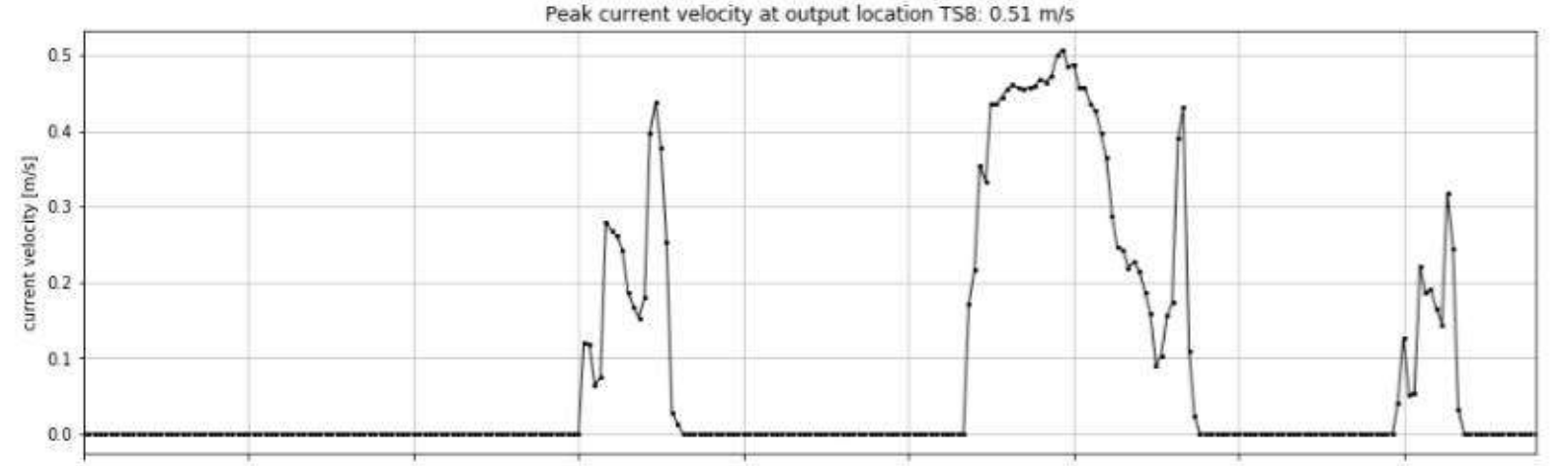
Peak current velocity at output location TS8: 0.51 m/s
current velocity [m/s]
0.5
0.4
0.3
0.2
0.1
0.0

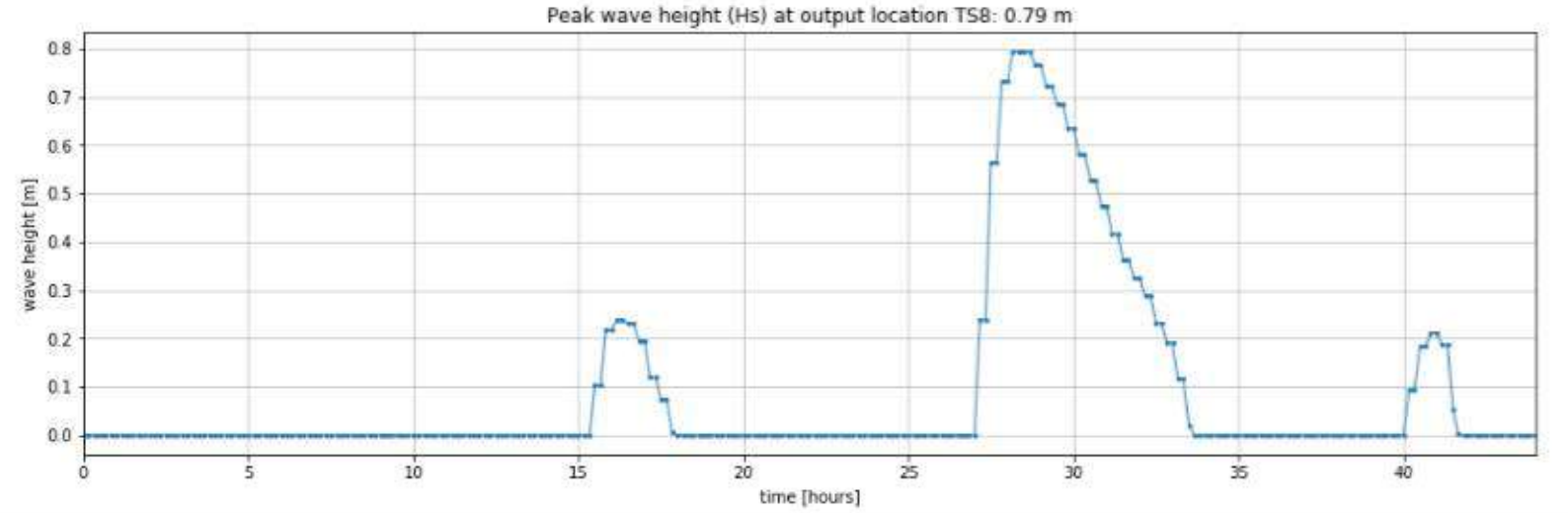
Peak wave height (Hs) at output location TS8: 0.79 m
wave height [m]
0.8
0.7
0.6
0.5
0.4
0.3
0.2
0.1
0.0
0
5
10
15
20
25
30
35
40
time [hours]

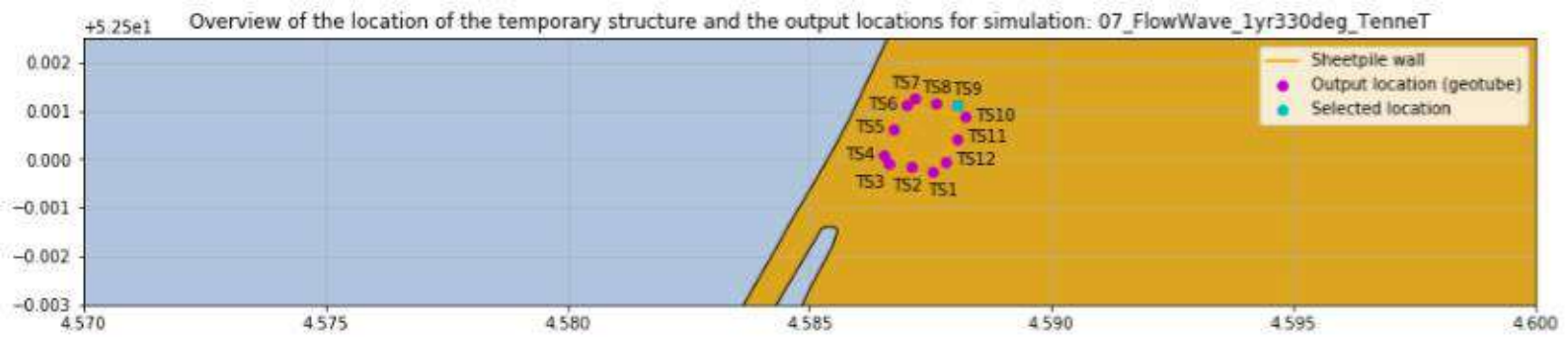
Overview of the location of the temporary structure and the output locations for simulation: 07_FlowWave_1yr330deg_TenneT
+5.25e1
Sheetpile wall
Output location (geotube)
Selected location
TS1
TS2
TS3
TS4
TS5
TS6
TS7
TS8
TS9
TS10
TS11
TS12
0.002
0.001
0.000
−0.001
−0.002
−0.003
4.570
4.575
4.580
4.585
4.590
4.595
4.600

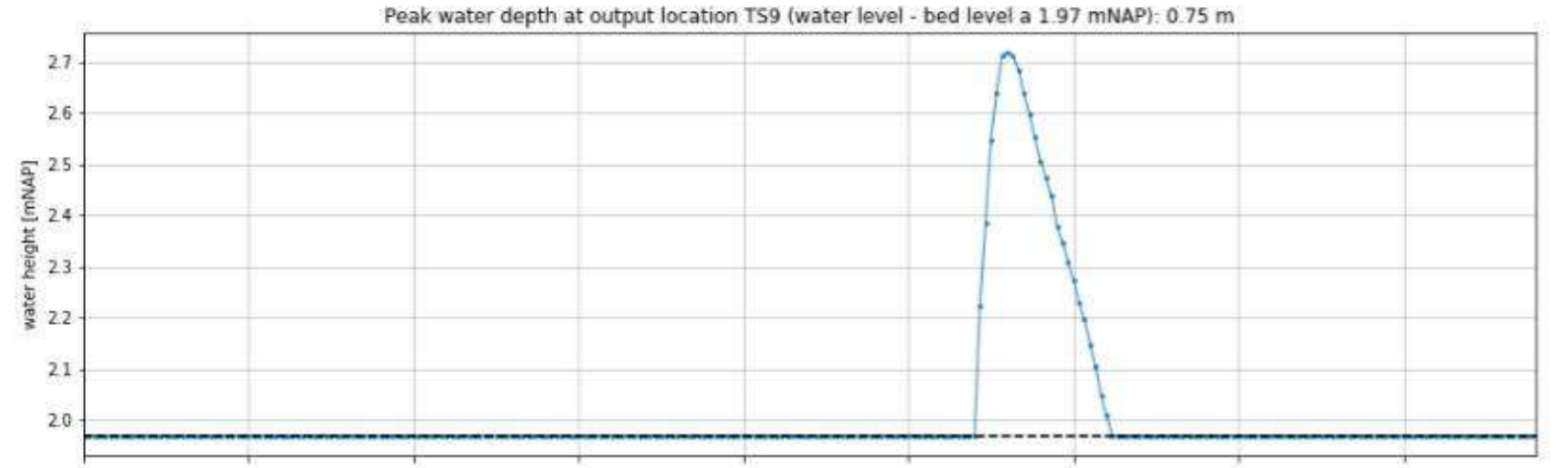
Peak water depth at output location TS9 (water level - bed level a 1.97 mNAP): 0.75 m
water height [mNAP]
2.7
2.6
2.5
2.4
2.3
2.2
2.1
2.0

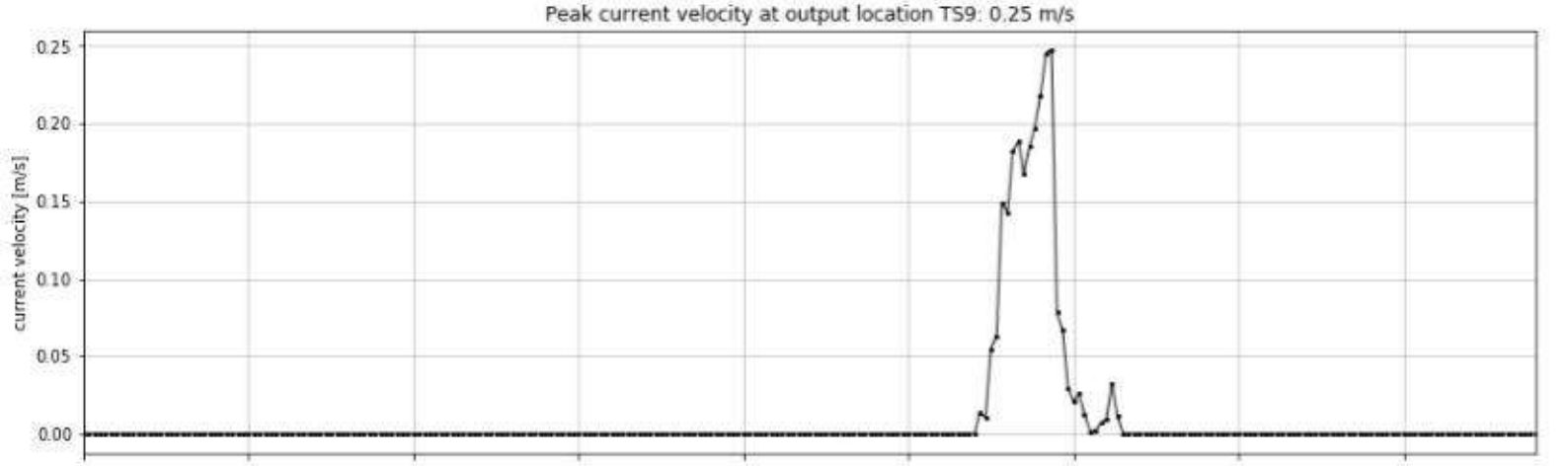
Peak current velocity at output location TS9: 0.25 m/s
current velocity [m/s]
0.25
0.20
0.15
0.10
0.05
0.00

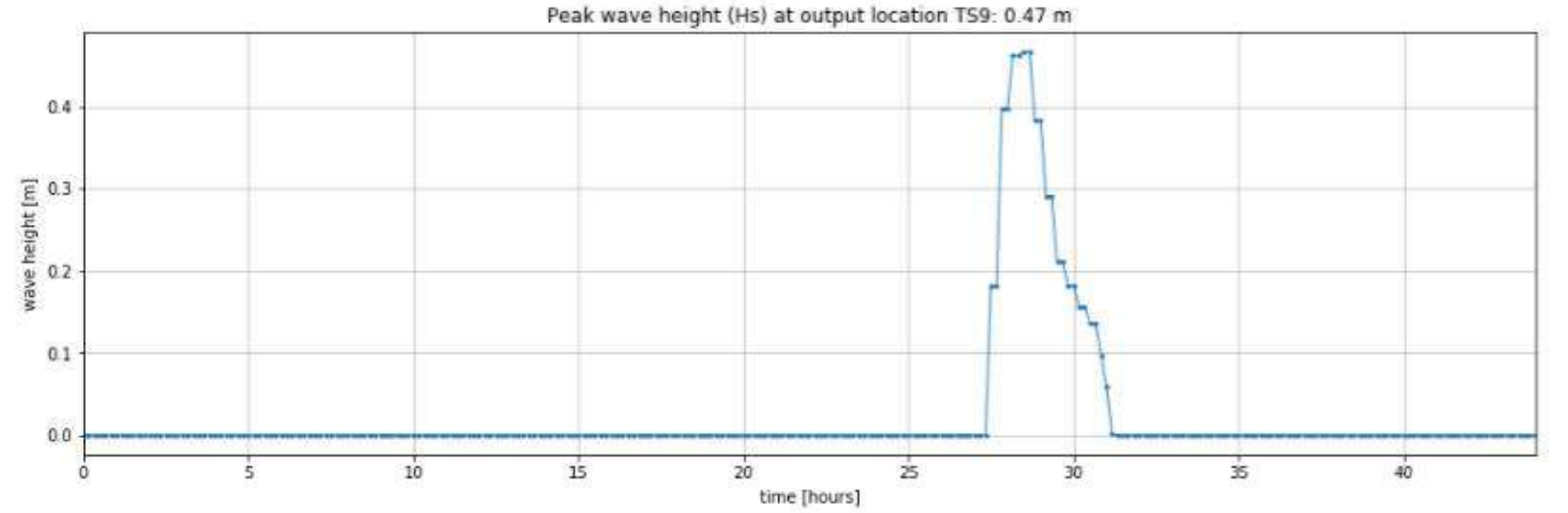
Peak wave height (Hs) at output location TS9: 0.47 m
wave height [m]
0.4
0.3
0.2
0.1
0.0
0
5
10
15
20
25
30
35
40
time [hours]

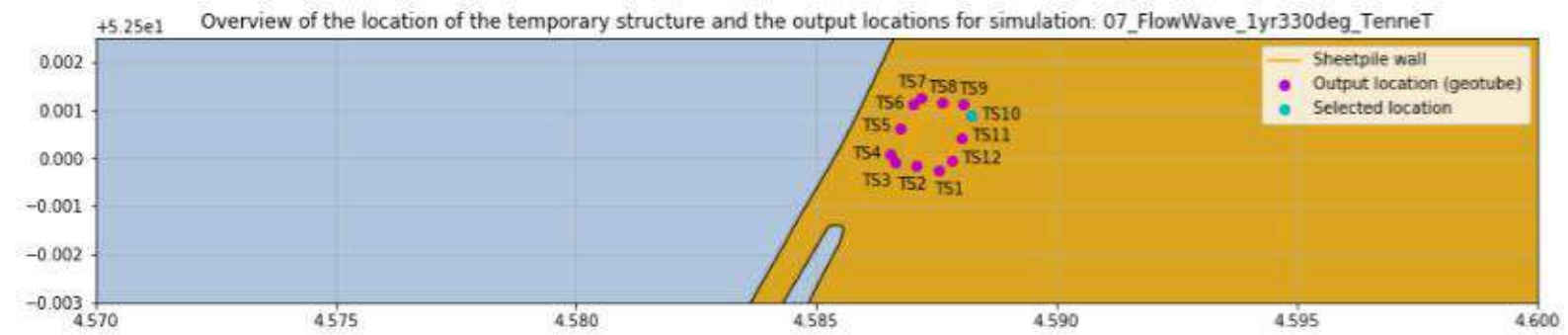
Overview of the location of the temporary structure and the output locations for simulation: 07_FlowWave_1yr330deg_TenneT
+5.25e1
Sheetpile wall
Output location (geotube)
Selected location
TS1
TS2
TS3
TS4
TS5
TS6
TS7
TS8
TS9
TS10
TS11
TS12
0.002
0.001
0.000
−0.001
−0.002
−0.003
4.570
4.575
4.580
4.585
4.590
4.595
4.600

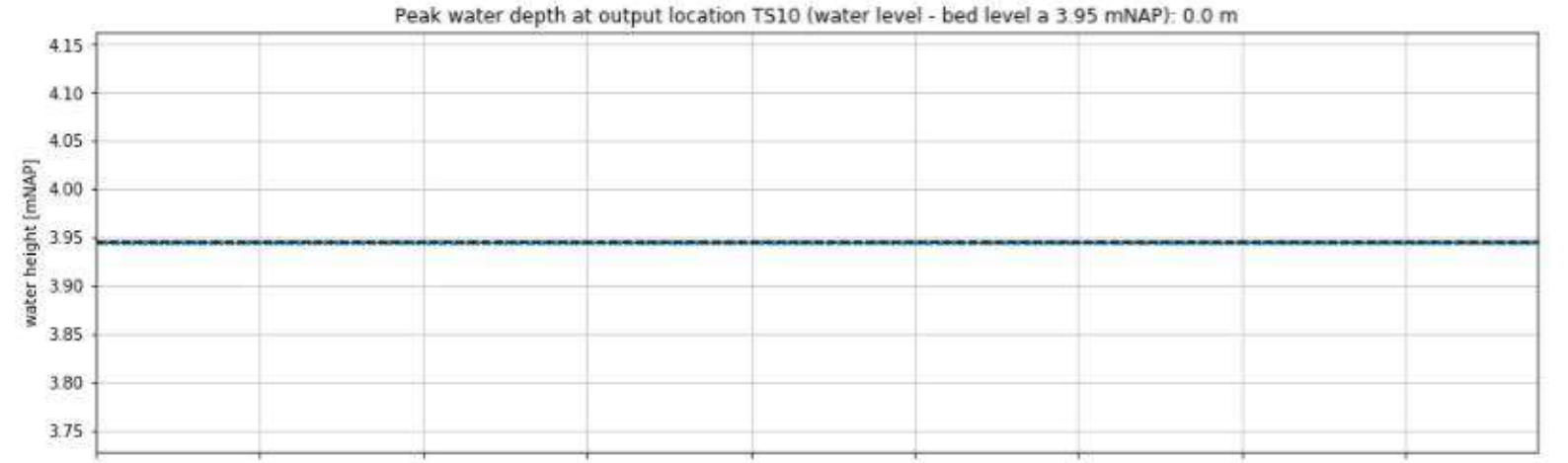
Peak water depth at output location TS10 (water level - bed level a 3.95 mNAP): 0.0 m
water height [mNAP]
4.15
4.10
4.05
4.00
3.95
3.90
3.85
3.80
3.75

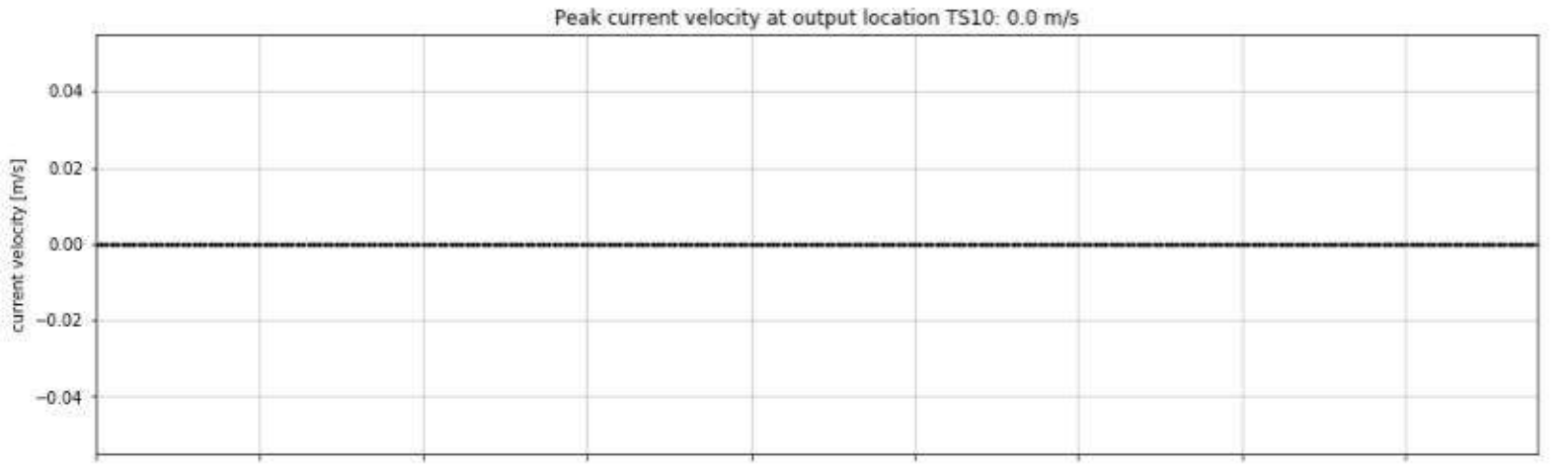
Peak current velocity at output location TS10: 0.0 m/s
current velocity [m/s]
0.04
0.02
0.00
−0.02
−0.04

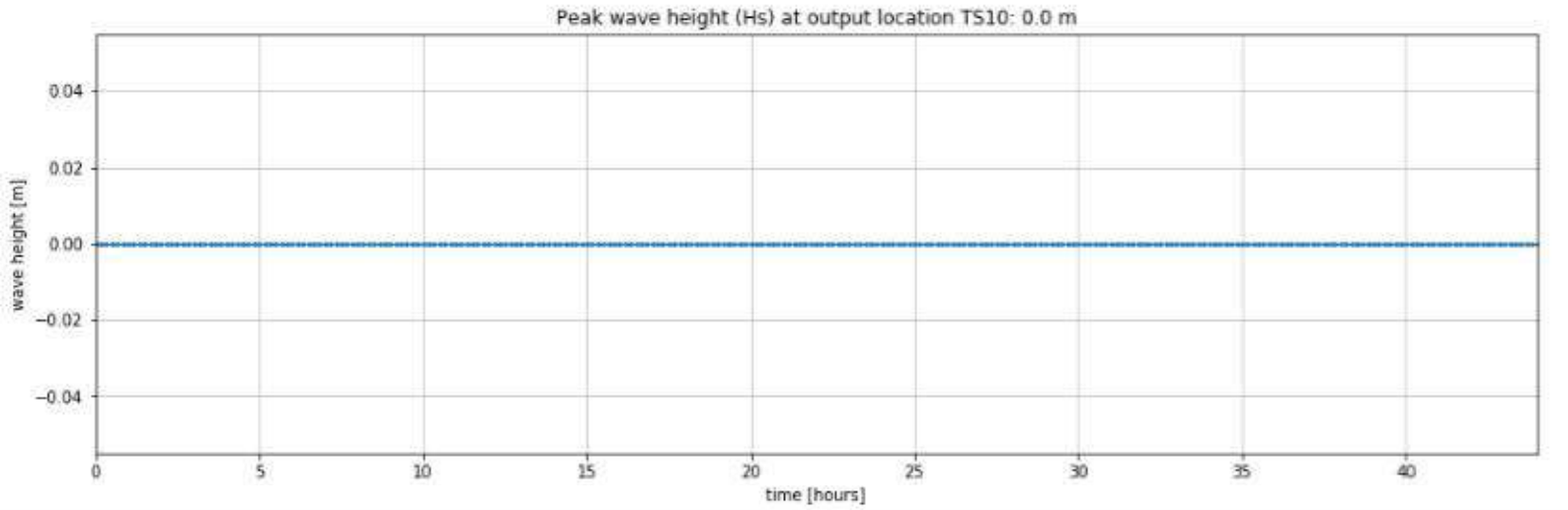
Peak wave height (Hs) at output location TS10: 0.0 m
wave height [m]
0.04
0.02
0.00
−0.02
−0.04
0
5
10
15
20
25
30
35
40
time [hours]

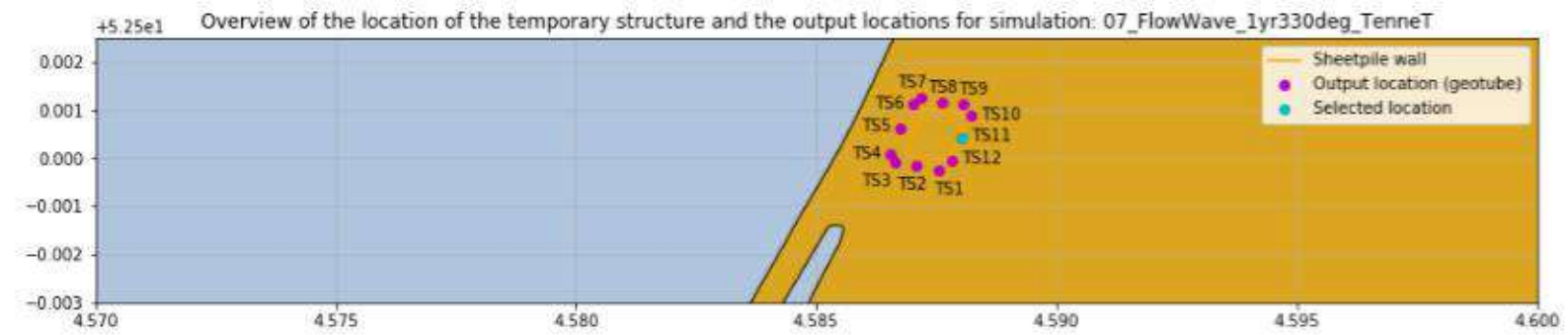
Overview of the location of the temporary structure and the output locations for simulation: 07_FlowWave_1yr330deg_TenneT
+5.25e1
Sheetpile wall
Output location (geotube)
Selected location
TS1
TS2
TS3
TS4
TS5
TS6
TS7
TS8
TS9
TS10
TS11
TS12
0.002
0.001
0.000
−0.001
−0.002
−0.003
4.570
4.575
4.580
4.585
4.590
4.595
4.600

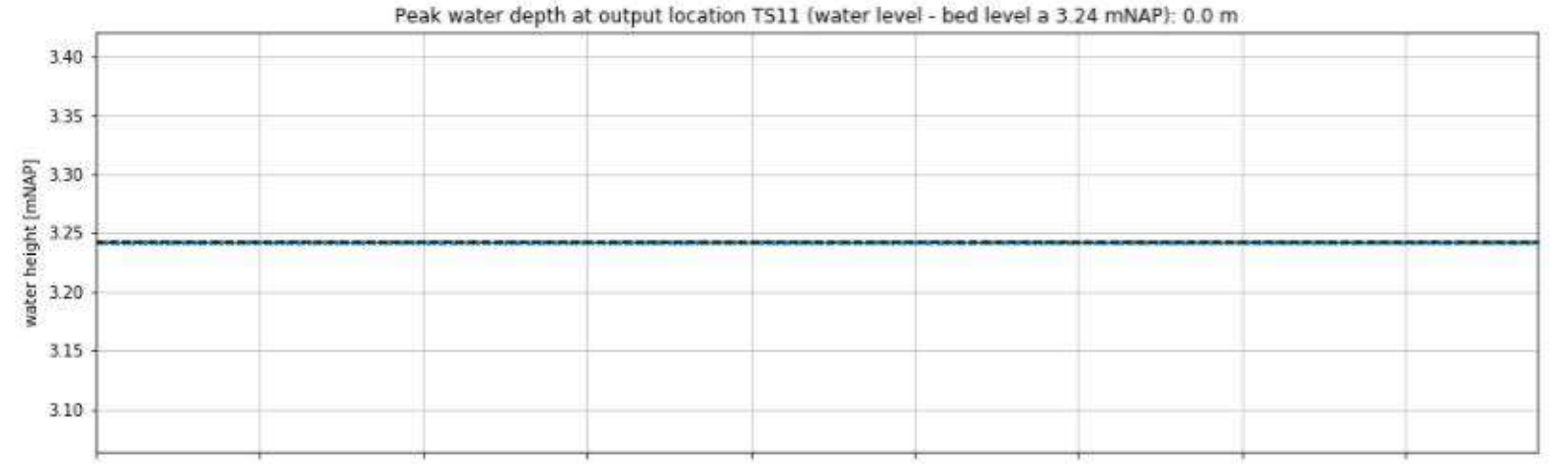
Peak water depth at output location TS11 (water level - bed level a 3.24 mNAP): 0.0 m
water height [mNAP]
3.40
3.35
3.30
3.25
3.20
3.15
3.10

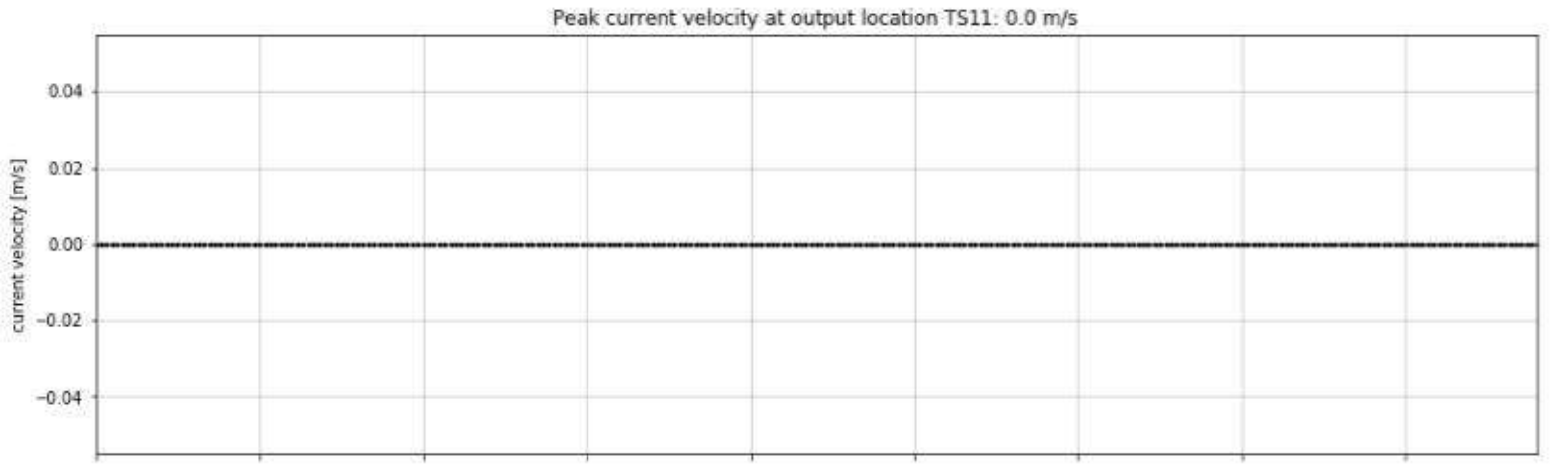
Peak current velocity at output location TS11: 0.0 m/s
current velocity [m/s]
0.04
0.02
0.00
−0.02
−0.04

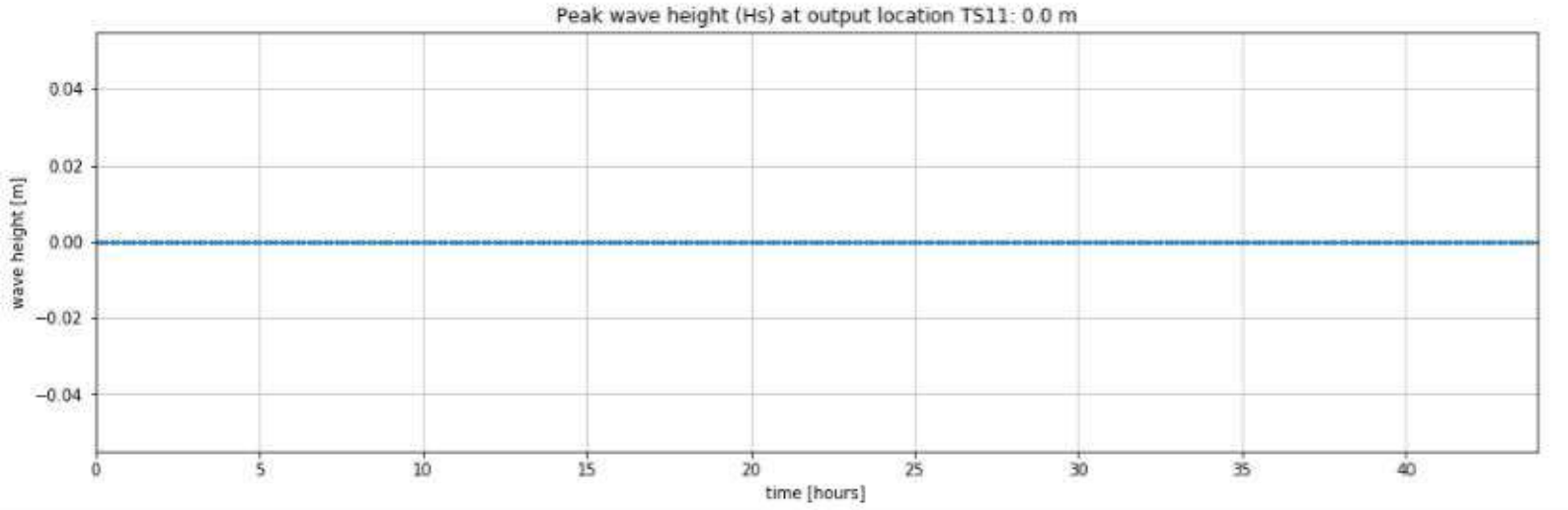
Peak wave height (Hs) at output location TS11: 0.0 m
wave height [m]
0.04
0.02
0.00
−0.02
−0.04
0
5
10
15
20
25
30
35
40
time [hours]

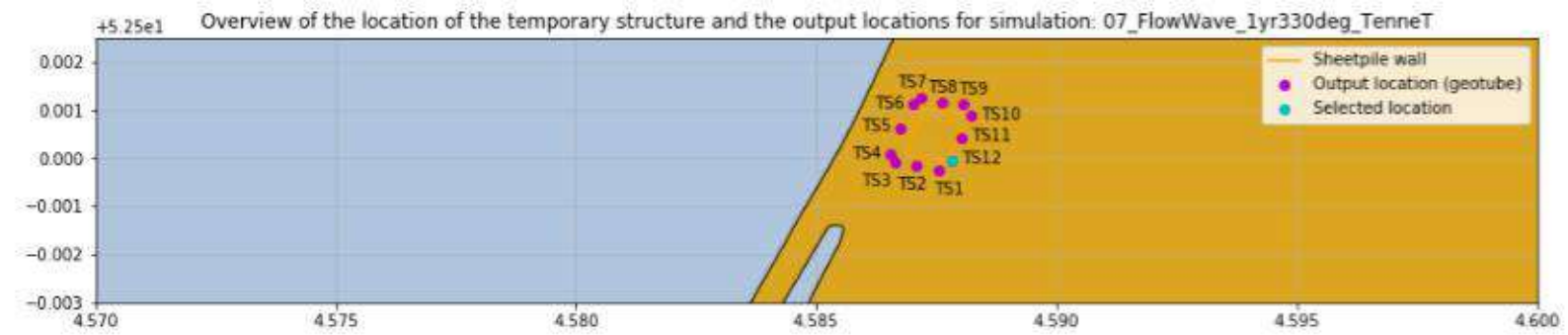
Overview of the location of the temporary structure and the output locations for simulation: 07_FlowWave_1yr330deg_TenneT
+5.25e1
Sheetpile wall
Output location (geotube)
Selected location
TS1
TS2
TS3
TS4
TS5
TS6
TS7
TS8
TS9
TS10
TS11
TS12
0.002
0.001
0.000
−0.001
−0.002
−0.003
4.570
4.575
4.580
4.585
4.590
4.595
4.600

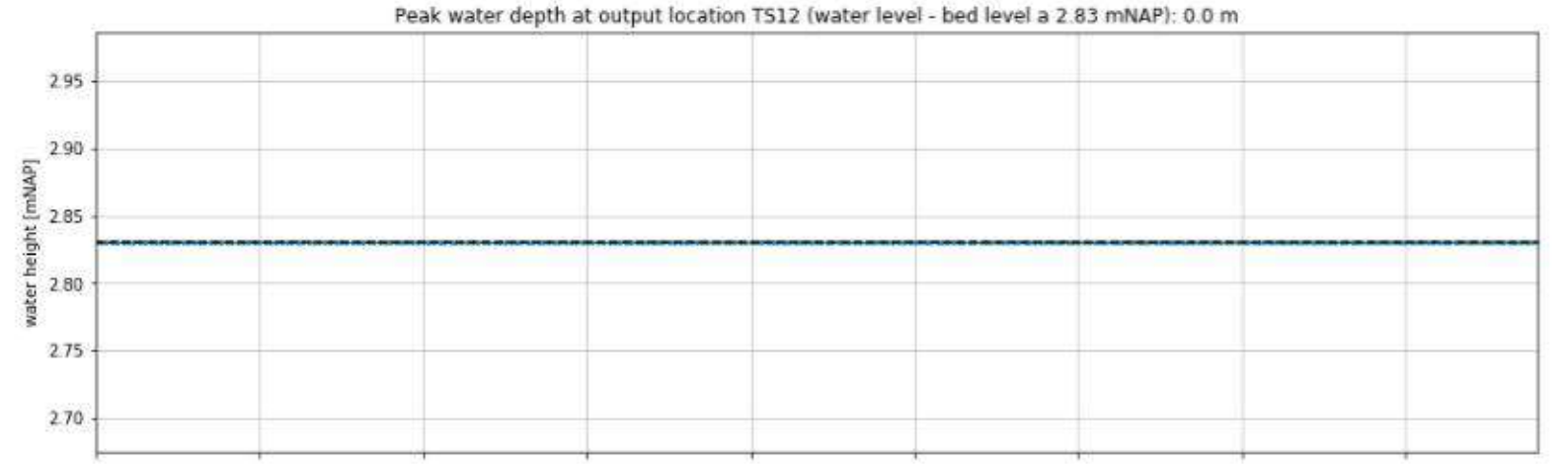
Peak water depth at output location TS12 (water level - bed level a 2.83 mNAP): 0.0 m
water height [mNAP]
2.95
2.90
2.85
2.80
2.75
2.70

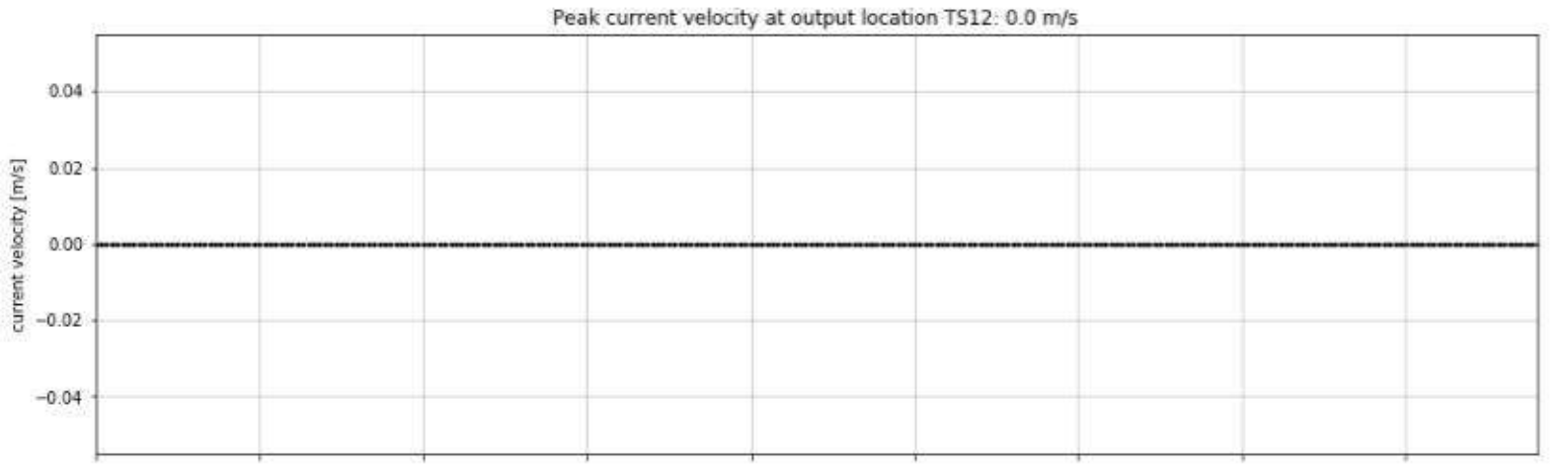
Peak current velocity at output location TS12: 0.0 m/s
current velocity [m/s]
0.04
0.02
0.00
−0.02
−0.04

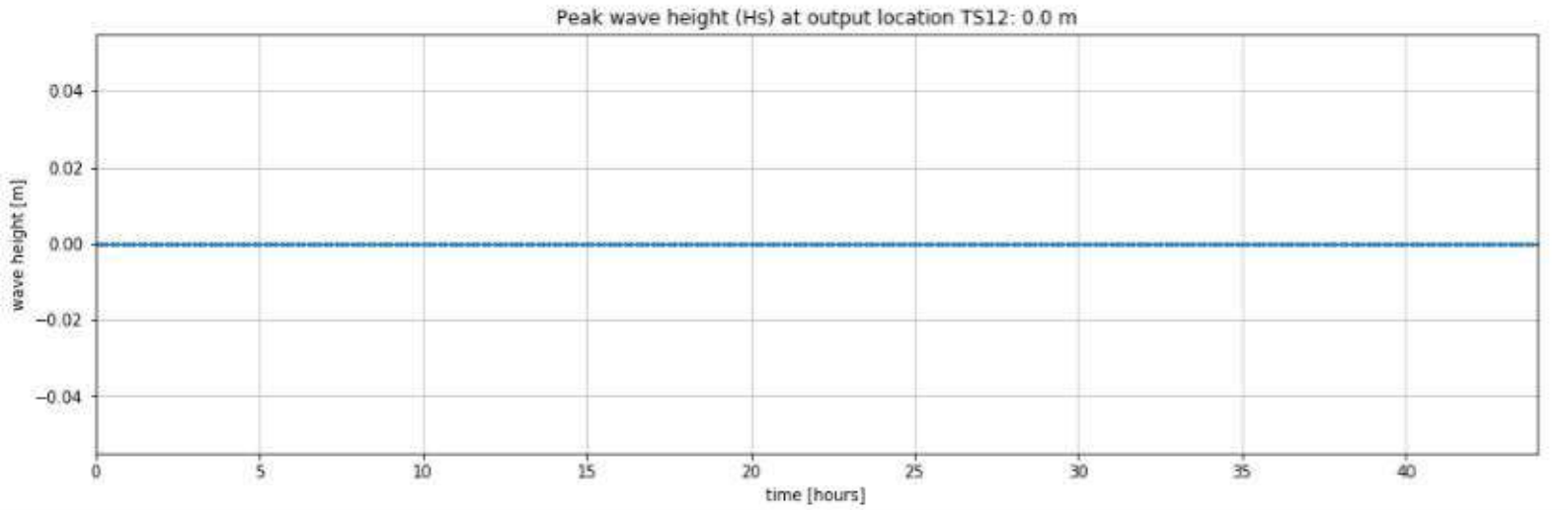
Peak wave height (Hs) at output location TS12: 0.0 m
wave height [m]
0.04
0.02
0.00
−0.02
−0.04
0
5
10
15
20
25
30
35
40
time [hours]

C.4 Flow-Wave 5yr storm 330 degrees – TenneT bathymetry

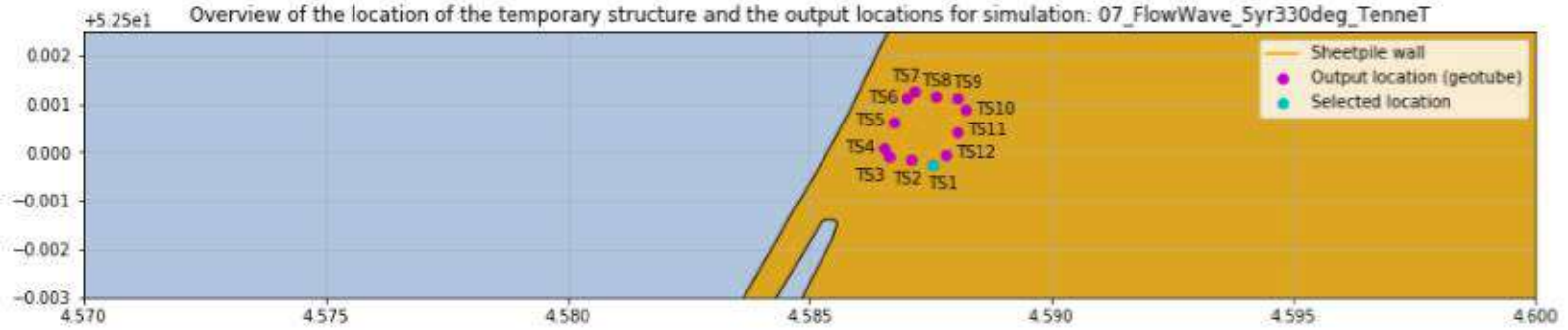
Overview of the location of the temporary structure and the output locations for simulation: 07_FlowWave_5yr330deg_TenneT
+5.25e1
Sheetpile wall
Output location (geotube)
Selected location
TS1
TS2
TS3
TS4
TS5
TS6
TS7
TS8
TS9
TS10
TS11
TS12
0.002
0.001
0.000
−0.001
−0.002
−0.003
4.570
4.575
4.580
4.585
4.590
4.595
4.600

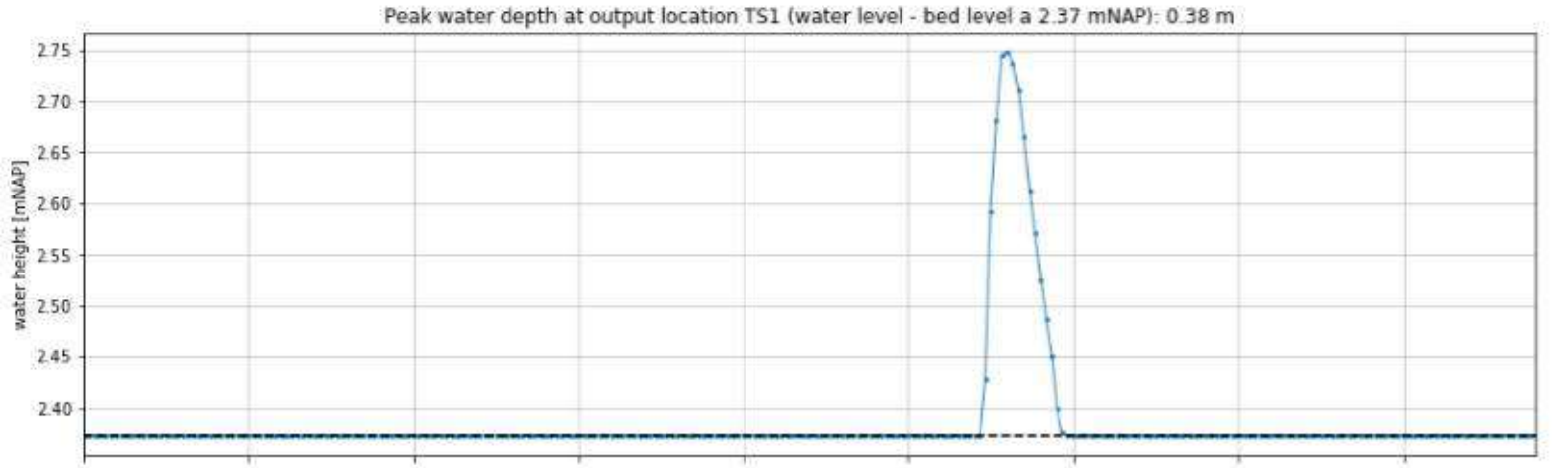
Peak water depth at output location TS1 (water level - bed level a 2.37 mNAP): 0.38 m
water height [mNAP]
2.75
2.70
2.65
2.60
2.55
2.50
2.45
2.40

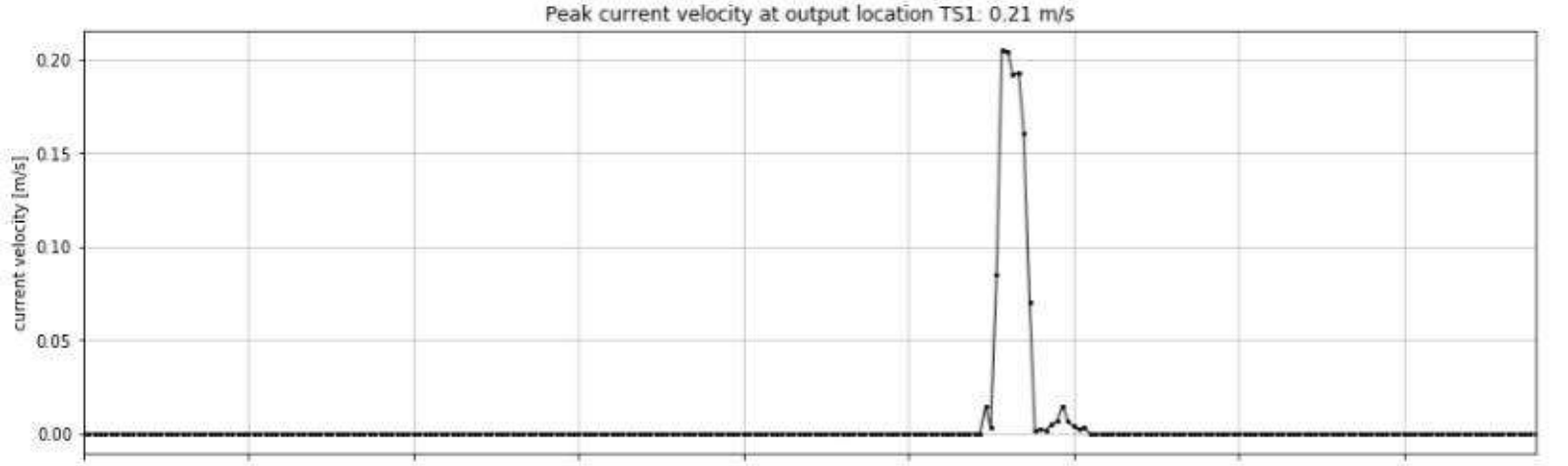
Peak current velocity at output location TS1: 0.21 m/s
current velocity [m/s]
0.20
0.15
0.10
0.05
0.00

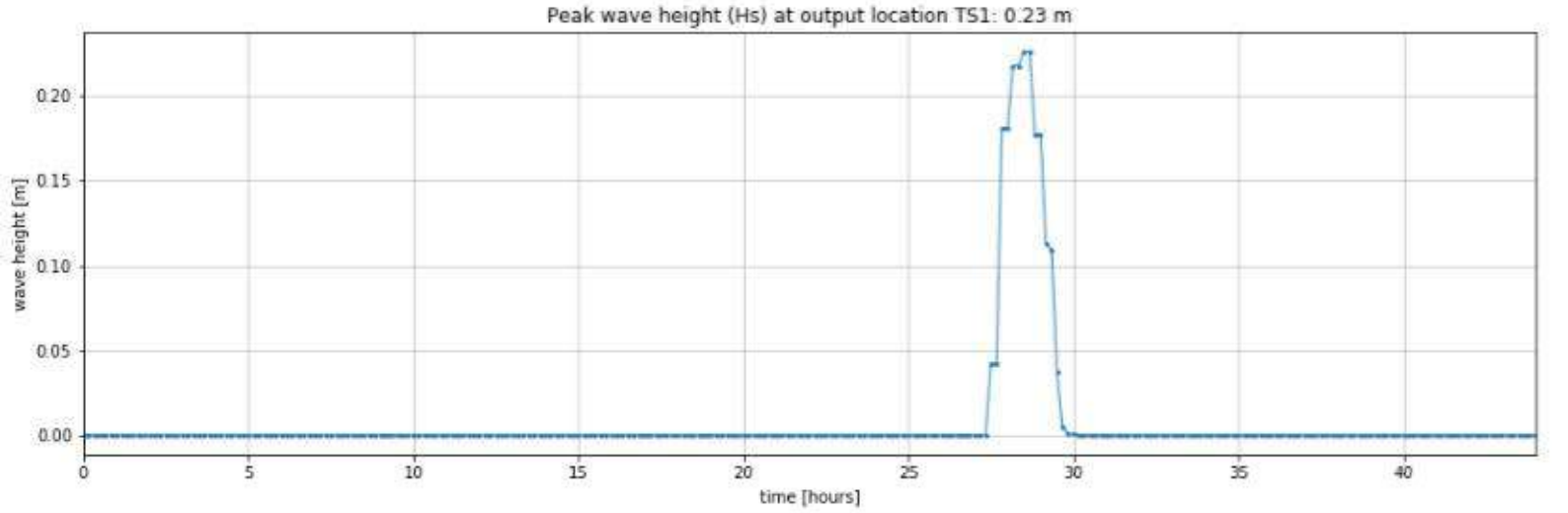
Peak wave height (Hs) at output location TS1: 0.23 m
wave height [m]
0.20
0.15
0.10
0.05
0.00
0
5
10
15
20
25
30
35
40
time [hours]

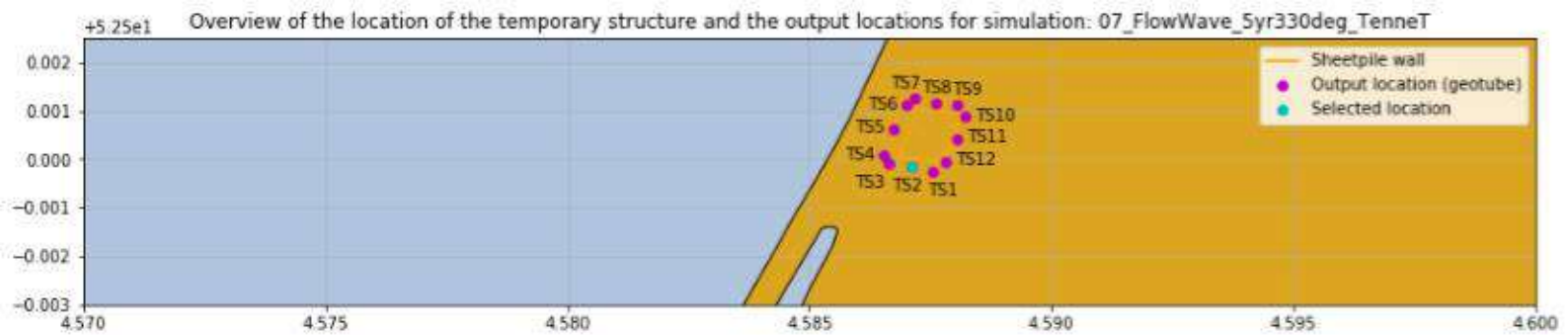
Overview of the location of the temporary structure and the output locations for simulation: 07_FlowWave_5yr330deg_TenneT
+5.25e1
Sheetpile wall
Output location (geotube)
Selected location
TS1
TS2
TS3
TS4
TS5
TS6
TS7
TS8
TS9
TS10
TS11
TS12
0.002
0.001
0.000
−0.001
−0.002
−0.003
4.570
4.575
4.580
4.585
4.590
4.595
4.600

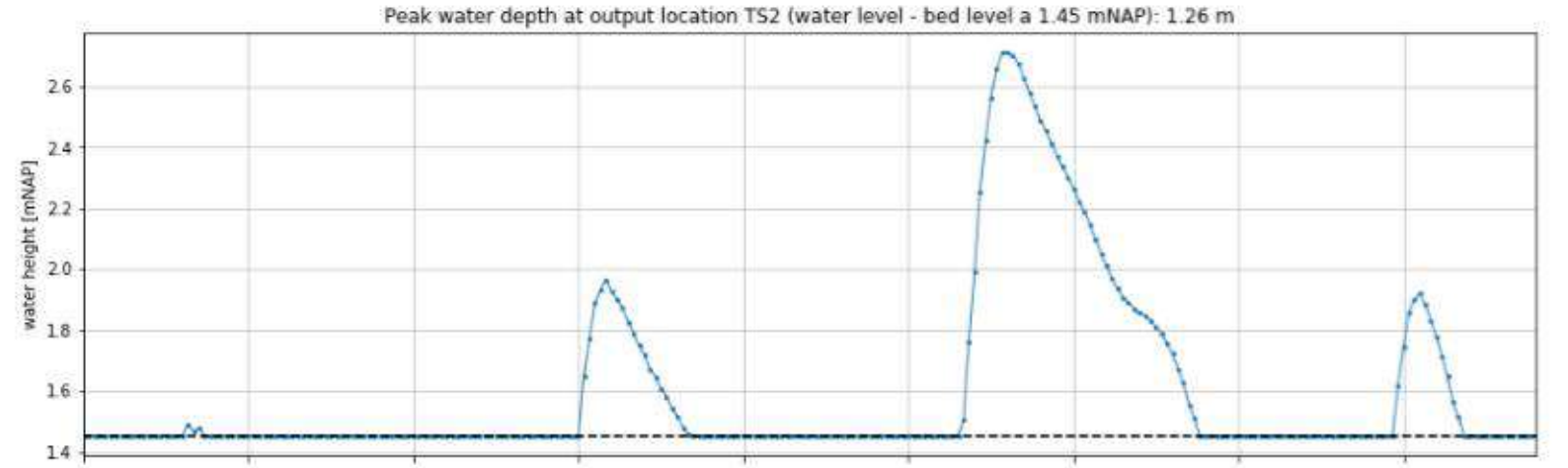
Peak water depth at output location TS2 (water level - bed level a 1.45 mNAP): 1.26 m
water height [mNAP]
2.6
2.4
2.2
2.0
1.8
1.6
1.4

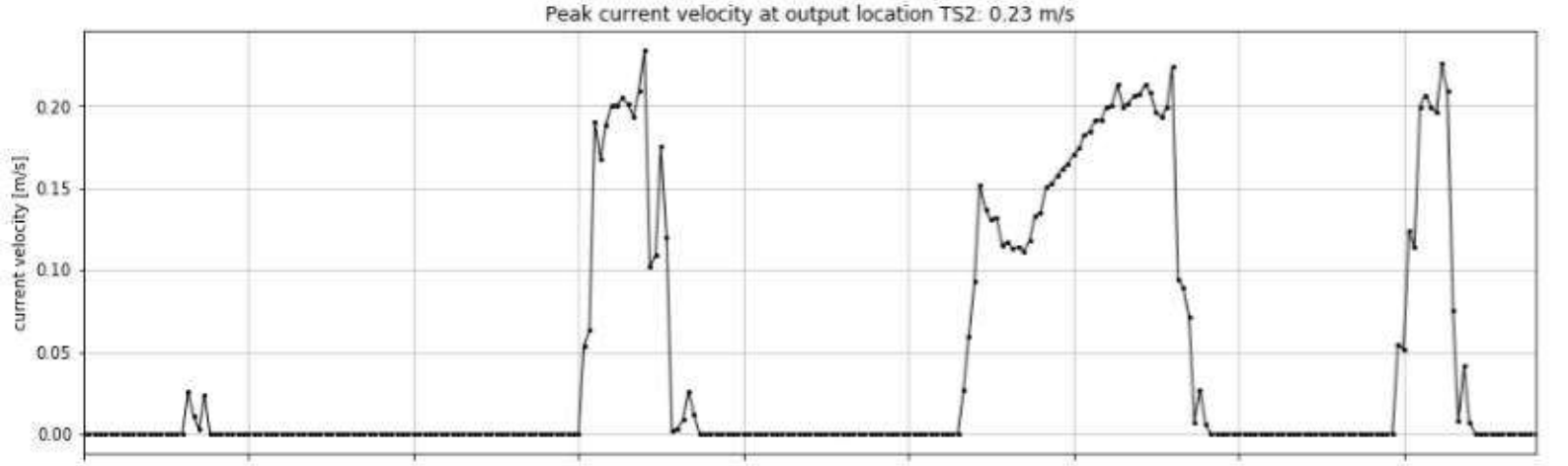
Peak current velocity at output location TS2: 0.23 m/s
current velocity [m/s]
0.20
0.15
0.10
0.05
0.00

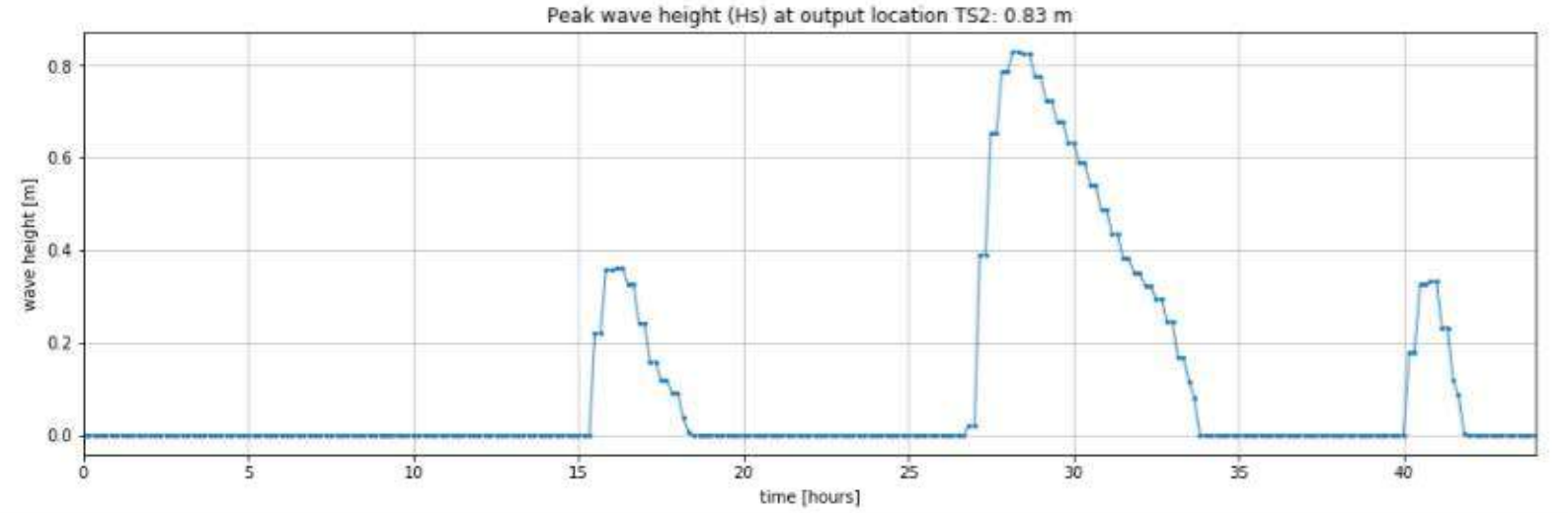
Peak wave height (Hs) at output location TS2: 0.83 m
wave height [m]
0.8
0.6
0.4
0.2
0.0
0
5
10
15
20
25
30
35
40
time [hours]

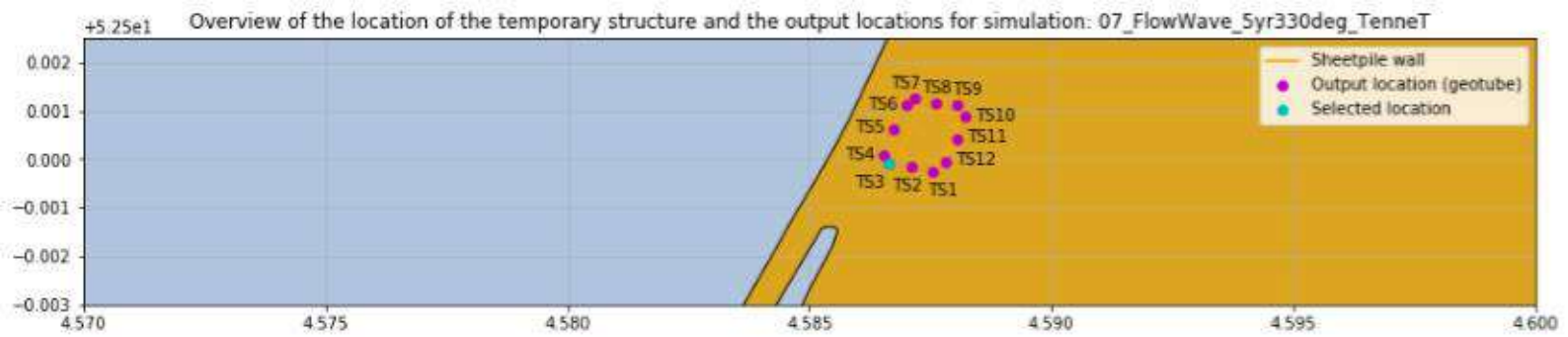
Overview of the location of the temporary structure and the output locations for simulation: 07_FlowWave_5yr330deg_TenneT
+5.25e1
Sheetpile wall
Output location (geotube)
Selected location
TS1
TS2
TS3
TS4
TS5
TS6
TS7
TS8
TS9
TS10
TS11
TS12
0.002
0.001
0.000
−0.001
−0.002
−0.003
4.570
4.575
4.580
4.585
4.590
4.595
4.600

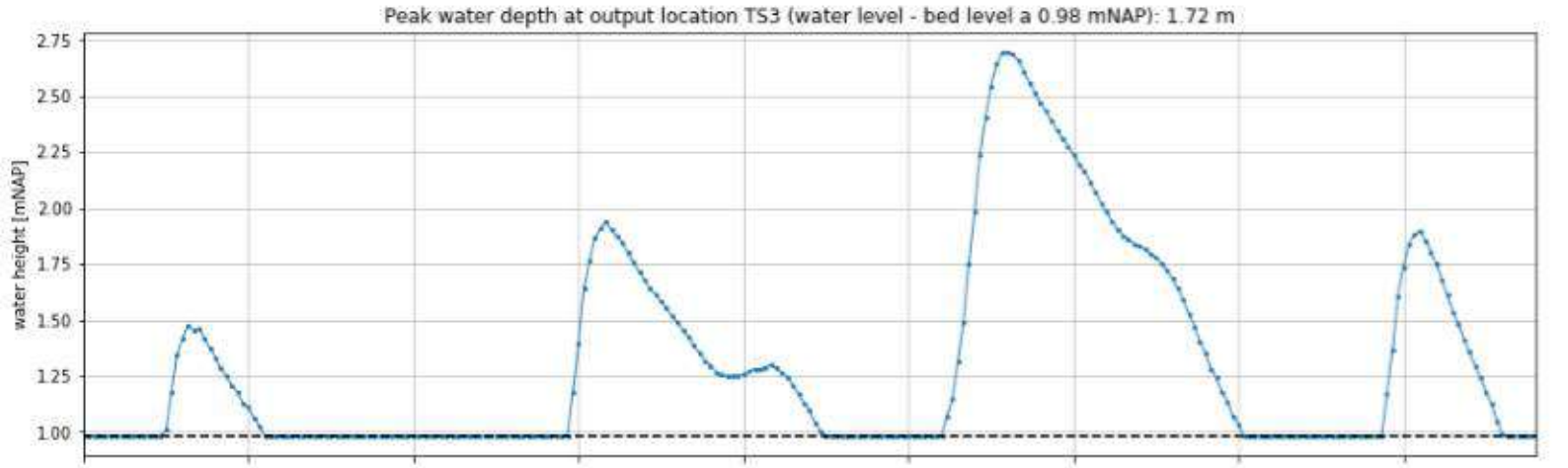
Peak water depth at output location TS3 (water level - bed level a 0.98 mNAP): 1.72 m
water height [mNAP]
2.75
2.50
2.25
2.00
1.75
1.50
1.25
1.00

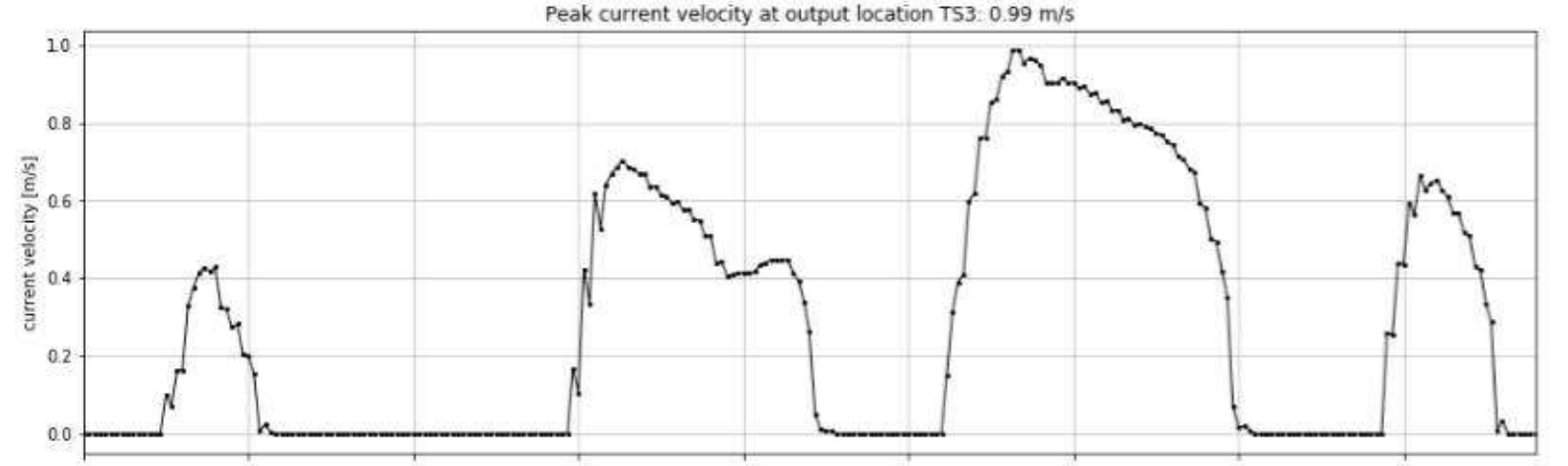
Peak current velocity at output location TS3: 0.99 m/s
current velocity [m/s]
1.0
0.8
0.6
0.4
0.2
0.0

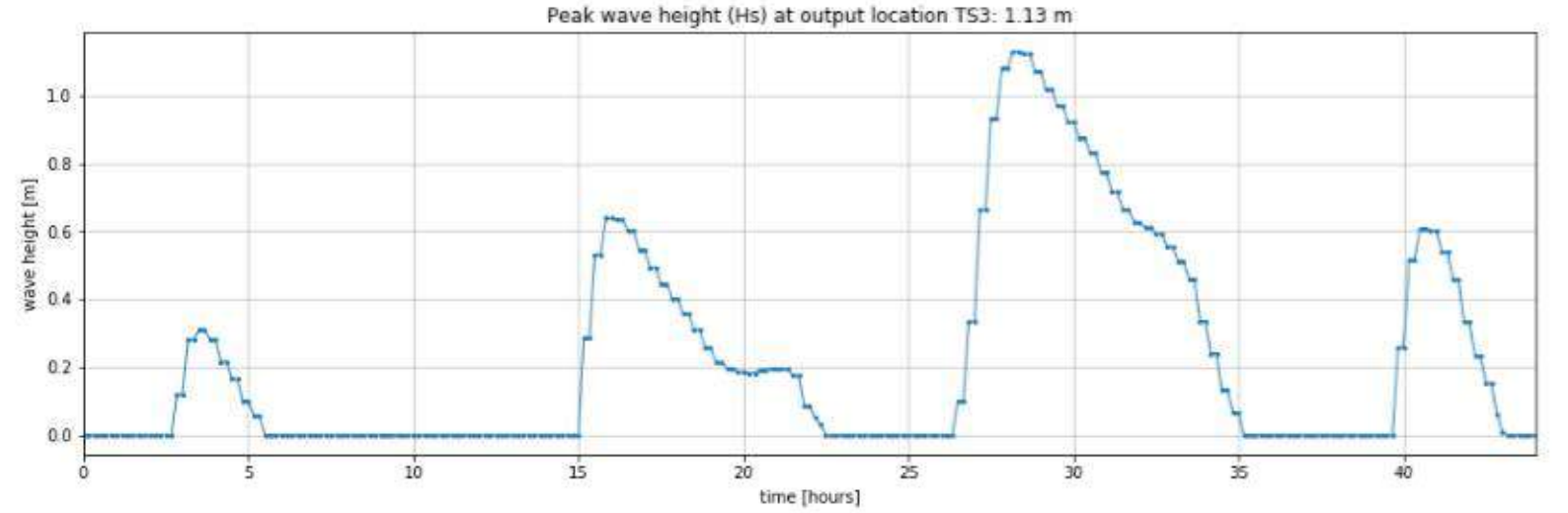
Peak wave height (Hs) at output location TS3: 1.13 m
wave height [m]
1.0
0.8
0.6
0.4
0.2
0.0
0
5
10
15
20
25
30
35
40
time [hours]

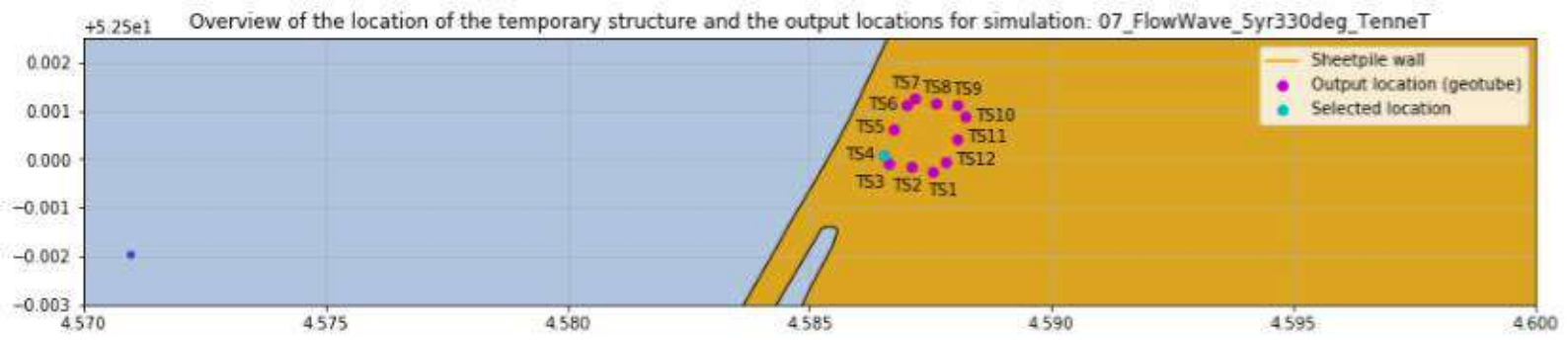
Overview of the location of the temporary structure and the output locations for simulation: 07_FlowWave_5yr330deg_TenneT
+5.25e1
Sheetpile wall
Output location (geotube)
Selected location
TS1
TS2
TS3
TS4
TS5
TS6
TS7
TS8
TS9
TS10
TS11
TS12

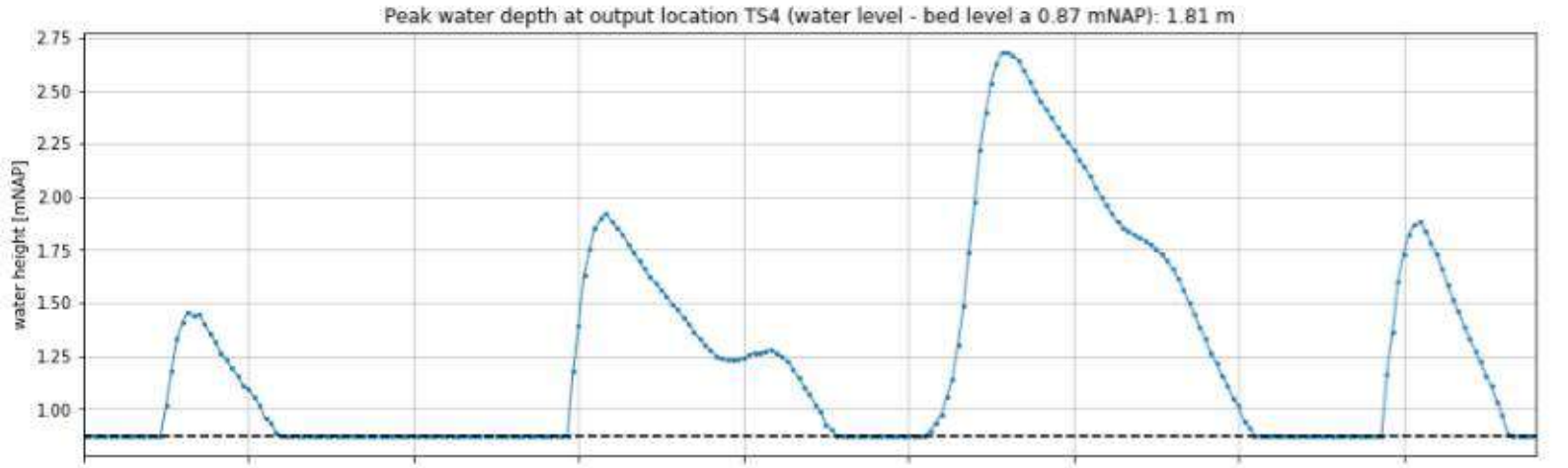
Peak water depth at output location TS4 (water level - bed level a 0.87 mNAP): 1.81 m
water height [mNAP]

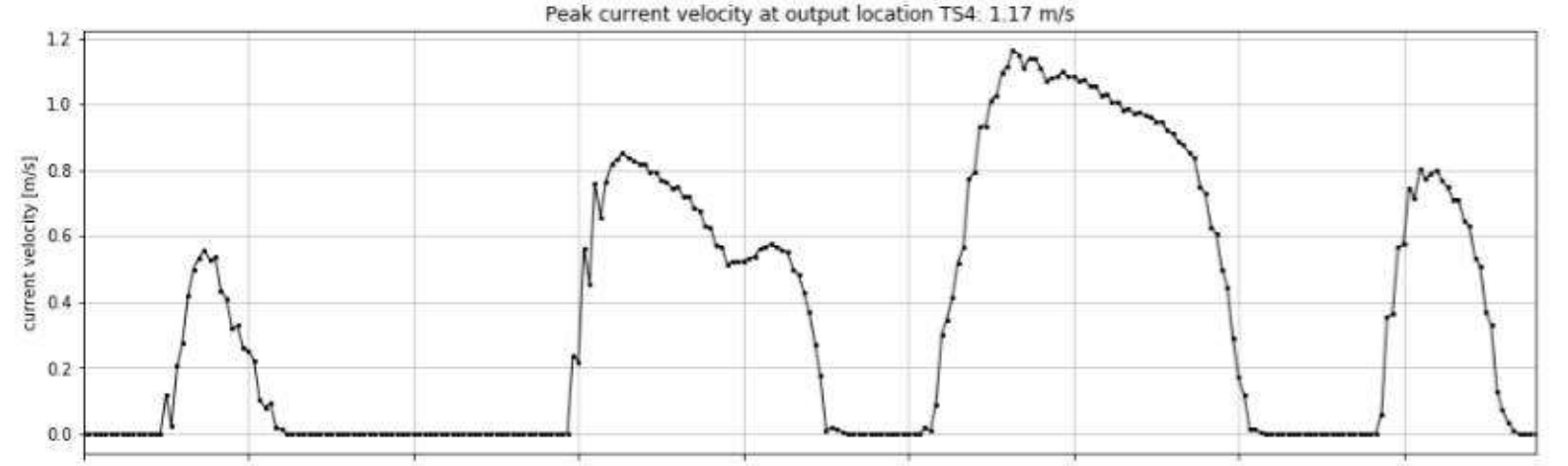
Peak current velocity at output location TS4: 1.17 m/s
current velocity [m/s]

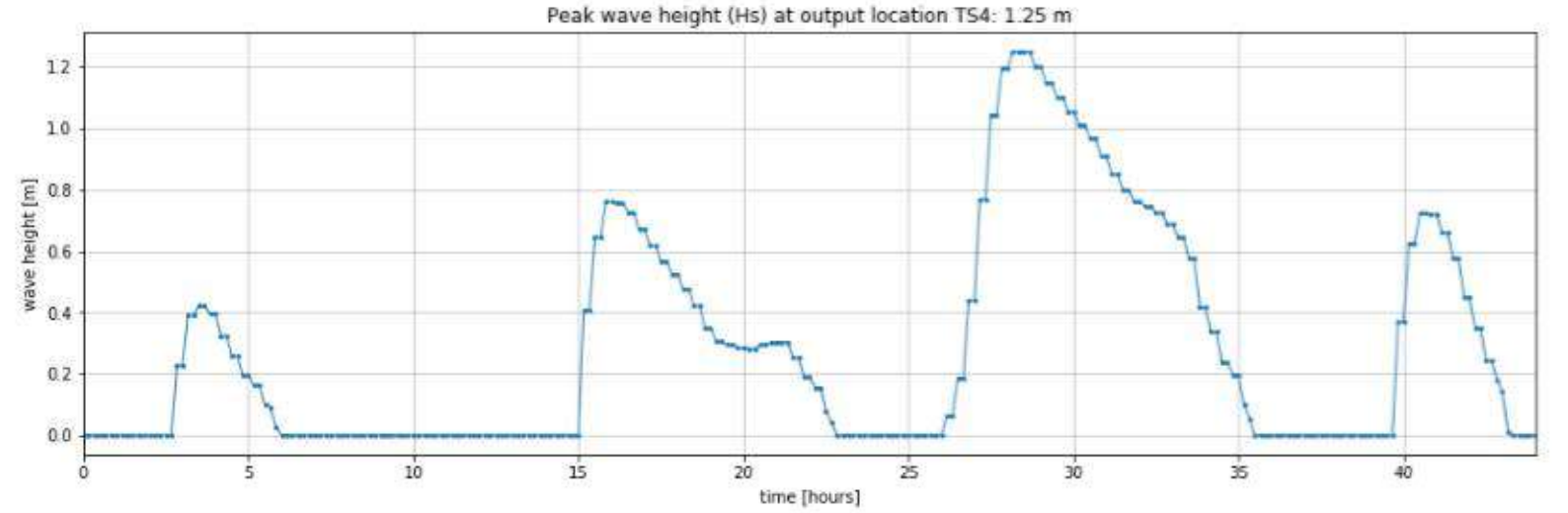
Peak wave height (Hs) at output location TS4: 1.25 m
wave height [m]
time [hours]

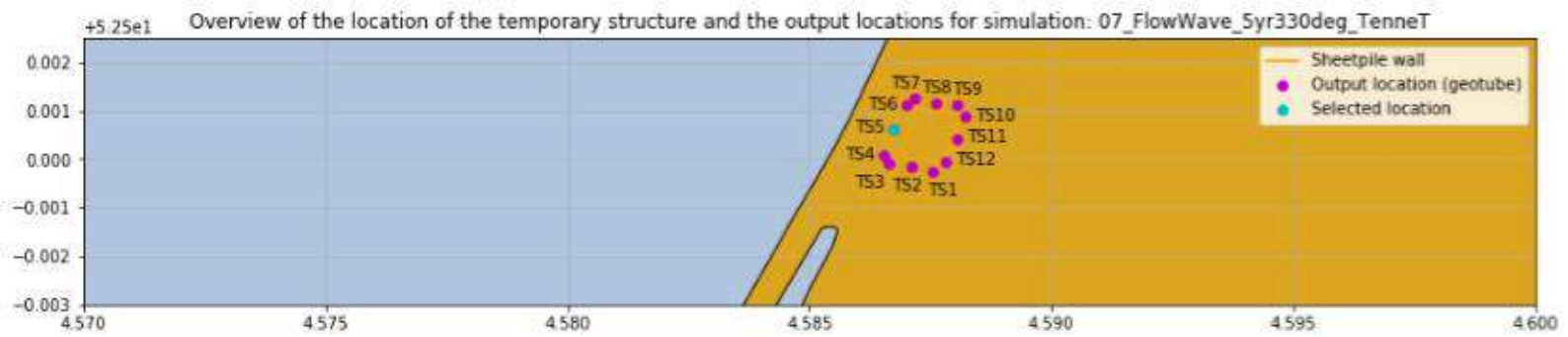
Overview of the location of the temporary structure and the output locations for simulation: 07_FlowWave_5yr330deg_TenneT
+5.25e1
Sheetpile wall
Output location (geotube)
Selected location
TS1
TS2
TS3
TS4
TS5
TS6
TS7
TS8
TS9
TS10
TS11
TS12
0.002
0.001
0.000
−0.001
−0.002
−0.003
4.570
4.575
4.580
4.585
4.590
4.595
4.600

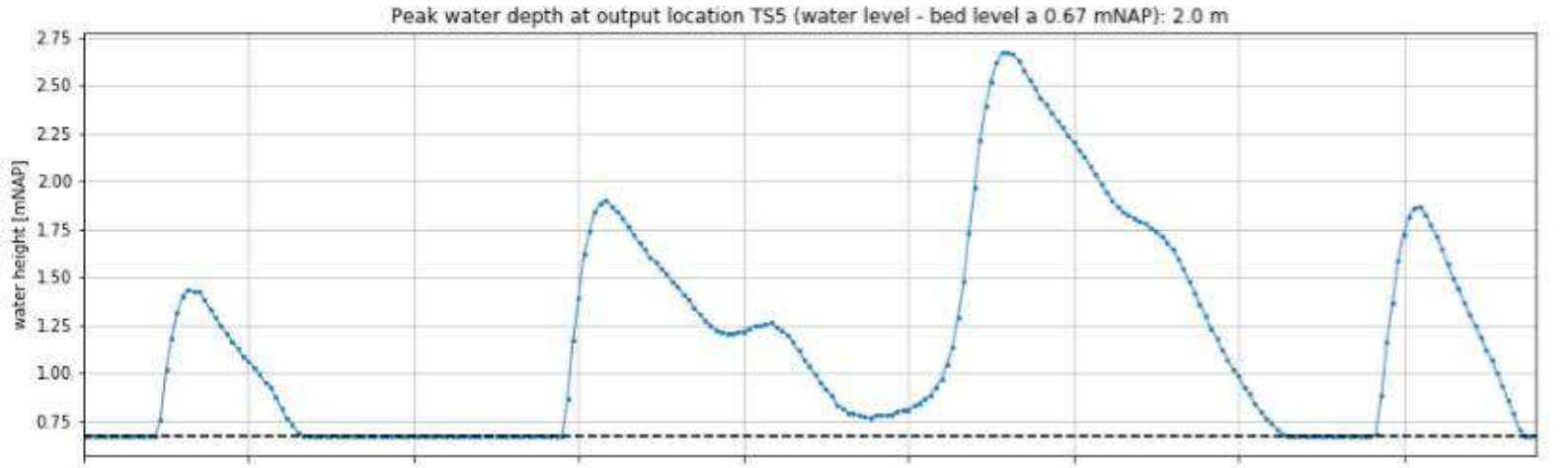
Peak water depth at output location TS5 (water level - bed level a 0.67 mNAP): 2.0 m
water height [mNAP]
2.75
2.50
2.25
2.00
1.75
1.50
1.25
1.00
0.75

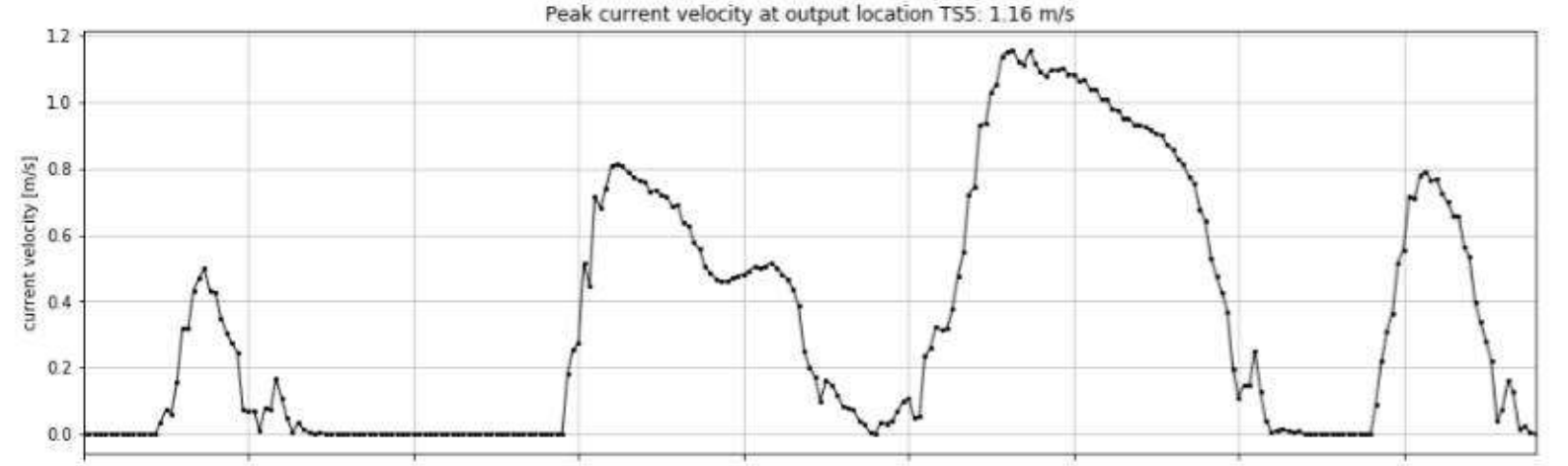
Peak current velocity at output location TS5: 1.16 m/s
current velocity [m/s]
1.2
1.0
0.8
0.6
0.4
0.2
0.0

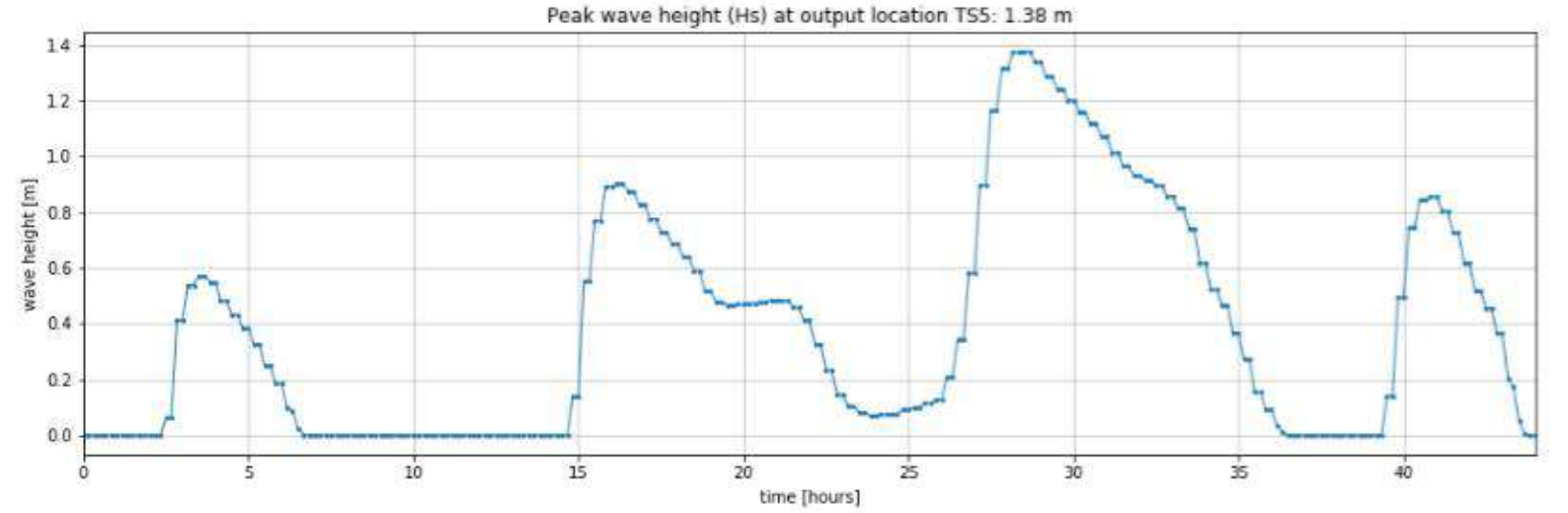
Peak wave height (Hs) at output location TS5: 1.38 m
wave height [m]
1.4
1.2
1.0
0.8
0.6
0.4
0.2
0.0
0
5
10
15
20
25
30
35
40
time [hours]

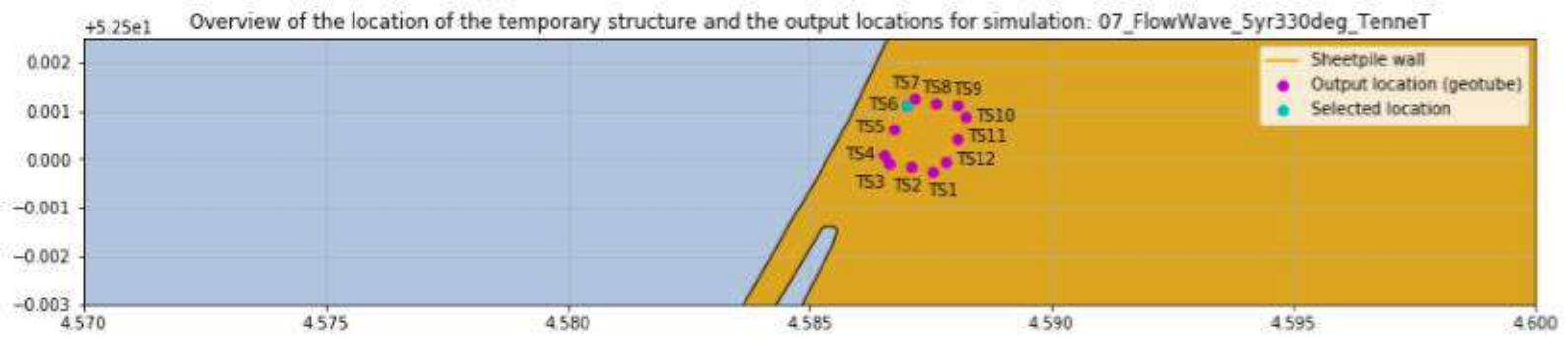
Overview of the location of the temporary structure and the output locations for simulation: 07_FlowWave_5yr330deg_TenneT
+5.25e1
Sheetpile wall
Output location (geotube)
Selected location
TS1
TS2
TS3
TS4
TS5
TS6
TS7
TS8
TS9
TS10
TS11
TS12
0.002
0.001
0.000
−0.001
−0.002
−0.003
4.570
4.575
4.580
4.585
4.590
4.595
4.600

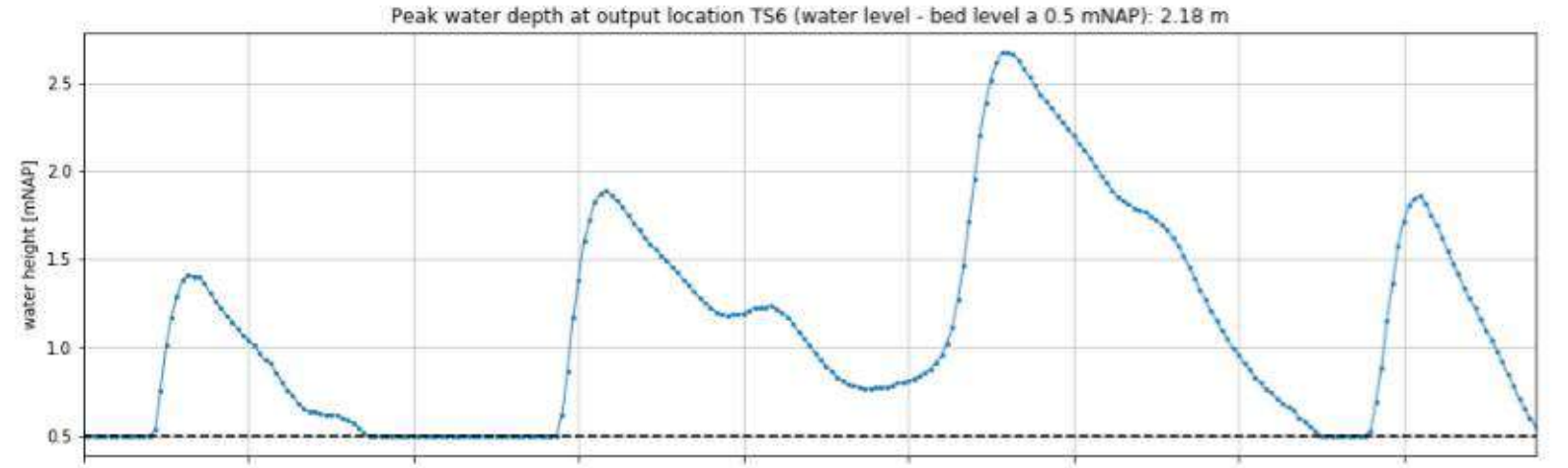
Peak water depth at output location TS6 (water level - bed level a 0.5 mNAP): 2.18 m
water height [mNAP]
2.5
2.0
1.5
1.0
0.5

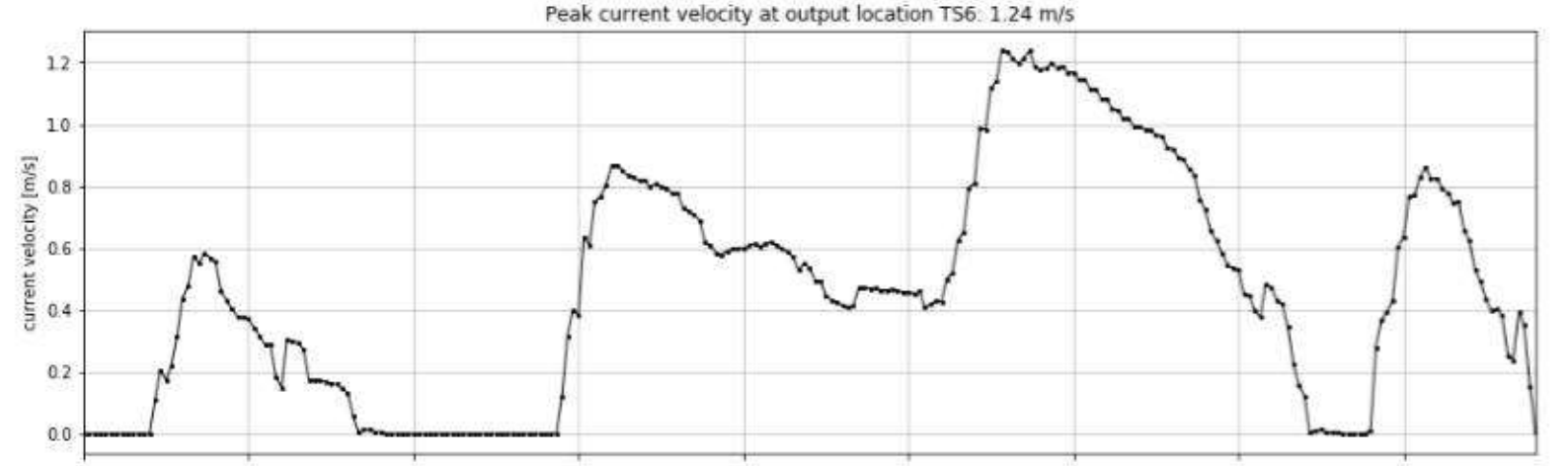
Peak current velocity at output location TS6: 1.24 m/s
current velocity [m/s]
1.2
1.0
0.8
0.6
0.4
0.2
0.0

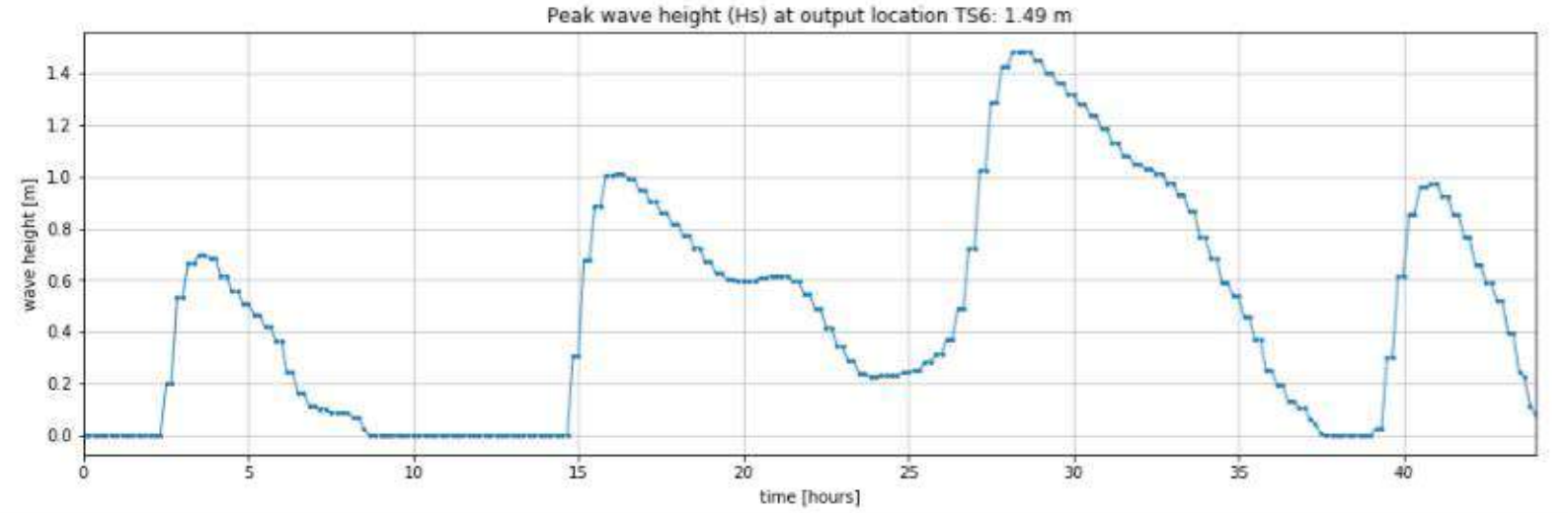
Peak wave height (Hs) at output location TS6: 1.49 m
wave height [m]
1.4
1.2
1.0
0.8
0.6
0.4
0.2
0.0
0
5
10
15
20
25
30
35
40
time [hours]

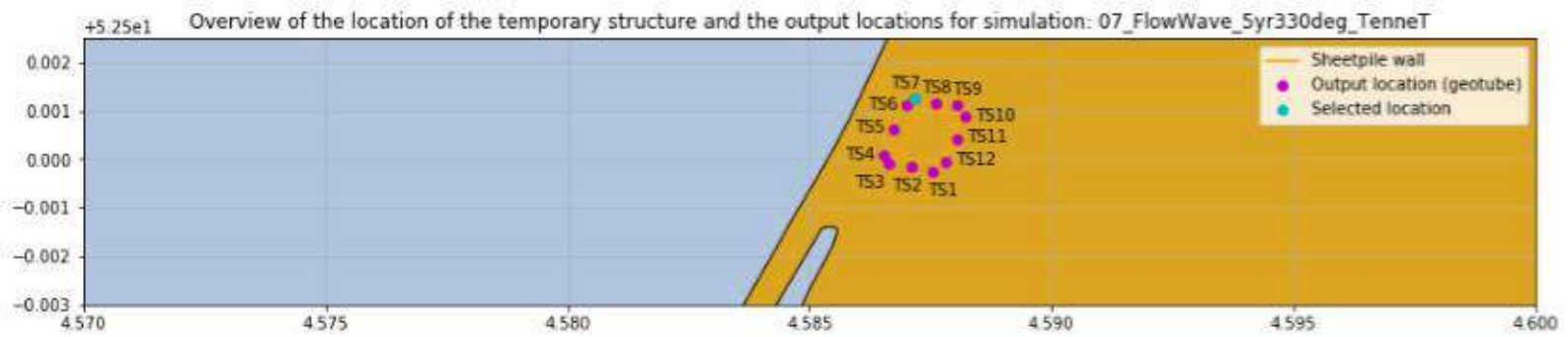
Overview of the location of the temporary structure and the output locations for simulation: 07_FlowWave_5yr330deg_TenneT
+5.25e1
Sheetpile wall
Output location (geotube)
Selected location
TS1
TS2
TS3
TS4
TS5
TS6
TS7
TS8
TS9
TS10
TS11
TS12
0.002
0.001
0.000
−0.001
−0.002
−0.003
4.570
4.575
4.580
4.585
4.590
4.595
4.600

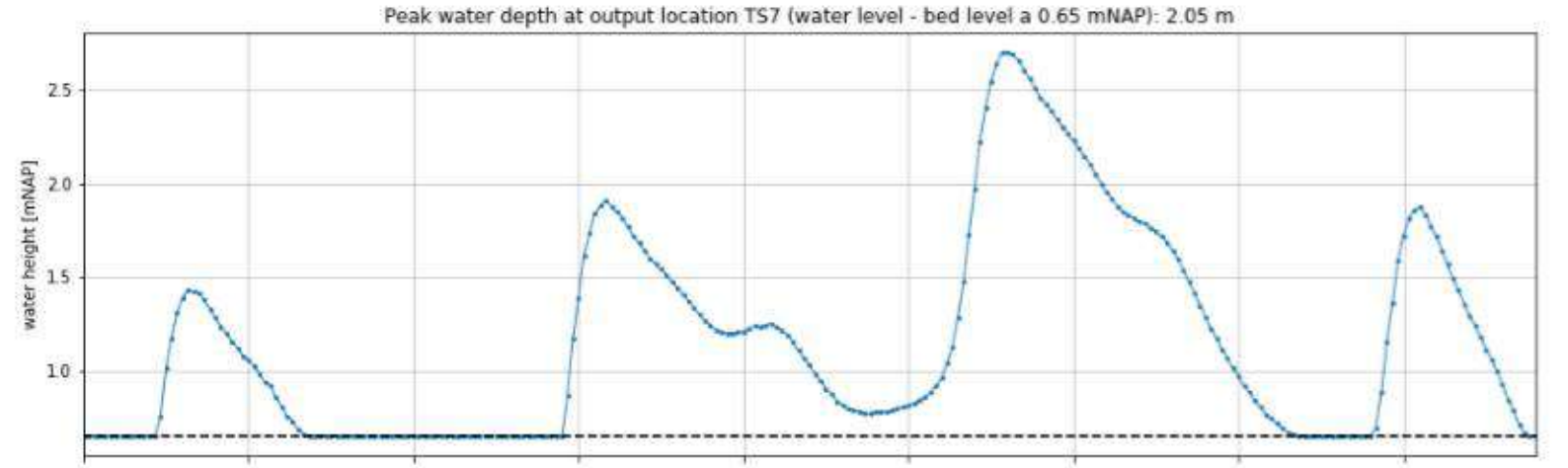
Peak water depth at output location TS7 (water level - bed level a 0.65 mNAP): 2.05 m
water height [mNAP]
2.5
2.0
1.5
1.0

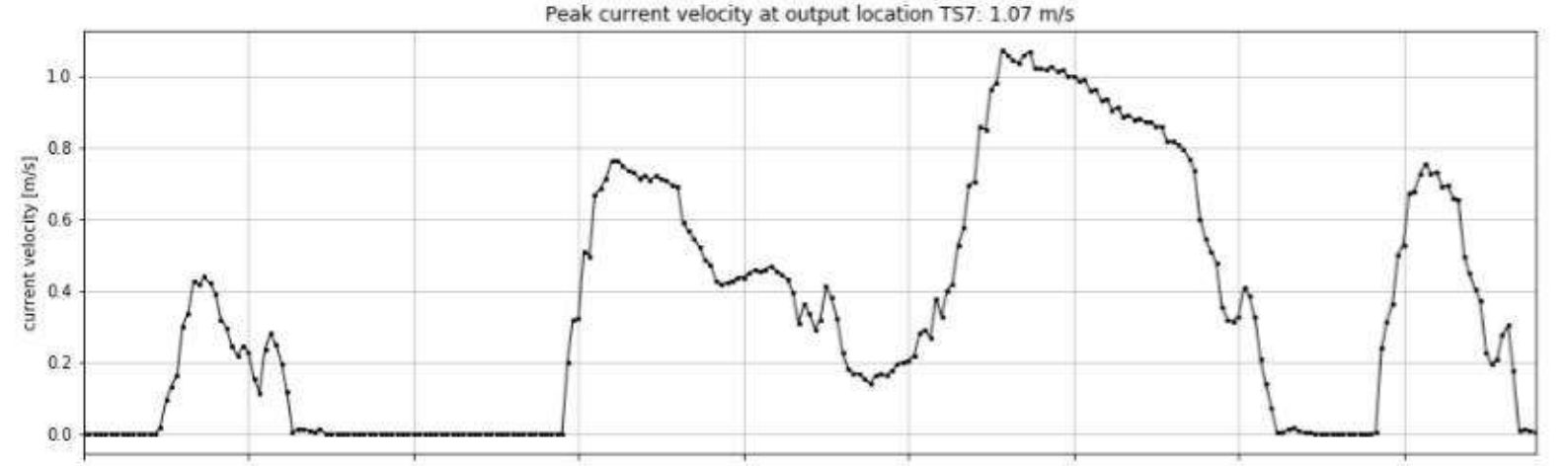
Peak current velocity at output location TS7: 1.07 m/s
current velocity [m/s]
1.0
0.8
0.6
0.4
0.2
0.0

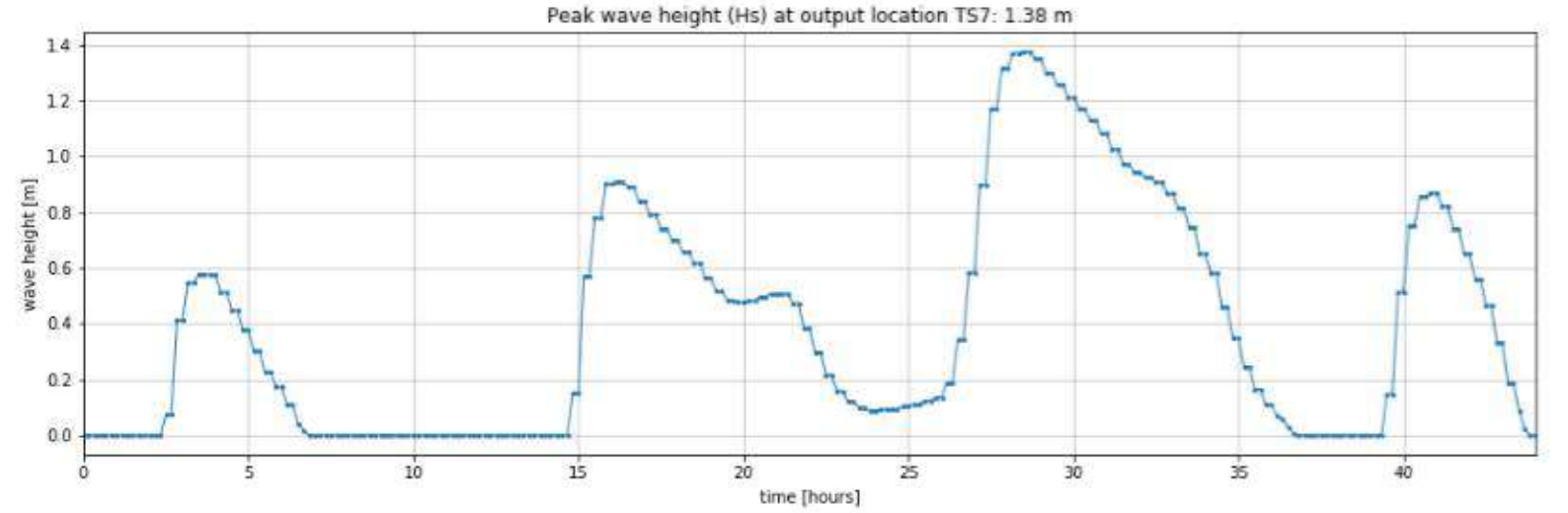
Peak wave height (Hs) at output location TS7: 1.38 m
wave height [m]
1.4
1.2
1.0
0.8
0.6
0.4
0.2
0.0
0
5
10
15
20
25
30
35
40
time [hours]

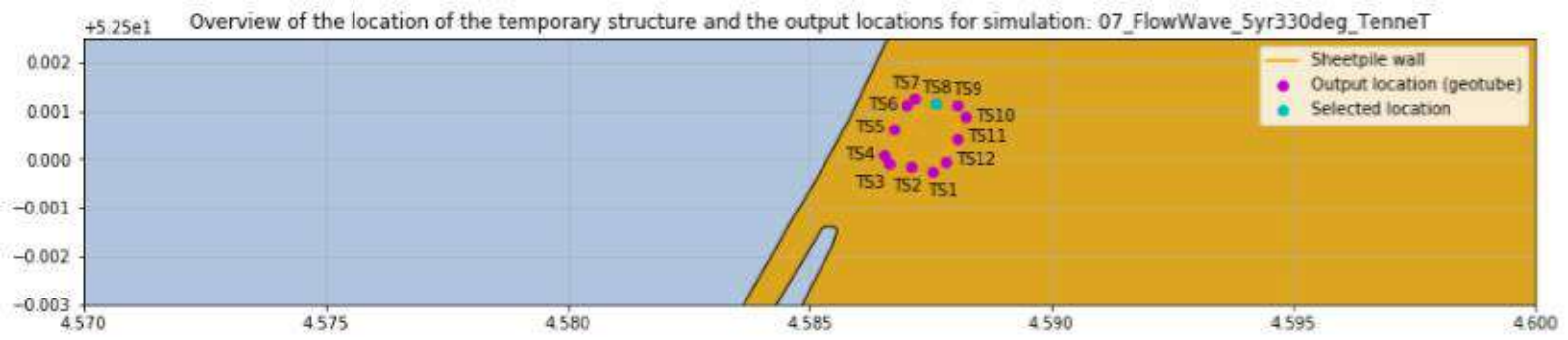
Overview of the location of the temporary structure and the output locations for simulation: 07_FlowWave_5yr330deg_TenneT
+5.25e1
Sheetpile wall
Output location (geotube)
Selected location
TS1
TS2
TS3
TS4
TS5
TS6
TS7
TS8
TS9
TS10
TS11
TS12
0.002
0.001
0.000
−0.001
−0.002
−0.003
4.570
4.575
4.580
4.585
4.590
4.595
4.600

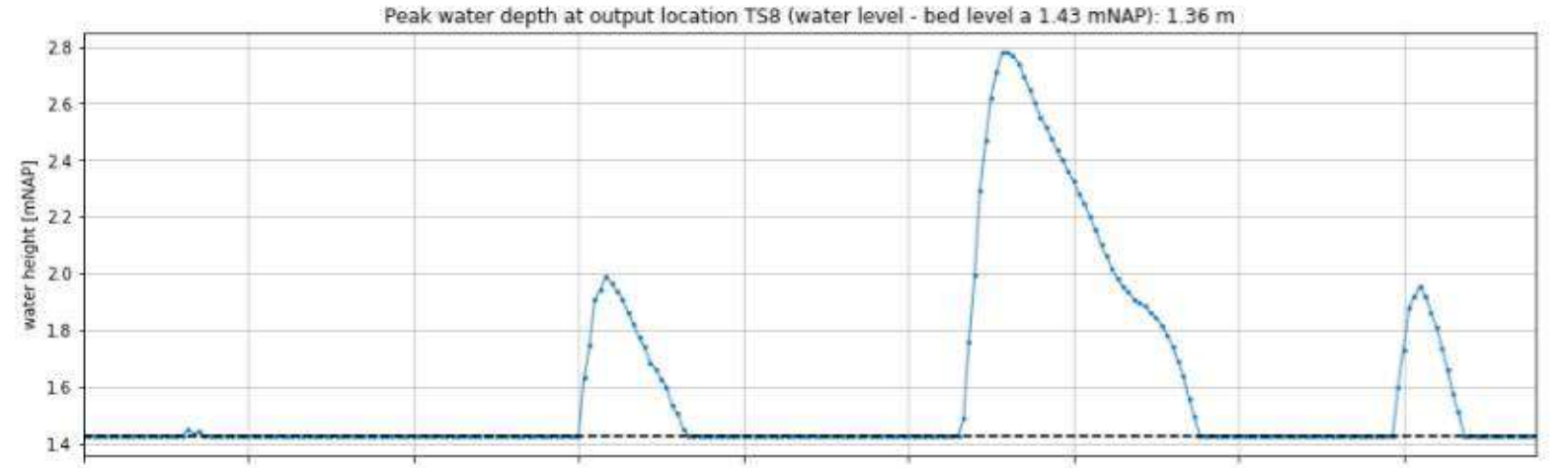
Peak water depth at output location TS8 (water level - bed level a 1.43 mNAP): 1.36 m
water height [mNAP]
2.8
2.6
2.4
2.2
2.0
1.8
1.6
1.4

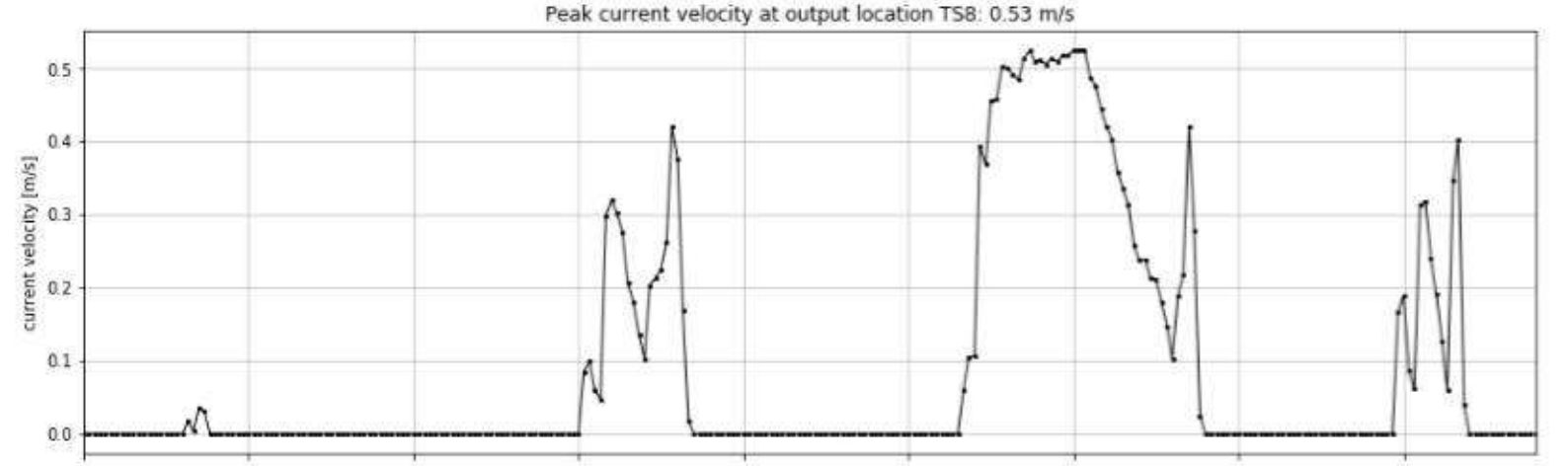
Peak current velocity at output location TS8: 0.53 m/s
current velocity [m/s]
0.5
0.4
0.3
0.2
0.1
0.0

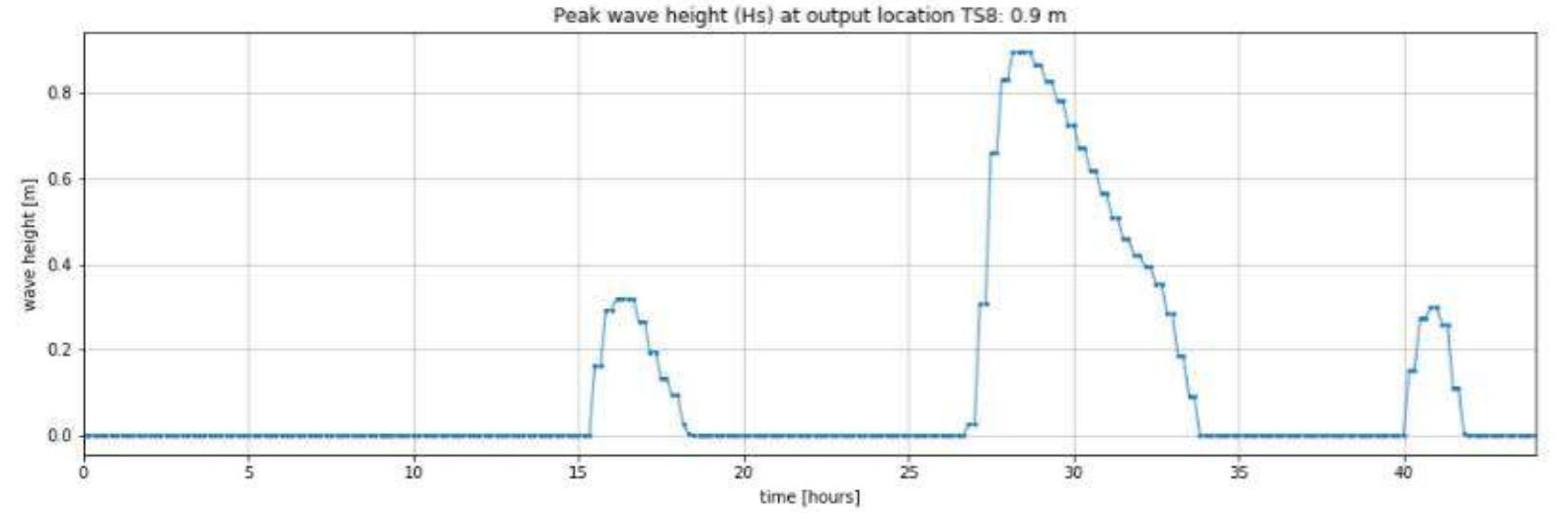
Peak wave height (Hs) at output location TS8: 0.9 m
wave height [m]
0.8
0.6
0.4
0.2
0.0
0
5
10
15
20
25
30
35
40
time [hours]

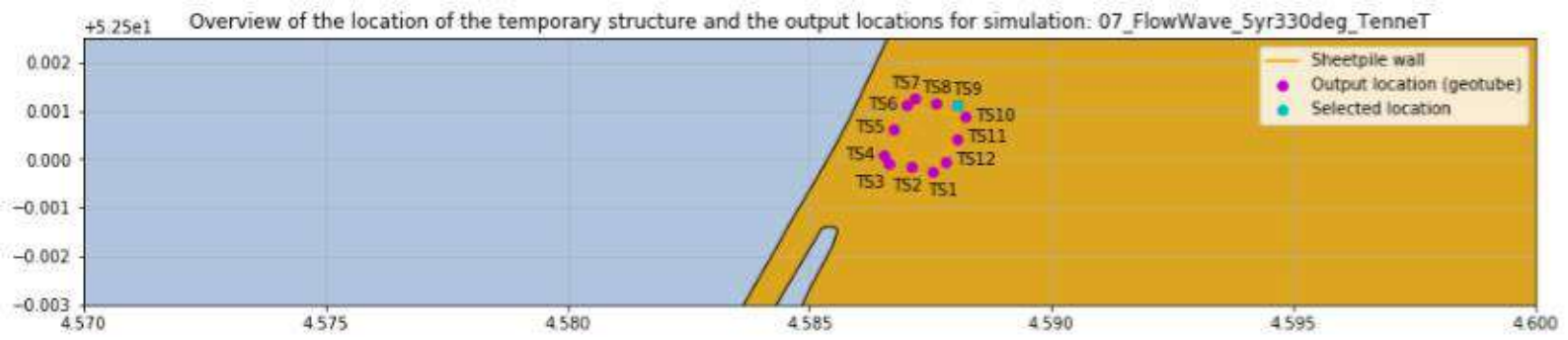
Overview of the location of the temporary structure and the output locations for simulation: 07_FlowWave_5yr330deg_TenneT
+5.25e1
Sheetpile wall
Output location (geotube)
Selected location
TS1
TS2
TS3
TS4
TS5
TS6
TS7
TS8
TS9
TS10
TS11
TS12
0.002
0.001
0.000
−0.001
−0.002
−0.003
4.570
4.575
4.580
4.585
4.590
4.595
4.600

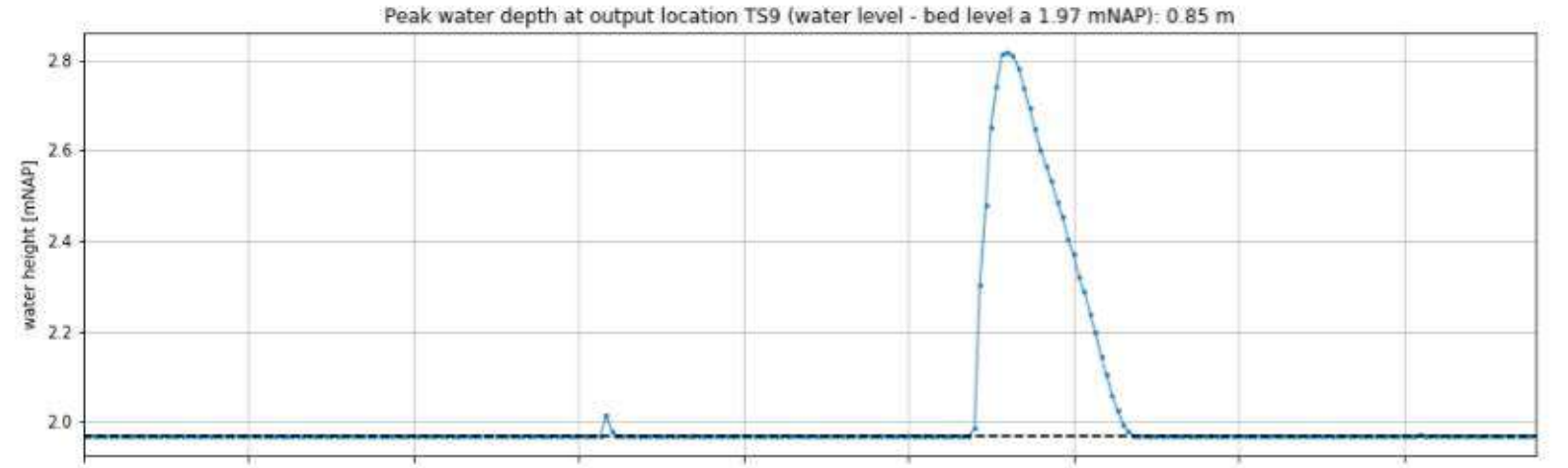
Peak water depth at output location TS9 (water level - bed level a 1.97 mNAP): 0.85 m
water height [mNAP]
2.8
2.6
2.4
2.2
2.0

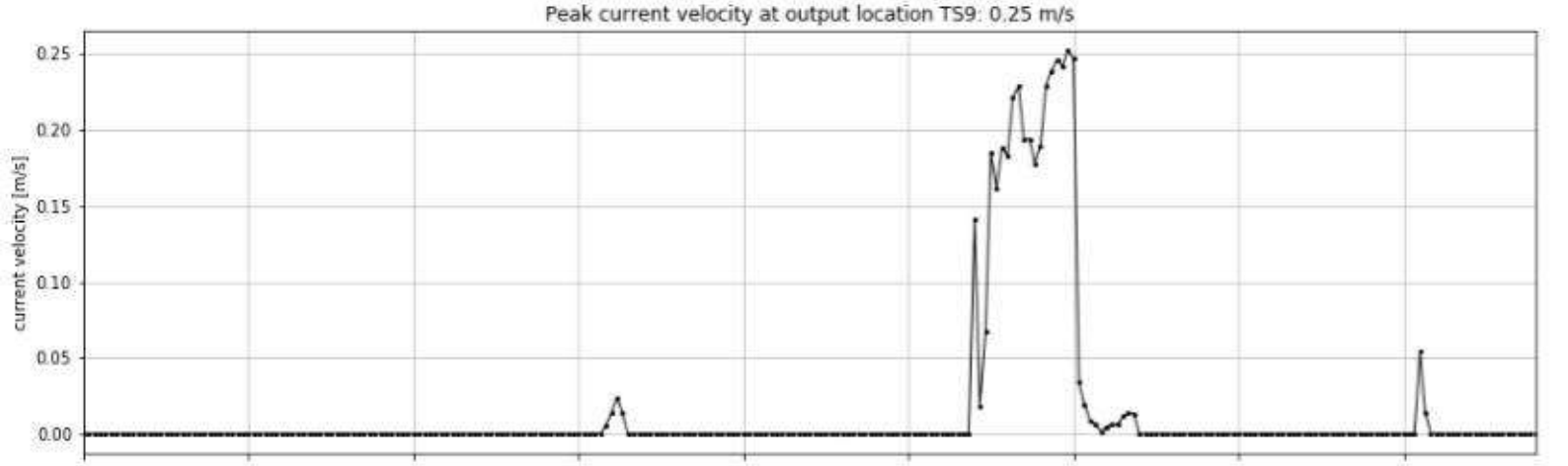
Peak current velocity at output location TS9: 0.25 m/s
current velocity [m/s]
0.25
0.20
0.15
0.10
0.05
0.00

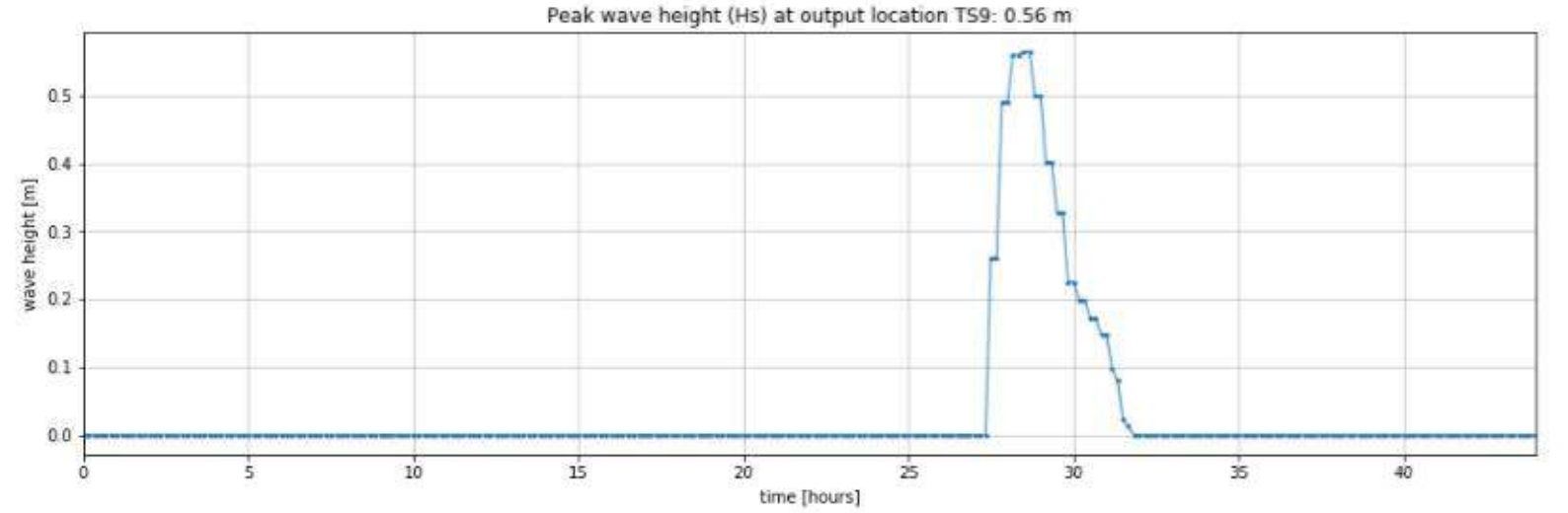
Peak wave height (Hs) at output location TS9: 0.56 m
wave height [m]
0.5
0.4
0.3
0.2
0.1
0.0
0
5
10
15
20
25
30
35
40
time [hours]

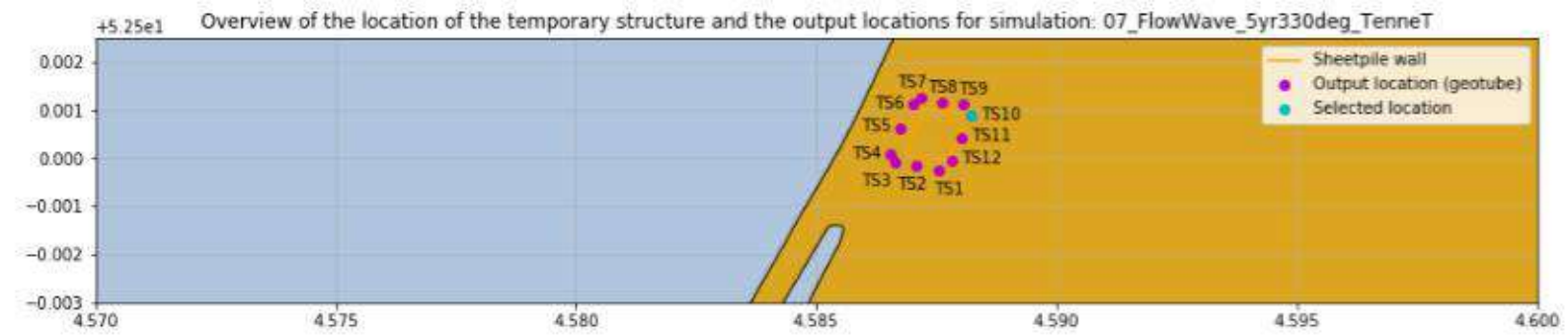
Overview of the location of the temporary structure and the output locations for simulation: 07_FlowWave_5yr330deg_TenneT
+5.25e1
Sheetpile wall
Output location (geotube)
Selected location
TS1
TS2
TS3
TS4
TS5
TS6
TS7
TS8
TS9
TS10
TS11
TS12
0.002
0.001
0.000
−0.001
−0.002
−0.003
4.570
4.575
4.580
4.585
4.590
4.595
4.600

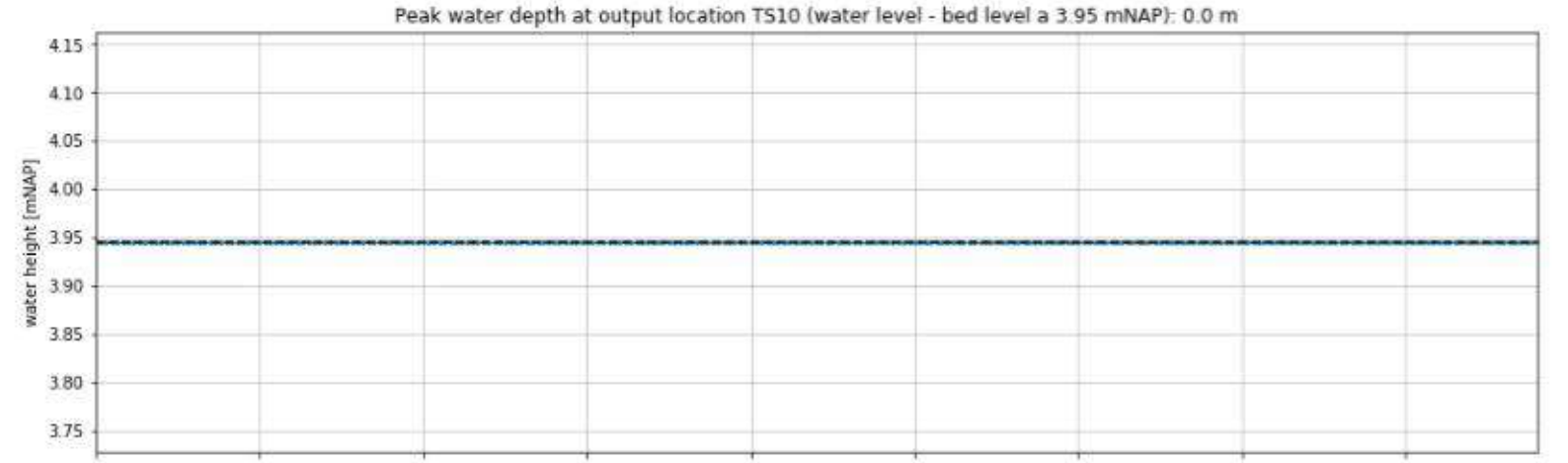
Peak water depth at output location TS10 (water level - bed level a 3.95 mNAP): 0.0 m
water height [mNAP]
4.15
4.10
4.05
4.00
3.95
3.90
3.85
3.80
3.75

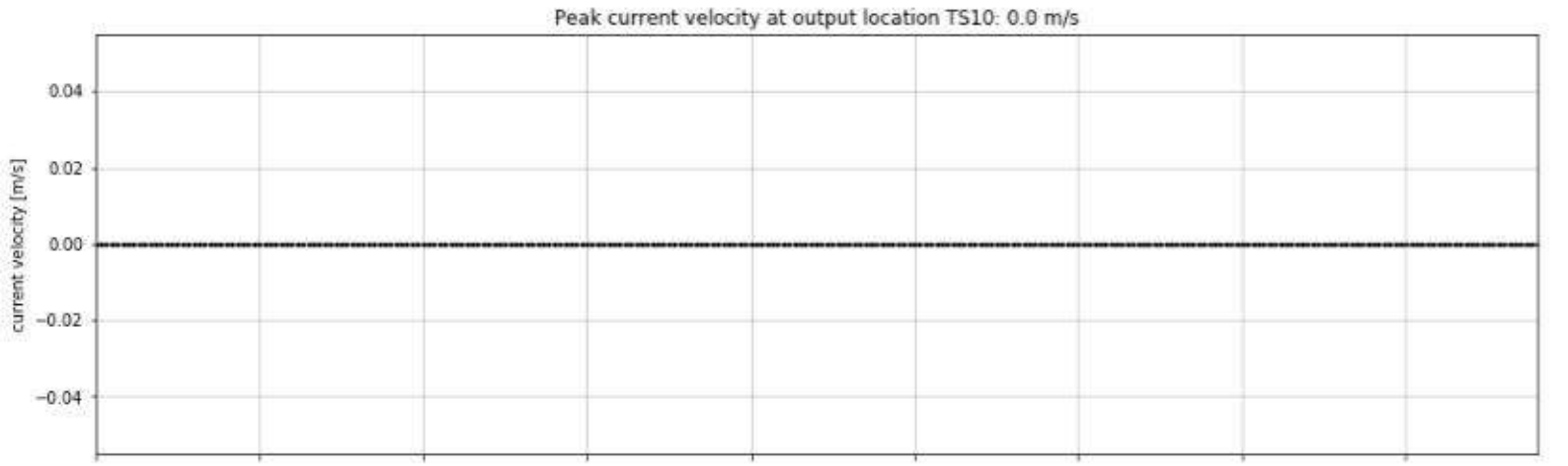
Peak current velocity at output location TS10: 0.0 m/s
current velocity [m/s]
0.04
0.02
0.00
−0.02
−0.04

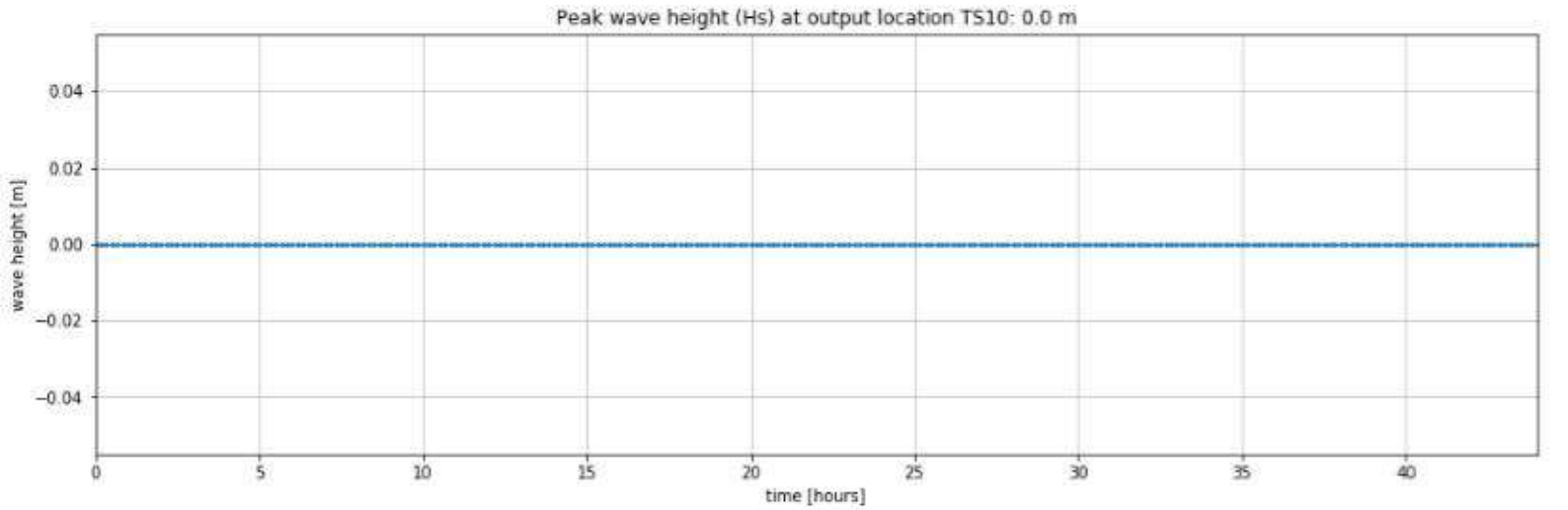
Peak wave height (Hs) at output location TS10: 0.0 m
wave height [m]
0.04
0.02
0.00
−0.02
−0.04
0
5
10
15
20
25
30
35
40
time [hours]

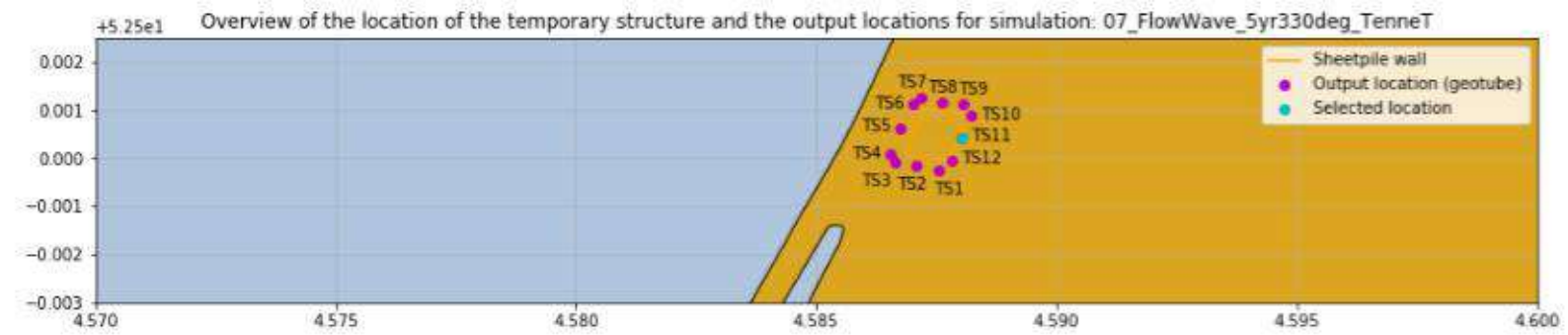
Overview of the location of the temporary structure and the output locations for simulation: 07_FlowWave_5yr330deg_TenneT
+5.25e1
Sheetpile wall
Output location (geotube)
Selected location
TS1
TS2
TS3
TS4
TS5
TS6
TS7
TS8
TS9
TS10
TS11
TS12
0.002
0.001
0.000
−0.001
−0.002
−0.003
4.570
4.575
4.580
4.585
4.590
4.595
4.600

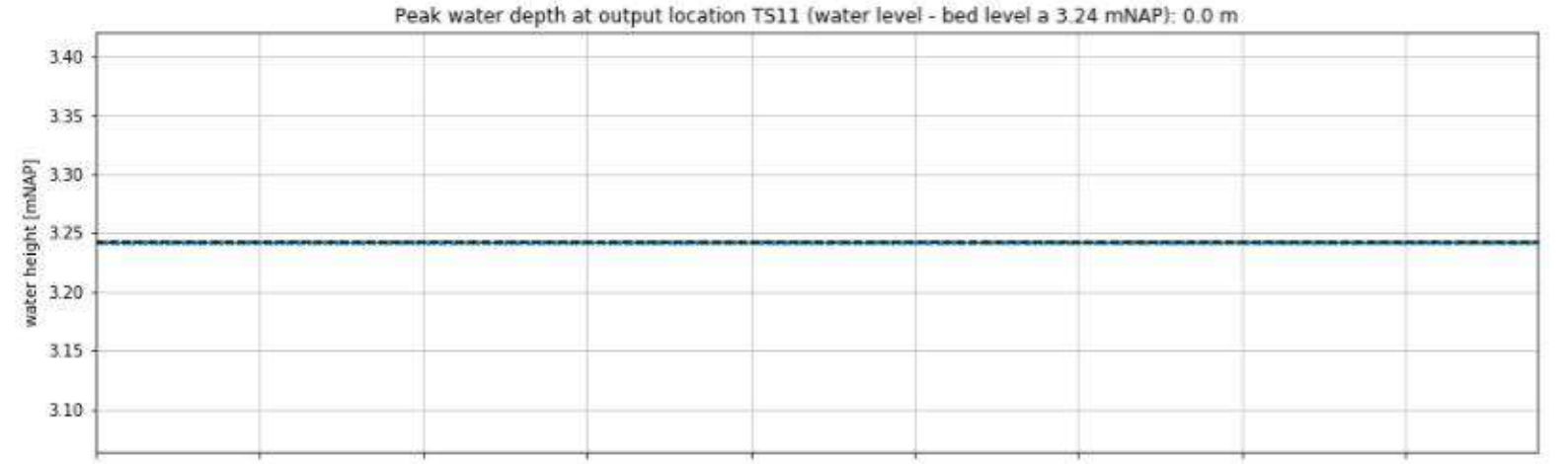
Peak water depth at output location TS11 (water level - bed level a 3.24 mNAP): 0.0 m
water height [mNAP]
3.40
3.35
3.30
3.25
3.20
3.15
3.10

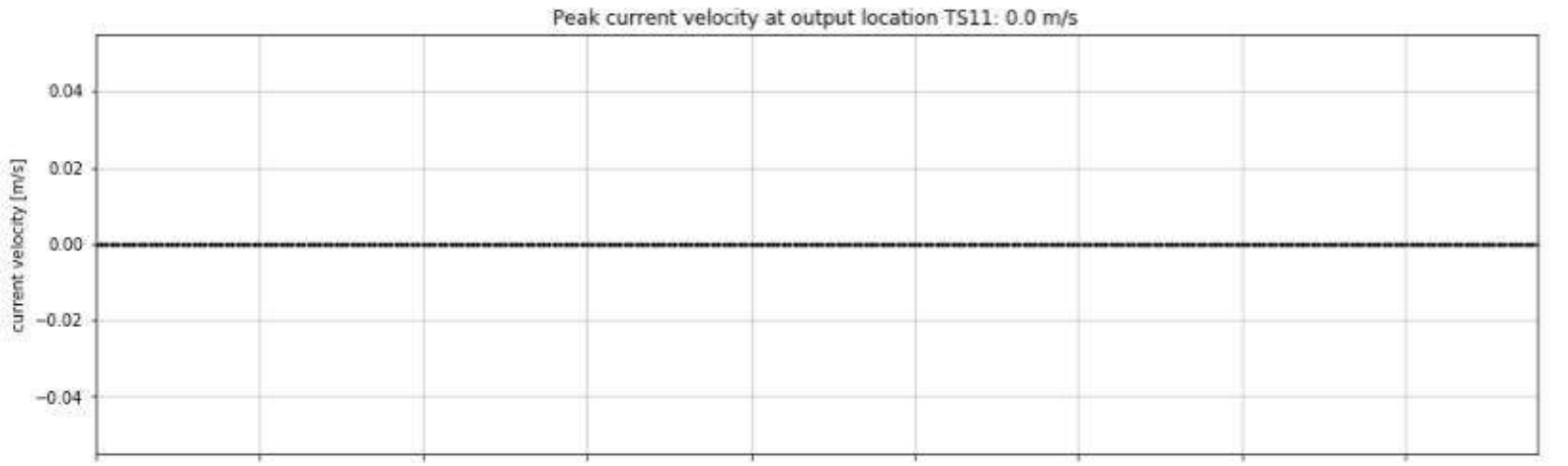
Peak current velocity at output location TS11: 0.0 m/s
current velocity [m/s]
0.04
0.02
0.00
−0.02
−0.04

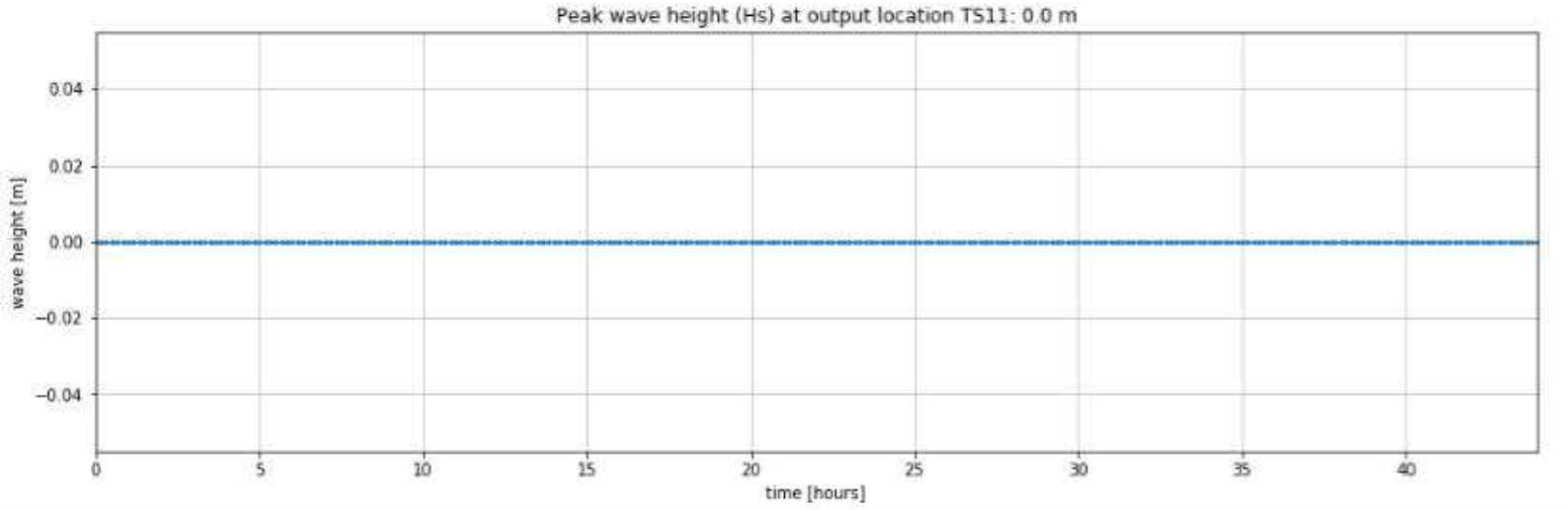
Peak wave height (Hs) at output location TS11: 0.0 m
wave height [m]
0.04
0.02
0.00
−0.02
−0.04
0
5
10
15
20
25
30
35
40
time [hours]

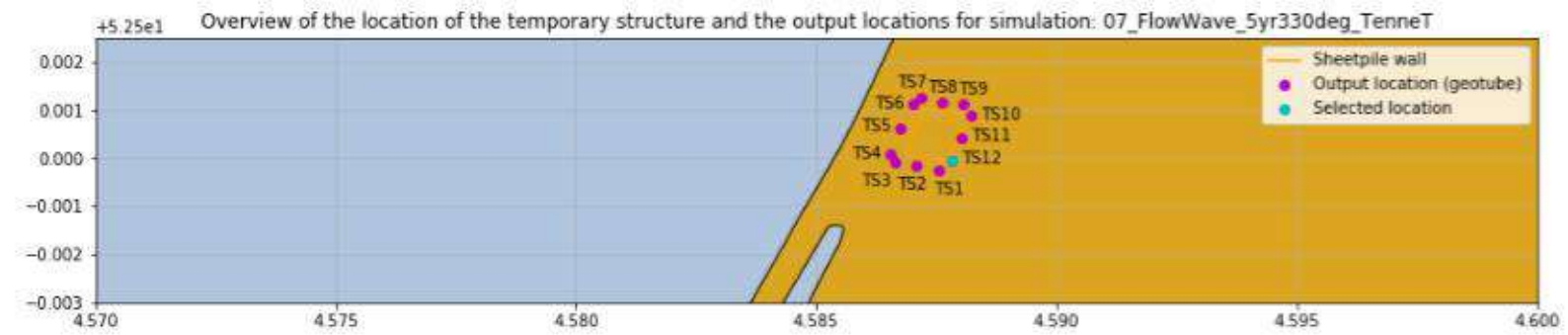
Overview of the location of the temporary structure and the output locations for simulation: 07_FlowWave_5yr330deg_TenneT
+5.25e1
Sheetpile wall
Output location (geotube)
Selected location
TS1
TS2
TS3
TS4
TS5
TS6
TS7
TS8
TS9
TS10
TS11
TS12
0.002
0.001
0.000
−0.001
−0.002
−0.003
4.570
4.575
4.580
4.585
4.590
4.595
4.600

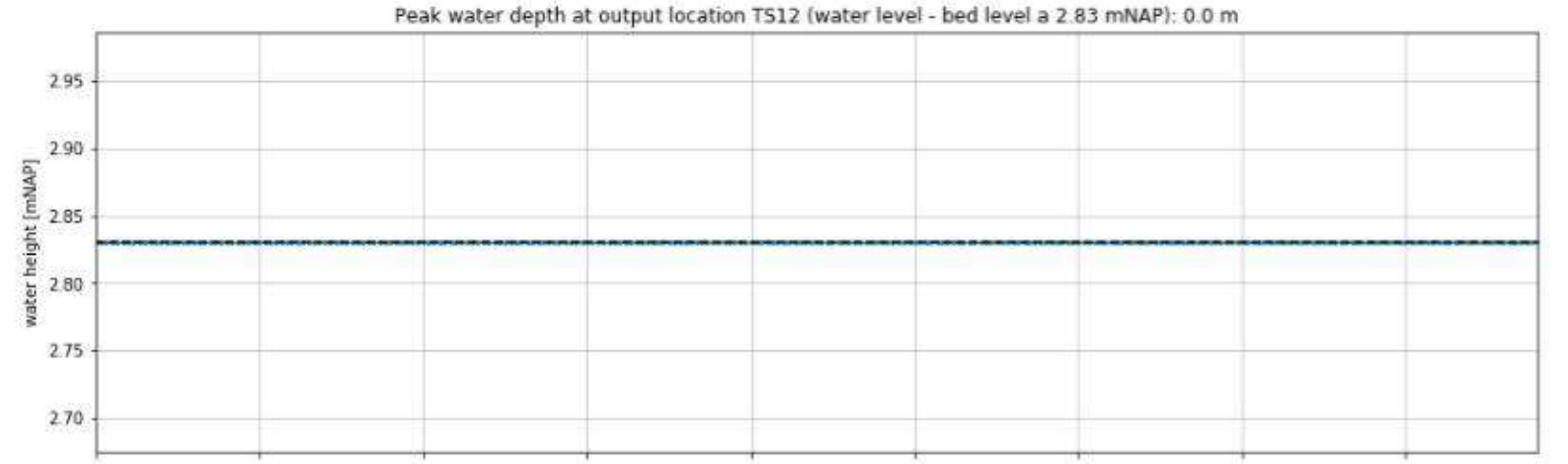
Peak water depth at output location TS12 (water level - bed level a 2.83 mNAP): 0.0 m
water height [mNAP]
2.95
2.90
2.85
2.80
2.75
2.70

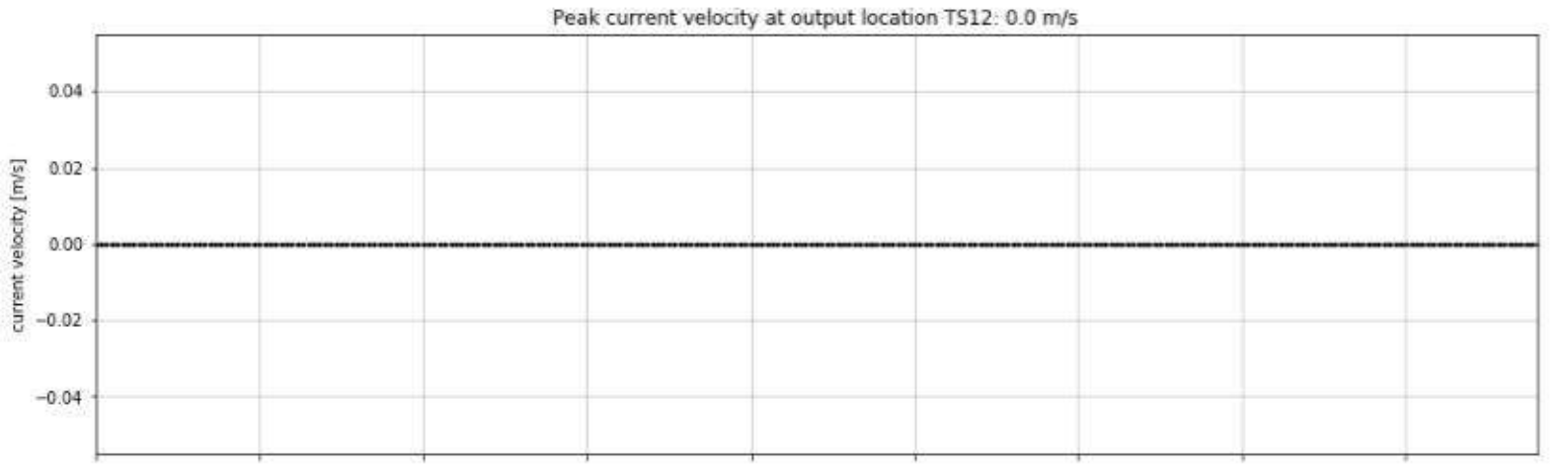
Peak current velocity at output location TS12: 0.0 m/s
current velocity [m/s]
0.04
0.02
0.00
−0.02
−0.04

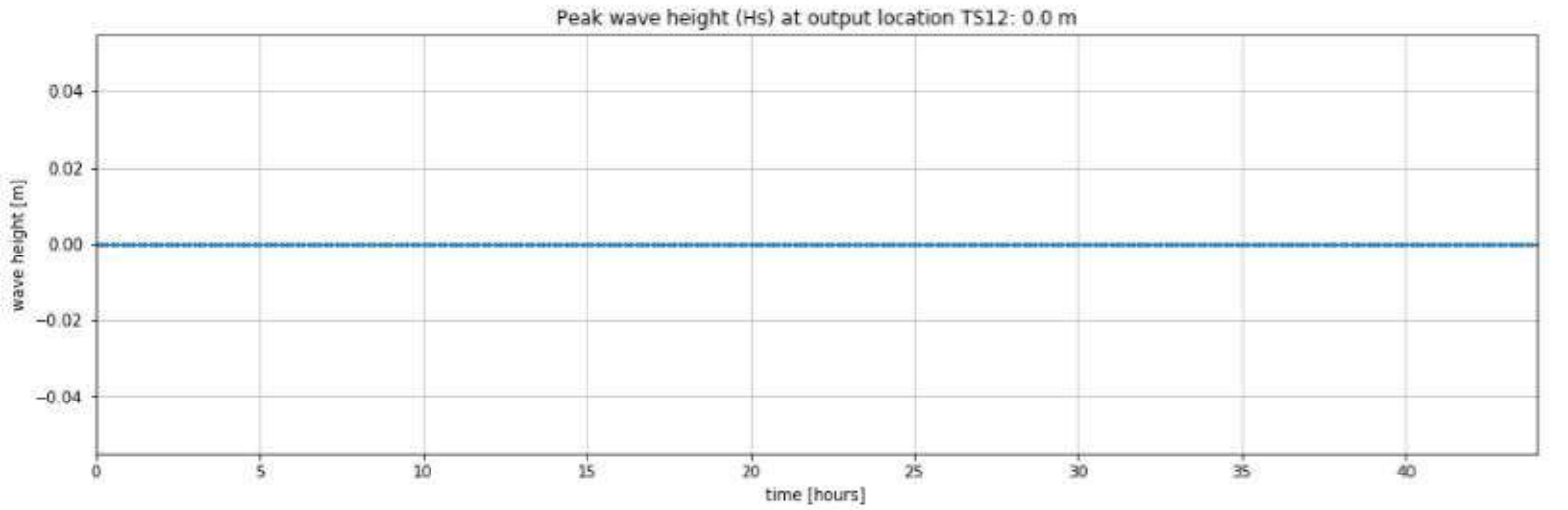
Peak wave height (Hs) at output location TS12: 0.0 m
wave height [m]
0.04
0.02
0.00
−0.02
−0.04
0
5
10
15
20
25
30
35
40
time [hours]

C.5 Flow-Wave 20 yr storm 330 degrees – TenneT bathymetry

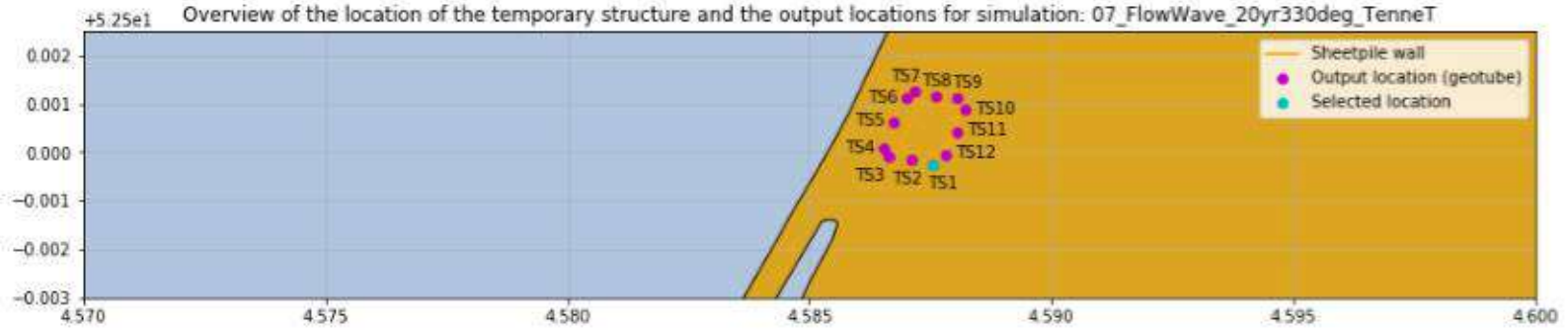
Overview of the location of the temporary structure and the output locations for simulation: 07_FlowWave_20yr330deg_TenneT
+5.25e1
Sheetpile wall
Output location (geotube)
Selected location
TS1
TS2
TS3
TS4
TS5
TS6
TS7
TS8
TS9
TS10
TS11
TS12
0.002
0.001
0.000
−0.001
−0.002
−0.003
4.570
4.575
4.580
4.585
4.590
4.595
4.600

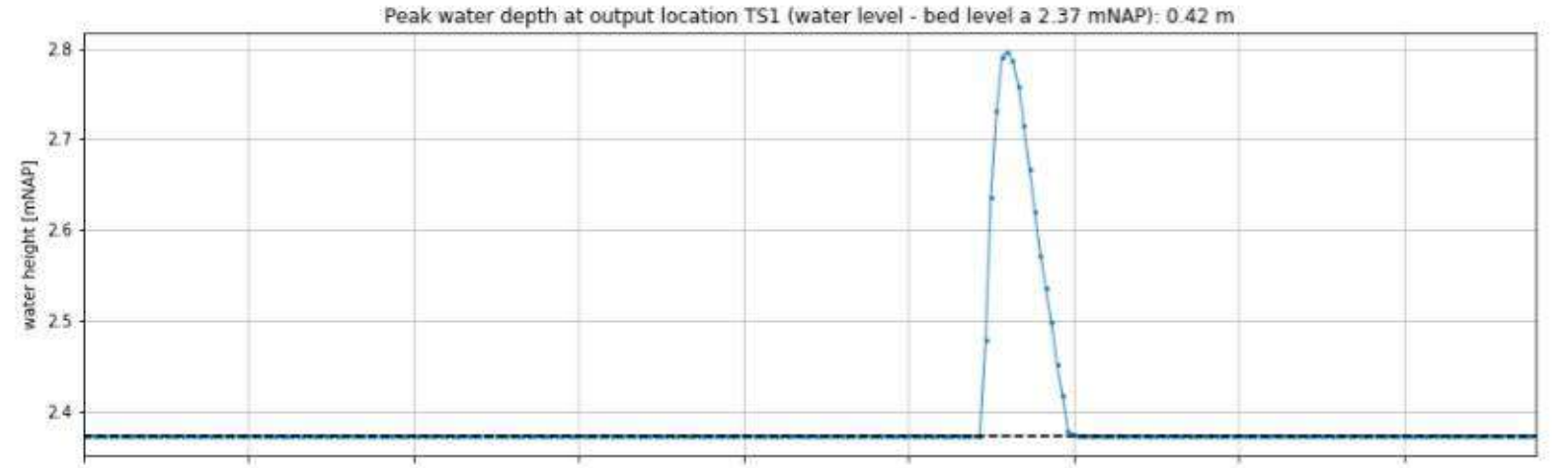
Peak water depth at output location TS1 (water level - bed level a 2.37 mNAP): 0.42 m
water height [mNAP]
2.8
2.7
2.6
2.5
2.4

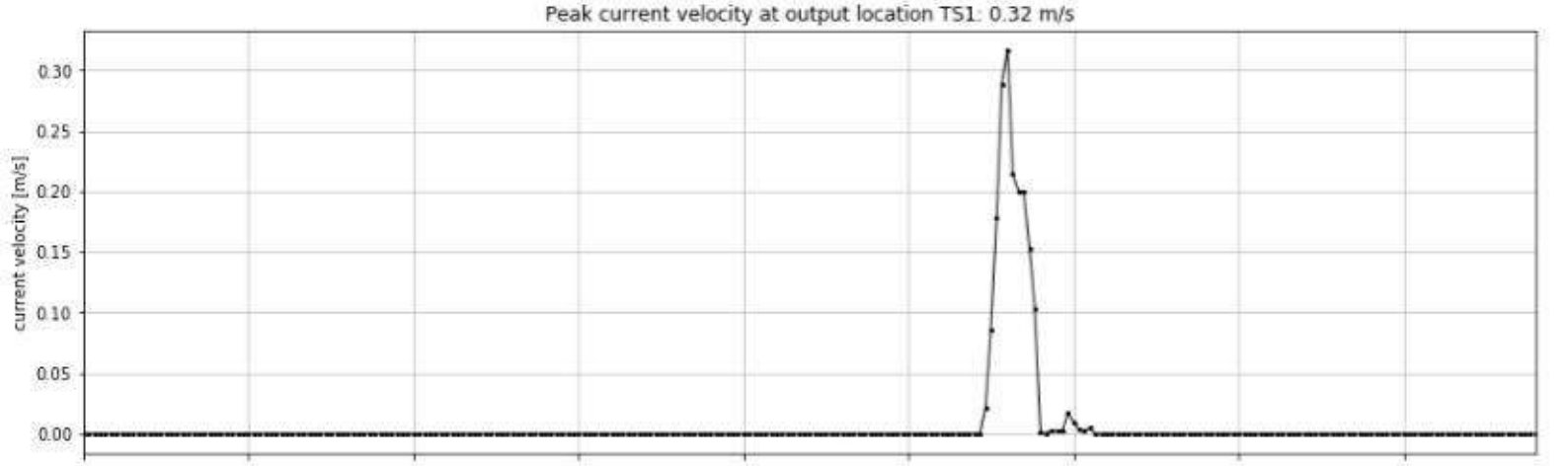
Peak current velocity at output location TS1: 0.32 m/s
current velocity [m/s]
0.30
0.25
0.20
0.15
0.10
0.05
0.00

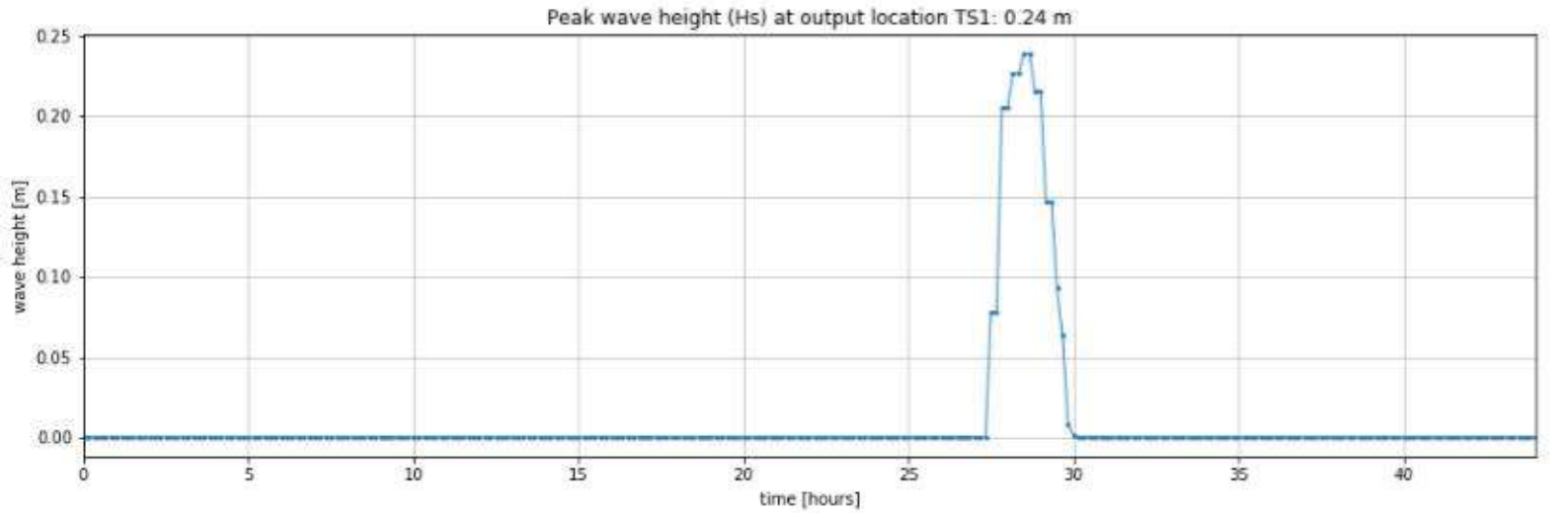
Peak wave height (Hs) at output location TS1: 0.24 m
wave height [m]
0.25
0.20
0.15
0.10
0.05
0.00
0
5
10
15
20
25
30
35
40
time [hours]

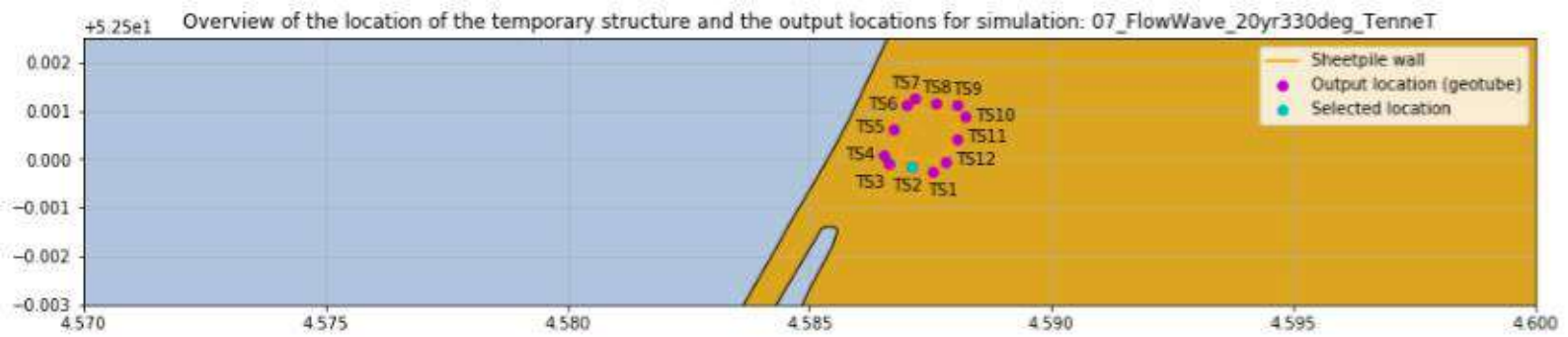
Overview of the location of the temporary structure and the output locations for simulation: 07_FlowWave_20yr330deg_TenneT
+5.25e1
Sheetpile wall
Output location (geotube)
Selected location
TS1
TS2
TS3
TS4
TS5
TS6
TS7
TS8
TS9
TS10
TS11
TS12
0.002
0.001
0.000
−0.001
−0.002
−0.003
4.570
4.575
4.580
4.585
4.590
4.595
4.600

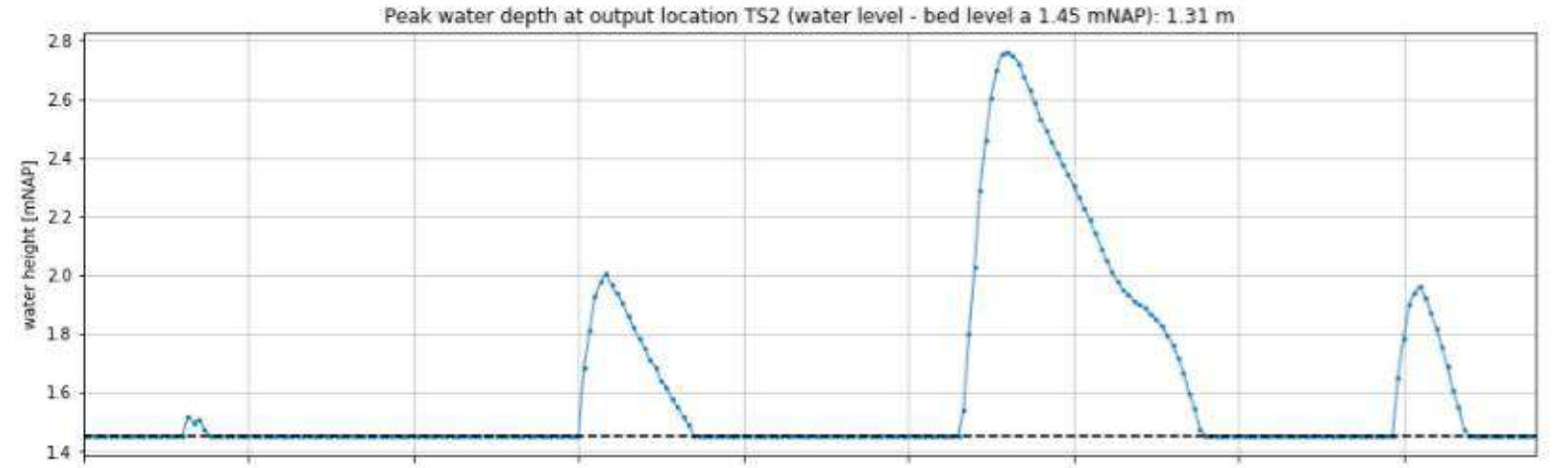
Peak water depth at output location TS2 (water level - bed level a 1.45 mNAP): 1.31 m
water height [mNAP]
2.8
2.6
2.4
2.2
2.0
1.8
1.6
1.4

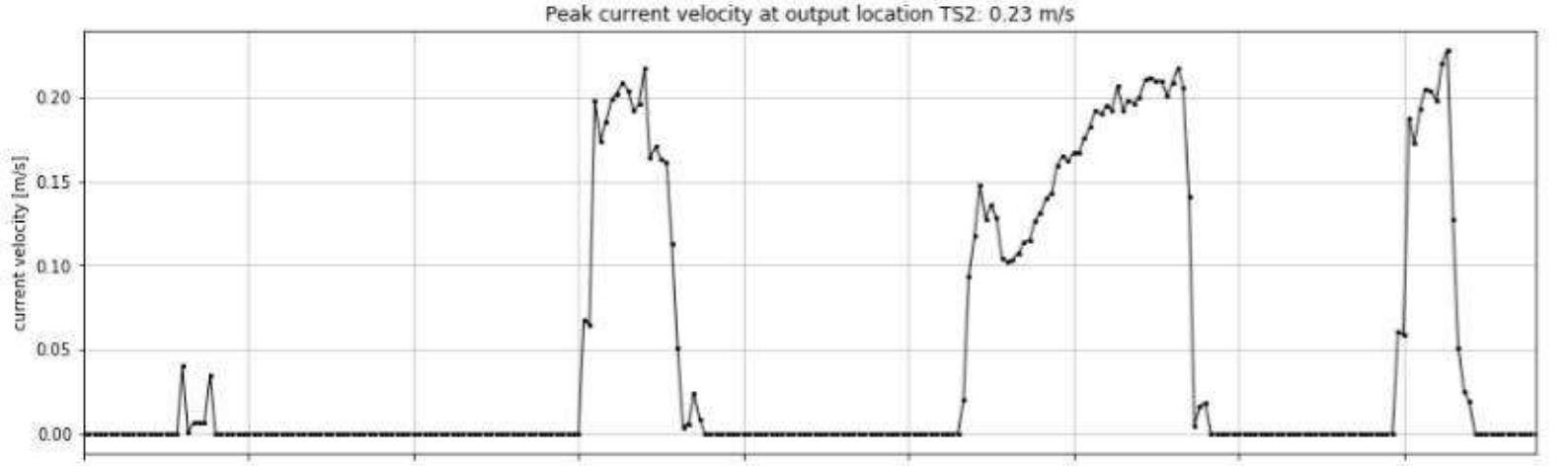
Peak current velocity at output location TS2: 0.23 m/s
current velocity [m/s]
0.20
0.15
0.10
0.05
0.00

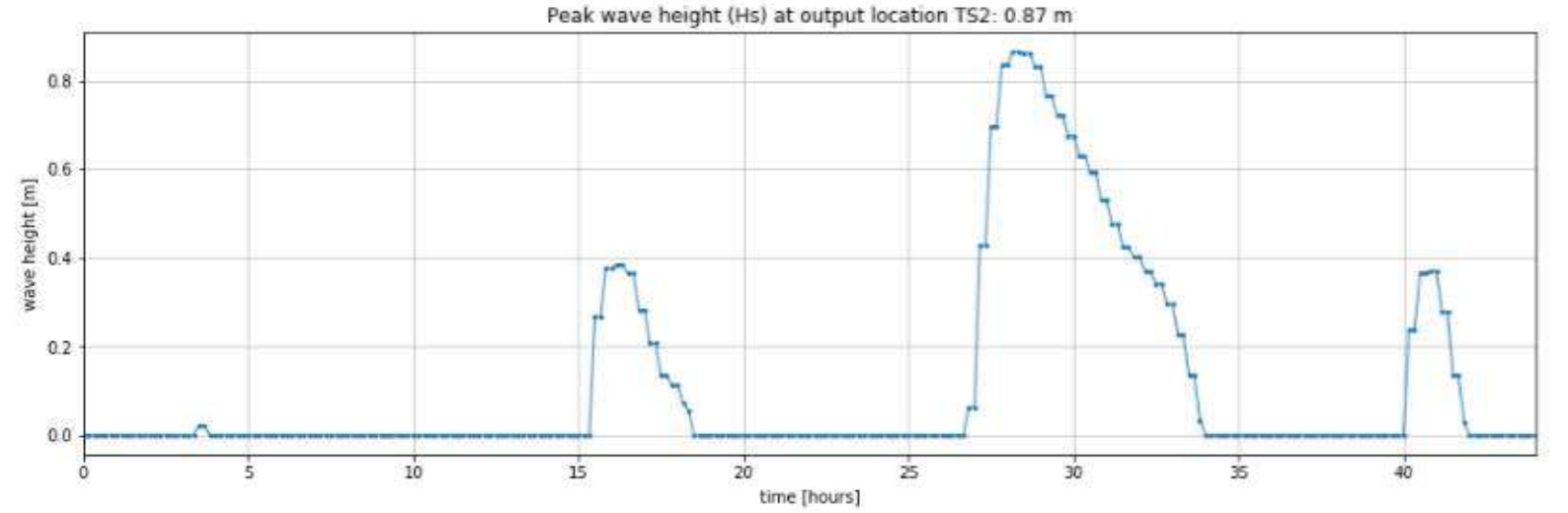
Peak wave height (Hs) at output location TS2: 0.87 m
wave height [m]
0.8
0.6
0.4
0.2
0.0
0
5
10
15
20
25
30
35
40
time [hours]

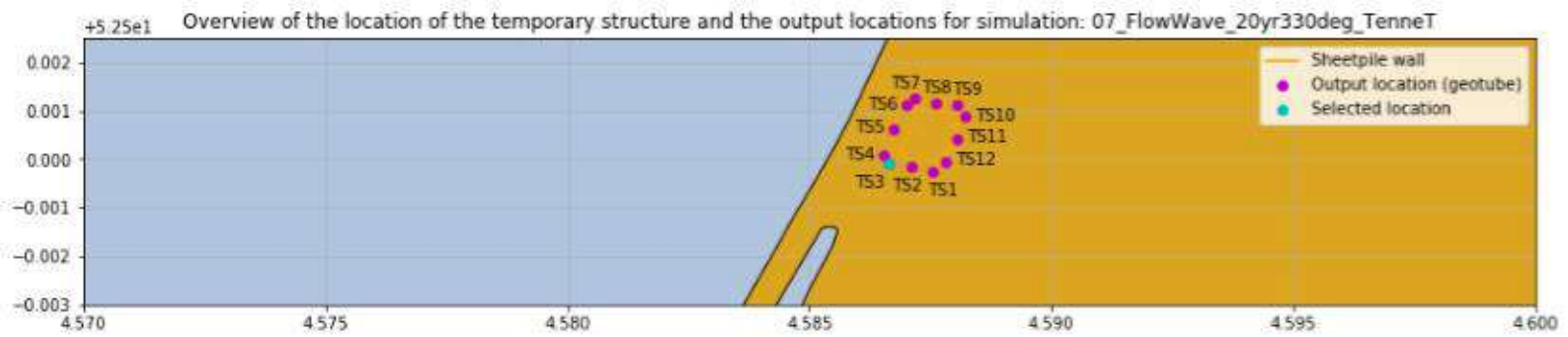
Overview of the location of the temporary structure and the output locations for simulation: 07_FlowWave_20yr330deg_TenneT
+5.25e1
Sheetpile wall
Output location (geotube)
Selected location
TS1
TS2
TS3
TS4
TS5
TS6
TS7
TS8
TS9
TS10
TS11
TS12
0.002
0.001
0.000
−0.001
−0.002
−0.003
4.570
4.575
4.580
4.585
4.590
4.595
4.600

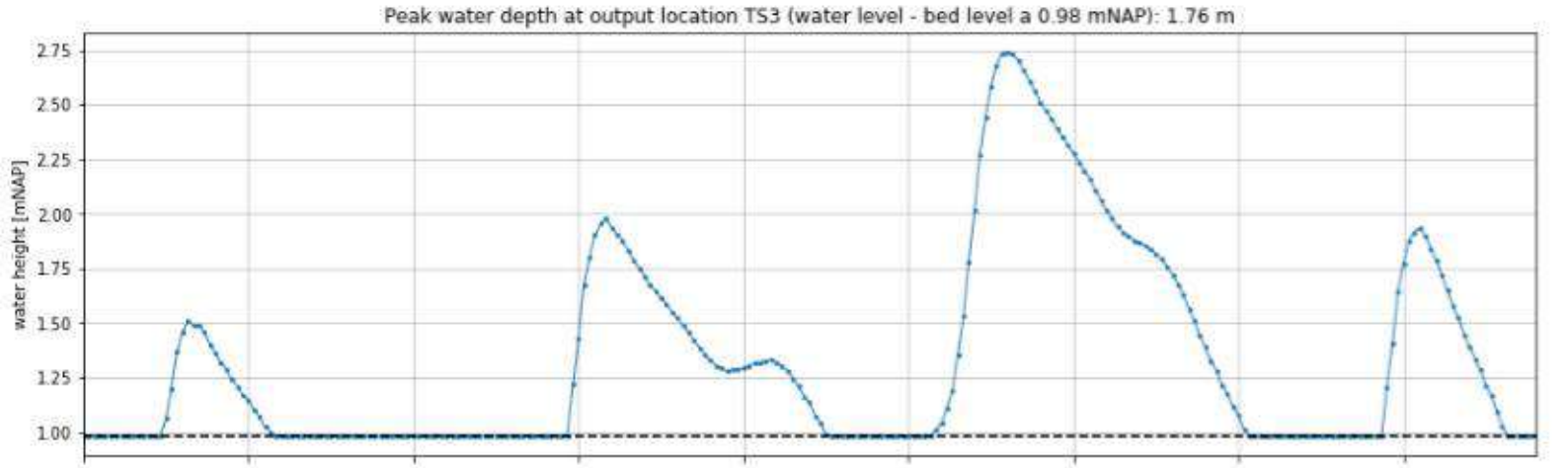
Peak water depth at output location TS3 (water level - bed level a 0.98 mNAP): 1.76 m
water height [mNAP]
2.75
2.50
2.25
2.00
1.75
1.50
1.25
1.00

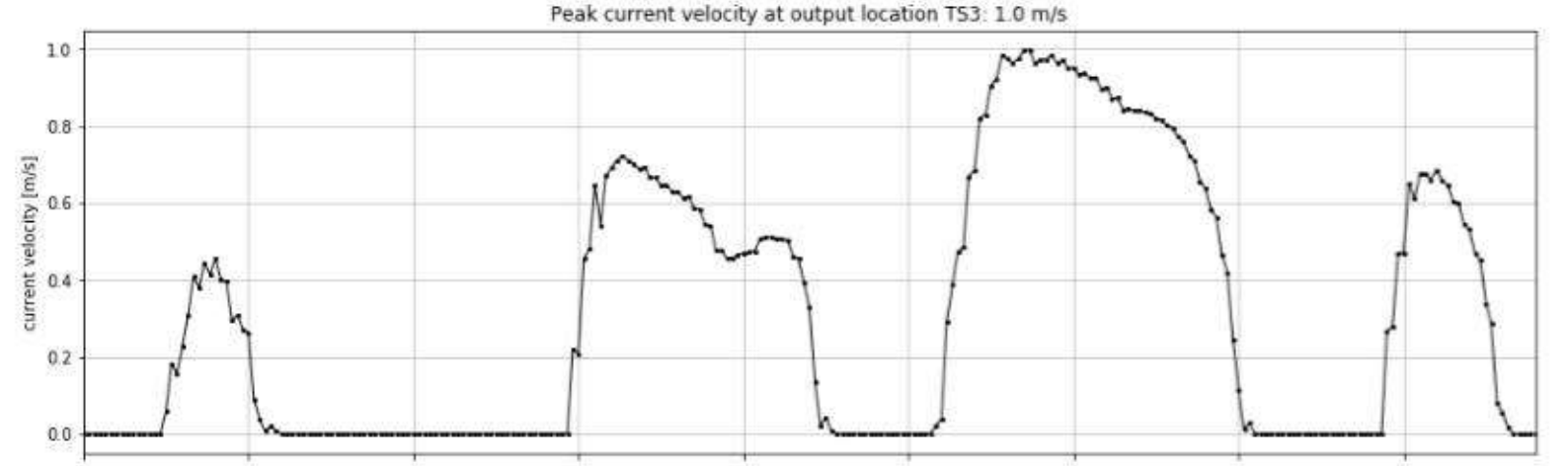
Peak current velocity at output location TS3: 1.0 m/s
current velocity [m/s]
1.0
0.8
0.6
0.4
0.2
0.0

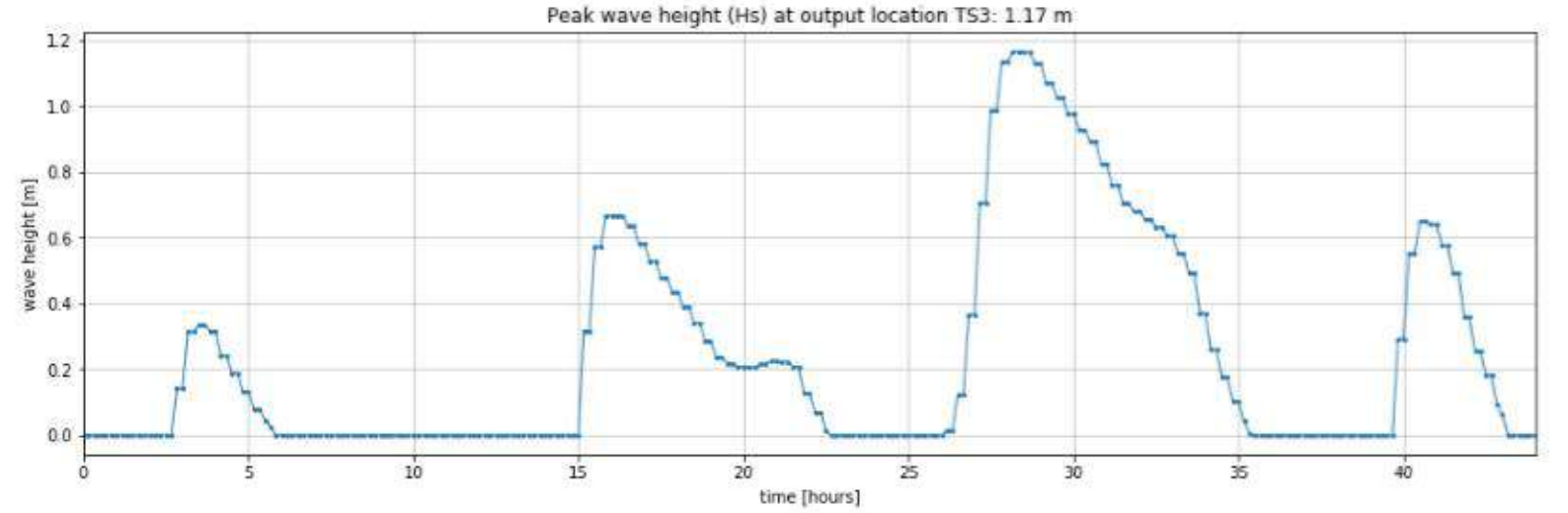
Peak wave height (Hs) at output location TS3: 1.17 m
wave height [m]
1.2
1.0
0.8
0.6
0.4
0.2
0.0
0
5
10
15
20
25
30
35
40
time [hours]

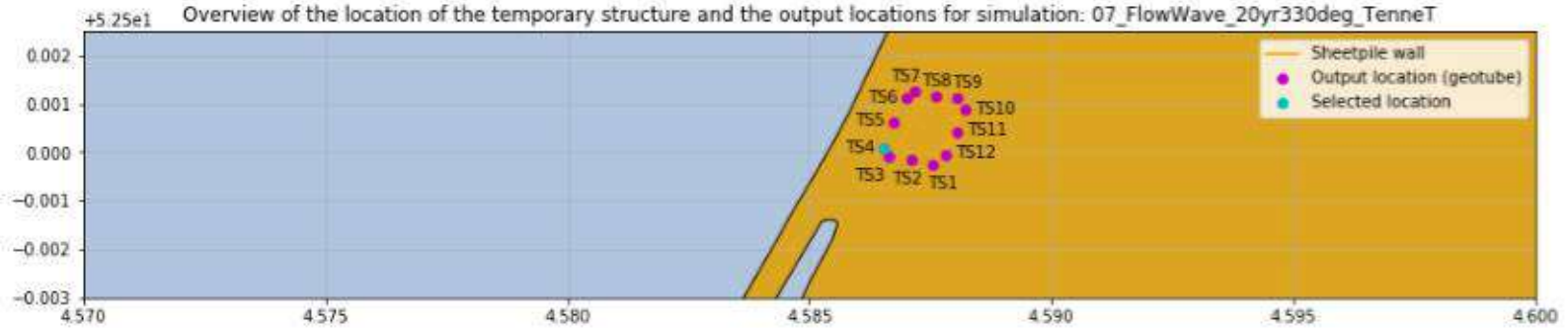
Overview of the location of the temporary structure and the output locations for simulation: 07_FlowWave_20yr330deg_TenneT
+5.25e1
Sheetpile wall
Output location (geotube)
Selected location
TS1
TS2
TS3
TS4
TS5
TS6
TS7
TS8
TS9
TS10
TS11
TS12
0.002
0.001
0.000
−0.001
−0.002
−0.003
4.570
4.575
4.580
4.585
4.590
4.595
4.600

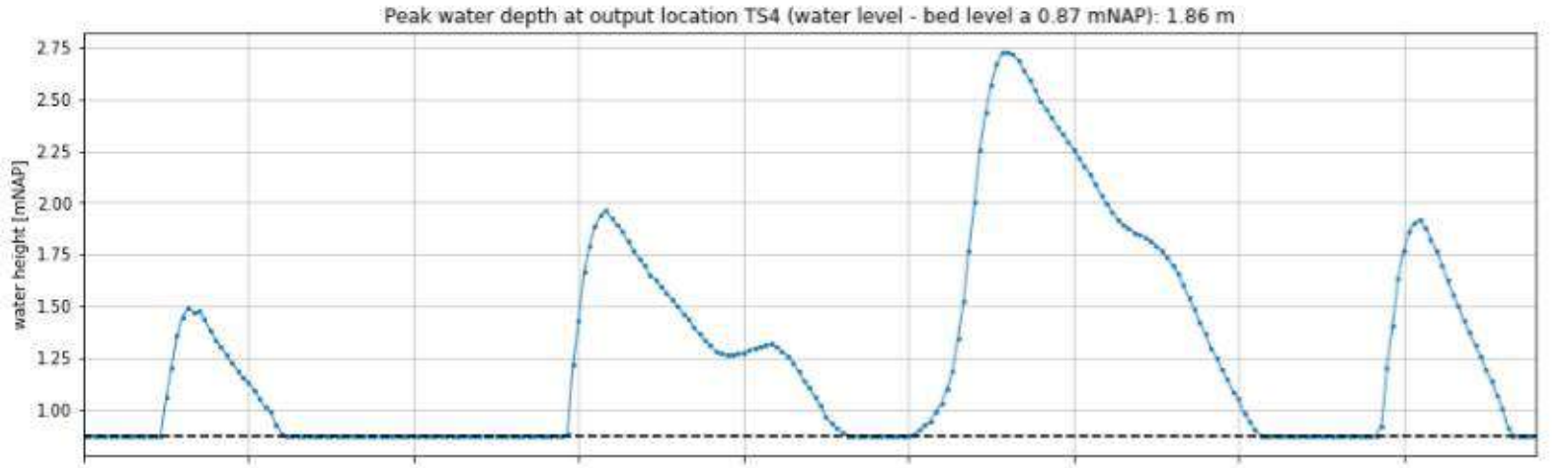
Peak water depth at output location TS4 (water level - bed level a 0.87 mNAP): 1.86 m
water height [mNAP]
2.75
2.50
2.25
2.00
1.75
1.50
1.25
1.00

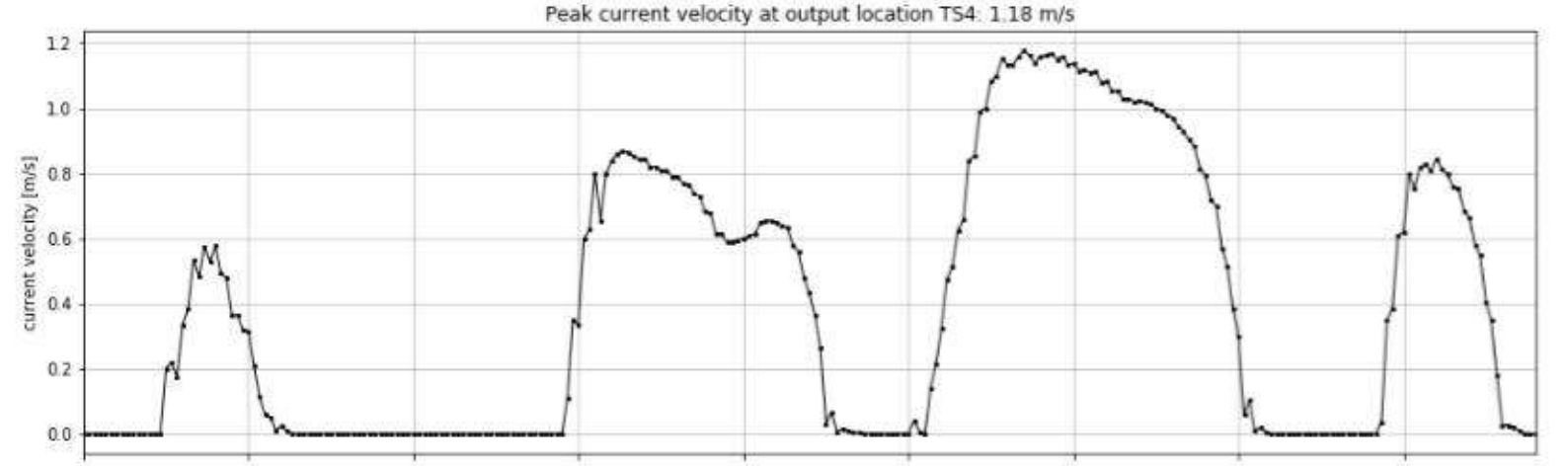
Peak current velocity at output location TS4: 1.18 m/s
current velocity [m/s]
1.2
1.0
0.8
0.6
0.4
0.2
0.0

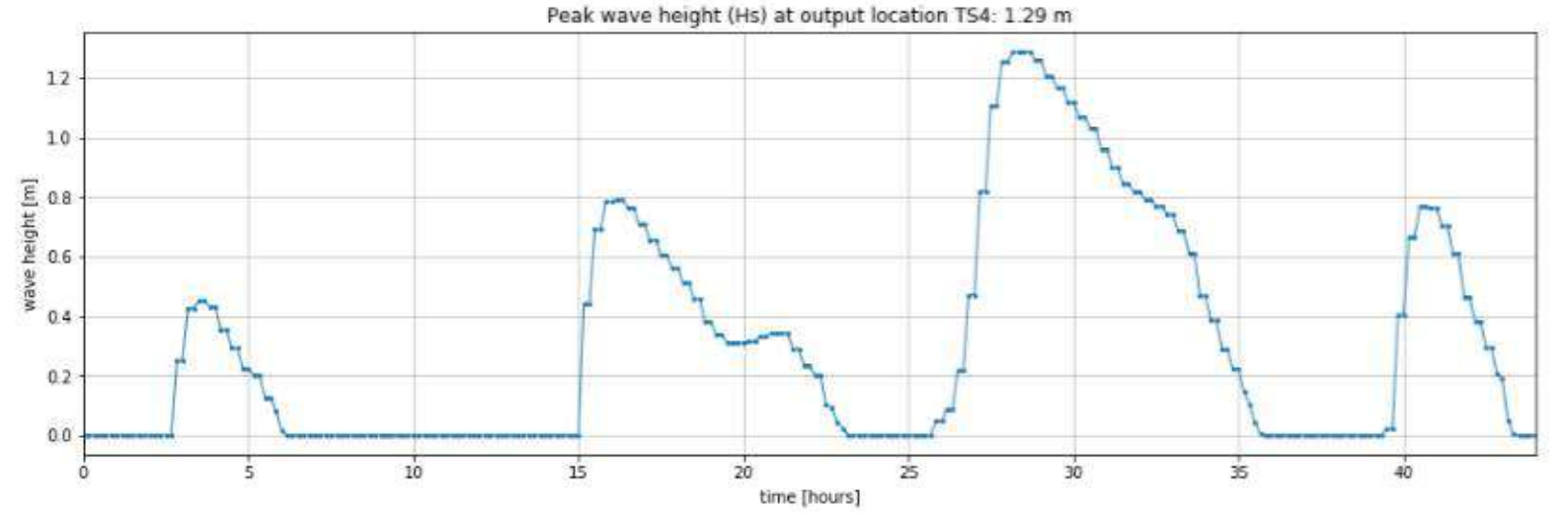
Peak wave height (Hs) at output location TS4: 1.29 m
wave height [m]
1.2
1.0
0.8
0.6
0.4
0.2
0.0
0
5
10
15
20
25
30
35
40
time [hours]

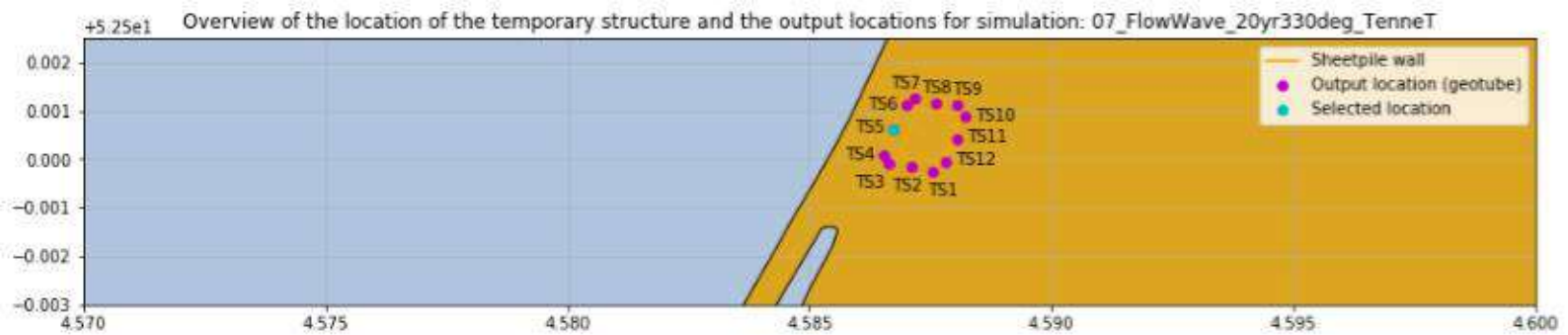
Overview of the location of the temporary structure and the output locations for simulation: 07_FlowWave_20yr330deg_TenneT
+5.25e1
Sheetpile wall
Output location (geotube)
Selected location
TS1
TS2
TS3
TS4
TS5
TS6
TS7
TS8
TS9
TS10
TS11
TS12
0.002
0.001
0.000
−0.001
−0.002
−0.003
4.570
4.575
4.580
4.585
4.590
4.595
4.600

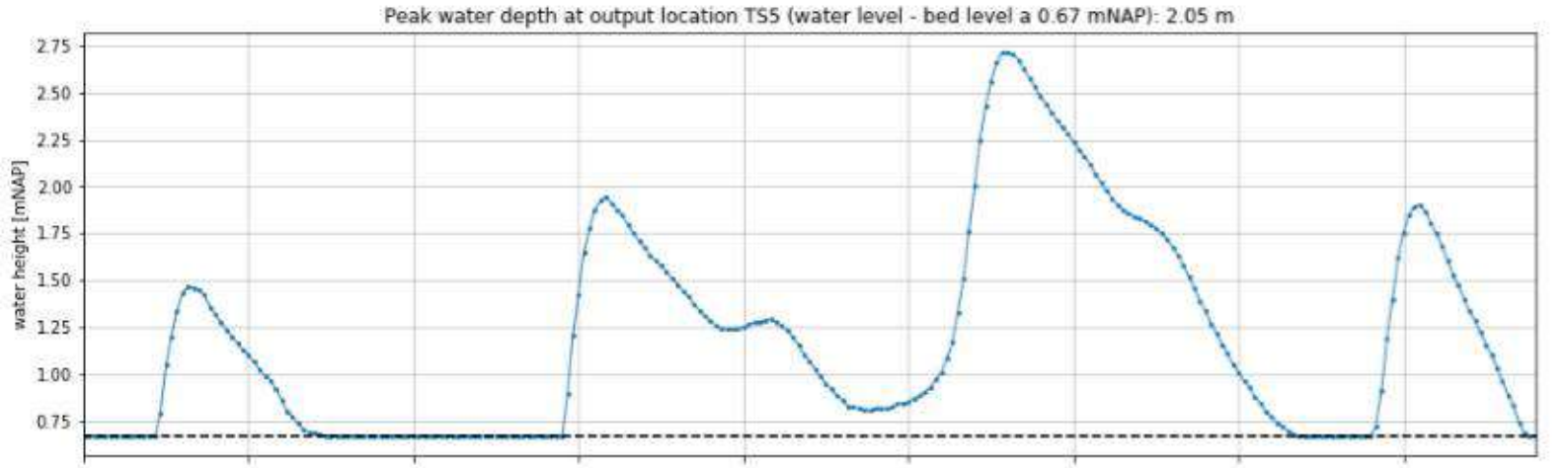
Peak water depth at output location TS5 (water level - bed level a 0.67 mNAP): 2.05 m
water height [mNAP]
2.75
2.50
2.25
2.00
1.75
1.50
1.25
1.00
0.75

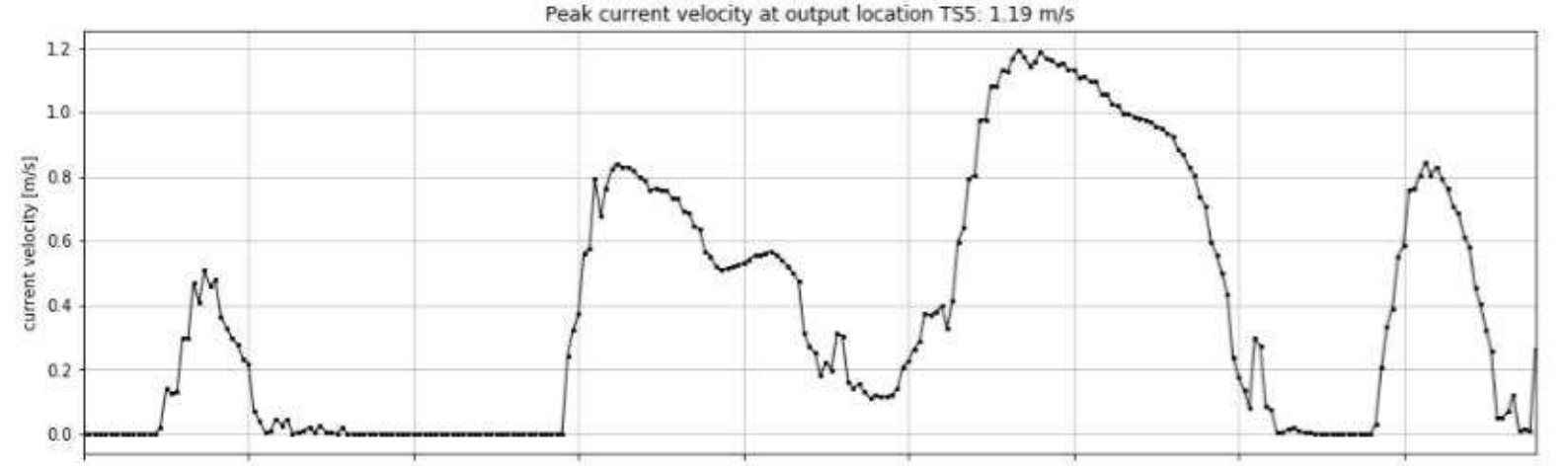
Peak current velocity at output location TS5: 1.19 m/s
current velocity [m/s]
1.2
1.0
0.8
0.6
0.4
0.2
0.0

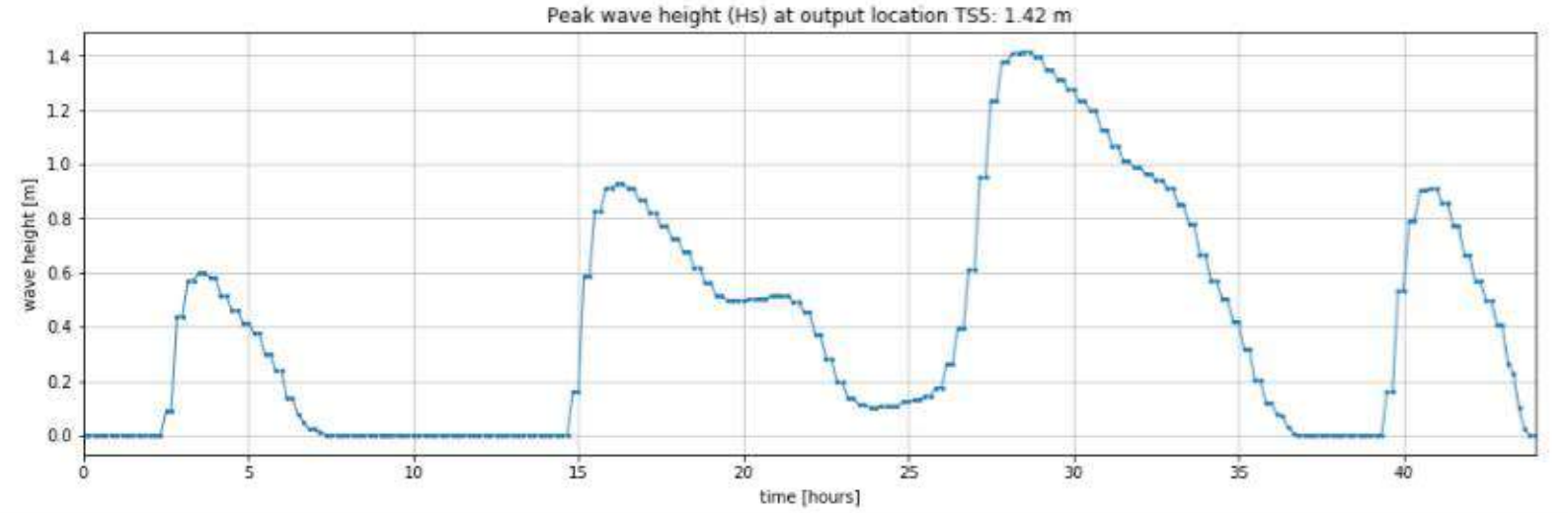
Peak wave height (Hs) at output location TS5: 1.42 m
wave height [m]
1.4
1.2
1.0
0.8
0.6
0.4
0.2
0.0
0
5
10
15
20
25
30
35
40
time [hours]

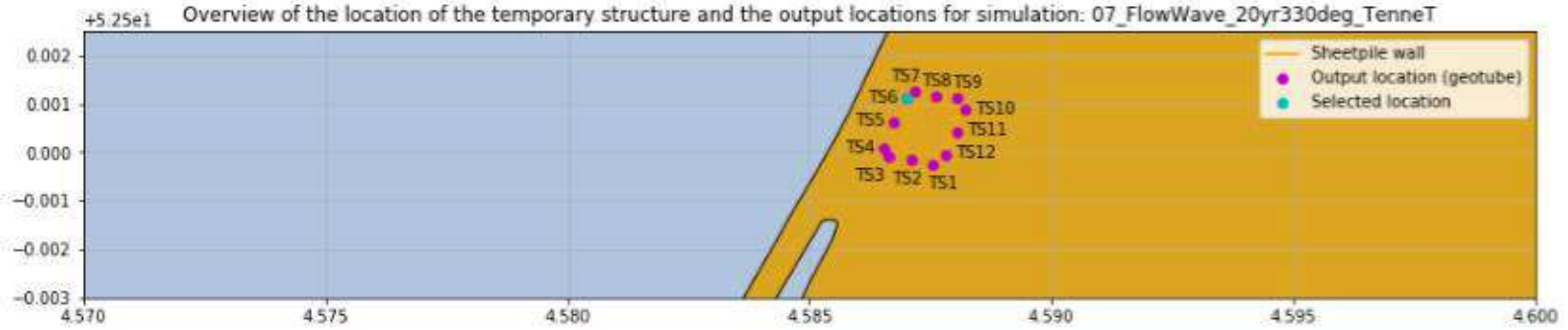
Overview of the location of the temporary structure and the output locations for simulation: 07_FlowWave_20yr330deg_TenneT
+5.25e1
Sheetpile wall
Output location (geotube)
Selected location
TS1
TS2
TS3
TS4
TS5
TS6
TS7
TS8
TS9
TS10
TS11
TS12
0.002
0.001
0.000
−0.001
−0.002
−0.003
4.570
4.575
4.580
4.585
4.590
4.595
4.600

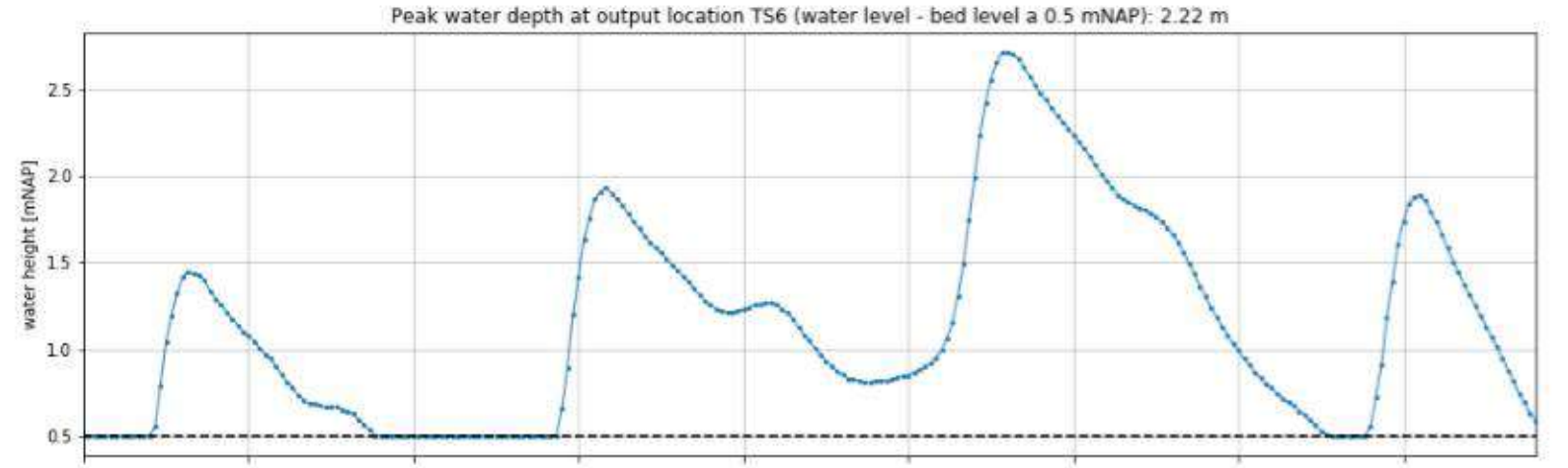
Peak water depth at output location TS6 (water level - bed level a 0.5 mNAP): 2.22 m
water height [mNAP]
2.5
2.0
1.5
1.0
0.5

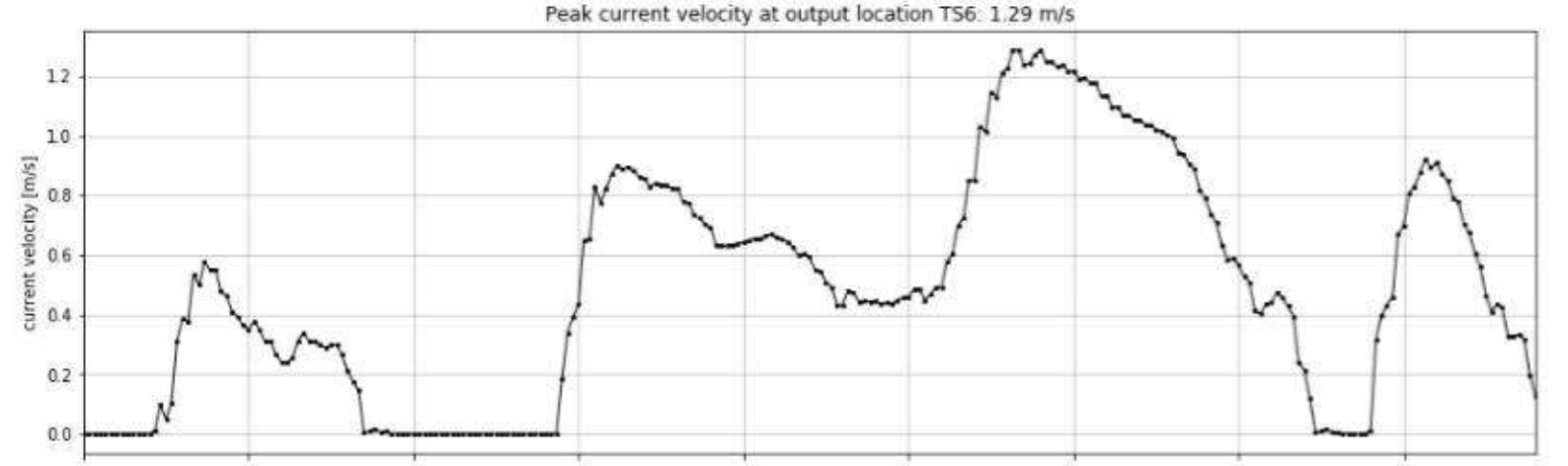
Peak current velocity at output location TS6: 1.29 m/s
current velocity [m/s]
1.2
1.0
0.8
0.6
0.4
0.2
0.0

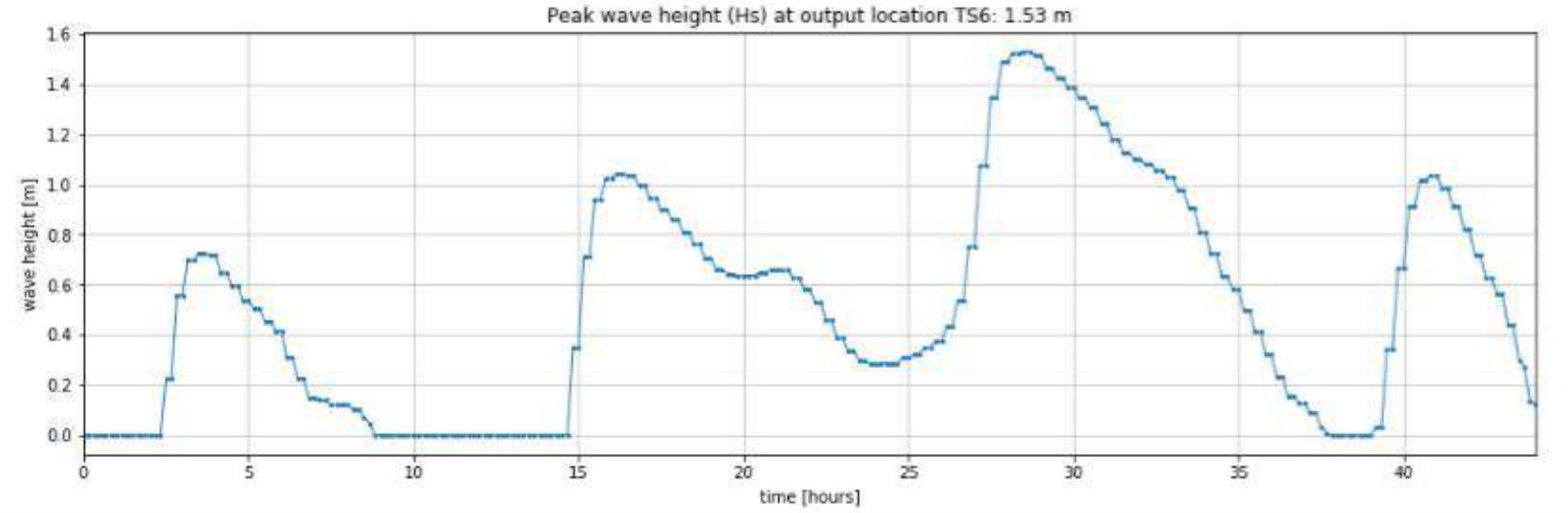
Peak wave height (Hs) at output location TS6: 1.53 m
wave height [m]
1.6
1.4
1.2
1.0
0.8
0.6
0.4
0.2
0.0
0
5
10
15
20
25
30
35
40
time [hours]

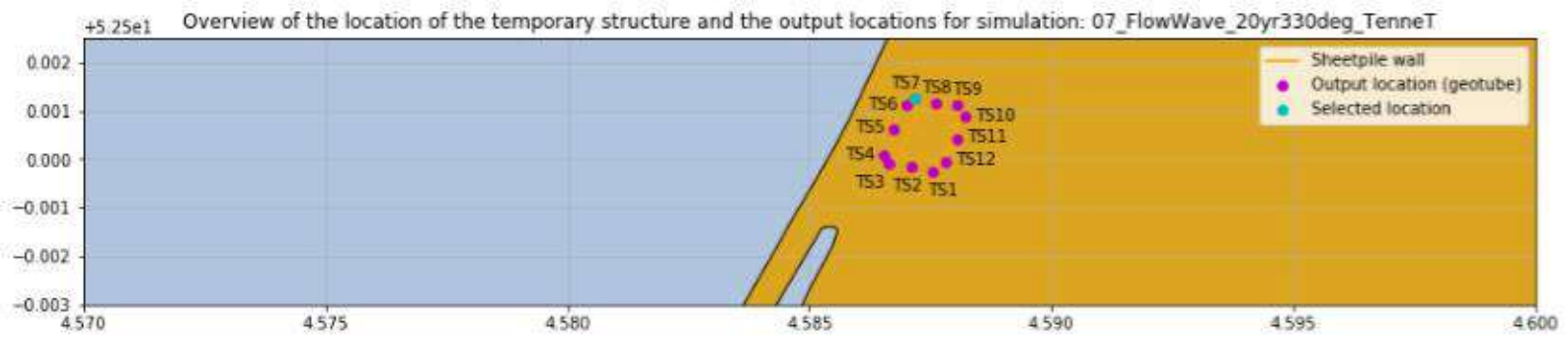
Overview of the location of the temporary structure and the output locations for simulation: 07_FlowWave_20yr330deg_TenneT
+5.25e1
Sheetpile wall
Output location (geotube)
Selected location
TS1
TS2
TS3
TS4
TS5
TS6
TS7
TS8
TS9
TS10
TS11
TS12
0.002
0.001
0.000
−0.001
−0.002
−0.003
4.570
4.575
4.580
4.585
4.590
4.595
4.600

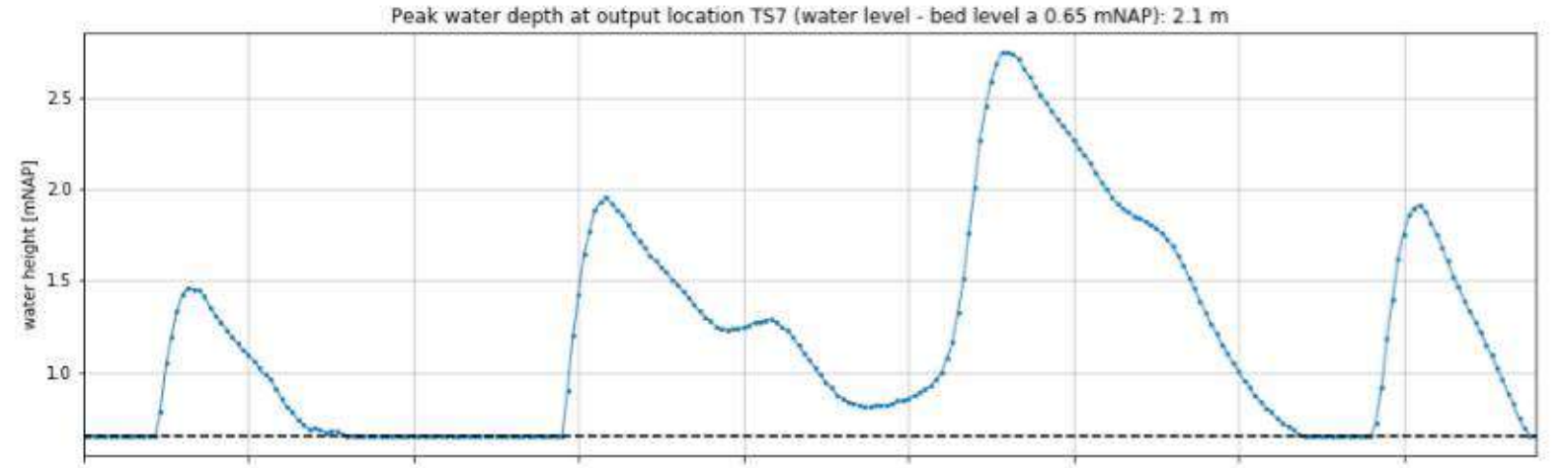
Peak water depth at output location TS7 (water level - bed level a 0.65 mNAP): 2.1 m
water height [mNAP]
2.5
2.0
1.5
1.0

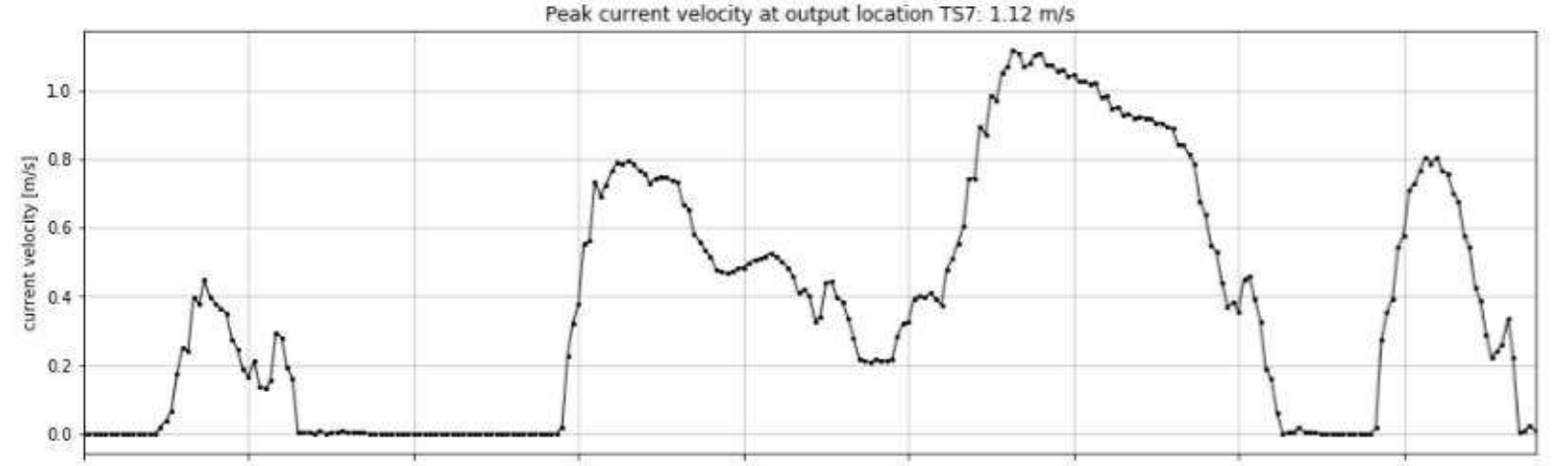
Peak current velocity at output location TS7: 1.12 m/s
current velocity [m/s]
1.0
0.8
0.6
0.4
0.2
0.0

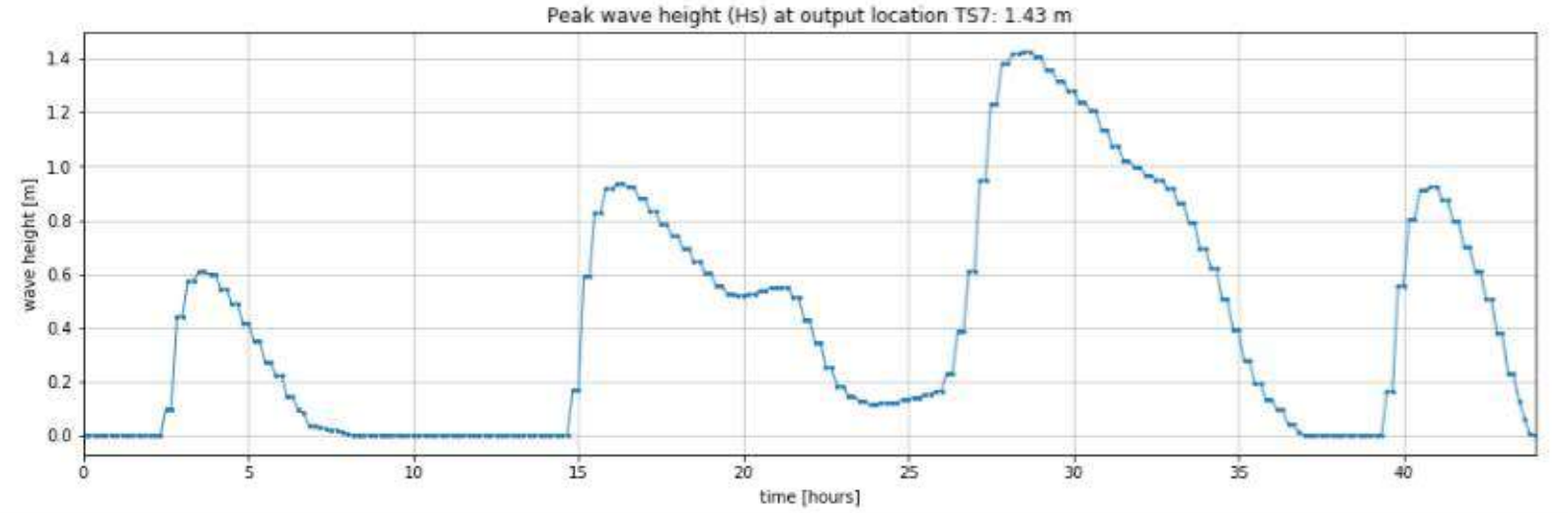
Peak wave height (Hs) at output location TS7: 1.43 m
wave height [m]
1.4
1.2
1.0
0.8
0.6
0.4
0.2
0.0
0
5
10
15
20
25
30
35
40
time [hours]

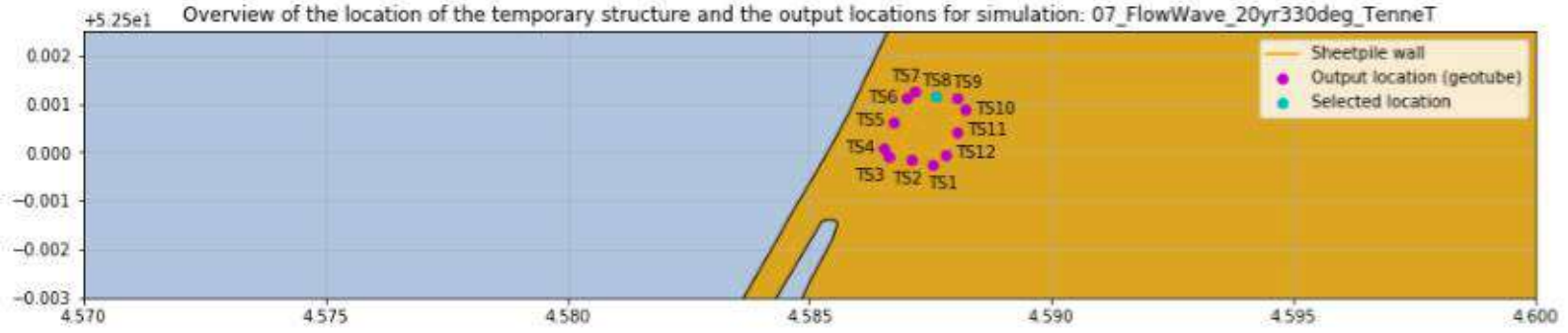
Overview of the location of the temporary structure and the output locations for simulation: 07_FlowWave_20yr330deg_TenneT
+5.25e1
Sheetpile wall
Output location (geotube)
Selected location
TS1
TS2
TS3
TS4
TS5
TS6
TS7
TS8
TS9
TS10
TS11
TS12
0.002
0.001
0.000
−0.001
−0.002
−0.003
4.570
4.575
4.580
4.585
4.590
4.595
4.600

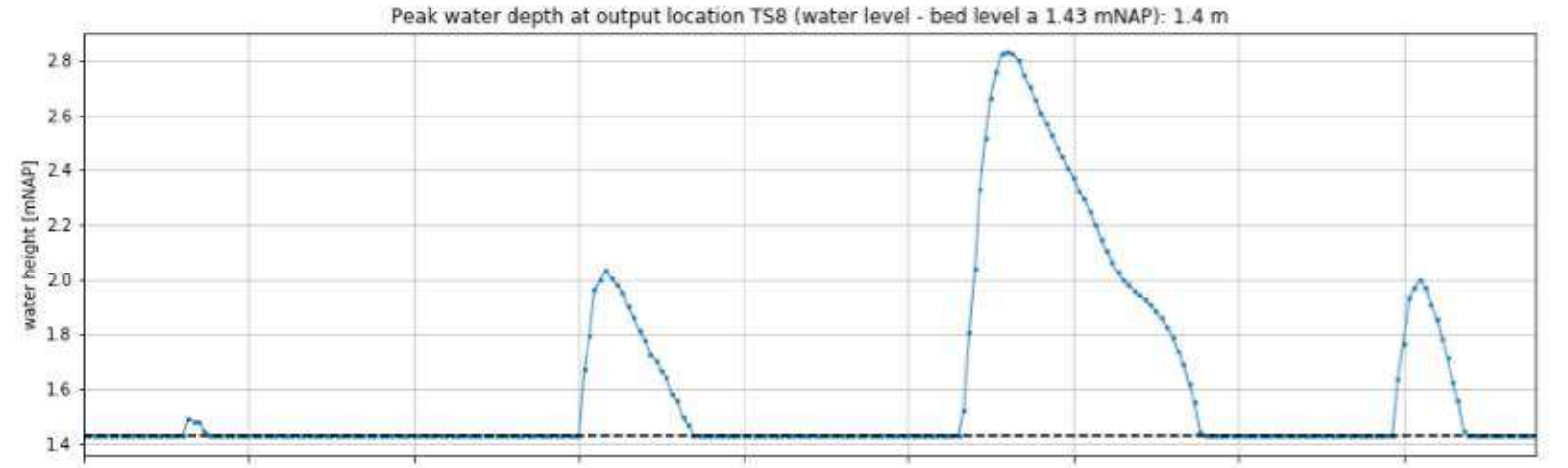
Peak water depth at output location TS8 (water level - bed level a 1.43 mNAP): 1.4 m
water height [mNAP]
2.8
2.6
2.4
2.2
2.0
1.8
1.6
1.4

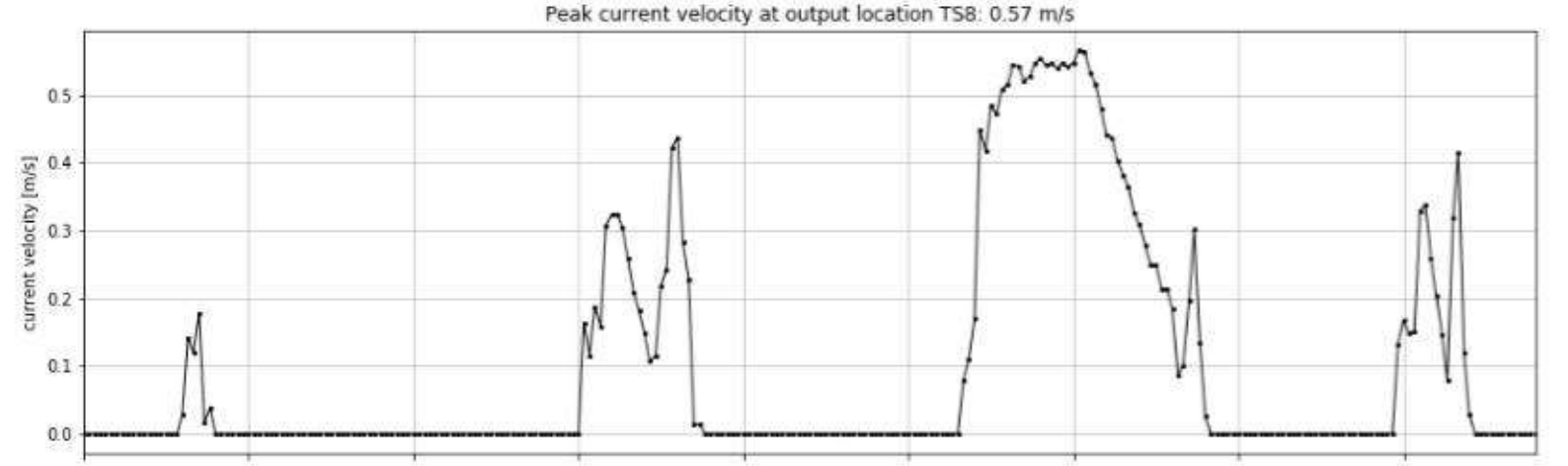
Peak current velocity at output location TS8: 0.57 m/s
current velocity [m/s]
0.5
0.4
0.3
0.2
0.1
0.0

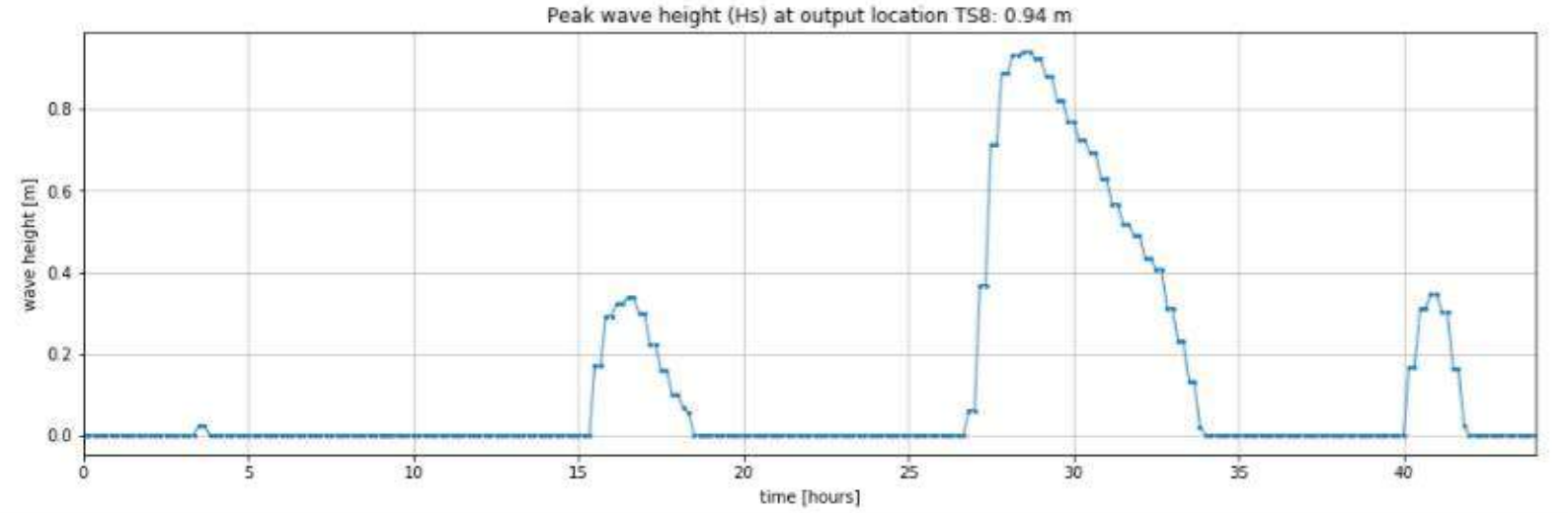
Peak wave height (Hs) at output location TS8: 0.94 m
wave height [m]
0.8
0.6
0.4
0.2
0.0
0
5
10
15
20
25
30
35
40
time [hours]

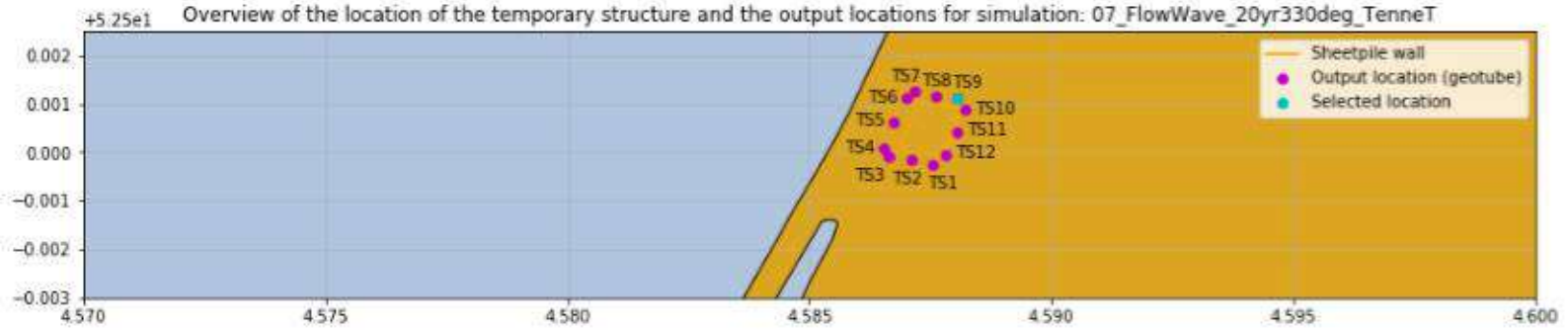
Overview of the location of the temporary structure and the output locations for simulation: 07_FlowWave_20yr330deg_TenneT
+5.25e1
Sheetpile wall
Output location (geotube)
Selected location
TS1
TS2
TS3
TS4
TS5
TS6
TS7
TS8
TS9
TS10
TS11
TS12
0.002
0.001
0.000
−0.001
−0.002
−0.003
4.570
4.575
4.580
4.585
4.590
4.595
4.600

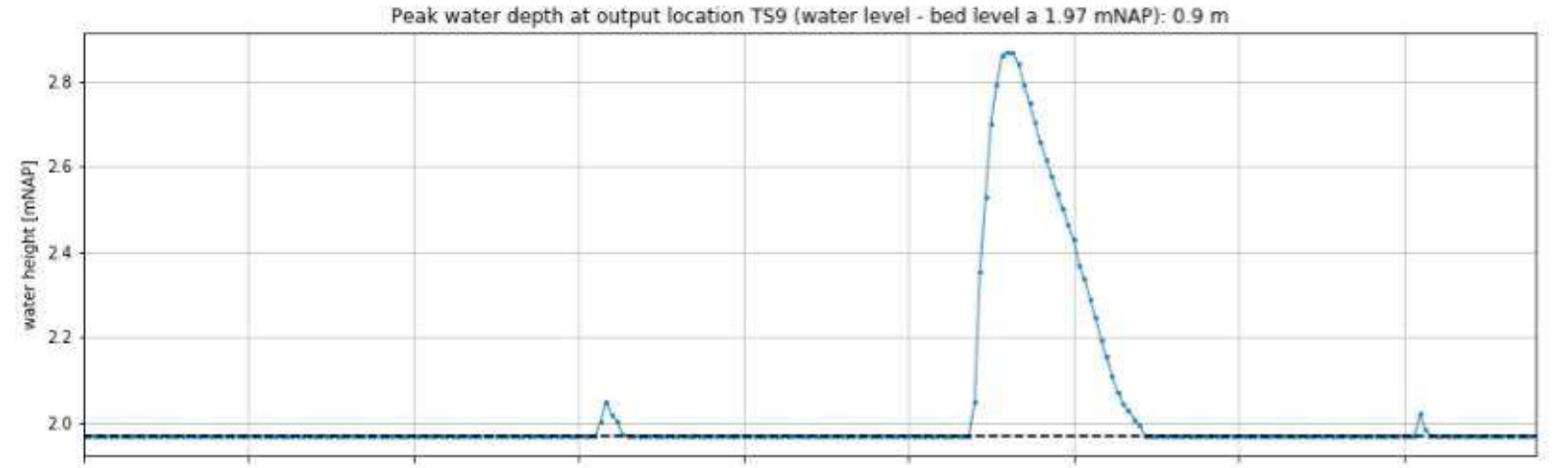
Peak water depth at output location TS9 (water level - bed level a 1.97 mNAP): 0.9 m
water height [mNAP]
2.8
2.6
2.4
2.2
2.0

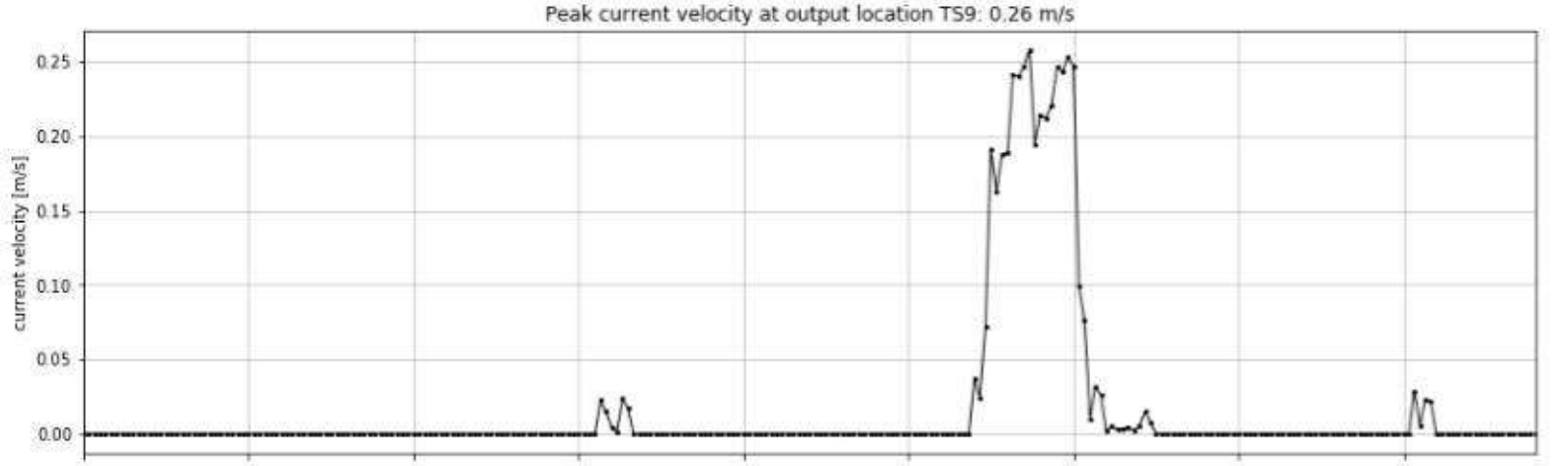
Peak current velocity at output location TS9: 0.26 m/s
current velocity [m/s]
0.25
0.20
0.15
0.10
0.05
0.00

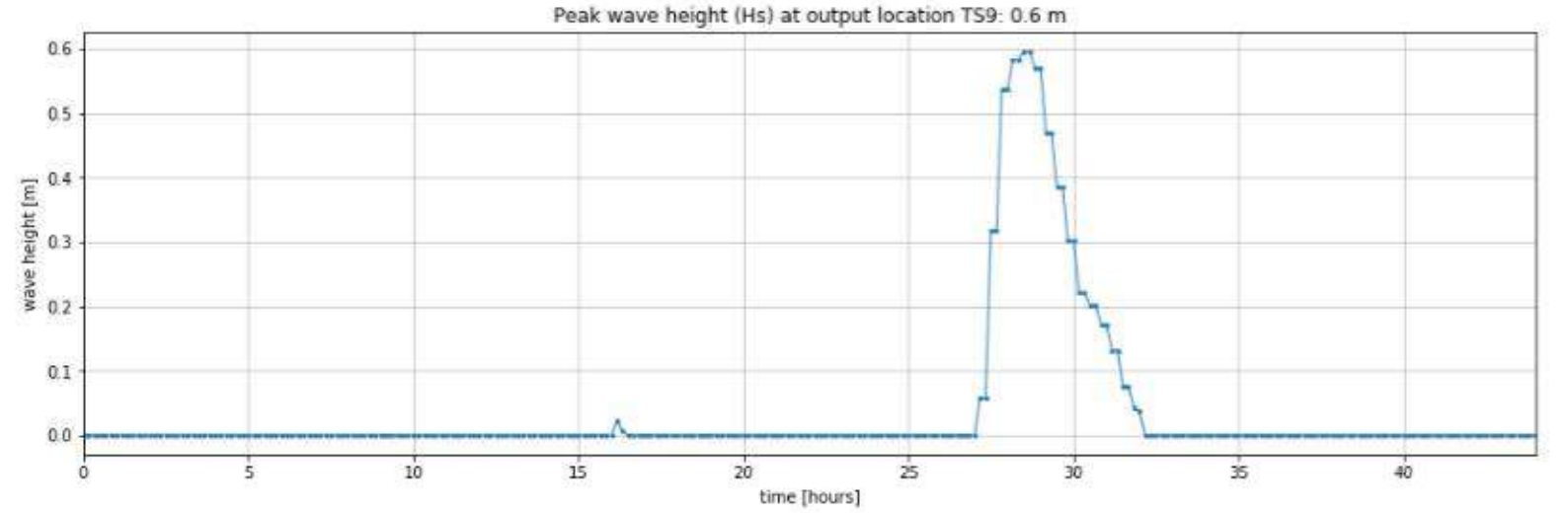
Peak wave height (Hs) at output location TS9: 0.6 m
wave height [m]
0.6
0.5
0.4
0.3
0.2
0.1
0.0
0
5
10
15
20
25
30
35
40
time [hours]

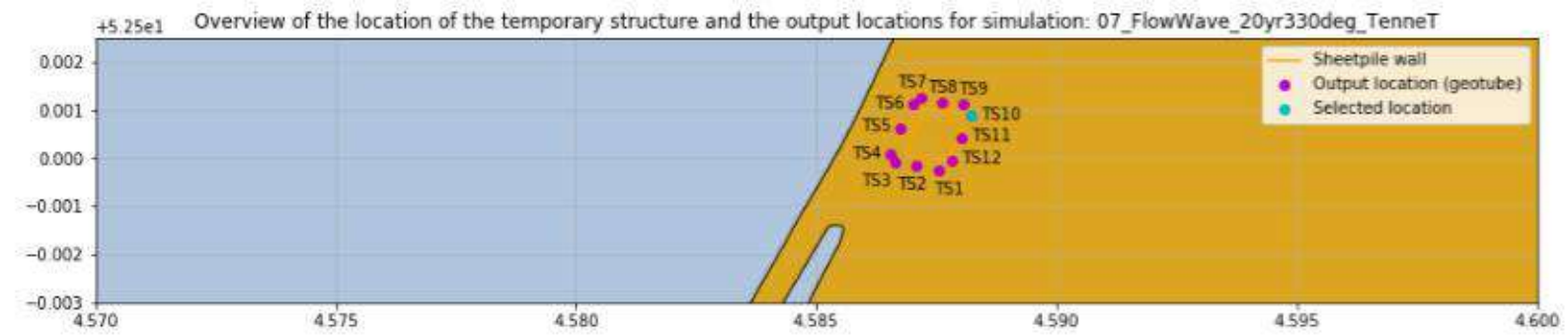
+5.25e1
Overview of the location of the temporary structure and the output locations for simulation: 07_FlowWave_20yr330deg_TenneT
Sheetpile wall
Output location (geotube)
Selected location
TS1
TS2
TS3
TS4
TS5
TS6
TS7
TS8
TS9
TS10
TS11
TS12
0.002
0.001
0.000
−0.001
−0.002
−0.003
4.570
4.575
4.580
4.585
4.590
4.595
4.600

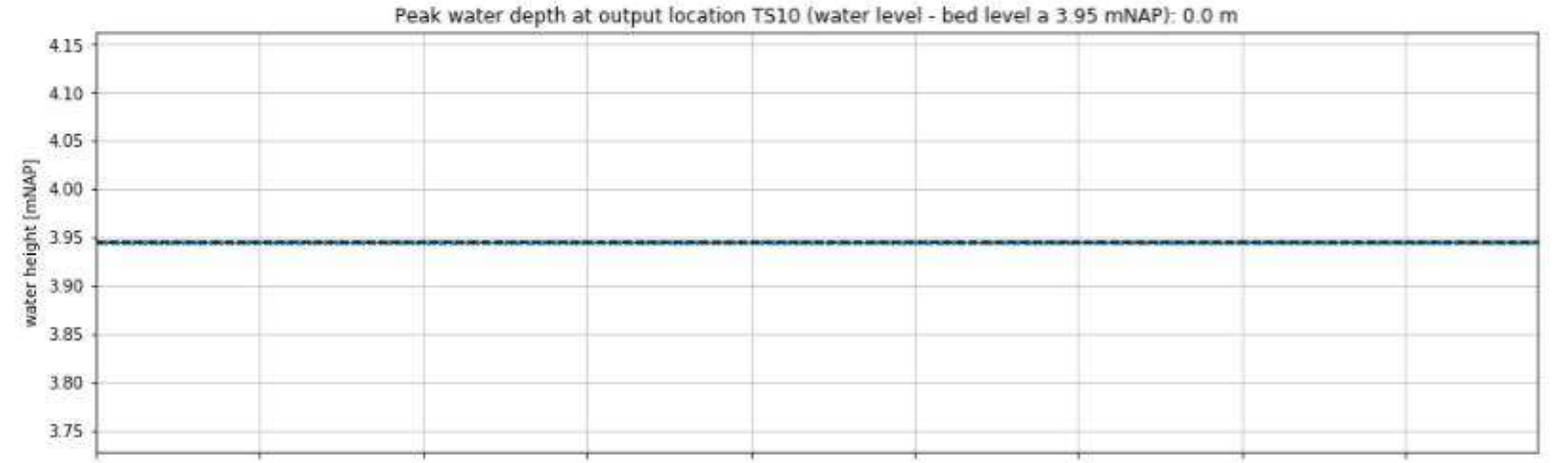
Peak water depth at output location TS10 (water level - bed level a 3.95 mNAP): 0.0 m
water height [mNAP]
4.15
4.10
4.05
4.00
3.95
3.90
3.85
3.80
3.75

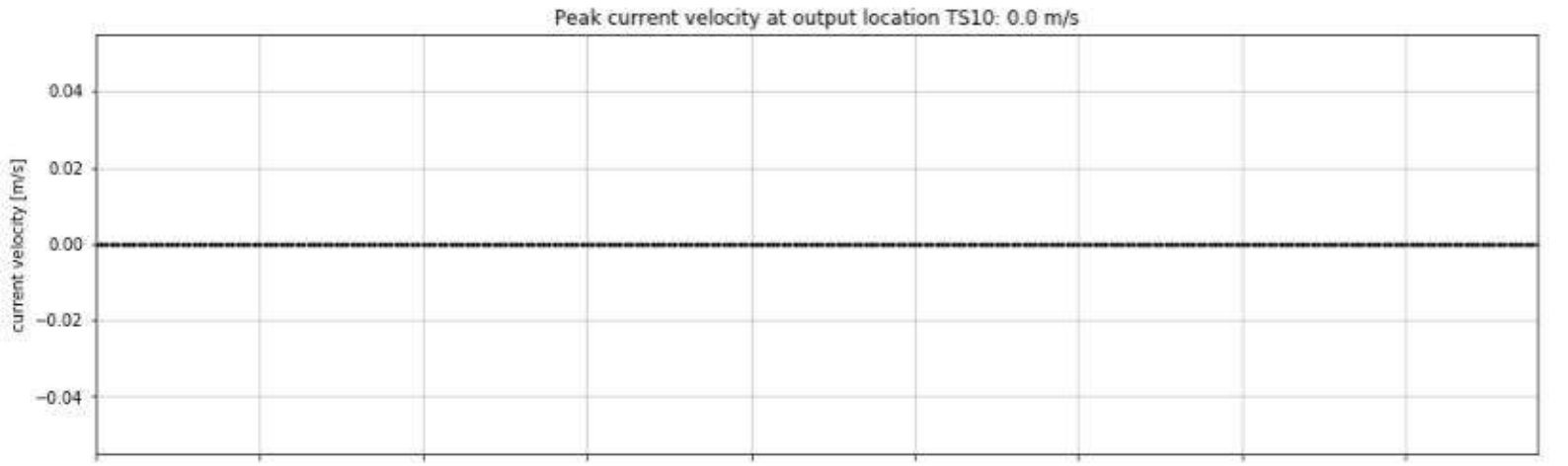
Peak current velocity at output location TS10: 0.0 m/s
current velocity [m/s]
0.04
0.02
0.00
−0.02
−0.04

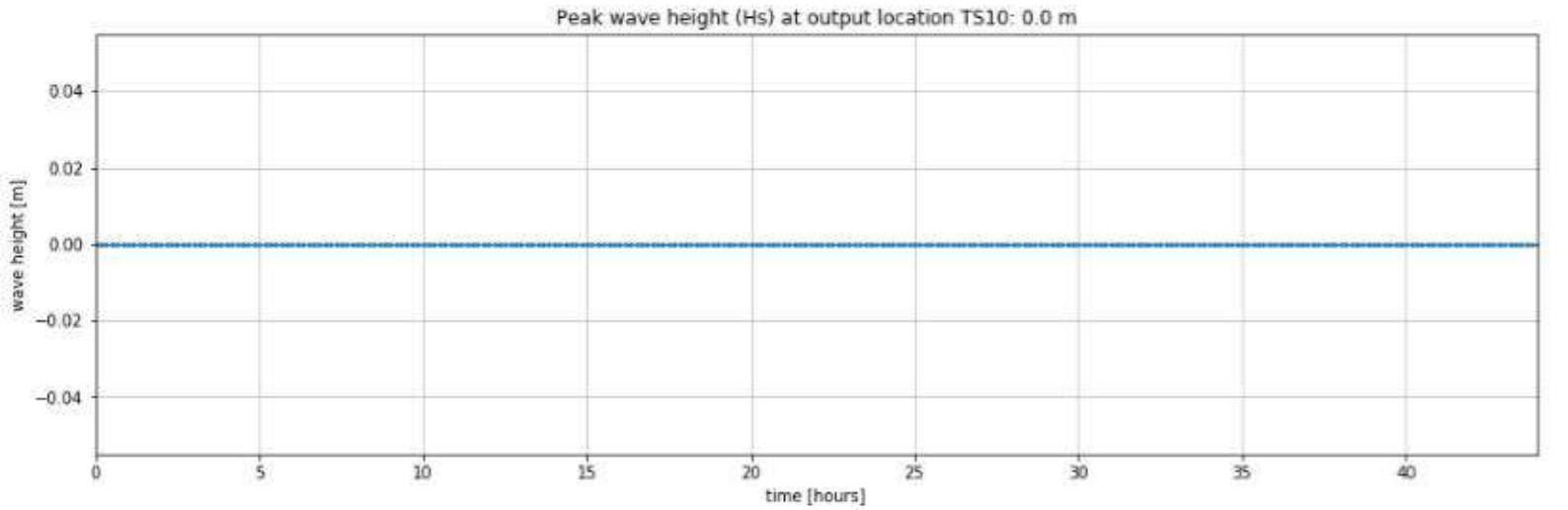
Peak wave height (Hs) at output location TS10: 0.0 m
wave height [m]
0.04
0.02
0.00
−0.02
−0.04
0
5
10
15
20
25
30
35
40
time [hours]

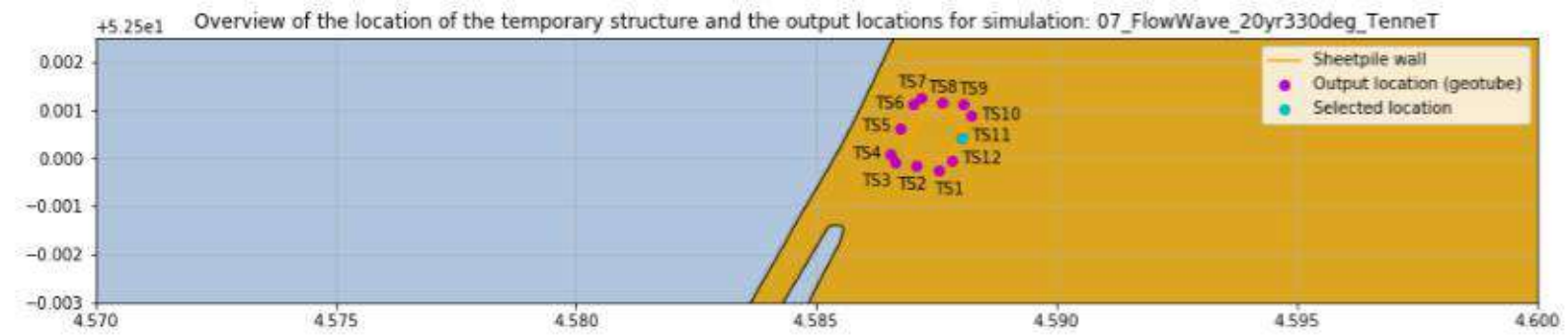
Overview of the location of the temporary structure and the output locations for simulation: 07_FlowWave_20yr330deg_TenneT
+5.25e1
Sheetpile wall
Output location (geotube)
Selected location
TS1
TS2
TS3
TS4
TS5
TS6
TS7
TS8
TS9
TS10
TS11
TS12
0.002
0.001
0.000
−0.001
−0.002
−0.003
4.570
4.575
4.580
4.585
4.590
4.595
4.600

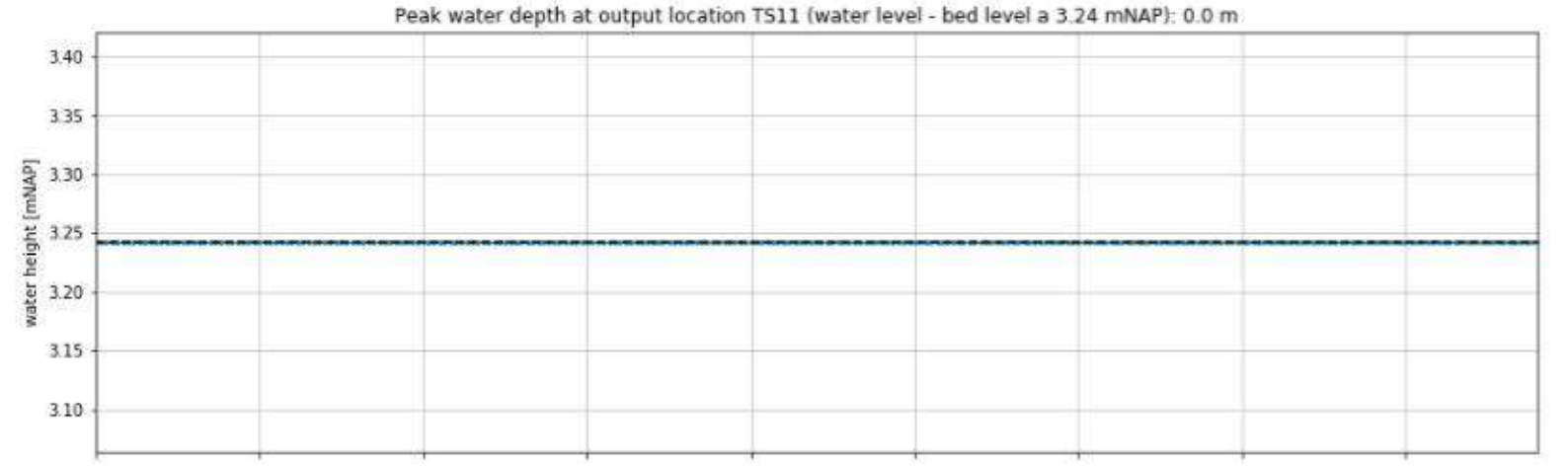
Peak water depth at output location TS11 (water level - bed level a 3.24 mNAP): 0.0 m
water height [mNAP]
3.40
3.35
3.30
3.25
3.20
3.15
3.10

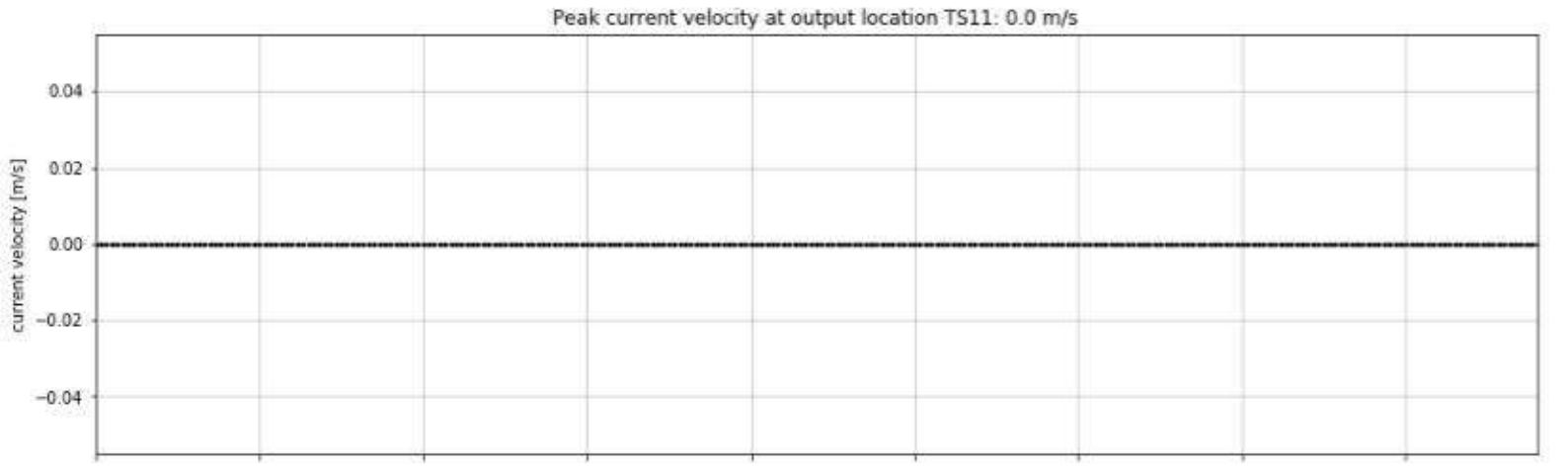
Peak current velocity at output location TS11: 0.0 m/s
current velocity [m/s]
0.04
0.02
0.00
−0.02
−0.04

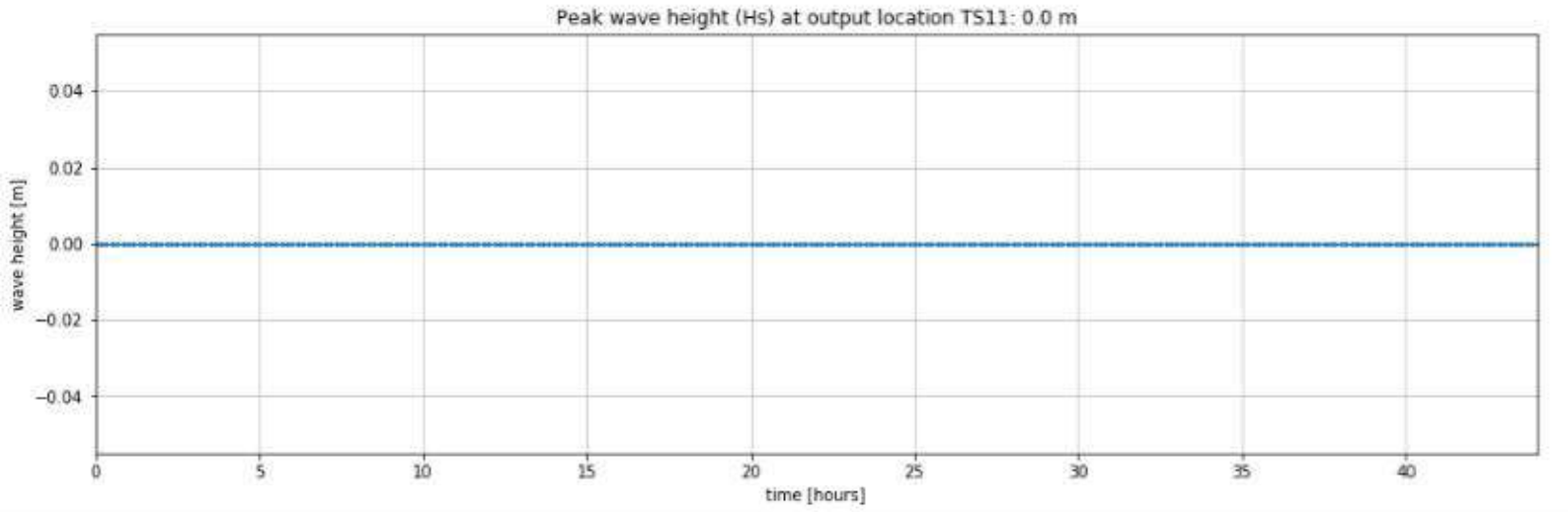
Peak wave height (Hs) at output location TS11: 0.0 m
wave height [m]
0.04
0.02
0.00
−0.02
−0.04
0
5
10
15
20
25
30
35
40
time [hours]

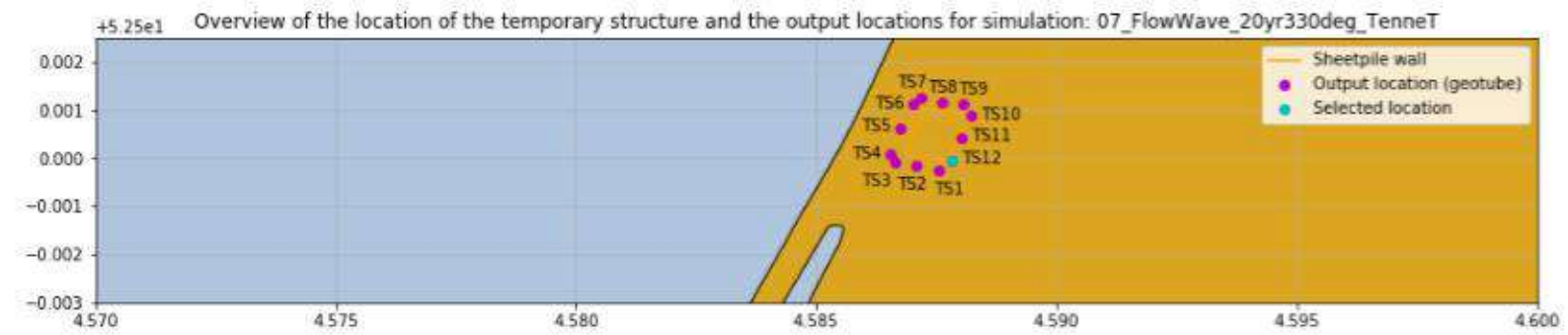
Overview of the location of the temporary structure and the output locations for simulation: 07_FlowWave_20yr330deg_TenneT
+5.25e1
Sheetpile wall
Output location (geotube)
Selected location
TS1
TS2
TS3
TS4
TS5
TS6
TS7
TS8
TS9
TS10
TS11
TS12
0.002
0.001
0.000
−0.001
−0.002
−0.003
4.570
4.575
4.580
4.585
4.590
4.595
4.600

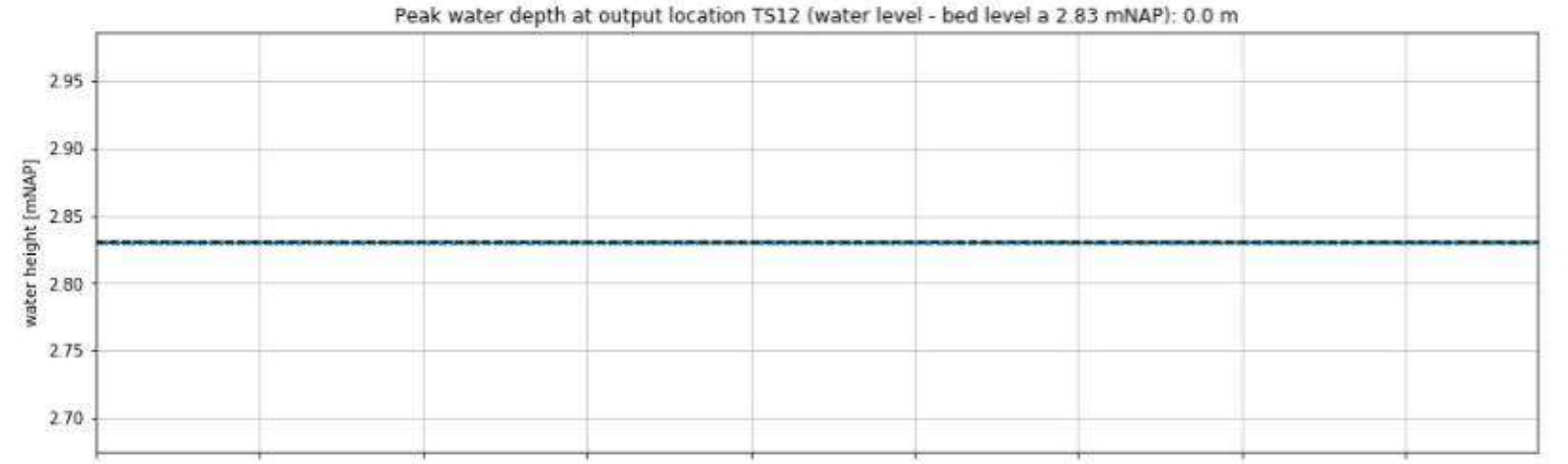
Peak water depth at output location TS12 (water level - bed level a 2.83 mNAP): 0.0 m
water height [mNAP]
2.95
2.90
2.85
2.80
2.75
2.70

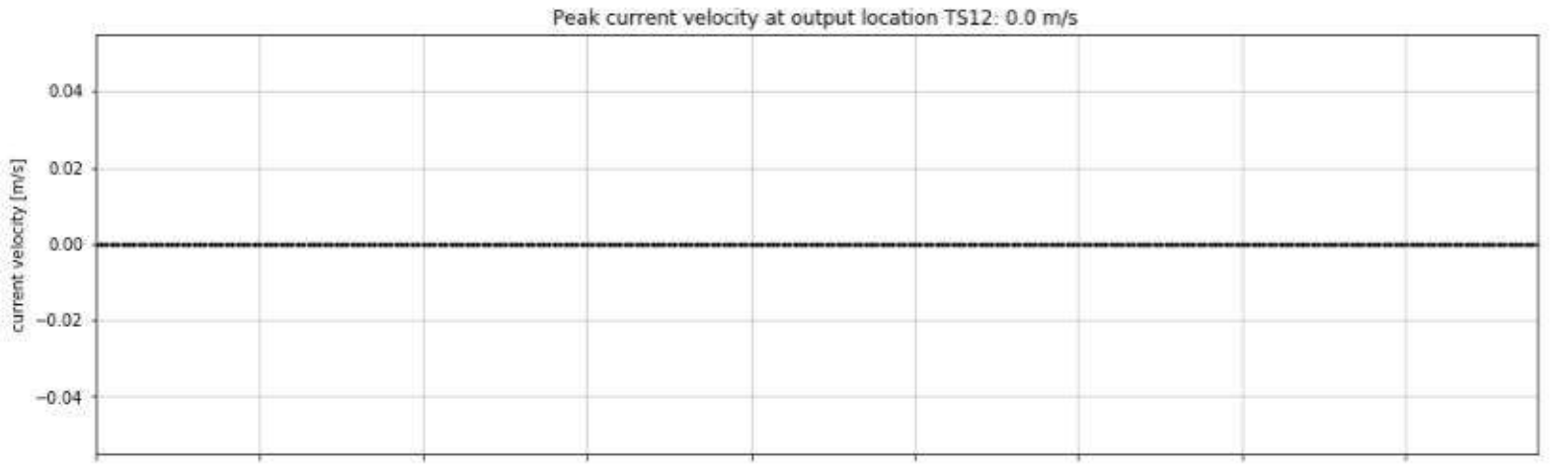
Peak current velocity at output location TS12: 0.0 m/s
current velocity [m/s]
0.04
0.02
0.00
−0.02
−0.04

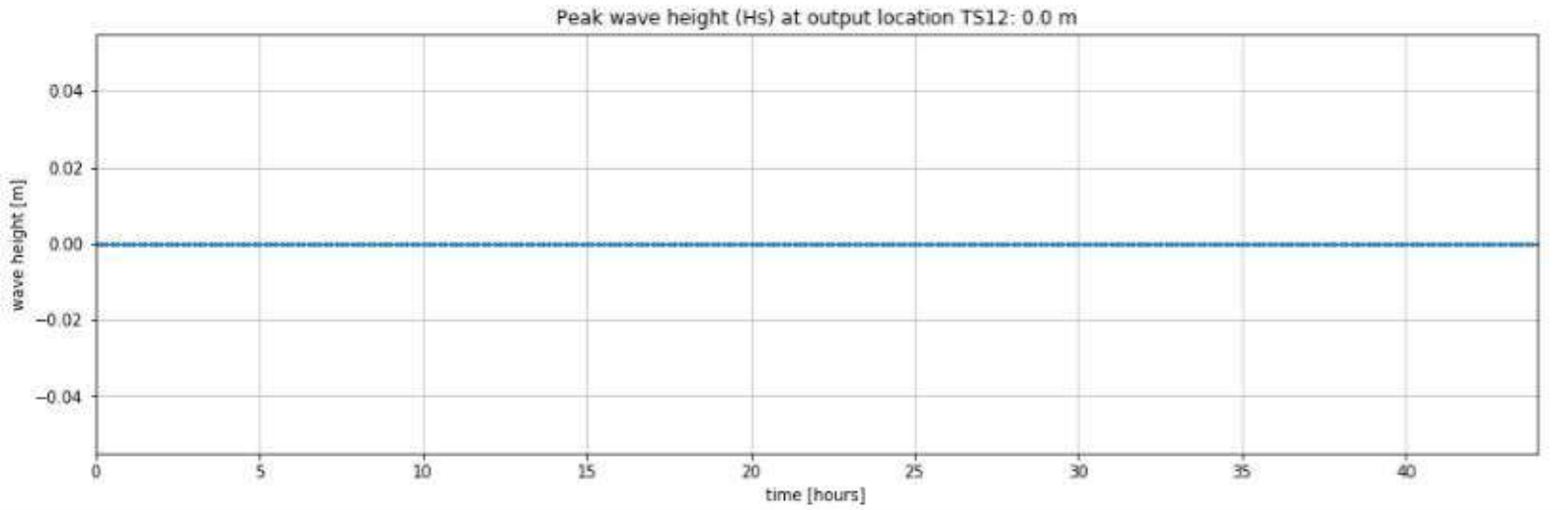
Peak wave height (Hs) at output location TS12: 0.0 m
wave height [m]
0.04
0.02
0.00
−0.02
−0.04
0
5
10
15
20
25
30
35
40
time [hours]

C.6 Flow-Wave 20 yr storm 330 degrees – Vaklodingen bathymetry

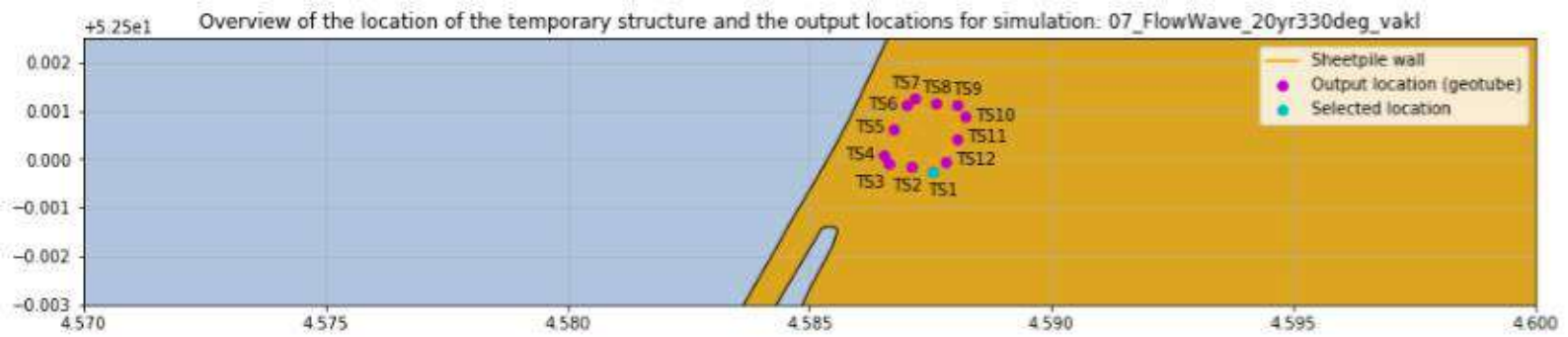
Overview of the location of the temporary structure and the output locations for simulation: 07_FlowWave_20yr330deg_vakl
+5.25e1
Sheetpile wall
Output location (geotube)
Selected location
TS1
TS2
TS3
TS4
TS5
TS6
TS7
TS8
TS9
TS10
TS11
TS12
0.002
0.001
0.000
−0.001
−0.002
−0.003
4.570
4.575
4.580
4.585
4.590
4.595
4.600

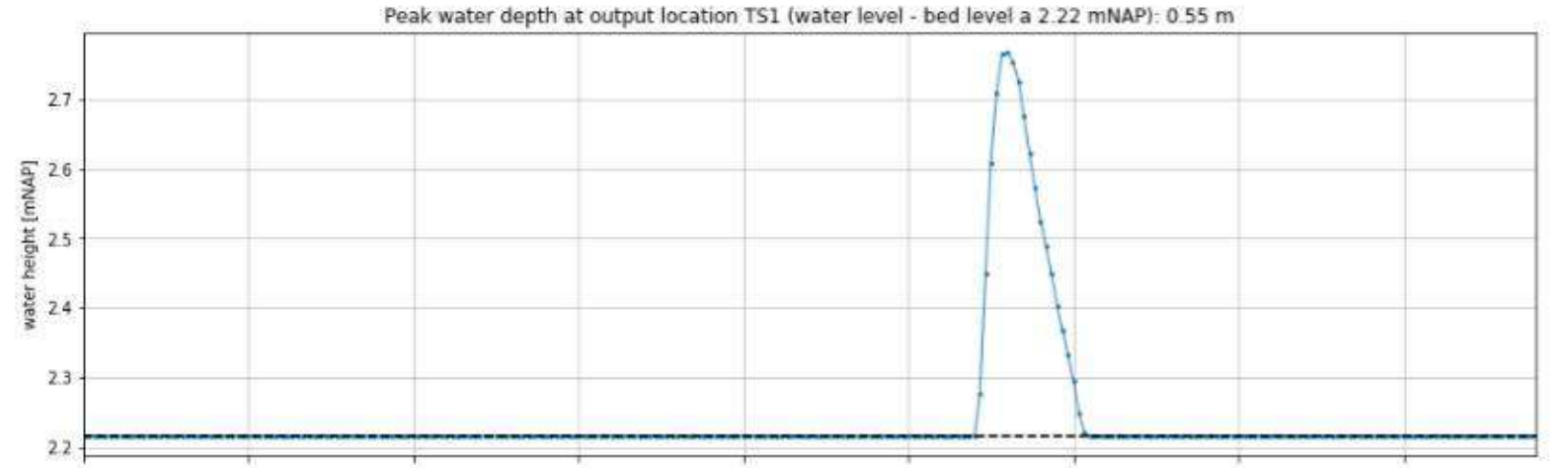
Peak water depth at output location TS1 (water level - bed level a 2.22 mNAP): 0.55 m
water height [mNAP]
2.7
2.6
2.5
2.4
2.3
2.2

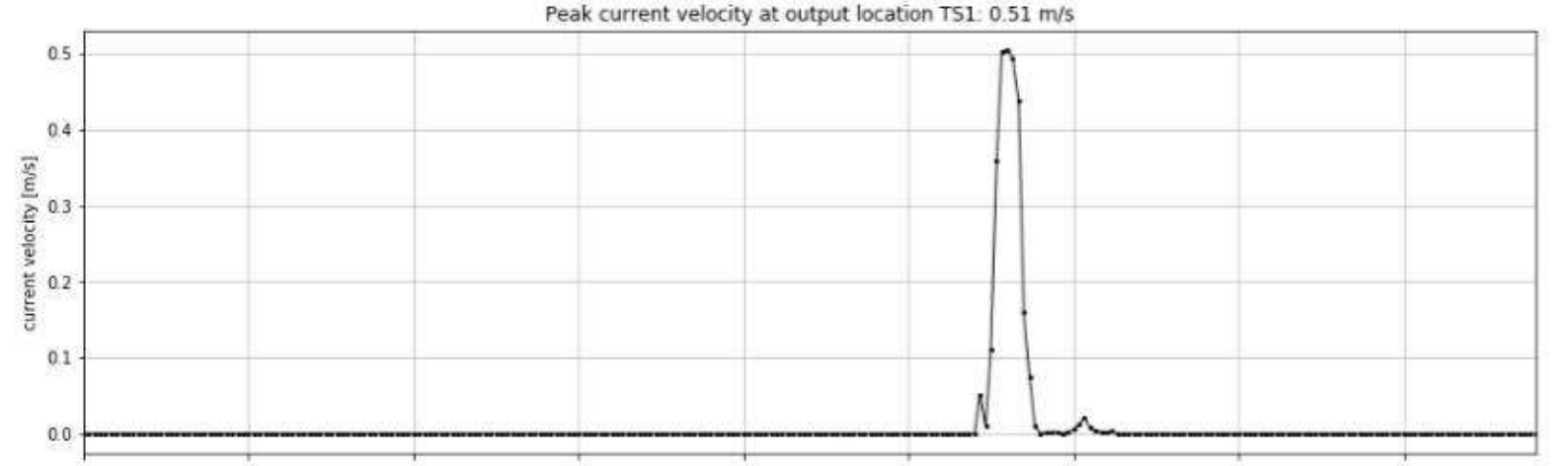
Peak current velocity at output location TS1: 0.51 m/s
current velocity [m/s]
0.5
0.4
0.3
0.2
0.1
0.0

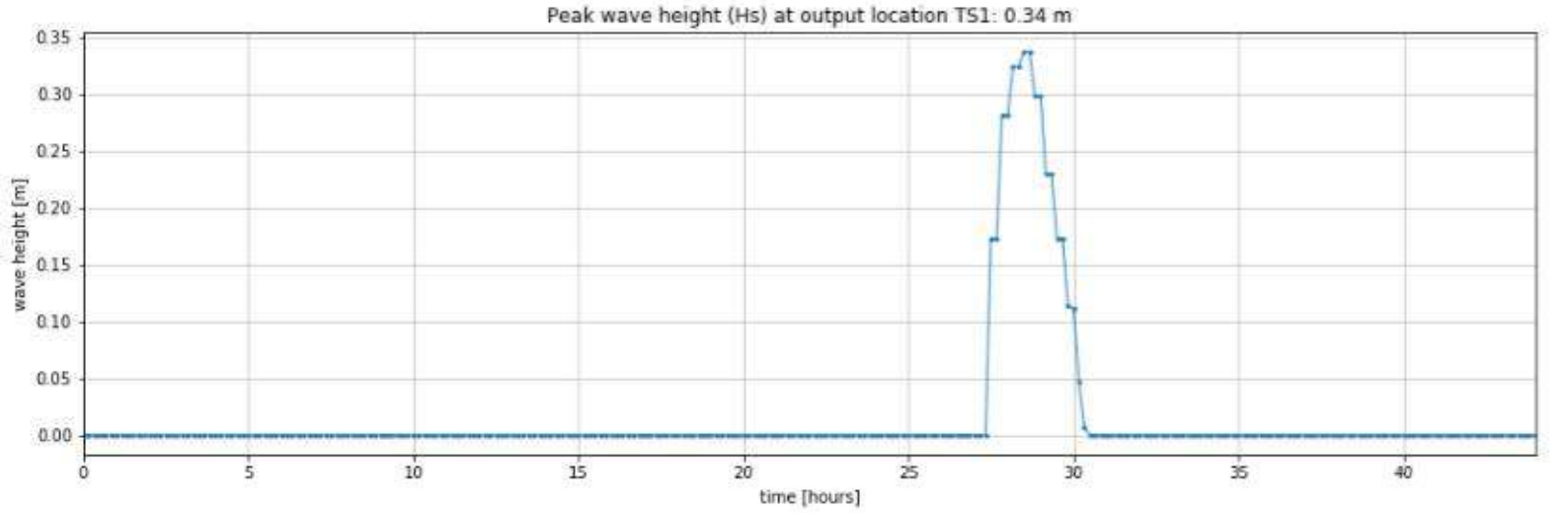
Peak wave height (Hs) at output location TS1: 0.34 m
wave height [m]
0.35
0.30
0.25
0.20
0.15
0.10
0.05
0.00
0
5
10
15
20
25
30
35
40
time [hours]

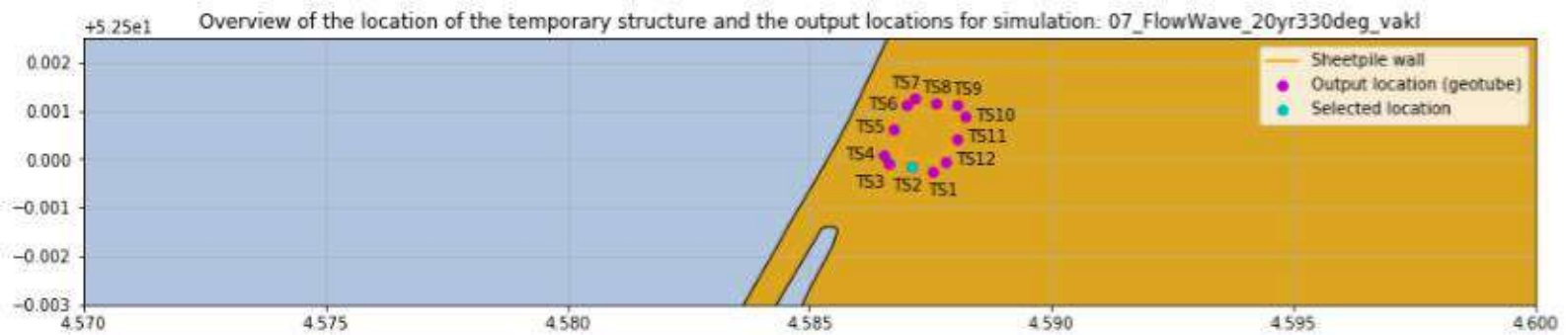
Overview of the location of the temporary structure and the output locations for simulation: 07_FlowWave_20yr330deg_vakl
+5.25e1
Sheetpile wall
Output location (geotube)
Selected location
TS1
TS2
TS3
TS4
TS5
TS6
TS7
TS8
TS9
TS10
TS11
TS12
0.002
0.001
0.000
−0.001
−0.002
−0.003
4.570
4.575
4.580
4.585
4.590
4.595
4.600

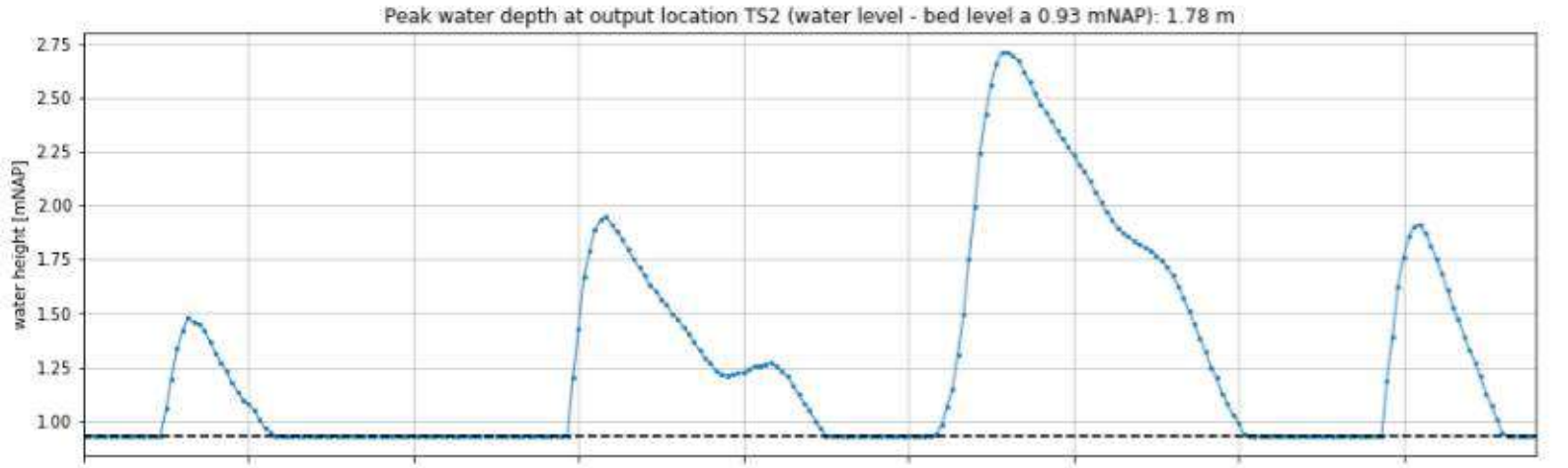
Peak water depth at output location TS2 (water level - bed level a 0.93 mNAP): 1.78 m
water height [mNAP]
2.75
2.50
2.25
2.00
1.75
1.50
1.25
1.00

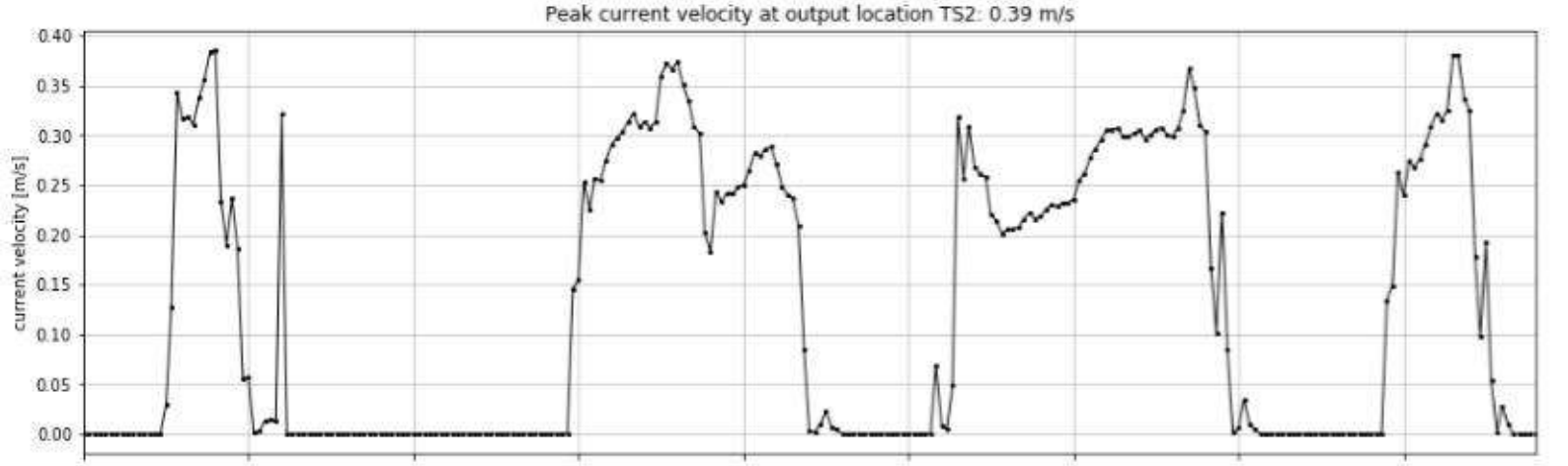
Peak current velocity at output location TS2: 0.39 m/s
current velocity [m/s]
0.40
0.35
0.30
0.25
0.20
0.15
0.10
0.05
0.00

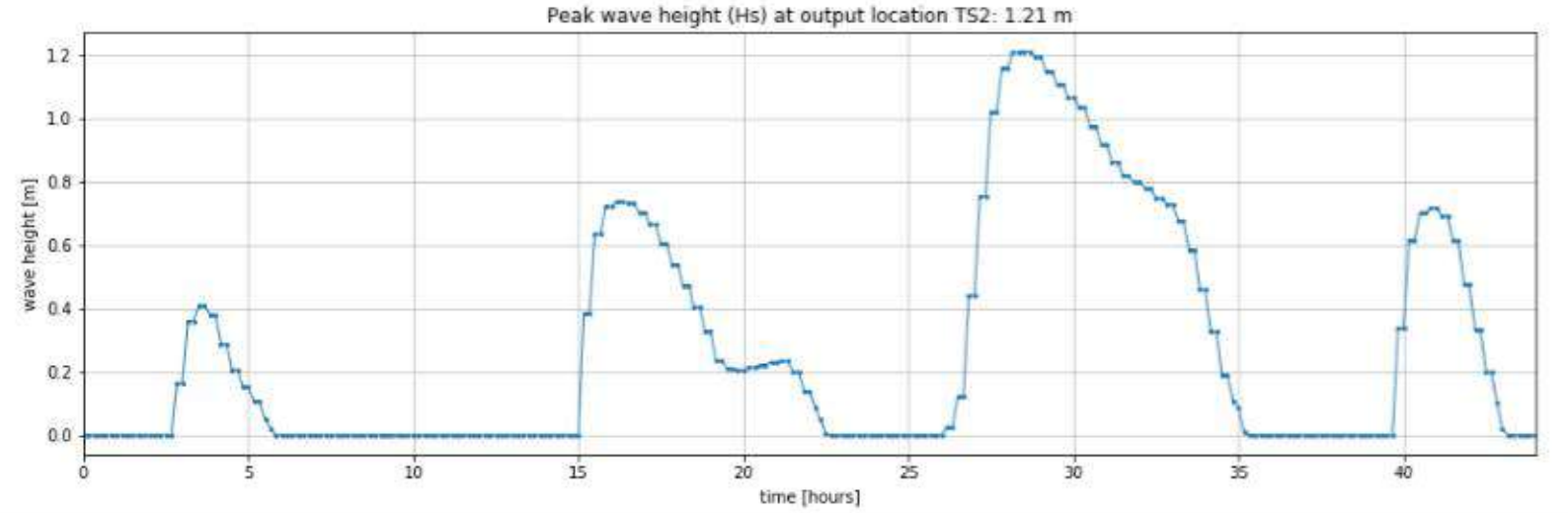
Peak wave height (Hs) at output location TS2: 1.21 m
wave height [m]
1.2
1.0
0.8
0.6
0.4
0.2
0.0
0
5
10
15
20
25
30
35
40
time [hours]

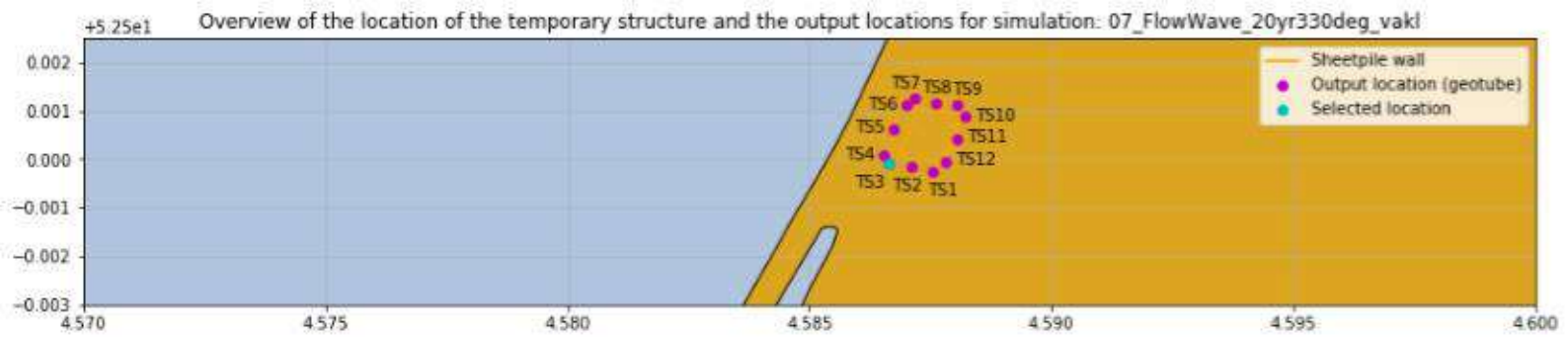
Overview of the location of the temporary structure and the output locations for simulation: 07_FlowWave_20yr330deg_vakl
+5.25e1
Sheetpile wall
Output location (geotube)
Selected location
TS1
TS2
TS3
TS4
TS5
TS6
TS7
TS8
TS9
TS10
TS11
TS12
0.002
0.001
0.000
−0.001
−0.002
−0.003
4.570
4.575
4.580
4.585
4.590
4.595
4.600

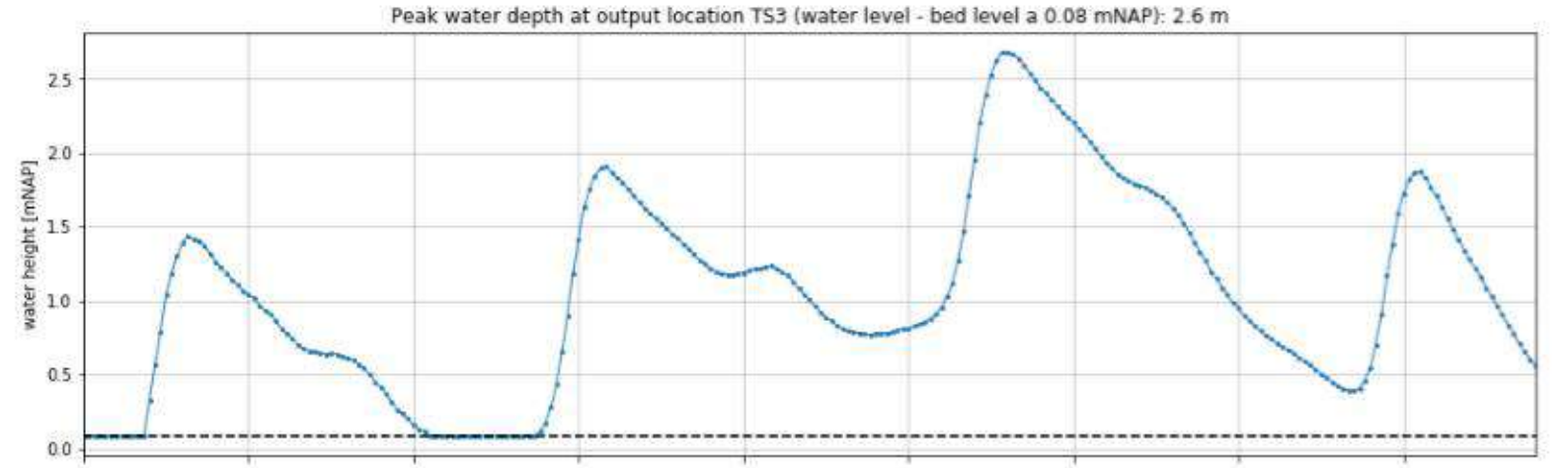
Peak water depth at output location TS3 (water level - bed level a 0.08 mNAP): 2.6 m
water height [mNAP]
0.0
0.5
1.0
1.5
2.0
2.5

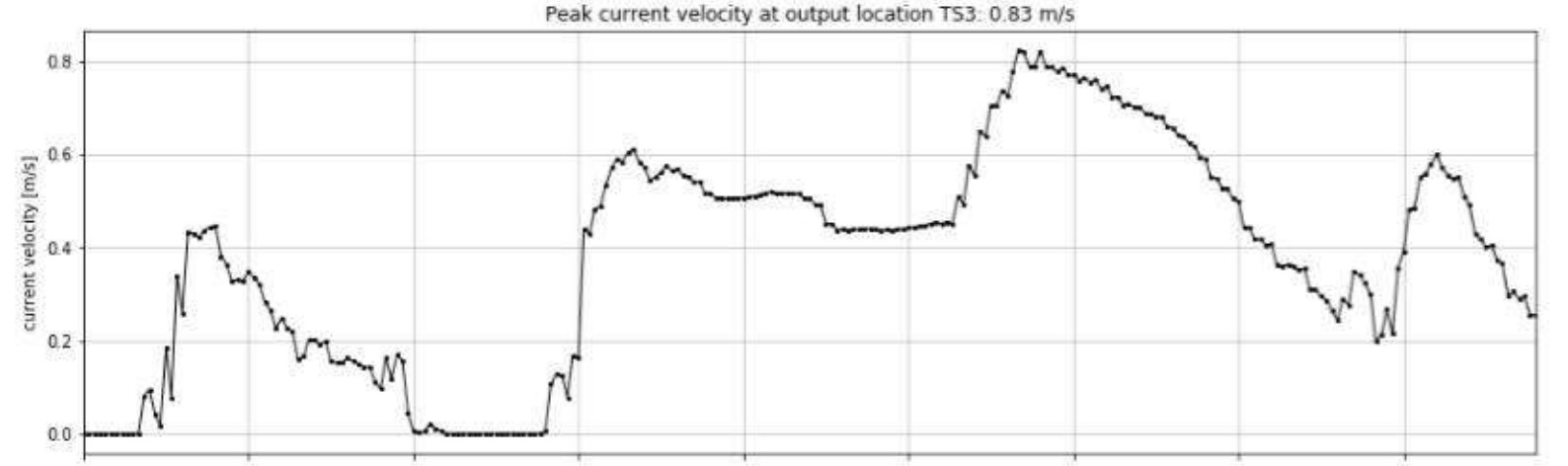
Peak current velocity at output location TS3: 0.83 m/s
current velocity [m/s]
0.0
0.2
0.4
0.6
0.8

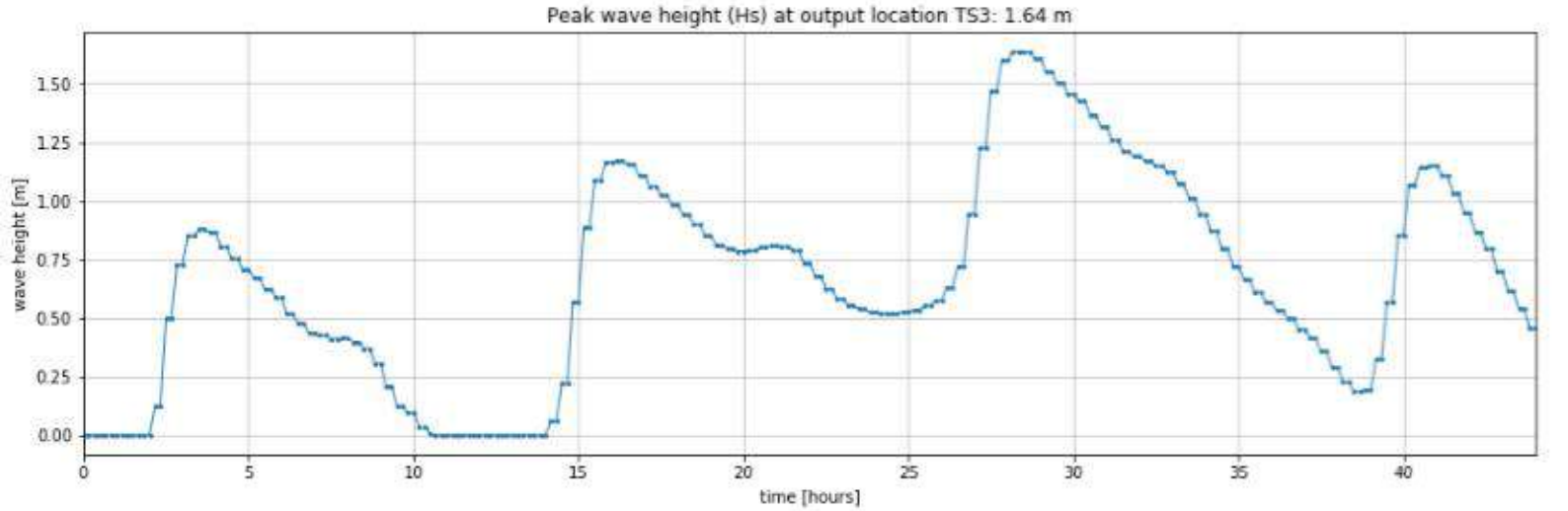
Peak wave height (Hs) at output location TS3: 1.64 m
wave height [m]
0.00
0.25
0.50
0.75
1.00
1.25
1.50
0
5
10
15
20
25
30
35
40
time [hours]

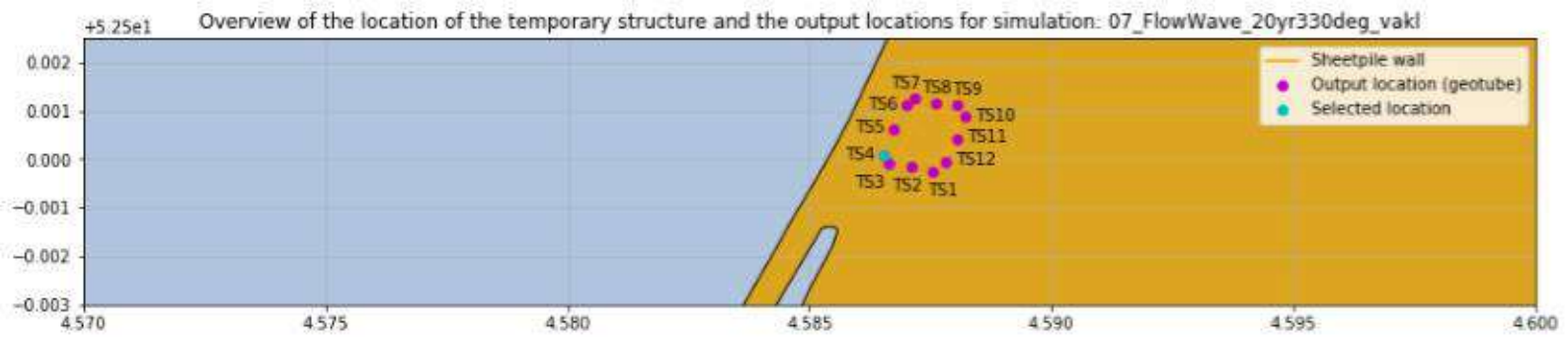
Overview of the location of the temporary structure and the output locations for simulation: 07_FlowWave_20yr330deg_vakl
+5.25e1
Sheetpile wall
Output location (geotube)
Selected location
TS1
TS2
TS3
TS4
TS5
TS6
TS7
TS8
TS9
TS10
TS11
TS12
0.002
0.001
0.000
−0.001
−0.002
−0.003
4.570
4.575
4.580
4.585
4.590
4.595
4.600

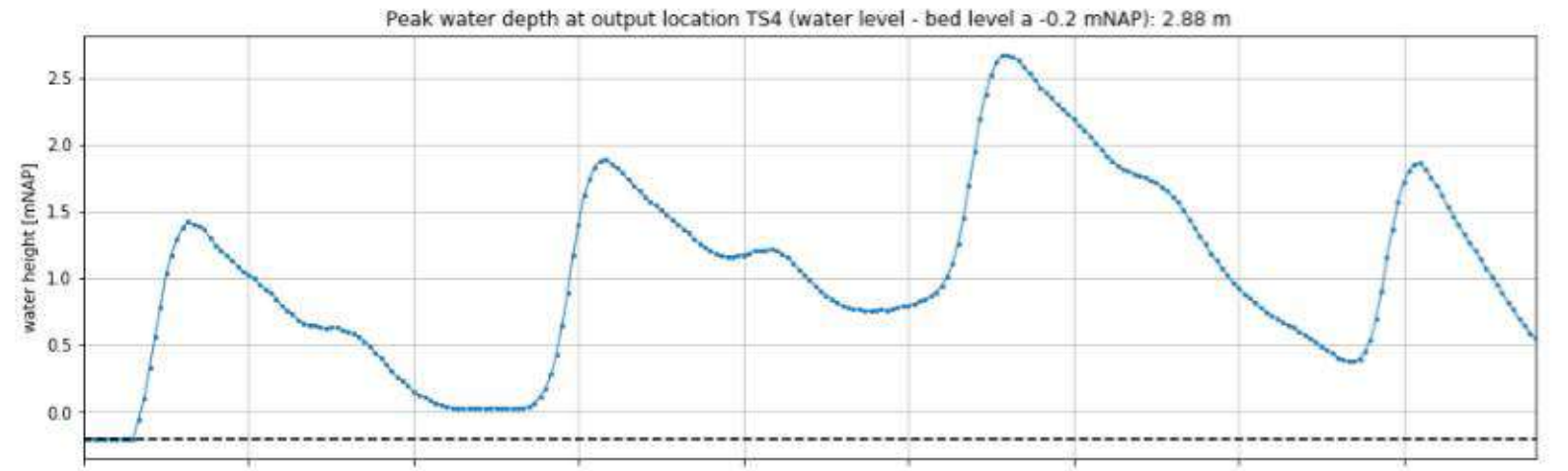
Peak water depth at output location TS4 (water level - bed level a -0.2 mNAP): 2.88 m
water height [mNAP]
2.5
2.0
1.5
1.0
0.5
0.0

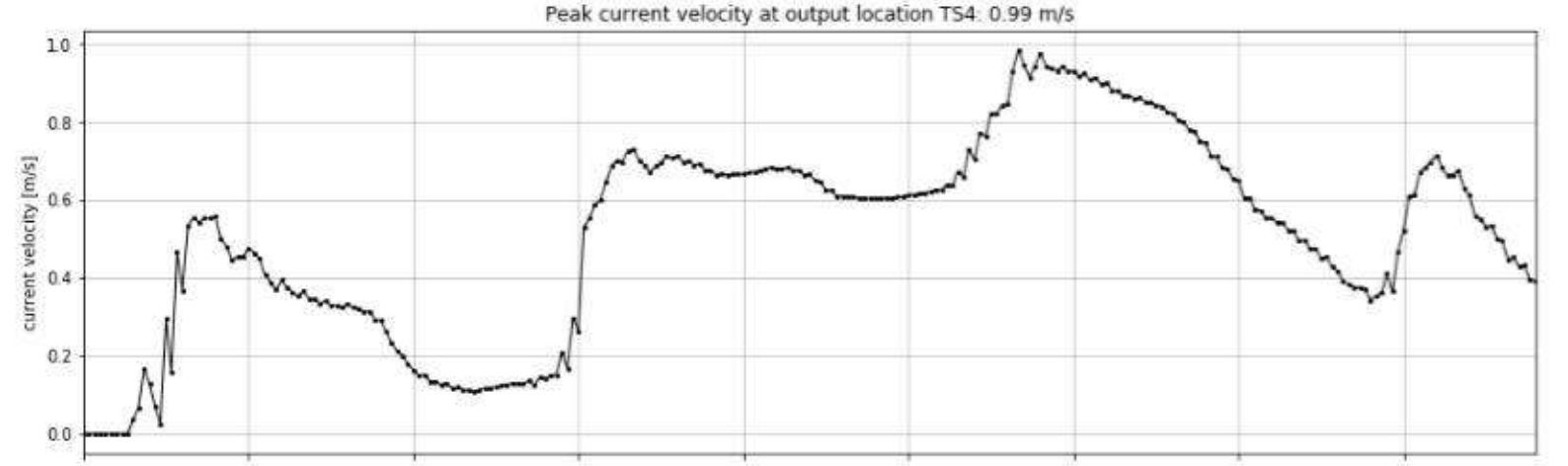
Peak current velocity at output location TS4: 0.99 m/s
current velocity [m/s]
1.0
0.8
0.6
0.4
0.2
0.0

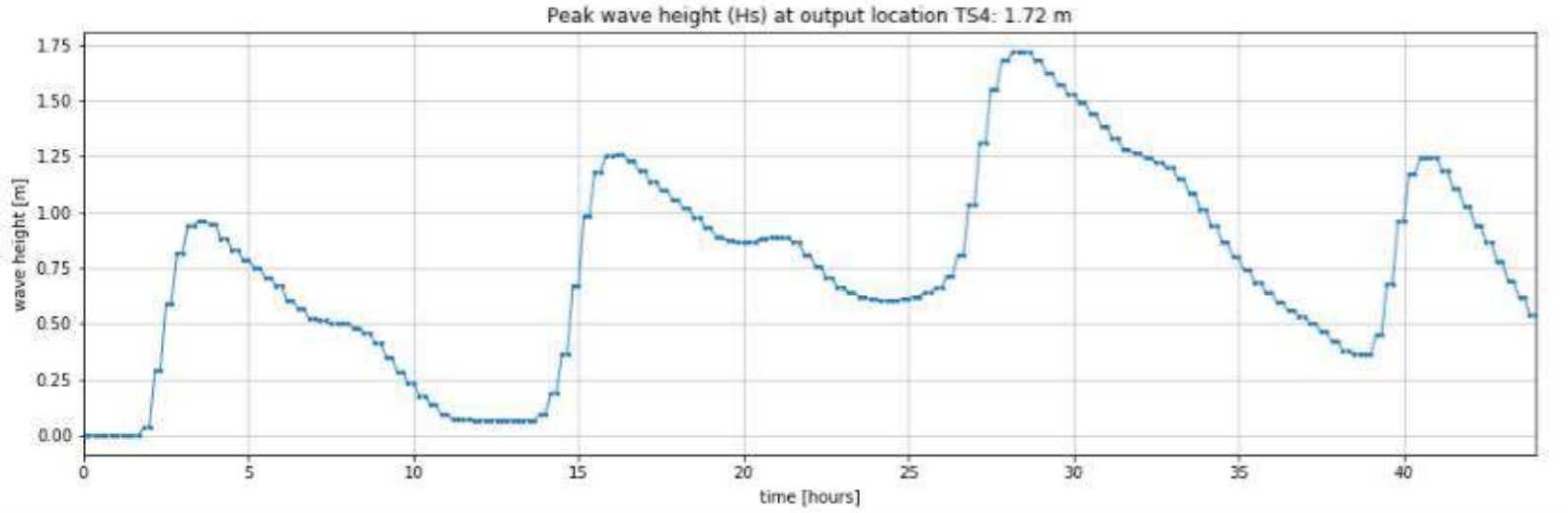
Peak wave height (Hs) at output location TS4: 1.72 m
wave height [m]
1.75
1.50
1.25
1.00
0.75
0.50
0.25
0.00
0
5
10
15
20
25
30
35
40
time [hours]

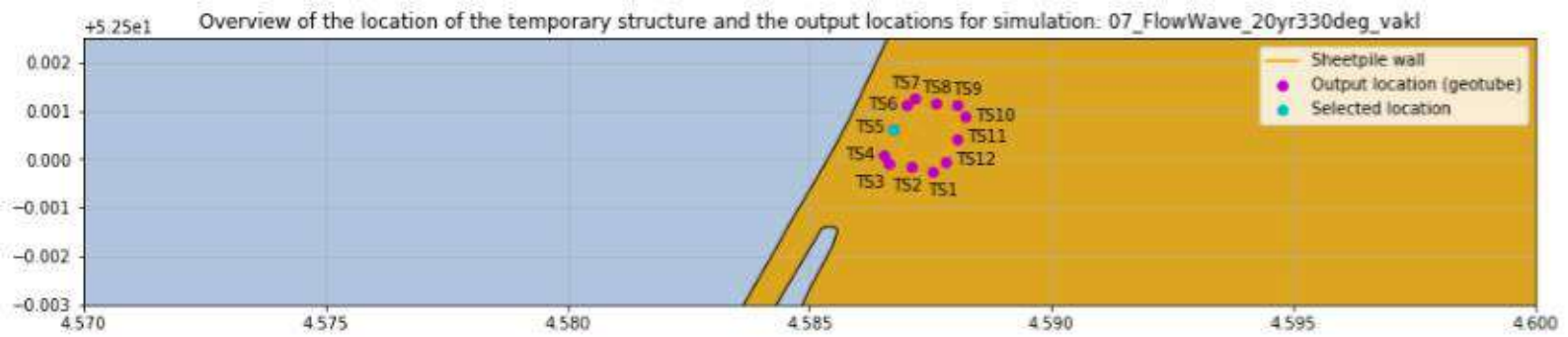
Overview of the location of the temporary structure and the output locations for simulation: 07_FlowWave_20yr330deg_vakl
+5.25e1
Sheetpile wall
Output location (geotube)
Selected location
TS1
TS2
TS3
TS4
TS5
TS6
TS7
TS8
TS9
TS10
TS11
TS12
0.002
0.001
0.000
−0.001
−0.002
−0.003
4.570
4.575
4.580
4.585
4.590
4.595
4.600

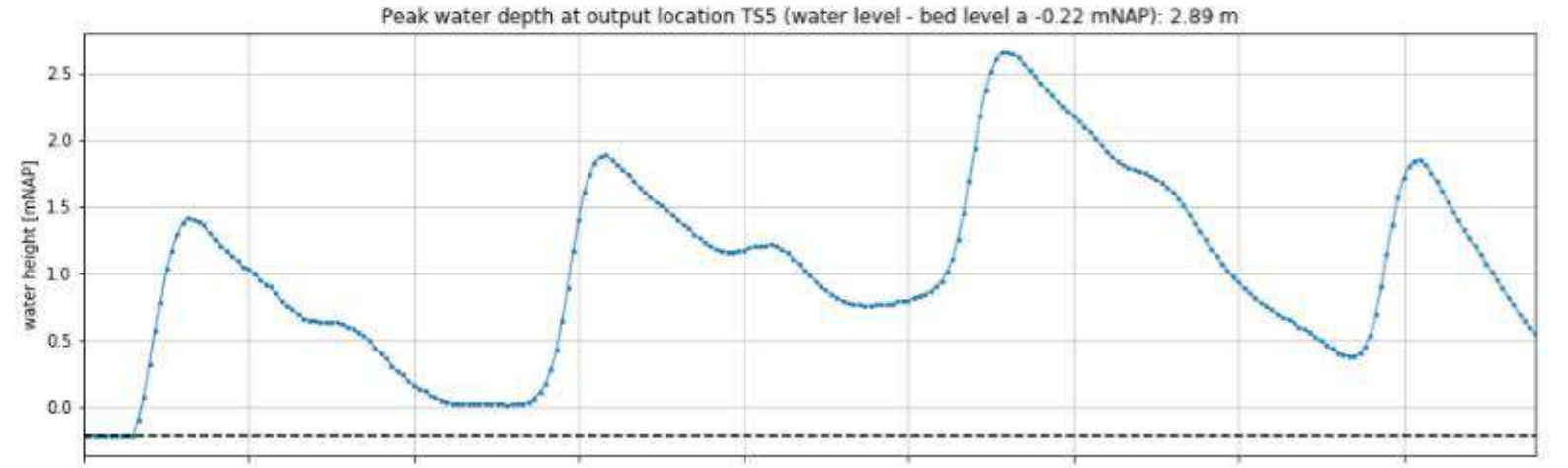
Peak water depth at output location TS5 (water level - bed level a -0.22 mNAP): 2.89 m
water height [mNAP]
2.5
2.0
1.5
1.0
0.5
0.0

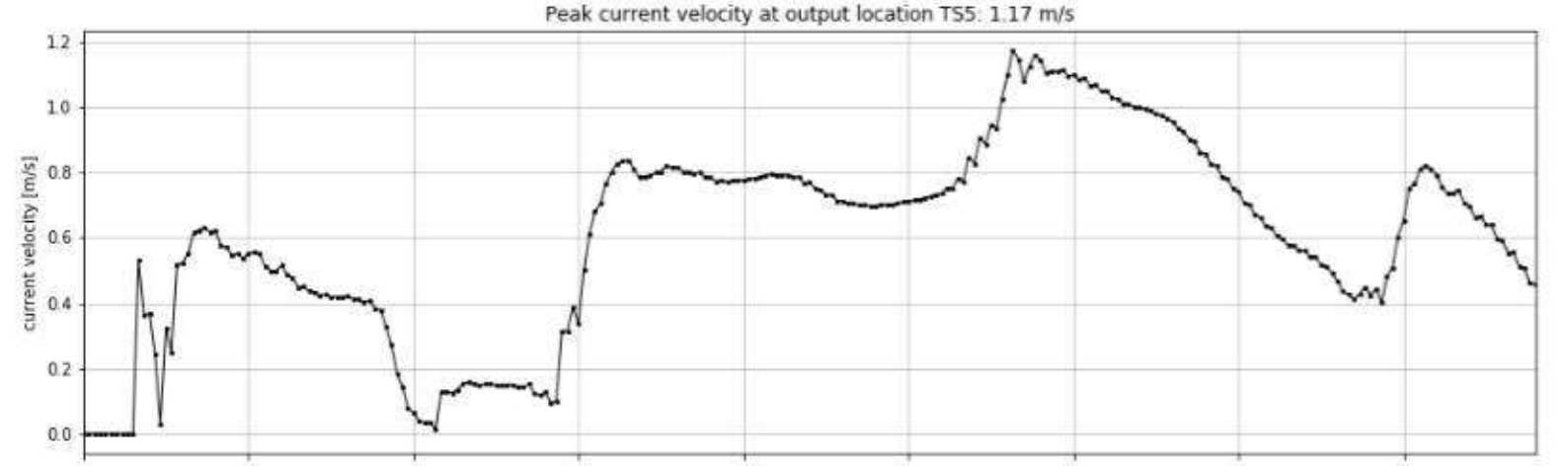
Peak current velocity at output location TS5: 1.17 m/s
current velocity [m/s]
1.2
1.0
0.8
0.6
0.4
0.2
0.0

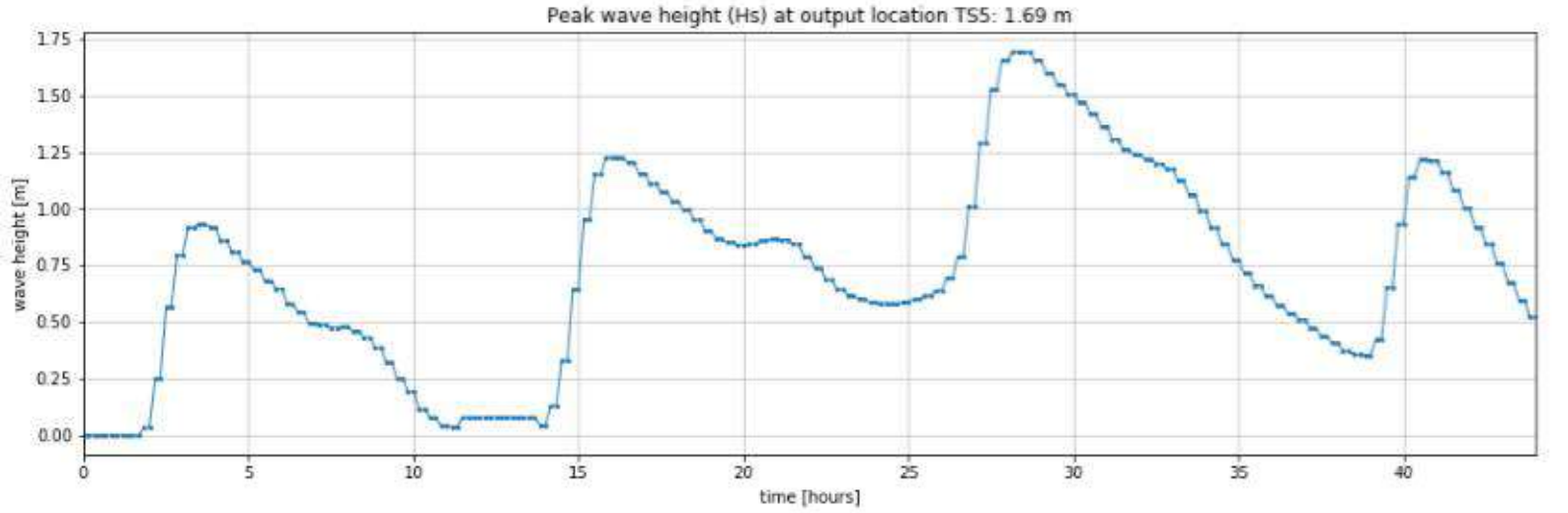
Peak wave height (Hs) at output location TS5: 1.69 m
wave height [m]
1.75
1.50
1.25
1.00
0.75
0.50
0.25
0.00
0
5
10
15
20
25
30
35
40
time [hours]

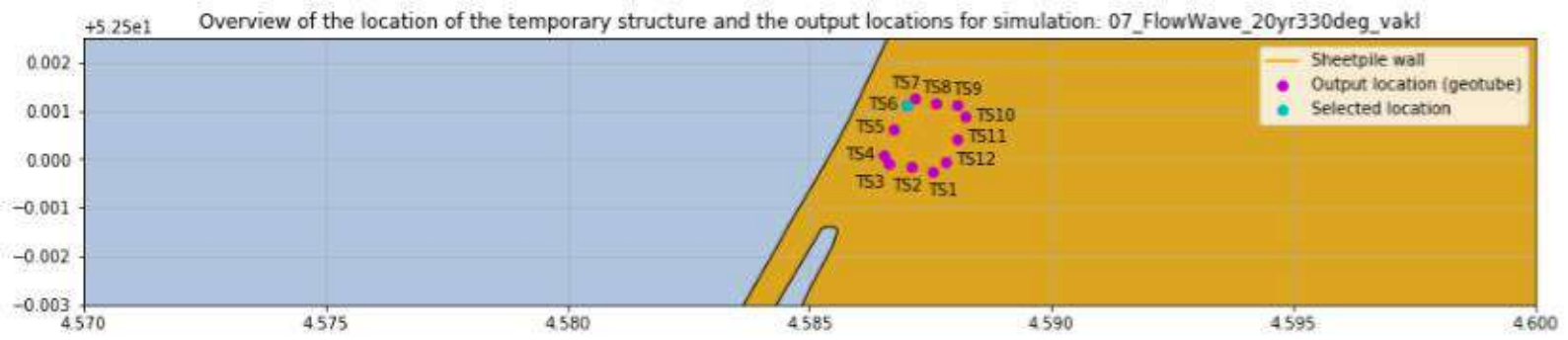
Overview of the location of the temporary structure and the output locations for simulation: 07_FlowWave_20yr330deg_vakl
+5.25e1
Sheetpile wall
Output location (geotube)
Selected location
TS1
TS2
TS3
TS4
TS5
TS6
TS7
TS8
TS9
TS10
TS11
TS12
0.002
0.001
0.000
−0.001
−0.002
−0.003
4.570
4.575
4.580
4.585
4.590
4.595
4.600

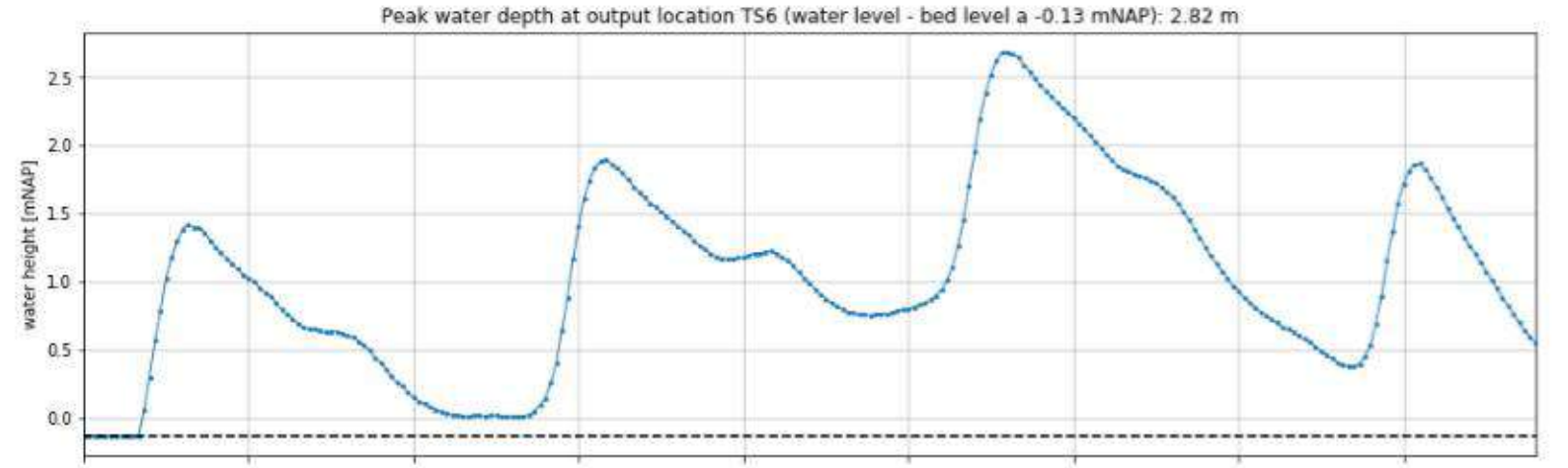
Peak water depth at output location TS6 (water level - bed level a -0.13 mNAP): 2.82 m
water height [mNAP]
2.5
2.0
1.5
1.0
0.5
0.0

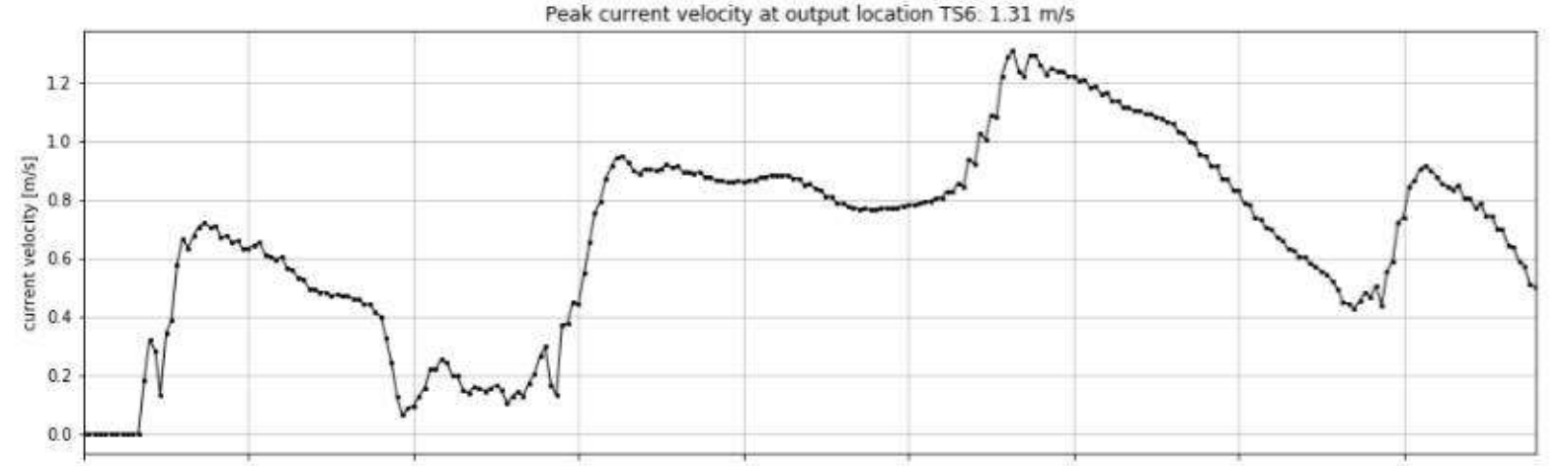
Peak current velocity at output location TS6: 1.31 m/s
current velocity [m/s]
1.2
1.0
0.8
0.6
0.4
0.2
0.0

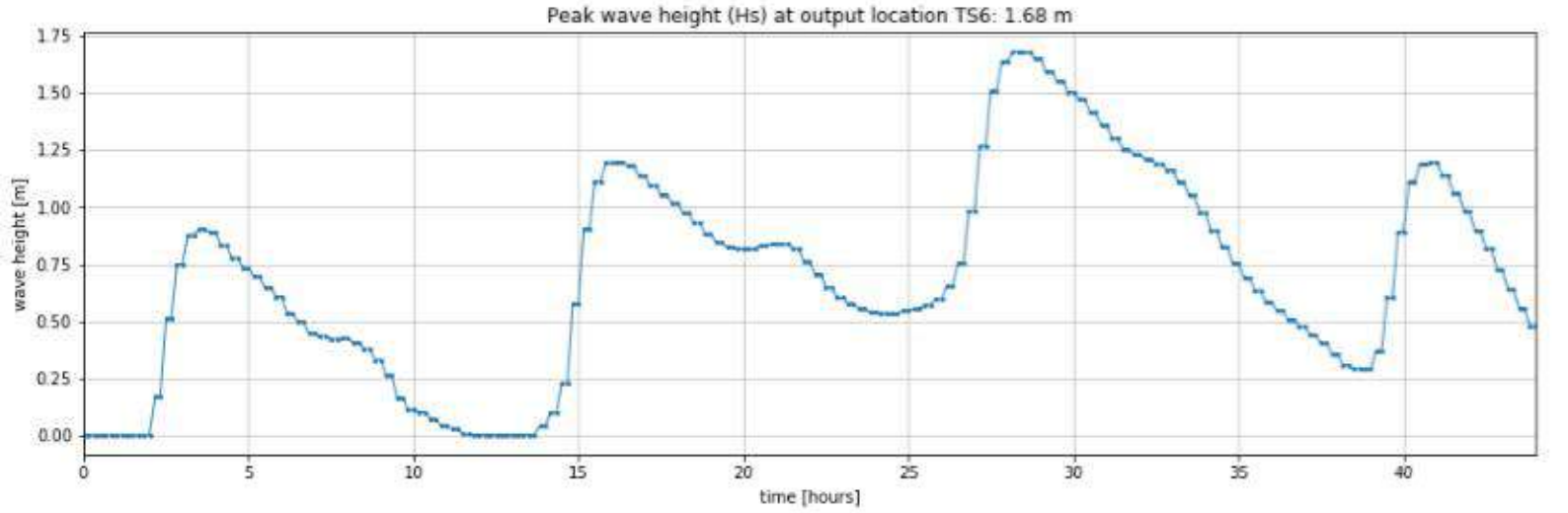
Peak wave height (Hs) at output location TS6: 1.68 m
wave height [m]
1.75
1.50
1.25
1.00
0.75
0.50
0.25
0.00
0
5
10
15
20
25
30
35
40
time [hours]

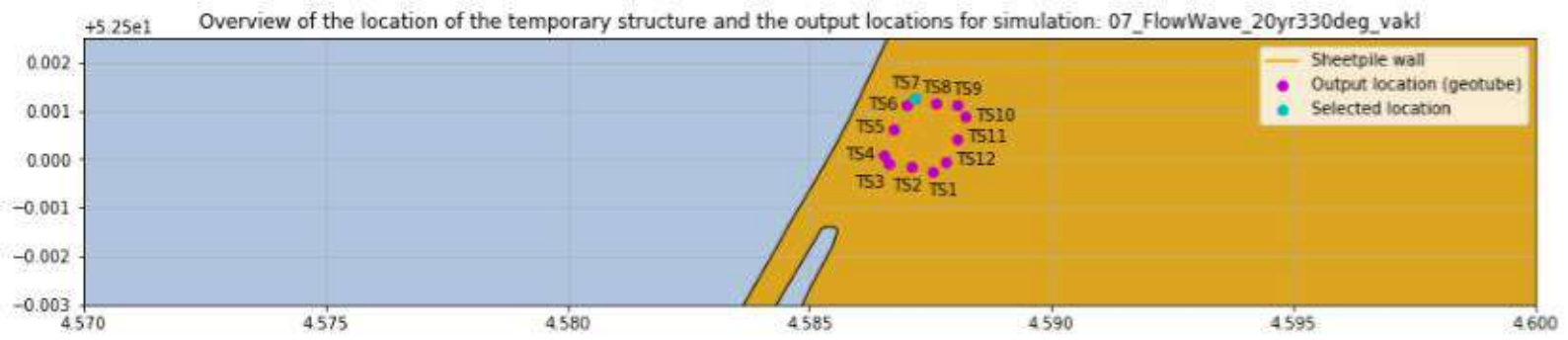
Overview of the location of the temporary structure and the output locations for simulation: 07_FlowWave_20yr330deg_vakl
+5.25e1
Sheetpile wall
Output location (geotube)
Selected location
TS1
TS2
TS3
TS4
TS5
TS6
TS7
TS8
TS9
TS10
TS11
TS12
0.002
0.001
0.000
−0.001
−0.002
−0.003
4.570
4.575
4.580
4.585
4.590
4.595
4.600

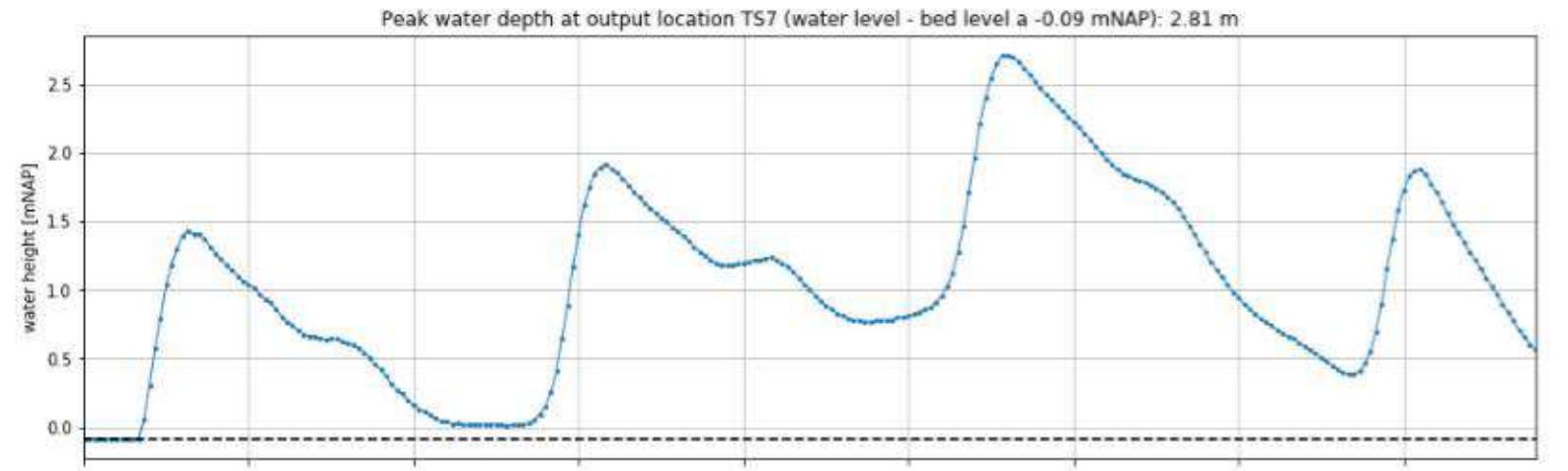
Peak water depth at output location TS7 (water level - bed level a -0.09 mNAP): 2.81 m
water height [mNAP]
2.5
2.0
1.5
1.0
0.5
0.0

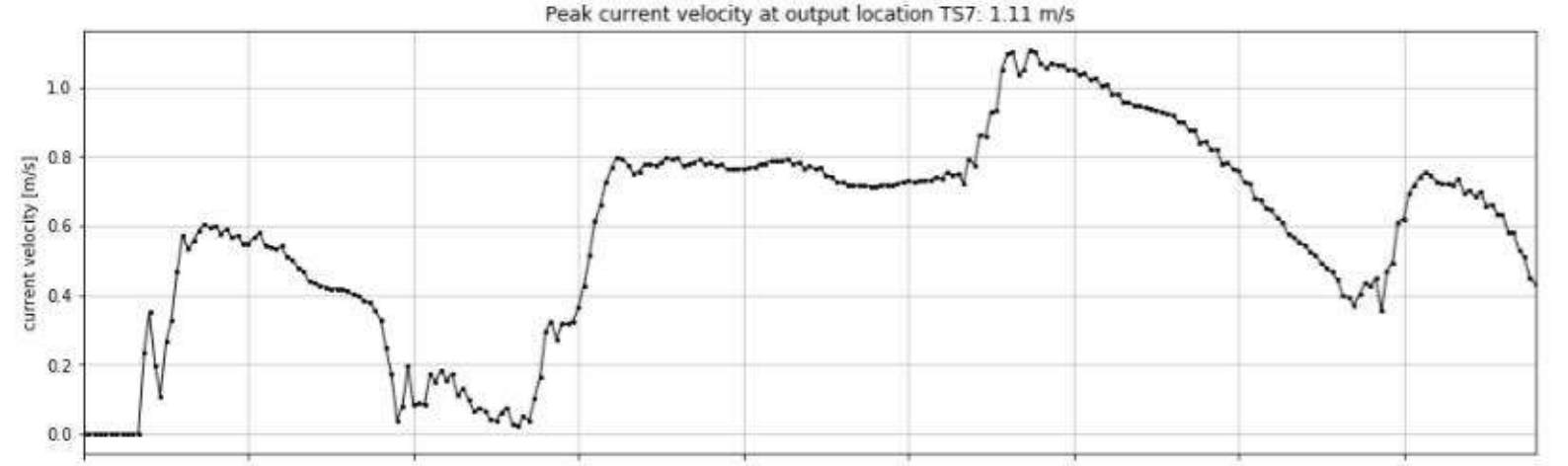
Peak current velocity at output location TS7: 1.11 m/s
current velocity [m/s]
1.0
0.8
0.6
0.4
0.2
0.0

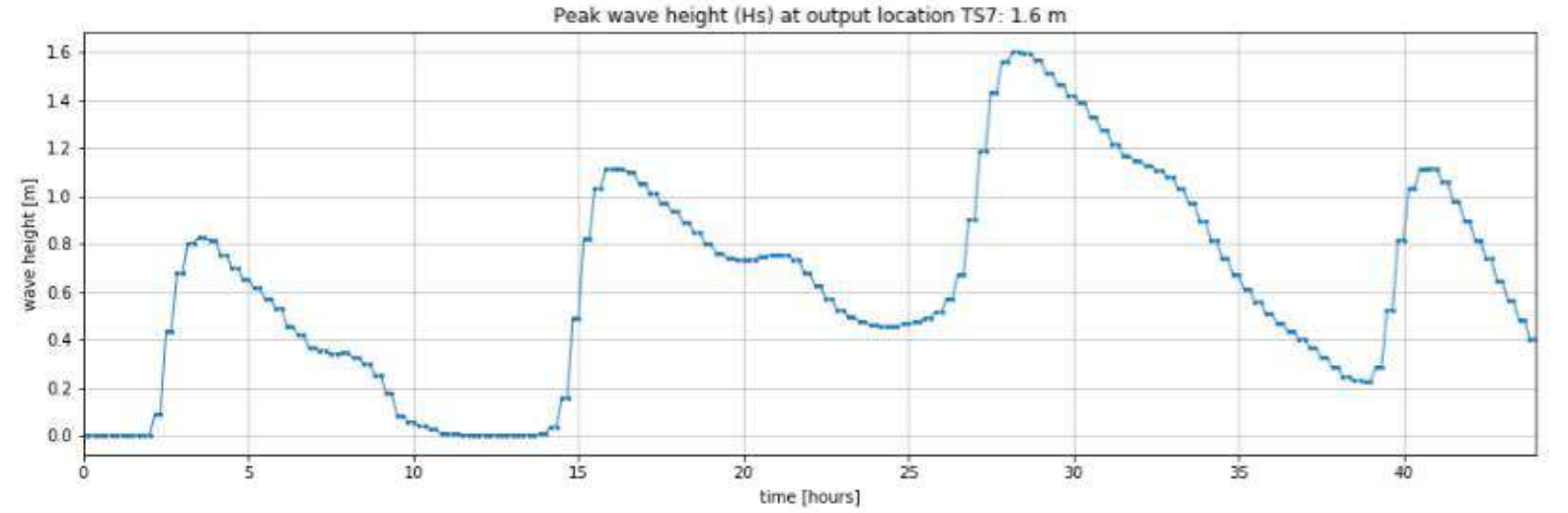
Peak wave height (Hs) at output location TS7: 1.6 m
wave height [m]
1.6
1.4
1.2
1.0
0.8
0.6
0.4
0.2
0.0
0
5
10
15
20
25
30
35
40
time [hours]

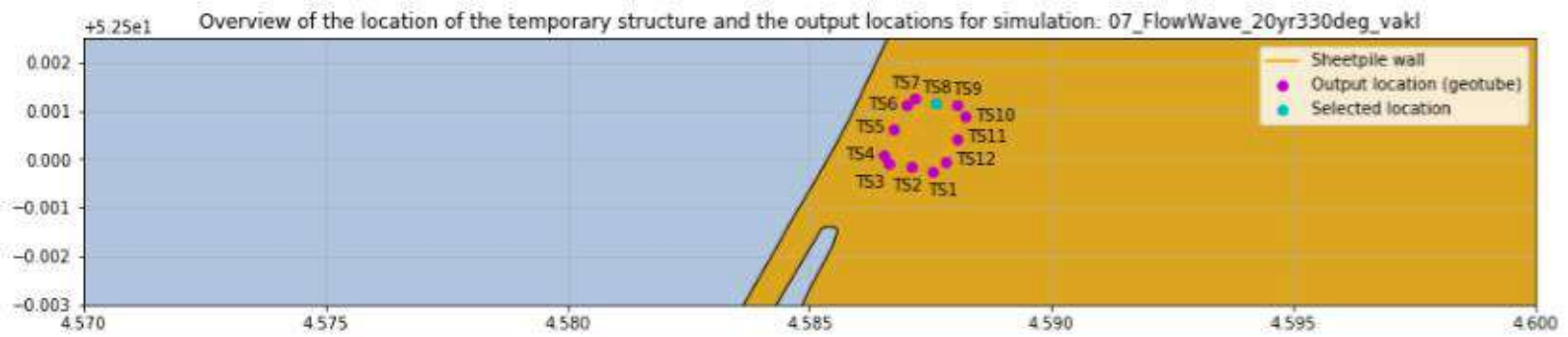
Overview of the location of the temporary structure and the output locations for simulation: 07_FlowWave_20yr330deg_vakl
+5.25e1
Sheetpile wall
Output location (geotube)
Selected location
TS1
TS2
TS3
TS4
TS5
TS6
TS7
TS8
TS9
TS10
TS11
TS12
0.002
0.001
0.000
−0.001
−0.002
−0.003
4.570
4.575
4.580
4.585
4.590
4.595
4.600

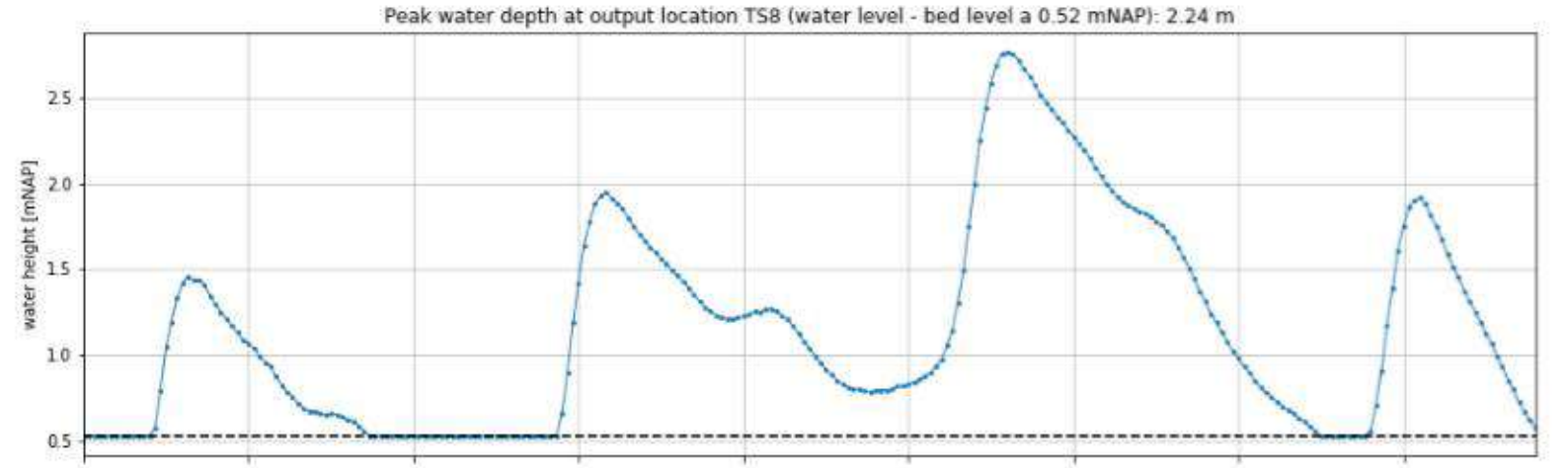
Peak water depth at output location TS8 (water level - bed level a 0.52 mNAP): 2.24 m
water height [mNAP]
2.5
2.0
1.5
1.0
0.5

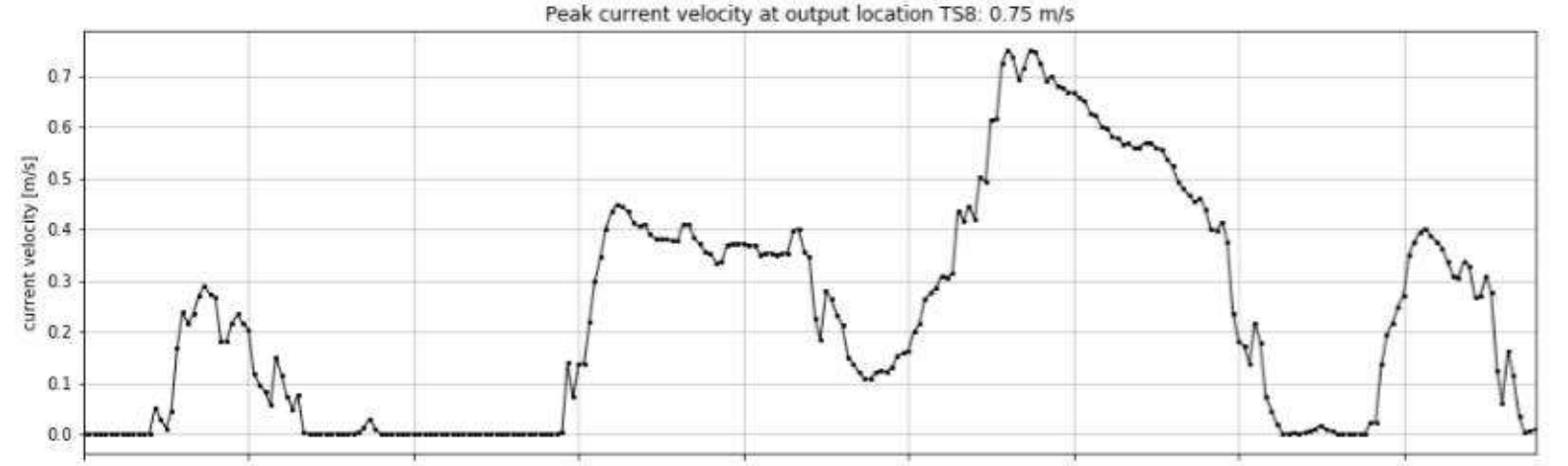
Peak current velocity at output location TS8: 0.75 m/s
current velocity [m/s]
0.7
0.6
0.5
0.4
0.3
0.2
0.1
0.0

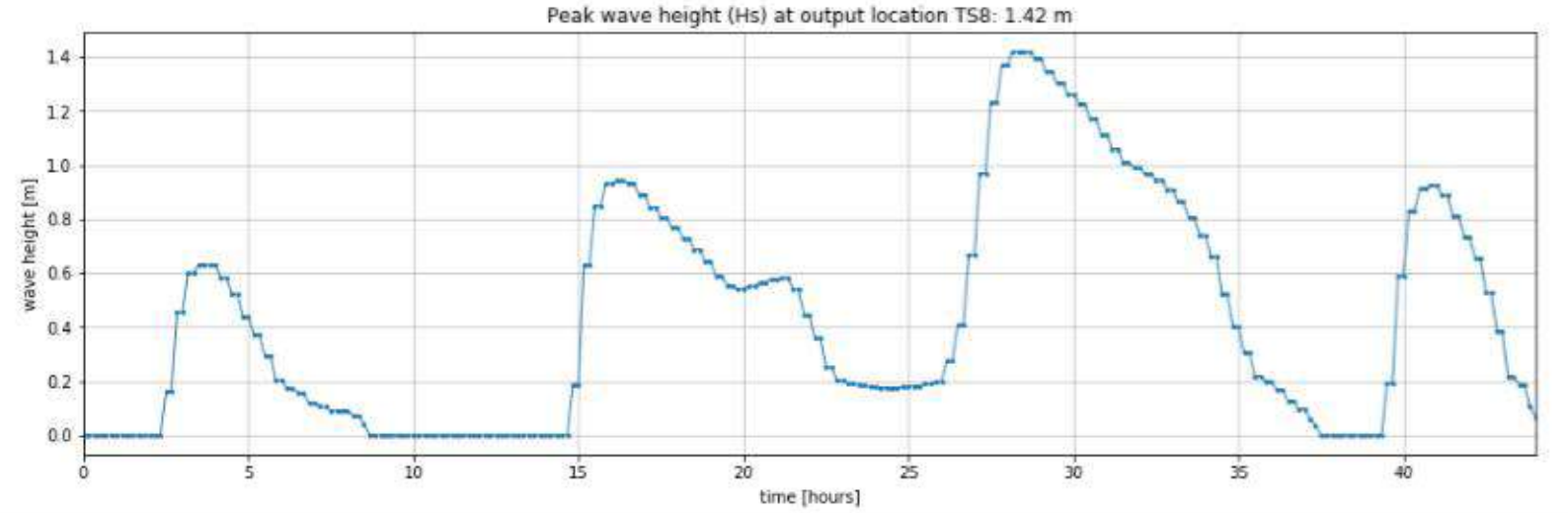
Peak wave height (Hs) at output location TS8: 1.42 m
wave height [m]
1.4
1.2
1.0
0.8
0.6
0.4
0.2
0.0
0
5
10
15
20
25
30
35
40
time [hours]

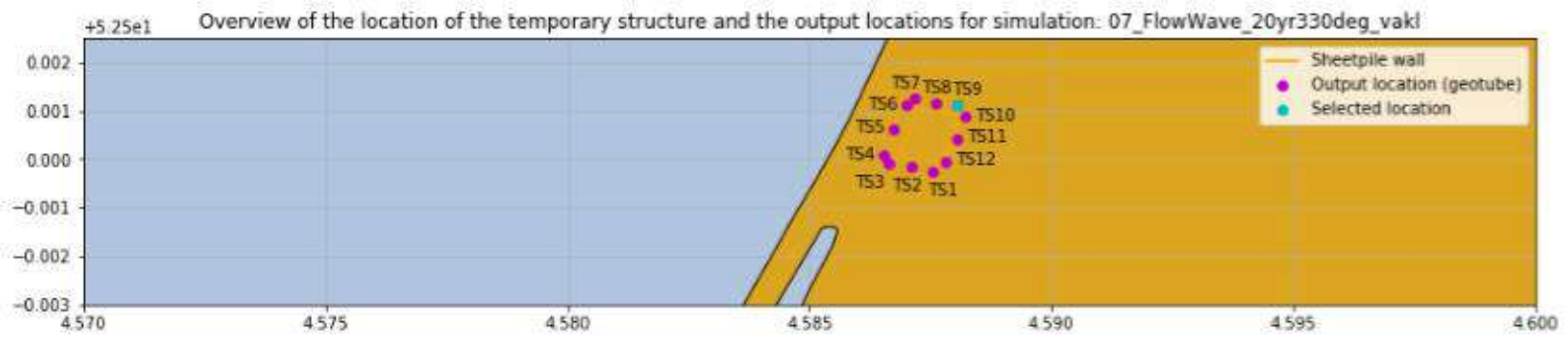
Overview of the location of the temporary structure and the output locations for simulation: 07_FlowWave_20yr330deg_vakl
+5.25e1
Sheetpile wall
Output location (geotube)
Selected location
TS1
TS2
TS3
TS4
TS5
TS6
TS7
TS8
TS9
TS10
TS11
TS12

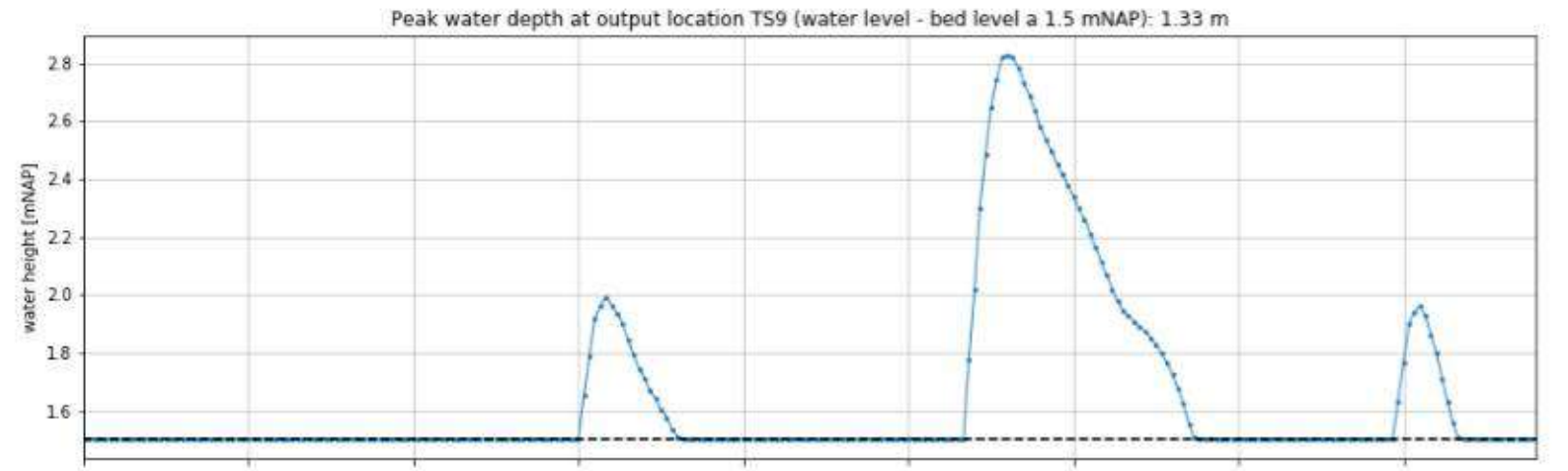
Peak water depth at output location TS9 (water level - bed level a 1.5 mNAP): 1.33 m
water height [mNAP]

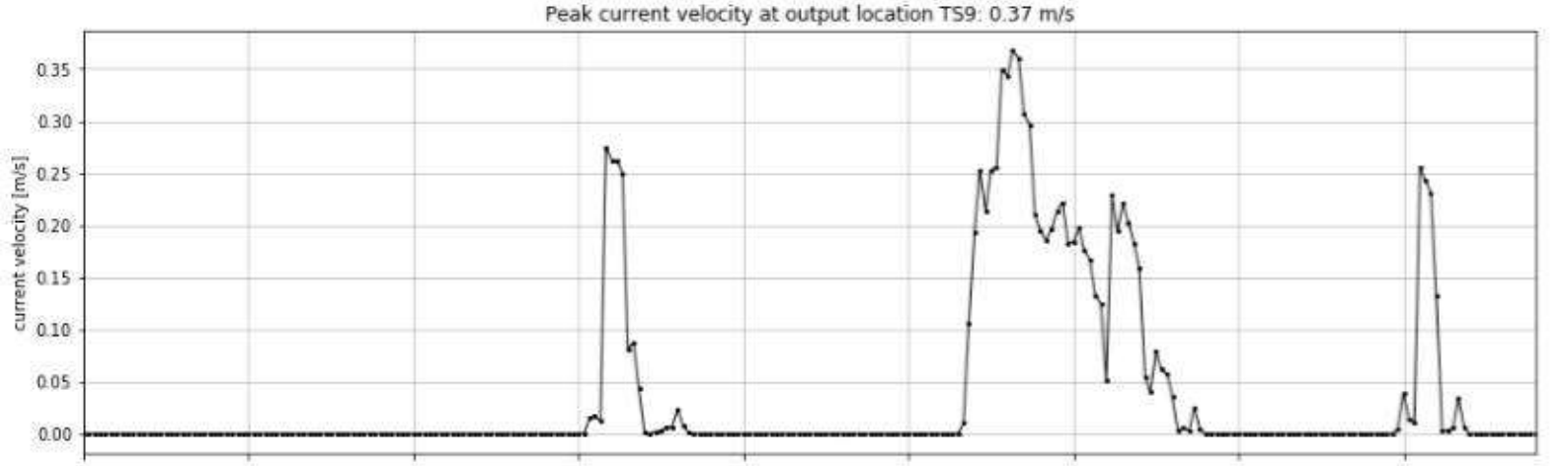
Peak current velocity at output location TS9: 0.37 m/s
current velocity [m/s]

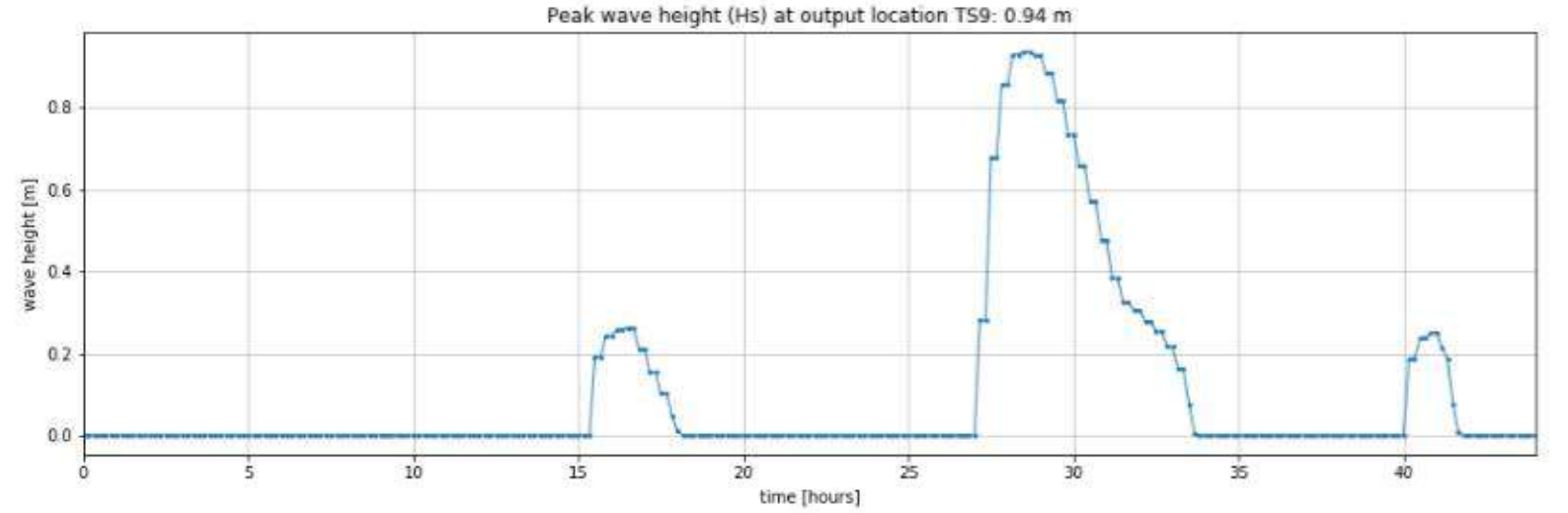
Peak wave height (Hs) at output location TS9: 0.94 m
wave height [m]
time [hours]

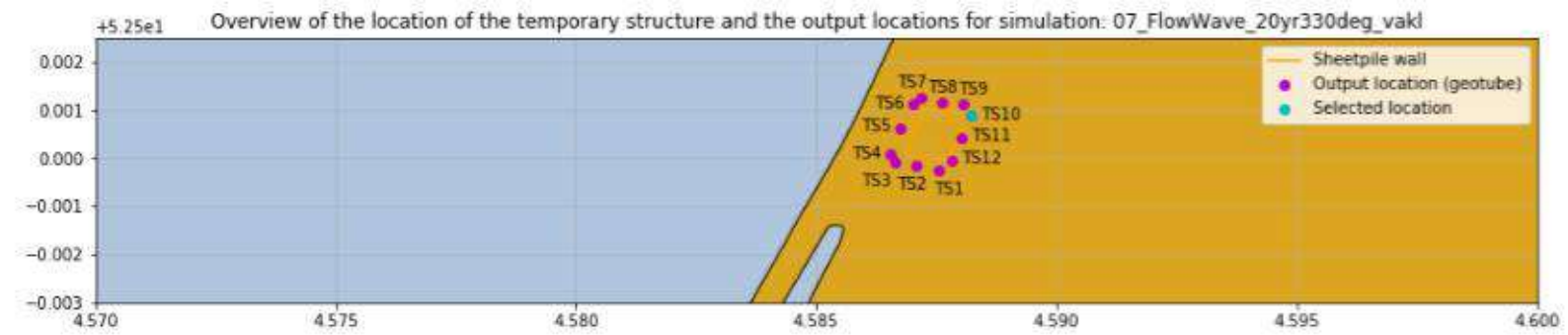
Overview of the location of the temporary structure and the output locations for simulation: 07_FlowWave_20yr330deg_vakl
+5.25e1
Sheetpile wall
Output location (geotube)
Selected location
TS1
TS2
TS3
TS4
TS5
TS6
TS7
TS8
TS9
TS10
TS11
TS12

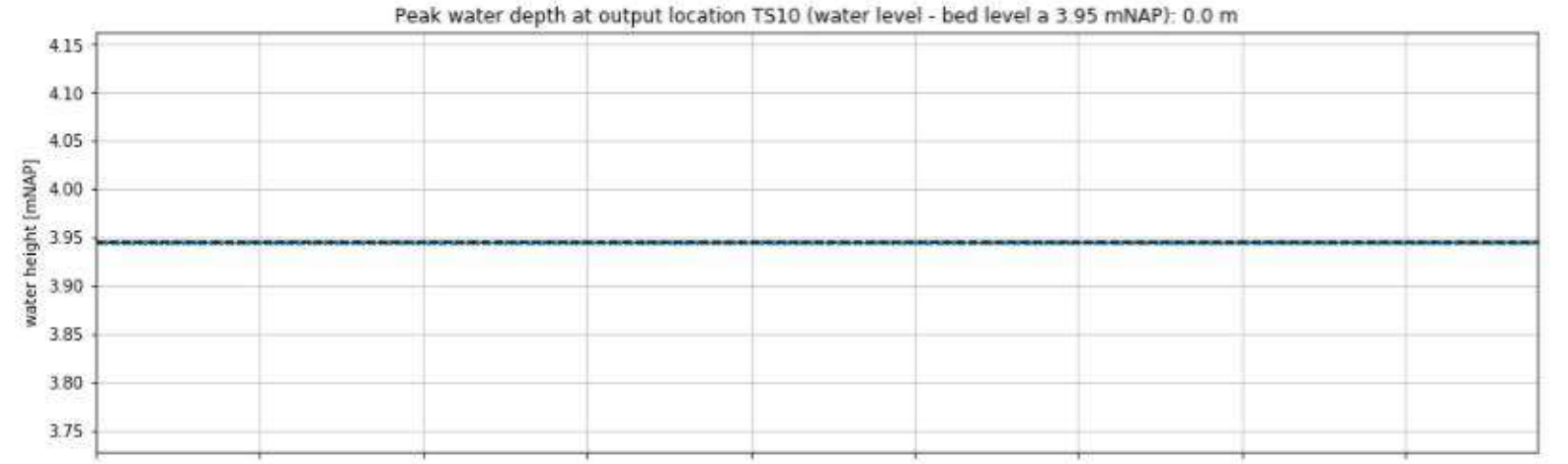
Peak water depth at output location TS10 (water level - bed level a 3.95 mNAP): 0.0 m
water height [mNAP]

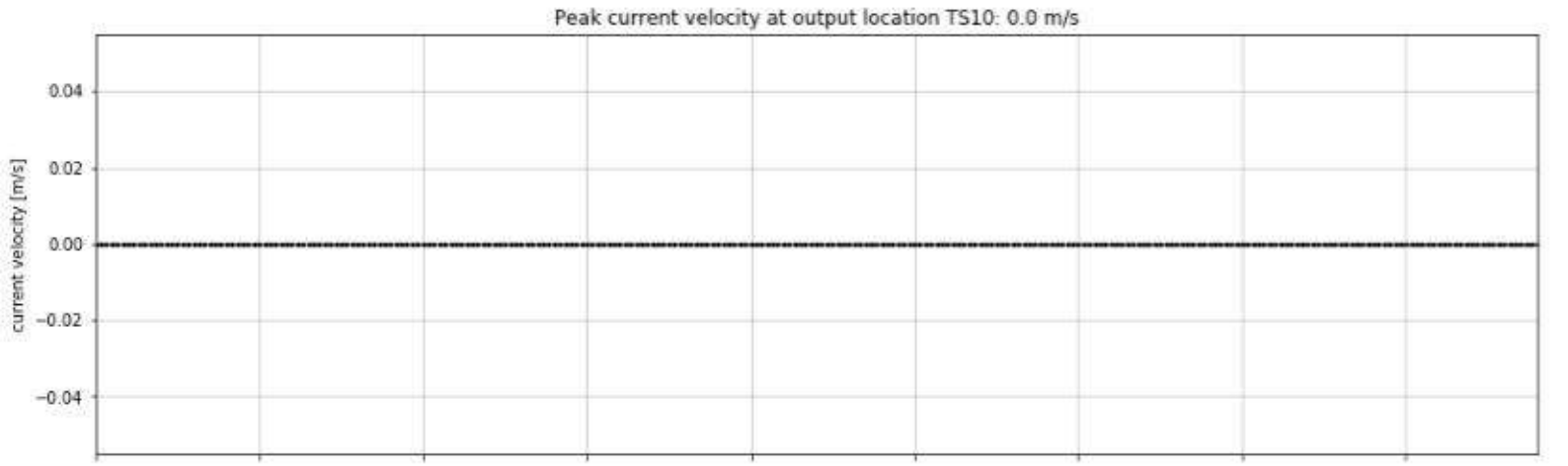
Peak current velocity at output location TS10: 0.0 m/s
current velocity [m/s]

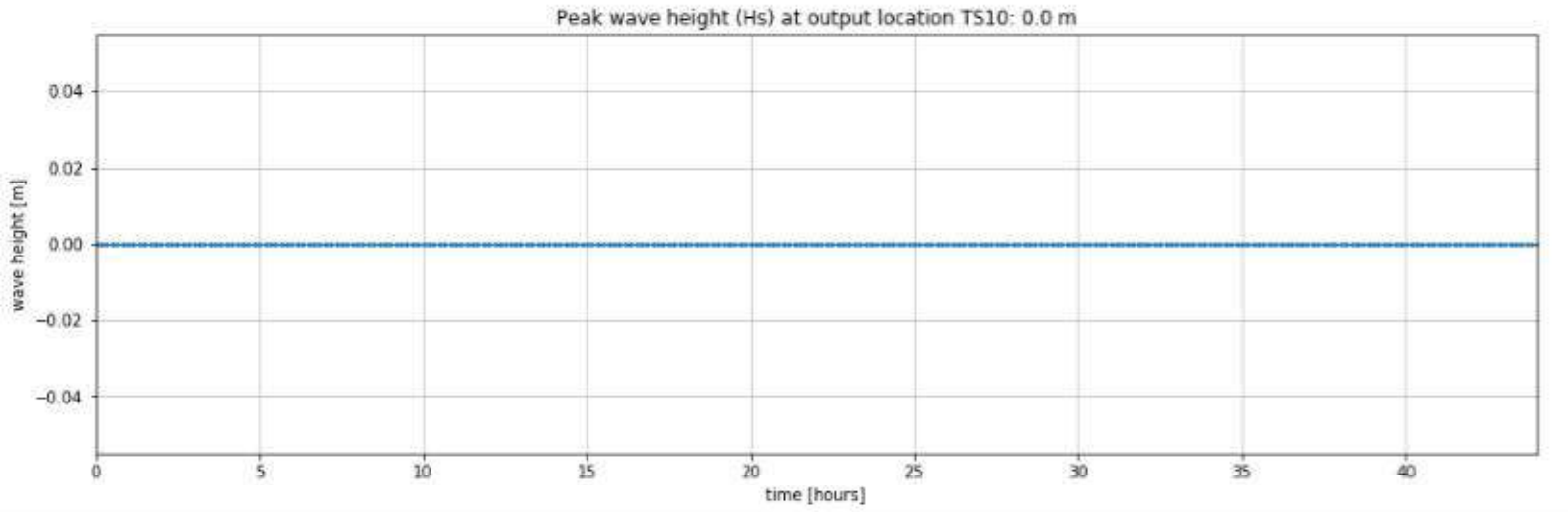
Peak wave height (Hs) at output location TS10: 0.0 m
wave height [m]
time [hours]

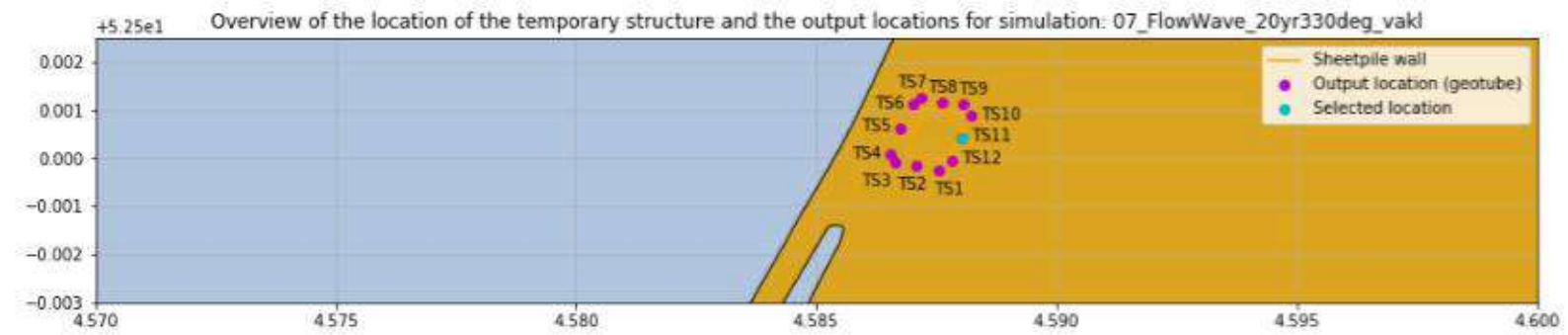
Overview of the location of the temporary structure and the output locations for simulation: 07_FlowWave_20yr330deg_vakl
+5.25e1
Sheetpile wall
Output location (geotube)
Selected location
TS1
TS2
TS3
TS4
TS5
TS6
TS7
TS8
TS9
TS10
TS11
TS12
0.002
0.001
0.000
−0.001
−0.002
−0.003
4.570
4.575
4.580
4.585
4.590
4.595
4.600

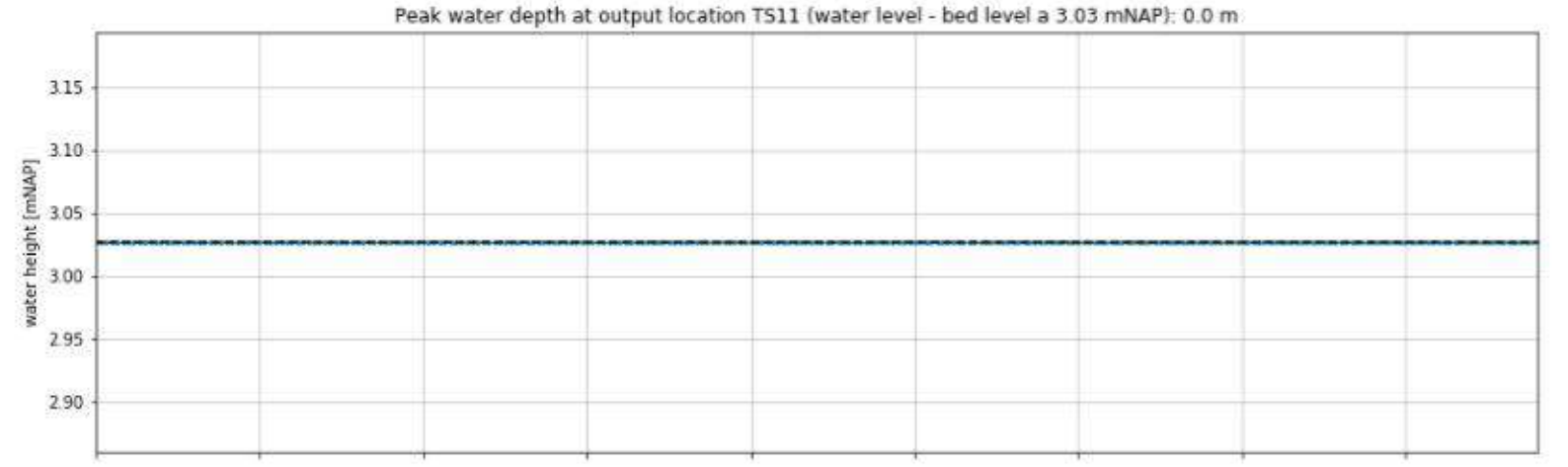
Peak water depth at output location TS11 (water level - bed level a 3.03 mNAP): 0.0 m
water height [mNAP]
3.15
3.10
3.05
3.00
2.95
2.90

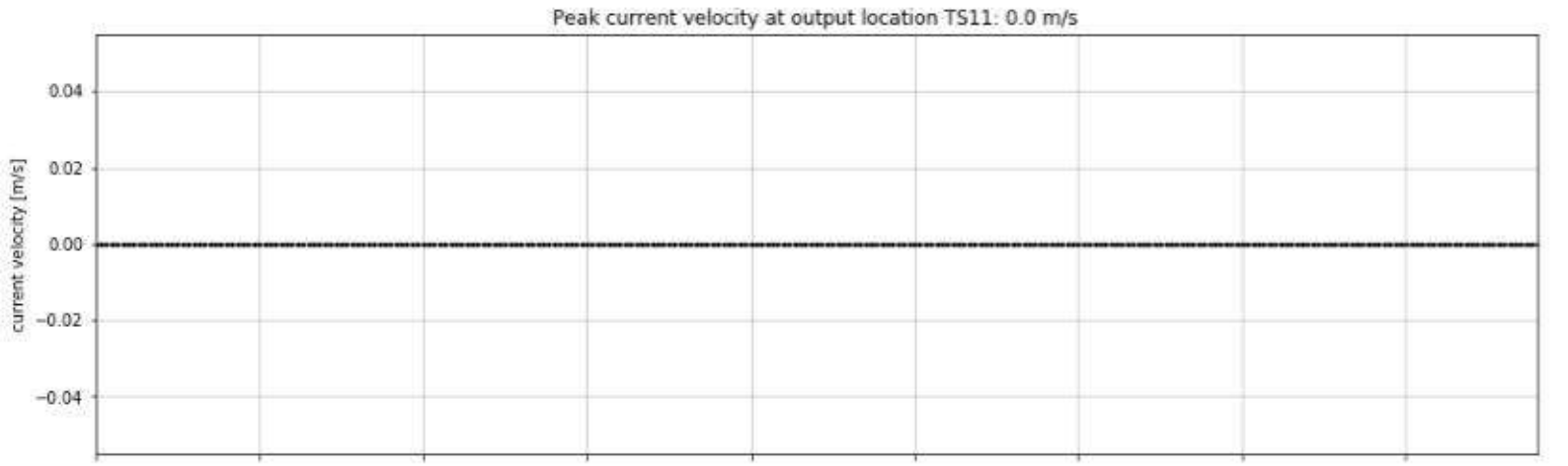
Peak current velocity at output location TS11: 0.0 m/s
current velocity [m/s]
0.04
0.02
0.00
−0.02
−0.04

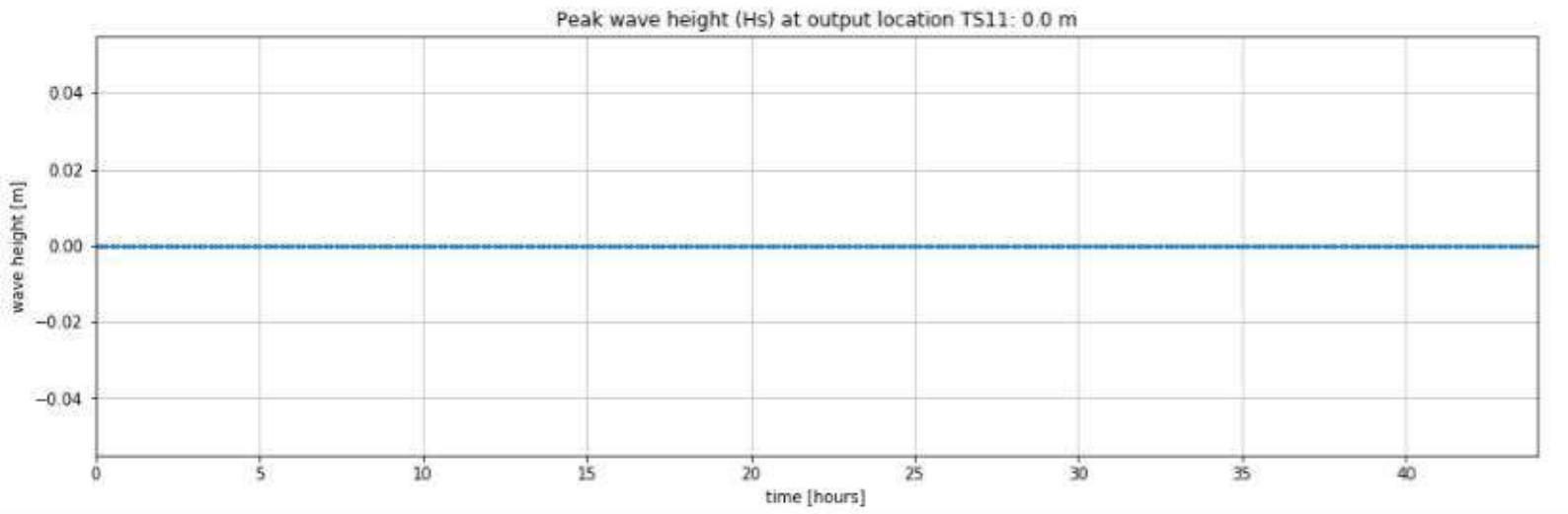
Peak wave height (Hs) at output location TS11: 0.0 m
wave height [m]
0.04
0.02
0.00
−0.02
−0.04
0
5
10
15
20
25
30
35
40
time [hours]

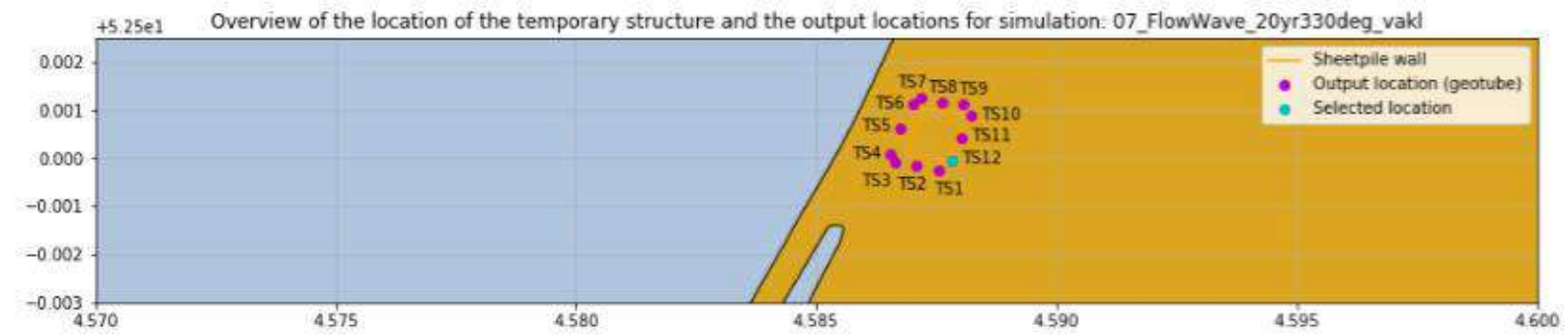
Overview of the location of the temporary structure and the output locations for simulation: 07_FlowWave_20yr330deg_vakl
+5.25e1
Sheetpile wall
Output location (geotube)
Selected location
TS1
TS2
TS3
TS4
TS5
TS6
TS7
TS8
TS9
TS10
TS11
TS12
0.002
0.001
0.000
−0.001
−0.002
−0.003
4.570
4.575
4.580
4.585
4.590
4.595
4.600

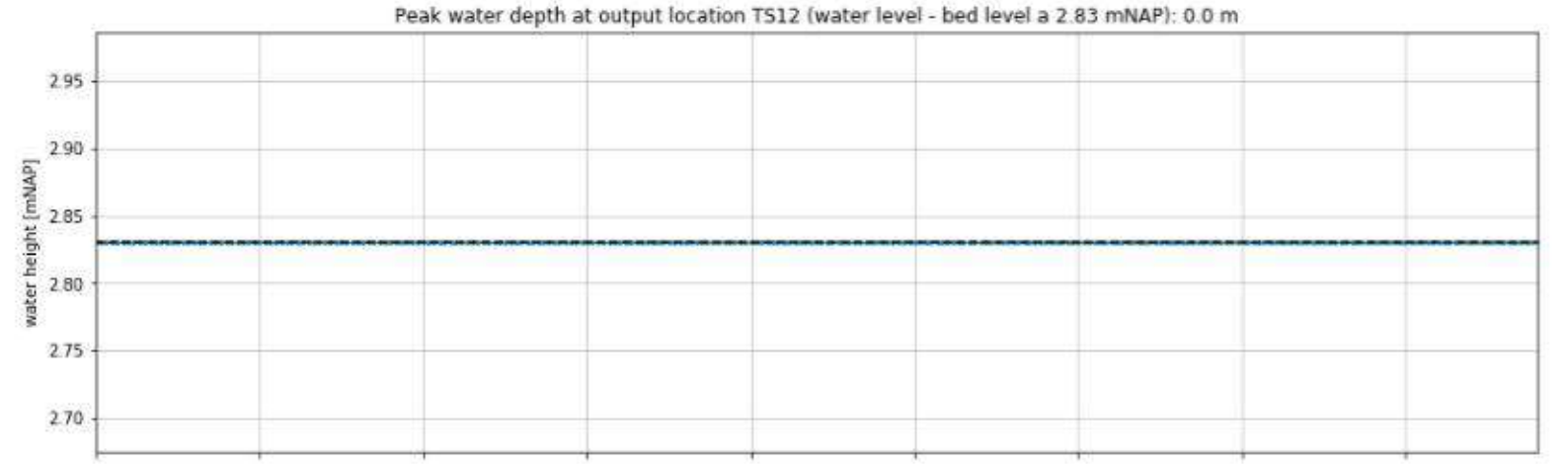
Peak water depth at output location TS12 (water level - bed level a 2.83 mNAP): 0.0 m
water height [mNAP]
2.95
2.90
2.85
2.80
2.75
2.70

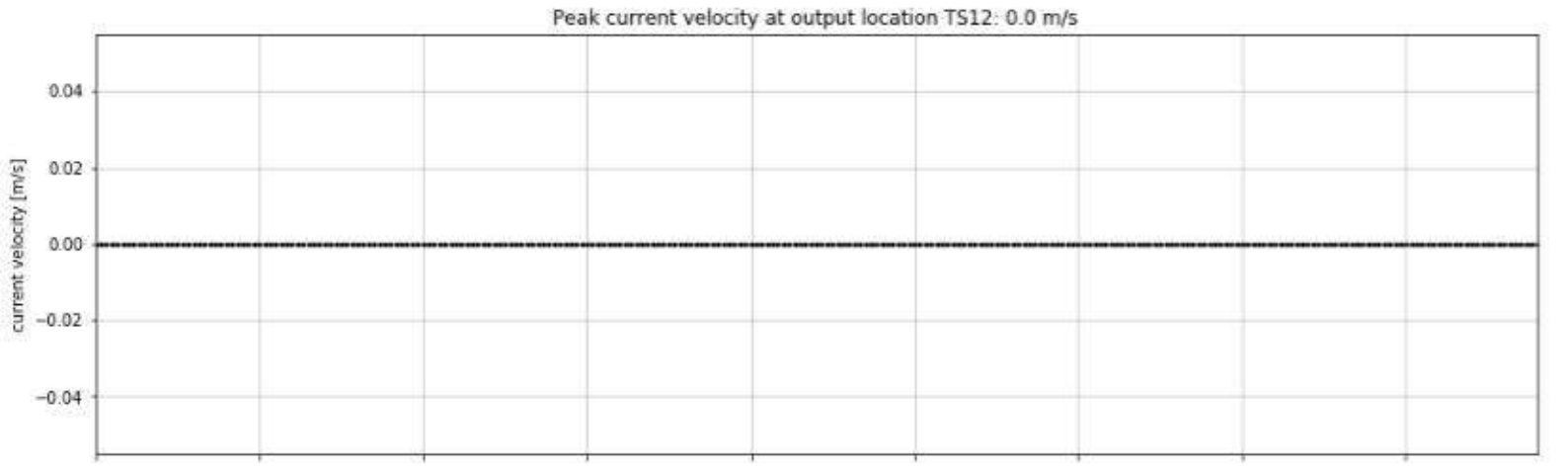
Peak current velocity at output location TS12: 0.0 m/s
current velocity [m/s]
0.04
0.02
0.00
−0.02
−0.04

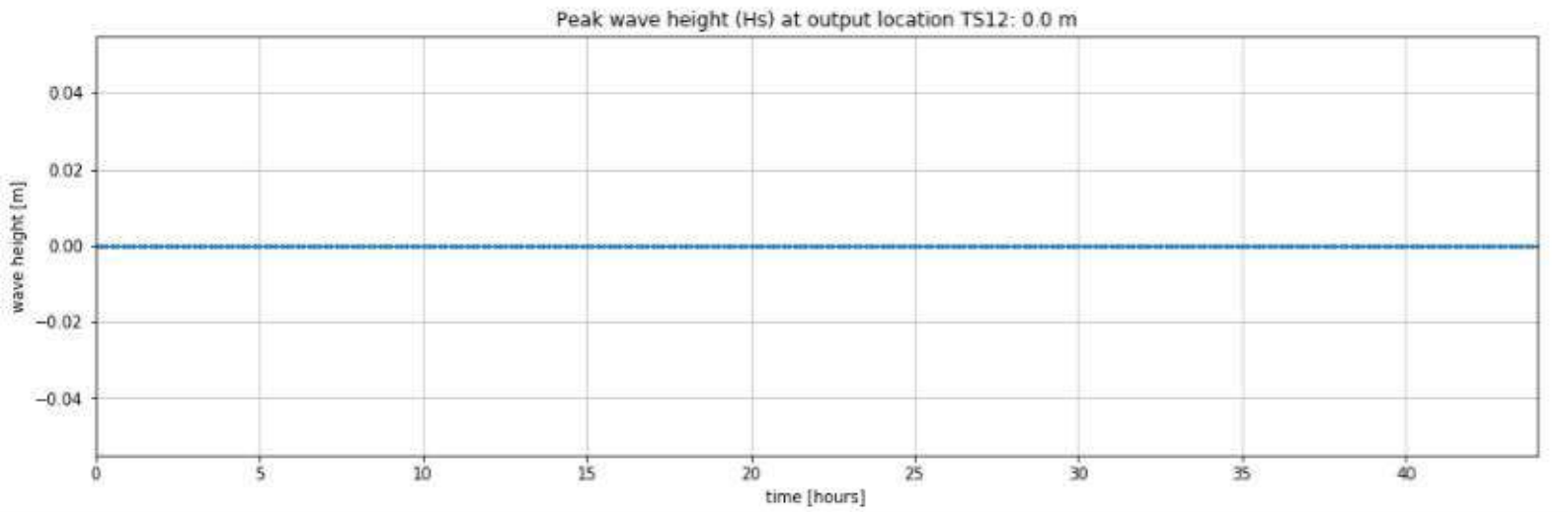
Peak wave height (Hs) at output location TS12: 0.0 m
wave height [m]
0.04
0.02
0.00
−0.02
−0.04
0
5
10
15
20
25
30
35
40
time [hours]

Deltares is an independent institute for applied research in the field of water and subsurface. Throughout the world, we work on smart solutions for people, environment and society.

Deltares

www.deltares.nl